Interplay between the transcription machinery and the responses to DNA damage and replication stress

Lilli Theres Eilertsen Bay

Department of Radiation Biology
Institute for Cancer Research
The Norwegian Radium Hospital
Oslo University Hospital

Dissertation submitted for the degree of Ph.D.

Institute of Clinical Medicine
Faculty of Medicine
University of Oslo

2023

Series of dissertations submitted to the
Faculty of Medicine, University of Oslo

ISBN 978-82-348-0275-1

Cover: UiO.
Print production: Graphic center, University of Oslo.

Table of Contents

Appendix: Papers I-III

Acknowledgements

The work presented in this thesis was carried out at the Department of Radiation Biology, Institute for Cancer Research, Norwegian Radium Hospital, Oslo University Hospital, in the period from 2018 to 2023. The funding received from The Research Council of Norway is gratefully acknowledged.

First, I want to express my gratitude to my main supervisor Helga B. Landsverk for the support and guidance I have received during the work on my PhD. Your mentorship and expertise have been invaluable throughout my PhD journey. I have really appreciated your enthusiasm for our work and that you always have time to discuss latest results or struggles. Thank you for everything that you have taught me. Secondly, I would like to thank my co-supervisor Randi G. Syljuåsen for the guidance, encouragement and support I have received over the years. Your extensive knowledge and passion for research is inspiring.

To previous and current members of Randi's group, thank you for creating a wonderful working environment. Your words of encouragement and valuable insights have not been taken for granted. It has been a pleasure to work with all of you. A special thanks to Lise E. Sandquist for all your contributions to this work. I would also like to highlight my office-colleagues throughout my PhD journey. To Adrian and Gro Elise, thank you for all the good laughs we have shared.

I would also like to acknowledge all co-authors for their contributions. For those of you that I may have failed to mention, your contributions have not gone unnoticed.

Finally, I want to thank my friends and family for all their support and constant love. A special thanks to my fiancé Einar. Your faith in me has been a constant source of motivation throughout my PhD journey. This work would not have been possible without you and Leonora.

Oslo, March 2023

Lilli Theres Eilertsen Bay

List of Papers

List of papers included in the thesis, referred to as Papers I-III in the text:

Paper I

WDR82/PNUTS-PP1 prevents transcription-replication conflicts by promoting RNA polymerase II degradation on chromatin.

Landsverk HB*, Sandquist LE*, Bay LTE*, Steurer B, Campsteijn C, Landsverk OJB, Marteijn JA, Petermann E, Trinkle-Mulcahy L, Syljuåsen RG.

*Shared first authorship

Cell Reports. 2020 Des 1; 33(9): 2211-1247.

Paper II

A novel, rapid and sensitive flow cytometry method reveals degradation of promoter proximal paused RNAPII in the presence and absence of UV.

Bay LTE, Syljuåsen RG, Landsverk HB.

Nucleic Acids Research. 2022 Aug; 50 (15): e89.

Paper III

The RNA polymerase II C-terminal domain promotes non-homologous end-joining (NHEJ) by recruiting DDX5 and CDC73.

Bay LTE, Trinkle-Mulcahy L, Eggen S, Syljuåsen RG, Landsverk HB.

Manuscript.

Other papers with contributions by the author, not included in the thesis:

Expanding roles of cell cycle checkpoint inhibitors in radiation oncology.

Hauge S, Eek Mariampillai A, Rødland GE, Bay LTE, Landsverk HB, Syljuåsen RG.

International Journal of Radiation Biology. 2021 Apr, 20: 1-10.

New link between the RNA polymerase II-CTD and replication stress.

Landsverk HB, Sandquist LE, Bay LTE, Syljuåsen RG.

Molecular & Cellular Oncology. 2021 Apr; 8 (3): 1910008.

Differential effects of combined ATR/Wee1 inhibition in cancer cells.

Rødland GE, Hauge S, Hasvold G, Bay LTE, Raabe TTH, Joel M, Syljuåsen RG.

Cancers. 2021 July; 13 (15): 3790.

Chromatin binding of RNA polymerase II and its phosphorylated forms through the cell cycle by flow cytometry.

Bay LTE, Stokke T, Syljuåsen RG, Landsverk HB.

In press at Bio-Protocol.

Summary

DNA damage is a major source of genomic instability and contributes to cancer development. On the other hand, inflicting lethal DNA damage is one of the most commonly used treatment strategies for cancer. DNA damage can e.g. be induced by agents that enhance the levels of replication stress. The survival of cancer cells is thus dependent on the responses to DNA damage and replication stress, where the transcription machinery emerges as a central factor. Understanding the role of transcription in the responses to DNA damage and replication stress is therefore of great importance.

The aim of this PhD thesis was to explore the interplay between transcription and the responses to DNA damage and replication stress. In paper I, we discovered novel roles for protein phosphatase 1 (PP1) nuclear targeting subunit (PNUTS)-PP1, the RNA polymerase II (RNAPII) C-terminal domain (CTD) phosphatase, and the docking protein WDR82 in suppressing replication stress. WDR82 has been shown to associate with PNUTS in the PTW-PP1 complex and binds RNAPII phosphorylated on serine 5 (pRNAPII S5). PNUTS-PP1 is known to dephosphorylate pRNAPII S5, and we discovered that WDR82 also promotes pRNAPII S5 dephosphorylation. Loss of pRNAPII S5 dephosphorylation affected the stability of RNAPII on chromatin, as we observed enhanced RNAPII residence time on chromatin after depletion of PNUTS/WDR82. With the proteasome inhibitor MG132, we discovered that RNAPII turnover was inhibited, indicating that PNUTS and WDR82 promoted degradation of RNAPII on chromatin. The replication stress response seen after depletion of PNUTS and WDR82 was dependent on transcription, as treatment with the transcription inhibitor THZ1 partially restored the DNA replication rate. This suggested that PNUTS-PP1/WDR82 promoted normal DNA replication by suppressing transcription-replication conflicts. We also found that the phospho-CTD interactor CDC73 was required for the enhanced RNAPII stability on chromatin seen after depletion of PNUTS/WDR82. Altogether, this suggests that WDR82 and PNUTS-PP1 are required to maintain a dynamic state of RNAPII to prevent conflicts with the replication fork.

As the interplay between transcription and the responses to replication stress and DNA damage is cell cycle dependent, we developed a flow cytometry technique that accurately measures RNAPII levels on chromatin in single cells through the cell cycle. In paper II, the technique was applied to measure cell cycle specific effects on RNAPII levels on chromatin in the presence and absence of DNA damage induced by ultraviolet radiation (UV). RNAPII is directly involved in the response to UV-induced bulky lesions, as lesion-stalled RNAPII signals to initiate transcription-coupled nucleotide excision repair (TC-NER). UV irradiation has been shown to induce a global “shutdown” of transcription, which causes reduced RNAPII pools and subsequent inhibition of transcription initiation. Interestingly, our results showed that transcription initiation was enhanced at early time points (15-30 min) after UV irradiation, which was primarily evident for the pRNAPII S5 form. Later, at 2h after UV irradiation, we observed a global inhibition of transcription, where the reduction in RNAPII levels on

chromatin was most pronounced for pRNAPII S5. As the elongating form of RNAPII is believed to encounter the UV-induced lesions and further targeted for degradation, we were surprised to see that pRNAPII S5 was specifically reduced at 2h after UV. pRNAPII S5 is associated with promoter proximal pausing, which is believed to be refractory to degradation. By inhibiting release into productive elongation with the transcription inhibitor 5,6-dichloro-1-β-ribofuranosylbenzimidazole (DRB), we were able to confirm that the promoter proximal paused RNAPII was specifically targeted for degradation after UV. Promoter proximal paused RNAPII was also shown to be targeted for degradation during unperturbed conditions. We also revealed cell cycle specific effects in the response to UV irradiation, as pRNAPII S2 levels were found to be more stable in S phase and pRNAPII S5 was degraded to a greater extent in S phase compared to G1 or G2 phases. Based on our results we proposed a new model for the effect of UV on the transcription cycle. We hypothesized that enhanced initiation of transcription after UV irradiation causes a phenomenon of "promoter proximal crowding", which resulted in premature termination via degradation of RNAPII.

The interplay between transcription and DNA damage was further explored in paper III, where we studied the role of transcription in the response to double-stranded breaks (DSBs) induced by ionizing radiation (IR). We observed a global inhibition of transcription after IR treatment, also at early time points (15-30 min). The reduction in RNAPII levels was especially notable for pRNAPII S2, suggesting that transcription elongation was suppressed by IR. PNUTS-PP1 was found to be required for the global inhibition of transcription upon IR-induced DNA damage. Notably, PNUTS depletion did not only recover IR-induced inhibition of transcription, but it also promoted a phospho-CTD mediated non-homologous end-joining (NHEJ) repair pathway. Several factors associated with NHEJ were enhanced on chromatin upon PNUTS depletion, while their chromatin association was inhibited with THZ1. As these NHEJ associated factors have been shown to bind the phospho-CTD, this suggested that the phosphorylation status of RNAPII CTD regulated their binding to chromatin. Moreover, RNA was found to be required for the recruitment of some NHEJ factors, but was not solely responsible for their enhanced chromatin association in PNUTS depleted cells. Additional factors, such as the phospho-CTD binding proteins CDC73 and DDX5, were required for the enhanced NHEJ frequency and influenced the recruitment of some NHEJ factors after PNUTS depletion. As the phospho-CTD and nascent RNA have been proposed to promote phase separation, we hypothesized that the phospho-CTD promoted NHEJ by forming nuclear condensates, involving nascent RNA, CDC73 and DDX5. However, this has to be further explored.

Taken together, our results support that the transcription machinery plays a central role in the DNA damage and replication stress responses. Our work has identified several new factors involved in the interplay between transcription and such genome integrity pathways.

Sammendrag (in Norwegian)

DNA-skade truer stabiliteten til genomet og kan føre til utvikling av kreft. Samtidig er det å påføre DNA-skade en av de mest brukte strategiene for å drepe kreftceller. Skaden kan blant annet påføres av stoffer som øker nivåene av replikasjonsstress. Kreftcellenes overlevelse er dermed avhengig av responsene til DNA-skade og replikasjonsstress, hvor transkripsjonsmaskineriet har vist seg å være sentral faktor. Det er dermed viktig å utforske rollen til transkripsjon i responsene til DNA-skade og replikasjonsstress.

Målet med denne avhandlingen var å utforske samspillet mellom transkripsjon og responsene til DNA-skade og replikasjonsstress. I artikkel I oppdaget vi nye roller for proteinfosfatase 1 (PP1)-kjerneadresserende subenhet (PNUTS)-PP1, fosfatasen til det C-terminale domenet (CTD) til RNA-polymerase II (RNAPII), og dokkingproteinet WDR82 i å hindre replikasjonsstress. WDR82 finnes i proteinkomplekset PTW-PP1 sammen med PNUTS, og har vist seg å binde RNAPII fosforylert på serin 5 (pRNAPII S5). PNUTS-PP1 er kjent for å defosforylere pRNAPII S5, og vi har nå oppdaget at WDR82 også promoterer pRNAPII S5-defosforylering. Tapet av pRNAPII S5-defosforylering viste seg å påvirke stabiliteten til RNAPII på kromatin, da vi observerte at RNAPII oppholdt seg lengre på kromatin etter nedregulering av PNUTS/WDR82. Behandling med proteasomhemmeren MG132 avlsørte at omsetningen av RNAPII på kromatin ble hindret, noe som indikerte at PNUTS og WDR82 promoterte degraderingen av RNAPII på kromatin. Replikasjonsstresset påført av nedreguleringen av PNUTS og WDR82 viste seg å være avhengig av transkripsjon, da behandling med transkripsjonshemmeren THZ1 delvis gjenopprettet hastigheten av DNA-replikasjon. Dette antydet at PNUTS-PP1/WDR82 promoterte normal DNA-replikasjon ved å hindre transkripsjon–replikasjon-konflikter. Vi avdekket også at CDC73, som er kjent for å binde fosforylert CTD av RNAPII, var nødvendig for den økte stabiliteten til RNAPII på kromatin etter nedreguleringen av PNUTS/WDR82. Kort oppsumert antyder dette at WDR82 og PNUTS-PP1 er nødvendige for å opprettholde RNAPII i en dynamisk tilstand for å unngå konflikter med replikasjonsgaffelen.

Siden samspillet mellom transkripsjon og responsene til replikasjonsstress og DNA-skade er avhengig av cellesyklus, utviklet vi en væskestrømscytometriteknikk som nøyaktig måler RNAPII-nivåer på kromatin i individuelle celler gjennom cellesyklusen. Denne teknikken ble videre brukt i artikkel II for å måle cellesyklusspesifikke effeker på kromatinnivåer av RNAPII med og uten DNA-skade påført ved UV-bestråling. RNAPII er kjent for å være direkte involvert i responsen til DNA-skade påført ved UV-bestråling, hvor RNAPII stans ved DNA-skaden signalerer igangsettingen av transkripsjonslenket nukleotidkuttingsreparasjon (TC-NER). UV-bestråling har også vært vist å medføre en global «nedstenging» av transkripsjon. Som en konsekvens blir den totale beholdningen av RNAPII i cellen redusert og ny initiering av transkripsjon hindres. Det var dermed interessant at vi observerte økt transkripsjonsinitiering ved tidlige tidspunkter (15-30 min) etter UV bestråling, hvor økningen var mest påfallende for pRNAPII S5. Siden elongerende RNAPII har vært ansett

som den formen av RNAPII som møter på UV-indusert skade, og deretter degraderes, ble vi overrasket over at pRNAPII S5 ble spesifikt redusert 2 timer etter UV-bestråling. pRNAPII S5 er assosiert med promotorproksimalt stanset RNAPII, og har blitt ansett å være beskyttet mot degradering. Vi bekreftet at promotorproksimalt stanset RNAPII ble spesifikt degradert ved å hindre frigjøringen av RNAPII til produktiv elongering med transkripsjonshemmeren 5,6-diklor-1-β-ribofuranosylbenzimidazol (DRB). Det viste seg at promotorproksimalt stanset RNAPII også ble degradert under uforstyrrede forhold. I tillegg avdekket vi cellesyklusspesifikke effekter i responsen til UV-bestråling, hvor pRNAPII S2-nivåene viste seg å være mer stabile i S-fasen og pRNAPII S5 ble degradert i større grad i S-fase sammenlignet med G1- og G2-fasene. Basert på våre resultater foreslo vi en ny modell for effektene av UV-bestråling på transkripsjonssyklusen. Vår hypotese gikk ut på at økt transkripsjonsinitiering etter UV-bestråling førte til fenomenet «promotorproksimal opphopning», som resulterte i prematur terminering av transkripsjon via degradering av RNAPII.

Samspillet mellom transkripsjon og DNA-skade ble videre addressert i artikkel nummer III, hvor vi studerte rollen til transkripsjon i responsen til dobbelttrådbrudd påført ved ioniserende stråling (IR). Vi observerte en global undertrykkelse av transkripsjon etter behandling med IR, også ved tidlige tidspunkter (15-30 min). Reduksjonen i RNAPII-nivåer var fremtredende for pRNAPII S2, noe som tydet på at transkripsjonselongeringen ble hindret etter behandling med IR. PNUTS-PP1 ble funnet å være nødvendig for den globale undertrykkelsen av transkripsjon etter IR-indusert DNA-skade. Merk at nedreguleringen av PNUTS ikke bare gjennopprettet undertrykkelsen av transkripsjonen etter IR, men også induserte en ikke-homolog endekobling (NHEJ)-reparajonsmekanisme som ble promotert av fosforylert CTD. Faktisk observerte vi at flere faktorer assosiert med NHEJ hadde økt kromatinbinding ved nedreguleringen av PNUTS, mens kromatinbidningen ble hindret med THZ1. Disse NHEJ-faktorene har blitt vist å binde fosforylert CTD, noe som antyder at fosforyleringsstatusen til RNAPII CTD regulerer kromatinbindingen av faktorene. Videre oppdaget vi at RNA var nødvendig for rekruteringen av noen av disse NHEJ-faktorene, men at RNA ene og alene ikke var ansvarlig for deres økte kromatinbinding etter nedreguleringen av PNUTS. Tilleggsfaktorer, slik som CDC73 og DDX5, som har blitt vist å binde fosforylert CTD, var nødvendig for den økte reparasjonen ved NHEJ, samt var involvert i rekruteringen av noen NHEJ-faktorer etter nedreguleringen av PNUTS. Siden fosforylert CTD og nylig produsert RNA har blitt foreslått å promotere faseseparasjon, foreslo vi en hypotese basert på at fosforylert CTD promoterte NHEJ-reparasjon ved å danne kondensater i kjernen, som også inneholdt RNA, CDC73 og DDX5. Dette må derimot utforskes videre.

Alt i alt støtter våre resultater opp under at transkripsjonsmaskineriet har en sentral rolle i responsene til DNA-skade og replikasjonsstress. Vårt arbeid har også identifisert flere nye faktorer involvert i samspillet mellom transkripsjon og slike signalveier som ivaretar integriteten til genomet.

1 Introduction

Faithful duplication of the genome during cell division is important to maintain genomic integrity. Although the process of DNA replication is strictly controlled, problems may arise that threaten the integrity of the genome. Such events that stall or block the progression of the replication machinery are collectively referred to as replication stress. There are numerous sources that can lead to impaired fork progression, and DNA damage is considered both a source and a consequence of replication stress [1]. As major sources of genomic instability, both replication stress and DNA damage contribute to cancer development [1-3]. Cancer is a large group of diseases associated with abnormal cell growth and bears the potential to spread to other parts of the body. One underlying mechanism of cancer is time dependent accumulation of genomic instability and DNA damage, which renders age as a major risk factor for developing cancer [4]. Defects in the DNA repair and replication stress responses contribute to carcinogenesis, however, they can also be exploited to improve the output of cancer treatments. Such defects can be specifically targeted in cancer cells as they are less common in normal tissue [3]. It is therefore of great importance to improve our knowledge on DNA damage and replication stress responses to explore how these defects can be targeted in cancer treatments.

Numerous studies have shown that transcription is a major source of replication stress and genomic instability [5, 6]. Some cancers display globally enhanced levels of transcription [7-10] and it has been shown that transcription inhibitors can improve the therapeutic outcome in such cancers [11-14]. Transcription is also emerging as a central factor in the DNA damage response. The main component of the transcription apparatus, RNA polymerase II, has been proposed to be involved in detection, repair and signaling following DNA damage [15-20]. As it continuously scans the genome during RNA synthesis, RNA polymerase II can be considered the ultimate surveyor of genomic integrity. Understanding how RNA polymerase II responds to replication stress and DNA damage will thus help to fully understand the DNA damage signaling and repair pathways and further improve our knowledge on cancer etiology.

1.1 The cell cycle

1.1.1 The cell cycle – regulation and checkpoints

The cell cycle is the process where the DNA is duplicated and a cell divides to generate two identical daughter cells. This process initiates when a resting cell moves from the resting phase (G0) into Gap phase 1 (G1), followed by the Synthesis phase (S), Gap phase 2 (G2) and Mitosis (M) (**Figure 1**). The G1, S and G2 phases together constitute the interphase. Mitosis can be further divided into prophase, metaphase, anaphase and telophase. After completion of mitosis, the cell divides to generate two daughter cells. These cells can further initiate a new cell cycle, or if the conditions do not support cell division, the daughter cells enter the resting phase, G0. Strict regulation of the cell cycle secures proper completion of one phase before entering the next. If a cell bypasses this regulation and enters the next phase prematurely, the cell may experience genomic instability and in worst case cell death. The transition from one phase to the next is therefore precisely timed by the activation of Cyclin-dependent kinases (CDKs), which is achieved by binding to specific Cyclins to form active heterodimers. A cell needs to pass three cell cycle checkpoints to complete one cycle of cell division. The activity of the different CDKs peaks in series to drive the progression of the cell cycle [21, 22].

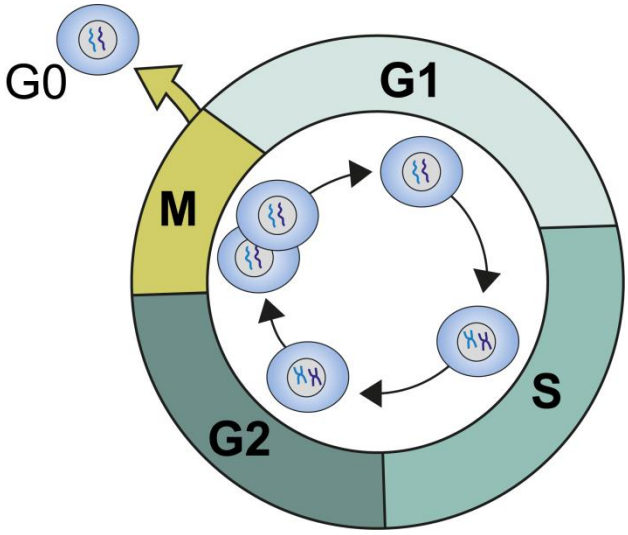

Figure 1: The cell cycle. The cell cycle consists of two gap phases G1 and G2, which separates the Synthesis phase (S) and Mitosis (M). The DNA is duplicated in S-phase prior to the production of two identical daughter cells during M-phase. If the conditions do not support a new round of cell division, the cell enters the G0 resting phase.

1.1.2 S-phase and DNA replication

In S-phase, the genome is copied into two identical versions through the process of DNA replication. It is important to maintain the genomic integrity and the process of DNA replication is therefore strictly regulated and supervised by several pathways. DNA replication starts with the licensing stage, where thousands of "pre-replication complexes" (pre-RCs) are loaded onto DNA at specific genomic locations, termed "replication origins". Licensing of origins requires low CDK activity and is therefore restricted to telophase [23] and G1-phase [24, 25]. The ORC (ATPases Origin Recognition Complex), together with Cdt1 (Chromatin licensing and DNA replication factor 1), Cdc6 (Cell division cycle 6) and the helicase MCM2-7 (Minichromosome Maintenance Protein 2-7), bind together at replication origins to form the pre-RC (**Figure 2**) [26].The helicase remains inactive until the cell enters S-phase and the CDK activity increases [24]. This is to prevent re-licensing of already replicated sequences in S-phase and to ensure that DNA is replicated only once per cell cycle [27]. On the other hand, it is important that enough origins are licensed, as under-replication also poses a threat to the genomic integrity. As licensing is limited to G1 and only happens once during a cell cycle, the cell "overcompensates" by licensing more origins than required for normal replication [25]. Whether an origin is fired or not depends on the replication program and is regulated by factors such as epigenetic marks, 3D genome architecture and transcriptional activity [28]. Although origins are termed as "early" or "late" firing, the process of origin firing occurs in a continuum throughout S-phase [29]. Origins that are unused during normal replication, termed "dormant" origins, can be fired later in the replication program to complete replication in the case of e.g. replication fork stalling [25].

As the cell proceeds into S-phase, replication is initiated by converting a licensed origin into an active replication fork. This process is highly regulated, where both current factors of the pre-RC complex are modified but also new factors are incorporated. Phosphorylation of the pre-RC complex by the kinases CDK2/Cyclin E and DDK (Dbf4-Dependent kinase) initiates origin firing and further promotes binding of CDC45 and GINS (Go-Ichi-Ni-San) to MCM2-7 [24, 30]. This leads to the formation of the pre-initiation complex (pre-IC). The MCM2-7 helicase is activated upon interaction with CDC45 and GINS [30], which further causes the DNA double stranded helix to unwind and form a replication bubble [31]. PCNA (Proliferating Cell Nuclear Antigen) encircles the double-stranded DNA and acts as a scaffold to tether proteins such as DNA polymerases to DNA to form two replication forks at each end of the bubble [32]. There are three types of DNA polymerases involved in replication: α generates short primers to initiate DNA synthesis, while δ and ε incorporates new nucleotides to assemble a new DNA strand on top of the template strand during elongation [31]. The DNA polymerases work bidirectionally from the origin to form two complementary DNA strands. If a replication fork encounters another active replication fork, the active helicase and PCNA are removed from chromatin and the replication fork gets disassembled [24].

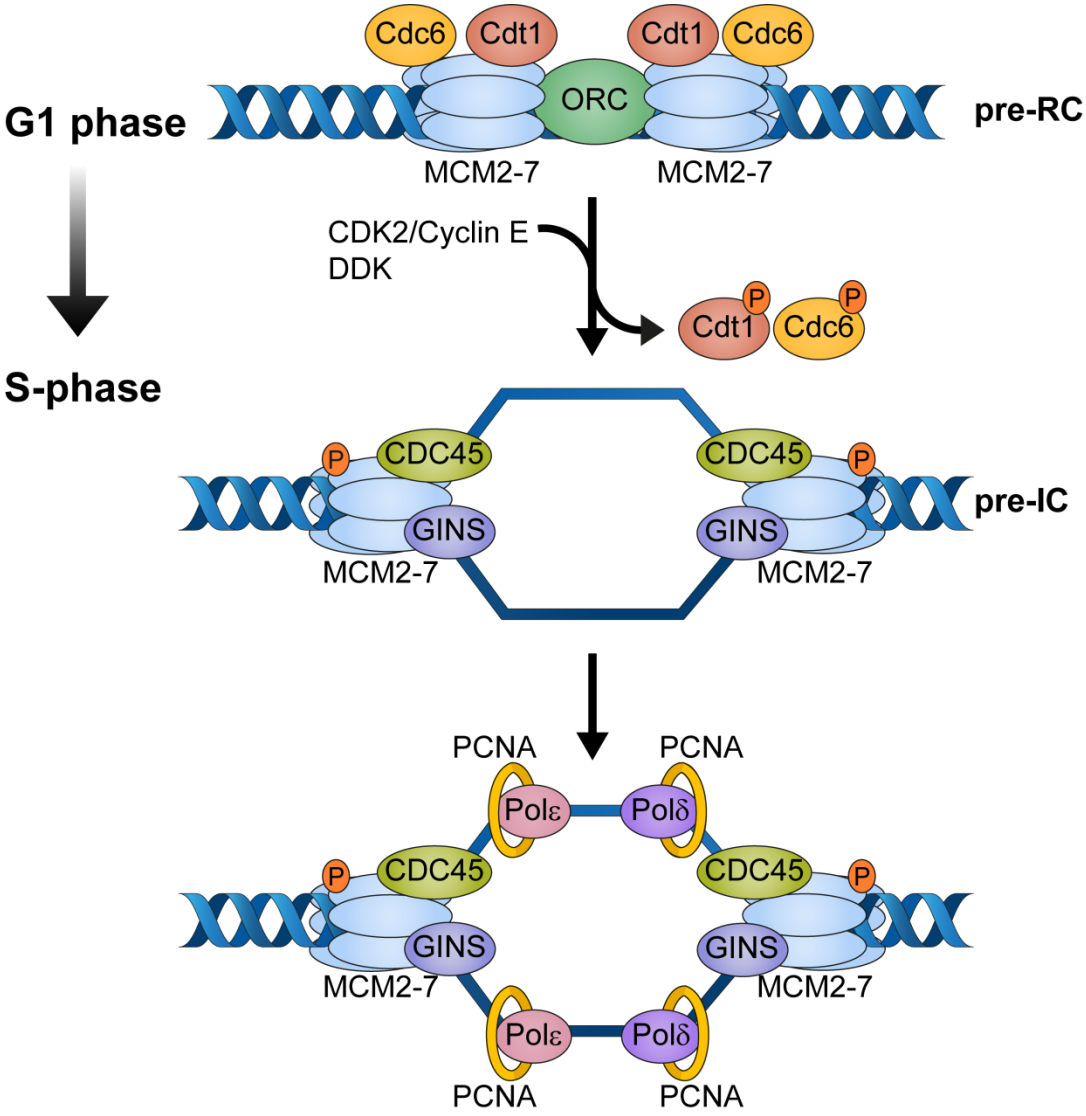

Figure 2: Initiation of DNA replication. In G1, DNA replication is initiated by loading of pre-replication complexes (pre-RCs) onto specific locations on DNA, termed "replication origins". These pre-RCs consist of ORC, Cdt1, Cdc6 and the MCM2-7 helicase. When the cell enters S-phase, increased CDK2/Cyclin E and DDK activity leads to activation of the helicase as it promotes binding of CDC45 and GINS to MCM2-7. Phosphorylation of Cdt1 and Cdc6 promotes their release from the pre-RCs and the remaining factors form the pre-initiation complex (pre-IC). Helicase activation facilitates melting of the DNA and the formation of a replication bubble. PCNA tethers the DNA polymerases ε and δ to DNA, to complete replisome assembly. See main text for details and references. Modified from [33]. Abbreviations: ORC, ATPases Orgin Recognition Complex; Cdt1, Chromatin licensing and DNA replication factor 1; Cdc6, Cell division cycle 6; MCM2-7, Minichromosome Maintenance Protein 2-7; CDK2, Cyclin-dependent kinase 2; DDK, Dbf4-Dependent kinase; GINS, Go-Ichi-Ni-San; PCNA, Proliferating Cell Nuclear Antigen.

During replication, the replication fork might encounter different events that distort the replication program. These events are collectively referred to as replication stress. This topic will be further explored in chapter 1.4.

1.2 Transcription

1.2.1 The transcription cycle

Transcription is the process of synthesizing RNA from the DNA code. RNA synthesis occurs throughout the cell cycle, except in mitosis when transcription is globally supressed [34-37]. There are several forms of RNA, where the main ones; messenger RNA (mRNA), transfer RNA (tRNA) and ribosomal RNA (rRNA), are used in the production of proteins. As mRNA carries the protein code, other types of RNA are termed non-coding RNA. In addition to tRNA and rRNA, there are numerous types of non-coding RNA that functions in gene expression via transcriptional and post-transcriptional regulation, and in epigenetic regulation [38]. The main mediators of transcription are RNA polymerases, where RNA polymerase II (RNAPII) is responsible for transcribing most of the genome in eukaryotic cells. RNAPII is a multi-subunit complex that contains a unique domain at the carboxy-terminus (CTD) of its largest subunit, RPB1. The CTD is conserved in fungi, plants and animals, ranging from 26 (in yeast) to 52 (in mammals) heptapeptide aminoacid repeats with the consensus sequence $Y_1S_2P_3T_4S_5P_6S_7$ [39-41]. During the transcription cycle, the CTD is subjected to post-translational modifications, mainly by phosphorylation. The pattern of different modifications is referred to as the "CTD code", which coordinates the recruitment of factors involved in transcription and RNA processing [41-43]. Amongst the different modifications of the CTD, the dynamic phosphorylation of serine 2 (pRNAPII S2) and serine 5 (pRNAPII S5) are the most studied. RNAPII at promoter proximal regions express high levels of pRNAPII S5, while pRNAPII S2 are associated with productive elongation [40]. pRNAPII S5 is also found in gene-internal regions and is enhanced on paused RNAPII at splice sites [44].

The transcription cycle is precisely timed and regulated at multiple steps. The main steps of the transcription cycle includes recruitment and formation of the preinitiation complex (PIC) at the promoter, release from the promoter and stalling at the promoter proximal pause site, promoter release followed by productive elongation, and finally termination (**Figure 3**) [45]. To initiate transcription, RNAPII and a set of general transcription factors (GTFs) are recruited to the promoter to form the PIC. The following transcription factors are required as a minimum for transcription initiation *in vitro*: TATA-binding protein (TBP), TFIIA, TFIIB, TFIIF, TFIIE and TFIIH [46]. PIC assembly is stimulated by the Mediator complex, which is required for recruitment of TFIIH to the promoter. Phosphorylation of the CTD on serine 5 by the TFIIH kinase CDK7 promotes the release of the Mediator and leads to promoter clearance of the RNAPII complex [47].

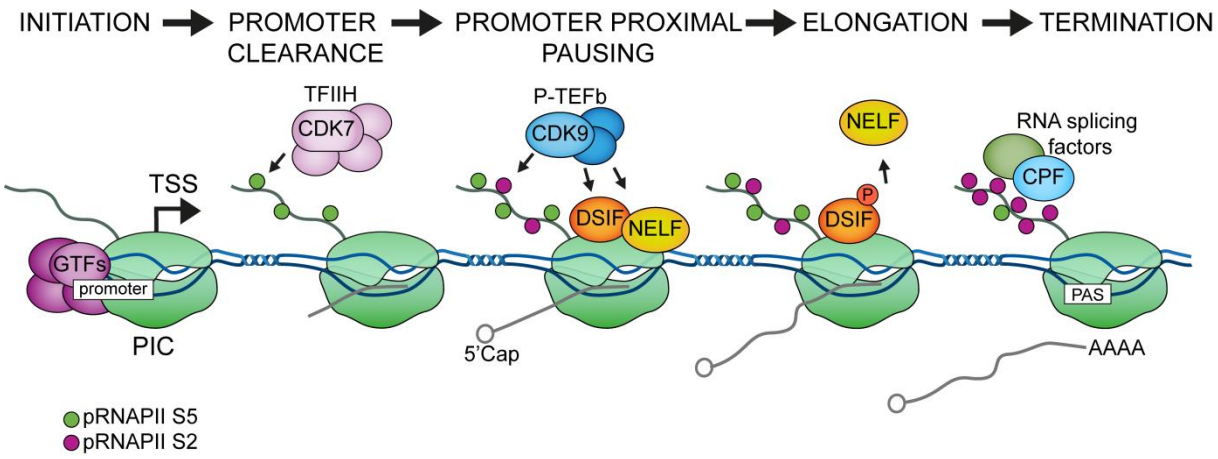

Figure 3: The transcription cycle. Transcription is initiated by the recruitment of PIC, which contains RNAPII and general transcription factors (GTFs), to the promoter. CDK7, within the TFIIH complex, phosphorylates pRNAPII S5 to promote promoter clearance. RNAPII progression is then stalled upon promoter proximal pausing, facilitated by DSIF and NELF. Premature termination and degradation of nascent RNA is prevented by the addition of a 5'cap. Pause release is triggered by the P-TEFb kinase by pRNAPII S2, but also by phosphorylation of DSIF and NELF, which causes NELF to dissociate. pRNAPII S2 levels peaks towards the 3'end and RNAPII progression slows upon encounter with a poly (A) signal (PAS). Termination factors, such as the RNA splicing machinery and polyadenylation factors (CPF) are recruited to pRNAPII S2 to terminate elongation and form mature mRNA. The capped and polyadenylated RNA is then released and RNAPII can be recycled for new rounds of transcription. See main text for details and references. Adapted from [48]. Abbreviations: PIC, pre-initiation complex; RNAPII, RNA polymerase II; pRNAPII S5, RNAPII CTD phosphorylated on serine 5; pRNAPII S2, RNAPII CTD phosphorylated on serine 2; DSIF, DRB sensitivity factor; NELF, negative elongation factor.

After 20-50 nucleotides downstream of the transcription start site (TSS), RNAPII is paused [49-51]. This promoter proximal pausing is considered a main rate-limiting step of transcription. Factors such as the DSIF complex (DRB sensitivity factor), composed of Spt5 and Spt4, and NELF (negative elongation factor) enforce promoter proximal pausing [45]. Spt5 binds RNAPII and promotes recruitment of capping enzymes [52] that recognizes serine 5 CTD repeats on RNAPII [53]. This is a critical event in promoting pause release as the addition of a 5' cap prevents degradation of nascent RNA and avoids premature termination of transcription [45, 54]. NELF then recognizes the RNAPII-Spt5 interface and prevents reactivation of RNAPII, leading to a paused state. Pause release is triggered by the recruitment of the P-TEFb kinase CDK9, which is responsible for phosphorylating RNAPII at serine 2, as well as NELF and Spt5. Phosphorylation of Spt5 causes NELF to dissociate from the elongation complex and transforms DSIF into a positive elongation factor that further promotes RNAPII to resume elongation. The dissociation of NELF by Spt5 exposes a binding site for the PAF1 complex (polymerase-associated factor 1) on RNAPII [45]. PAF1c has been shown to regulate phosphorylation of the RNAPII CTD, promoter proximal pausing and pause release [55, 56]. P-TEFb promotes the recruitment of PAF1c to facilitate phosphorylation of RNAPII CTD and further promote its release from promoter proximal pausing [45, 55-57]. Another factor considered as necessary for release into active elongation is Spt6. This

elongation factor has been shown to bind the phosphorylated CTD of RNAPII to open the RNA clamp formed by DSIF [58]. In addition, it possesses histone chaperone activity, which facilitates disassembly and reassembly of nucleosomes as RNAPII transcribes the genome [59]. It has been proposed that the formation of an activated RNAPII elongation complex requires the combined action of P-TEFb, PAF1c and Spt6 [58].

Serine 2 phosphorylation increases throughout elongation and reaches a plateau as RNAPII moves towards the end of the gene. At the end of the gene, termination factors, such as the RNA splicing machinery and polyadenylation factors (CPF), are recruited to pRNAPII S2 [40, 60]. This leads to the formation of mature mRNA and finally termination of elongation. Termination is associated with a slowdown of RNAPII when it transcribes across a poly (A) signal (PAS) [61]. There are two models for how RNAPII is released from chromatin during termination: the allosteric model and the torpedo model. In the allosteric model, the RNAPII elongation complex is subjected to a change in conformation and/or destabilized upon sensing PAS, which is likely due to the recruitment of CPF or release of antitermination factors. This model does not depend on cleavage of the transcript. In the torpedo model, cleavage of the transcript at PAS allows for 5'-3' exoribonuclease 2 (XRN2) exonuclease to degrade the transcript downstream of the cleavage site [62]. As the rate of XRN2 is faster than RNAPII, it hunts down RNAPII like a torpedo to displace RNAPII from chromatin [63]. Transcription has to be terminated properly, as it otherwise can disturb other RNA polymerases or lead to conflicts between transcription and replication [61]. As terminating RNAPII is believed to be recycled for new rounds of transcription [64], failure to terminate can impact the total RNAPII pool, which can further inhibit initiation of new rounds of transcription. Transcription can also be terminated prematurely from the promoter proximal pause site or during productive elongation to limit pervasive transcription [65-67].

Throughout the transcription cycle, RNAPII associates with a great variety of factors to drive RNA production. Emerging results suggest that RNAPII associates with factors of transcription and RNA metabolism through biomolecular condensates [68-72]. These membraneless organelles are formed by spontaneous separation of a homogenous mixture into two co-existing liquid phases, where high levels of proteins and nucleic acids form condensates in a less dense bulk liquid phase [73]. This thermodynamically driven process of liquid-liquid phase separation (LLPS) is driven by weak multivalent interactions between chemical groups or intrinsically disordered regions (IDRs) in proteins and nucleic acids [74]. The low complexity IDRs and repetitive structure of the CTD drives RNAPII to form such biomolecular condensates [68-72]. Studies have shown that hypophosphorylated CTD of RNAPII promotes formation of condensates with the Mediator complex and other transcription initiation factors, while hyperphosphorylated RNAPII CTD is associated with splicing condensates [70-72]. Phosphorylation of the CTD disrupts initiation condensates [72, 75], while 5,6-dichloro-1-β-ribofuranosylbenzimidazole (DRB), which inhibits release into productive elongation [76], blocks the formation of splicing condensates [70]. This suggests

that the phosphorylation status of RNAPII depicts its ability to phase separate with distinct factors involved in transcription. RNA and DNA also harbor domains that enable them to bind to proteins and other molecules of nucleic acids [73]. Long non-coding RNA (lncRNA) is especially associated with biomolecular condensates and has been proposed to drive phase separation as a molecular scaffold [77].

1.3 The DNA damage response

DNA holds the genetic code that makes an organism, and like a recipe it contains the instructions for how to make all the proteins required for an organism to live. Protecting the integrity of the DNA is therefore of great significance and is performed by specialized surveillance systems collectively called the DNA damage response (DDR). This network of signaling pathways recognizes the DNA lesion and initiates the proper cellular signaling cascade to repair the damage and finally protect the genome. The cell possesses many pathways to remodel and repair the DNA. To avoid unnecessary and possibly detrimental changes to the DNA, the repair response needs to be coordinated in time and space, but also adapted to the type of DNA lesion. DNA damage can occur from a great variety of sources, internal and external, leading to different types of lesions. The majority of lesions are single stranded breaks (SSBs) or molecular changes in a base or a nucleotide; however, double stranded breaks (DSBs) also occur [78, 79]. If damaged DNA is not properly repaired it might cause genomic instability, apoptosis or senescence, which can further promote carcinogenesis or premature aging [78-80].

1.3.1 Internal sources of DNA damage

Damage can arise during normal cell-intrinsic processes, including DNA replication, transcription and oxidative stress. The DNA double helix conformation both stabilizes and protects DNA against degradation, metabolic activation and the formation of secondary structures. However, during replication and transcription, the double helix is unwound and opened up; leading to exposed stretches of single-stranded DNA (ssDNA). These structures are more vulnerable to chemical and enzymatic degradation and require the protection of ssDNA binding proteins [81]. Replication forks that stall upon encounter with an obstacle may further collapse and cause DSBs if they are not protected [82, 83]. In addition, both transcription and replication creates supercoiling and subsequently torsional stress as the polymerases move along the DNA [84, 85]. This torsional stress is resolved by DNA topoisomerases, which catalyses controlled breakage of one or both strands of DNA [86, 87]. Any errors that may occur during the relief of torsional stress can cause the DNA to be broken at unwanted sites and stretches of ssDNA can be exposed [88]. Furthermore, incorporation of the wrong base during DNA replication will lead to a mismatch in base pairing [84]. Oxidative stress can also cause DNA damage via reactive oxygen species (ROS). These are natural by-products from oxidative metabolism and inflammation [89], but they can also be generated in response to xenobiotics, cytokines and bacterial invasion [90]. ROS oxidize bases of the DNA and form conversions and mismatches that structurally distort the DNA and can lead to the formation of SSBs [91, 92]. If oxidized bases occur on opposing strands, attempted repair by base excision repair (BER) can lead to the formation of DSBs [93].

1.3.2 External genotoxic agents

External sources to DNA damage are ultraviolet radiation (UV) and ionizing radiation (IR), which cause physical damage to the DNA. DNA damage can also be induced by genotoxic chemical compounds, such as hydroxyurea, camptothecin and aphidicolin. In contrast to physical sources, some chemical compounds do not directly damage the DNA, but rather interfere with replication [94]. A major source of physical damage is UV, which causes the formation of pyrimidine dimers and 6-4 photoproducts in the DNA that can block the progression of replication and transcription [95]. Replication forks stalled at UV-induced bulky lesions lead to the formation of SSBs as repair intermediates. If these intermediates remain unrepaired they can lead to the formation of DSBs upon DNA replication [96]. In addition, UV-induced damage arrests the progression of productively elongating RNAPII [97]. Lesion-stalled RNAPII further initiates transcription-coupled nucleotide excision repair (TC-NER) [15], which causes a global "shutdown" of transcription [98, 99]. If the transcription block is not resolved by repair or bypass, elongating RNAPII is subjected to proteasome-mediated degradation as a "last resort" mechanism [100-102]. While we are regularly exposed to UV from the sun, IR is mostly restricted to medical treatments such as radiotherapy or medical examination by X-ray imaging. However, we are continuously exposed to low amounts of IR from radioactive materials that occur naturally in the environment, as well as from cosmic background radiation [79]. IR is a photon or particle with the ability to turn an atom into an ion by the removal of an electron. DNA damage is induced directly upon the ionization event or from the creation of free radicals. IR can produce a broad spectrum of DNA damage, where the most harmful one is DSBs [103, 104]. It has been estimated that for each DSB, IR produces more than 10 SSBs per cell [105, 106]. A SSB can turn into a DSB if another SSB is located in close proximity on the opposite strand. These two-ended DSBs are repaired mainly by non-homologous end-joining (NHEJ) [107, 108].

1.3.3 Initiating the DNA damage response

The DDR is initiated by specific sensor proteins, which are determined by the type of DNA lesion, as well as the cell cycle phase. Information about the type of damage and where it is located is collected from these sensor proteins and relayed by signal transducers to effector proteins (**Figure 4**). Through signaling cascades, the information is conveyed from protein to protein through different types of post-translational modifications such as phosphorylations, poly(ADP-ribosylations), ubiquitylations etc. The response exerted by the effector proteins involves induction of cell cycle checkpoints, DNA repair, cell death, chromatin remodelling and changes to replisome stability, transcription and energy metabolism [78, 79].

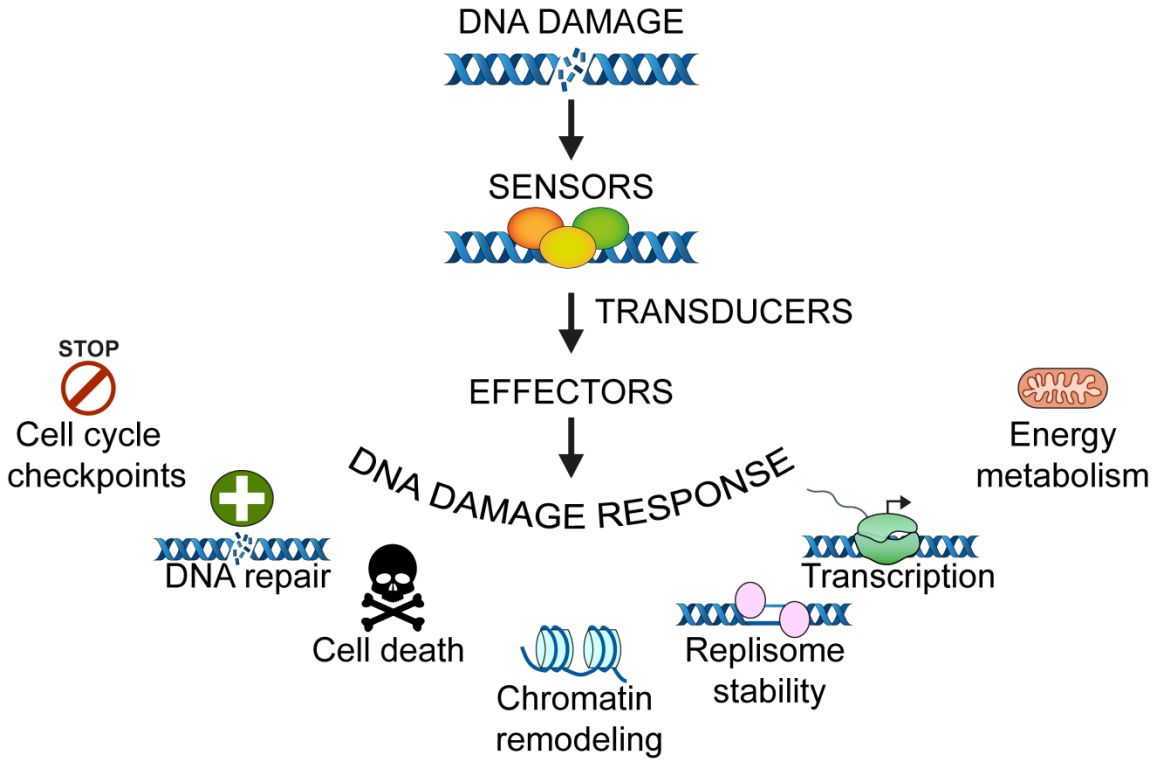

Figure 4: The DNA damage response. The DNA damage response is a network of signaling pathways that aim to repair the lesion and protect the genomic integrity. The response is initiated when sensor proteins detect the DNA damage. Information about the type of DNA lesion and its location is further relayed by signal transducer to effector proteins. The DNA damage response can involve cell cycle checkpoints, DNA repair, cell death, remodeling of chromatin, stabilization of the replisome and changes to transcription and energy metabolism. See main text for references and details. Modified from [79, 109].

The apical mediators of the DDR are Ataxia-telangiectasia Mutated kinase (ATM), Ataxia-telangiectasia and Rad3-related kinase (ATR), and DNA-dependent protein kinase (DNA-PK). These three related kinases are all members of the phosphoinositide-3-kinase-related protein kinase (PIKK) family and share domain architecture and several modes of action [110]. ATM and DNA-PK are activated primarily by DSBs, and facilitate their repair by homologous recombination (HR), via ATM signaling, or by non-homologous end joining (NHEJ), via DNA-PK. While ATM also initiates phosphorylation cascades of proteins involved in other DNA repair pathways [111] and checkpoint activation [110], DNA-PK is mainly involved in DSBs repair by NHEJ [78]. ATR, on the other hand, responds to a much wider range of genotoxic stresses, as it recognizes stretches of ssDNA coated with replication protein A (RPA) via its binding-partner ATRIP. ATR is involved in repair of ssDNA intermediates formed during DNA repair or replication stress [112], but is also critical for DSB repair and checkpoint responses induced by DSBs [113]. Upon activation, these three kinases phosphorylate downstream substrates on their serine and threonine followed by glutamine residues [110]. As many as 700 proteins are substrates for ATM and ATR [114], which reflects the diversity of responses that can be initiated upon detection of DNA damage. Another common feature is that they all require accessory proteins to be recruited

to the site of DNA damage. DNA-PK is recruited by the Ku heterodimer (Ku70/80) [115-117], ATM by the MRN complex (MRE11, RAD50 and NBS1) [117-119] and ATR by ATRIP [117, 120].

PARP1 is considered another damage sensor, and is recruited to the site of DNA damage within seconds. As a member of the Poly (ADP-ribose) polymerases (PAPRs), PARP1 binds to the site of damage to modify the chromatin structure. Here it attaches negatively charged poly (ADP-ribose) (PAR) chains via the process of PARylation [121, 122], which results in chromatin relaxation [123]. PAPR1 is involved in multiple repair pathways, and is activated by both SSBs and DSBs. In addition to sensing DNA damage, it is involved in the efficacy of repair and recruitment of DDR factors, such as ATM, NBS1 and MRE11, where the two latter are components of the MRN complex [123].

RNAPII has been proposed to be involved in detection, repair and signaling following DNA damage. As a damage sensor, RNAPII is believed to act through the process of "recognition by proxy". Notably, RNAPII does not recognize DNA damage directly, but rather its impaired progression signals the presence of an obstacle or DNA lesion and further stimulates the recruitment of repair factors [15-20]. As RNAPII continually scans the genome during productive elongation, in all cell cycle phases except mitosis, it can be considered the ultimate surveyor of genomic integrity. In the presence of bulky DNA damage, such as produced upon UV, RNAPII stalls and recruits central factors of the TC-NER repair pathway [124]. Upon loss of TC-NER, stalling of RNAPII led to increased levels of the stress response protein p53 [125] via a mechanism that depended on ATR and RPA [126]. p53 is considered a "guardian of the genome" and is a major marker of several DDR mechanisms [127]. Activation of p53 upon RNAPII stalling could provide one mechanism of how RNAPII acts as a damage sensor and indicates that RNAPII could sense damage independently of the type of lesion. Supporting this, RNAPII stalled at base insertions or interstrand crosslinks, induced by actinomycin D and psoralen respectively, also caused enhanced p53 levels [126]. As RNAPII has a stable association with the chromatin and stalls upon encounter with several types of DNA damage [128], it can be considered 100-10,000 fold more specific than any other DNA damage sensor [126]. On the other hand, how lesion-stalled RNAPII differs from RNAPII stalled during normal transcription needs to be further explored.

1.3.4 DNA damage repair pathways

A cell experiences tens of thousands of DNA lesions each day [129] and harbours several repair mechanisms to detect these lesions and further promote their repair. Most lesions are repaired by a catalytic signaling cascade involving multiple proteins, while a few are subjected to direct protein-mediated reversal. Small errors, such as single base alterations or lesions that cause helix distortions in short stretches of the DNA, are targeted by mismatch repair (MMR), base excision repair (BER) or nucleotide excision repair (NER) [79]. The latter,

which recognizes lesions that causes helix distortions, can be divided into two sub pathways based on their mechanism of lesion recognition: transcription coupled NER (TC-NER) and global-genome NER (GG-NER). TC-NER acts on lesions that block transcription, which leads to RNAPII stalling, while GG-NER acts independently of transcription [130, 131]. Moreover, interstrand and intrastrand crosslinks or SSBs causes more extensive damage and are repaired by the interstrand crosslink repair pathways (Fanconi repair pathway), NER or the single strand break repair pathway (SSBR), respectively. The most detrimental DNA lesion is DSBs, where the two major repair pathways are non-homologous end-joining (NHEJ) and homologous recombination (HR) [79].

1.3.5 Repair of DNA double stranded breaks

As one of the most lethal forms of DNA damage, DSBs can cause rearrangements of the genome and lead to cell death [132]. The formation of DSBs triggers the phosphorylation of H2AX on S139 (termed γH2AX), which further promotes the assembly of DDR proteins at the break site [78, 133]. DSBs can be observed in the microscope as local accumulations of repair factors in the nucleus, also called foci. γH2AX is a well-known marker of such foci [134], but also 53BP1, RPA, RAD51 and several other repair factors has the ability to form IR-induced foci [78, 135]. During DNA replication, one-ended DSBs spontaneously occur when the replication fork encounters unrepaired DNA lesions, which leads to fork collapse [82, 83]. These one-ended DSBs favor HR mediated repair. Two-ended DSBs produced by IR can be repaired by HR in G2 or S-phases, however, the majority are repaired by NHEJ pathways, [107, 108], consisting of classical-NHEJ (cNHEJ), Polθ-mediated end-joining (TMEJ) and single-strand annealing (SSA). As the most dominant pathway, NHEJ is estimated to repair approximately 80% of IR-induced DSBs [136, 137]. One main difference between the DSB-repair pathways is that HR, TMEJ and SSA require end resection, while resected DNA substrates inhibits cNHEJ [135, 138].

HR is limited to S and G2 phases as it requires CDK1 and CDK2 activity [139-141] and homologous DNA template provided by sister chromatids (**Figure 5**) [135, 142]. Repair is initiated by MRN and CtIP in combination with other nucleases that process the 5’ DNA strand at the lesion to produce a long 3’ ssDNA end. The ssDNA is then applied in the search of a template sequence, followed by resection using the homologous sister chromatid as a template. There are different HR pathways that can finalize the DSB repair, however, they all have in common that the sequence surrounding the DSB is replaced with the homologous DNA template [135, 142]. Alternatively, if resection reveals homologous repetitive sequences flanking the DSB ends, repair might be directed towards SSA, another repair pathway. The single stranded DSB ends are then annealed at the homologous repetitive sequences and the intervening sequence is removed by nucleases. Any resulting nicks or gaps are filled by DNA synthesis and DNA ligases. As SSA results in the deletion of one DNA

repeat and the intervening sequence between the repetitive sequences, it is considered highly mutagenic [142].

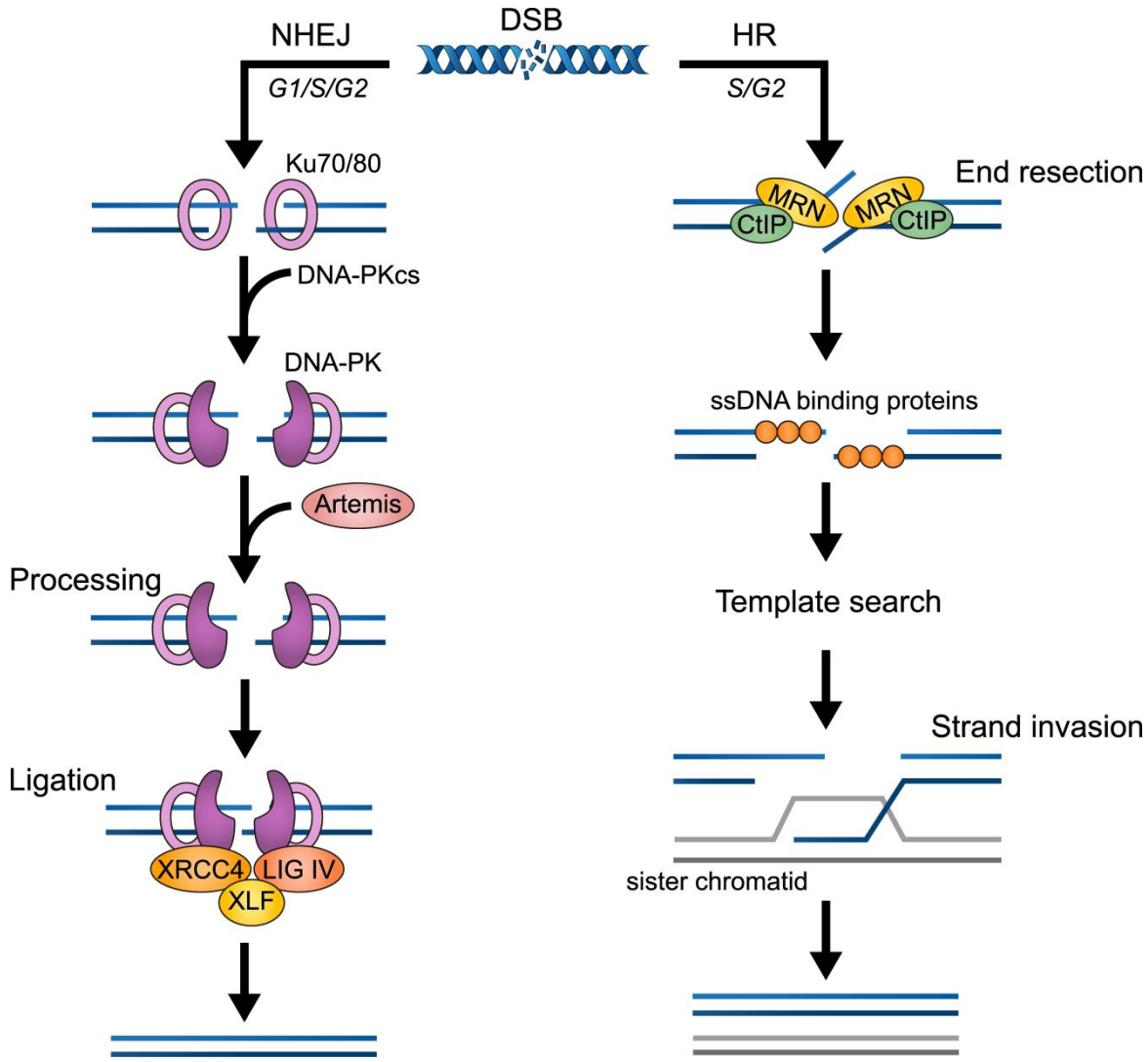

Figure 5: The two major repair pathways of DNA double stranded breaks. Double stranded breaks (DSBs) are mainly repaired by either NHEJ or HR. Pathway choice is largely dependent on the cell cycle stage, as HR is limited to S and G2 phases. As the most dominant pathway, NHEJ is initiated by the recruitment of the Ku70/80 heterodimer to the DSB. DNA-PKcs are then recruited to form the DNA-PK complex, which further promotes direct ligation of the DSB by the XRCC4-Lig IV-XLF complex. Additional processing of the DSB ends prior to ligation is facilitated by enzymes such as Artemis. HR cannot directly ligate the broken ends, and require a homologous DNA template for repair. Recruitment of the MRN complex (MRE11, RAD50 and NBS1) and CtIP promotes 5' end resection, which produces long 3'ss DNA ends that are further applied in the search of a repair template. The single-stranded DNA (ssDNA) is protected and stabilized by ssDNA binding proteins. The sister chromatid is then used as template to replace the sequence surrounding the DSB to facilitate repair. See main text for details and references. Adapted from [135]. Abbreviations: NHEJ, non-homologous end-joining; HR, homologous recombination; Lig IV, Ligase IV.

In contrast to HR and SSA, cNHEJ reseals the broken DNA ends without the need of sequence homology or major end processing. cNHEJ has been suggested to dominate in

G0/G1, however, studies has shown that cNHEJ is active throughout interphase and even predominates in G2 [138, 143, 144]. Upon initiation of the cNHEJ pathway, the Ku70/80 heterodimer is rapidly recruited to the DSB, where it acts as a scaffold for other NHEJ proteins (**Figure 5**). Firstly, Ku70/80 recruits DNA-PKcs (catalytic subunit of DNA-PK) to form the DNA-PK complex. Active DNA-PK causes phosphorylation of several cNHEJ and related repair factors. Direct joining of the DNA ends is performed by the XRCC4-DNA ligase IV-XLF complex. XRCC4 acts to stabilize DNA ligase IV and promotes its activity, while XLF is required for gap filling and aligning the ends prior to ligation [107, 138, 143]. If the ends are aligned and compatible, the cNHEJ factors mentioned are sufficient to directly ligate the DSB. However, non-cohesive ends, such as the more complex DSBs created by IR, cannot be directly ligated and require additional processing enzymes, such as the endonuclease Artemis [107, 138, 143]. Other factors have also been implicated to promote NHEJ [145-155]; however, their role and function in NHEJ are less explored.

TMEJ is more error prone than cNHEJ as it involves insertions and deletions, and has no mechanism in place to ensure that the sequence close to the DSB is restored. This alternative NHEJ pathway is considered to engage if HR or cNHEJ have failed in repair of the DSB. Repair is occasionally facilitated by microhomology structures near the DSB site and requires the polymerase Polθ to directly ligate the broken DNA ends [138, 156]. Exactly which factors are involved in this pathway is unclear, however, the MRN complex [157], PARP1 [158], and CtIP [159] have been implicated in TMEJ-mediated repair. PARP1 has been indicated to aid in the recruitment of Polθ to the broken DNA ends [160]. Microhomology directed annealing of the broken ends leads to the formation of an unrepaired tail, which is removed by nucleases. The gap is then filled by Polθ-mediated DNA synthesis, followed by ligation by either DNA ligase III or I [138, 156].

Pathway choice is largely regulated by the DNA damage sensors: the Ku70/80 heterodimer is recruited to the DSB site within seconds to promote cNHEJ repair, while PARP1 competes with Ku70/80 to direct repair away from cNHEJ by promoting end resection [161]. 53BP1 also participates in the pathway choice as it inhibits end resection and thus promotes cNHEJ [162]. While cNHEJ is active throughout interphase, HR requires CDK activity [139-141] and homologous sequences as template for DNA repair [135, 142] and is thus confined to S and G2 phases. Cell cycle dependent regulation of pathway choice is largely coordinated by 53BP1 and BRCA1. In G1, 53BP1 rapidly recruits RIF1 (RAP1-interacting factor homolog) to protect against BRCA1-mediated end resection [150, 163, 164]. As cells move into S-phase, BRCA1 drives the removal of 53BP1 and promotes end resection and repair by HR [150, 163, 165]. The exact molecular mechanism underlying the choice of DSB repair pathway remains unclear. It has been proposed that RIF1 is gradually detached from 53BP1 and replaced with SCAI (suppressor of cancer cell invasion). SCAI is then believed to inhibit the 53BP1/RIF1-mediated block of end resection to facilitate BRCA1-mediated repair, which may involve resection-dependent NHEJ in G1 and HR in S/G2 [166].

RIF1 may also be inhibited upon recruitment of the SWI2/SNF2 member CSB, which binds RIF1 and remodels chromatin at the DSB site to promote BRCA1 binding [167]. In addition to chromatin structure at the DSB, the complexity of the DNA ends and local transcription status may also influence the choice of repair pathway [168, 169].

1.3.6 The role of RNA polymerase II in repair of DSBs

DSBs can occur within transcriptionally active and inactive regions of the genome. Transcription is emerging as a central factor in the DDR, but its exact role and how it responds to DSBs is incompletely understood. It has been shown that transcription elongation is repressed indirectly by ATM, DNA-PK or PARP1-mediated signaling cascades [170-172]. ATM silences transcription by local and global post-translational modifications to the chromatin, which involves a transition from “active” to “repressive” histone marks. This ATM-mediated silencing may occur over hundreds of kilobases from the DSB site. ATM is believed to stall and maintain RNAPII levels at transcriptional sites away from the DSB [173], while DNA-PK mediates eviction of RNAPII from the DSB site [174]. Removal of RNAPII is obtained by DNA-PK facilitated recruitment of the E3 ubiquitin ligase WWP2, which polyubiquitinates RNAPII for proteasomal degradation [175]. DNA-PK mediated silencing of transcription is local, as adjacent genes remain unaffected, and aims to avoid collisions between RNAPII and the repair machinery [174]. Transcription can also be inhibited upon the formation of DSBs by PARP1-mediated PARylation of RNAPII. The transcription factor NELF-E is recruited to RNAPII in a PARP1-dependent manner, where it inhibits promoter proximal release into gene bodies [176]. Altogether, these mechanisms aim to inhibit transcription to promote DSB repair.

On the other hand, several studies have shown that RNAPII and nascent RNA are necessary for DSB repair in humans, suggesting that transcription could also promote DSB repair [171, 177-180]. It has been shown that DSB ends can act as promoters [177, 179, 181-184] and recruit RNAPII through a MRN complex-mediated mechanism [179, 181]. Factors of the pre-initiation complex have also been shown to be recruited to DSBs [183, 184], supporting that transcription may initiate from the break site. At the site of DSBs, DICER and DROSHA are involved in the formation of small stretches of non-coding RNAs (sncRNA) which are termed DNA-damage response RNAs (DDRNAs) and DSB-induced RNA (diRNA) [178, 180, 185]. The production of such RNA species requires RNAPII-mediated transcription, which proceeds bidirectionally from the break site [179, 186]. Many repair proteins are recruited to the break site by sncRNAs, as their recruitment is inhibited by RNase A [180, 185]. Long non-coding RNA (lncRNA) has also been implicated in DSB repair, as they promote NHEJ and direct the assembly of NHEJ effector proteins [187, 188]. Non-coding RNAs have also been shown to facilitate HR by the formation of DNA:RNA hybrids with resected DNA, which promotes BRCA1 recruitment [182]. Enhanced levels of RNA:DNA hybrids at the DSB sites can be caused by enhanced promoter proximal pausing and premature termination of

transcription [189]. Moreover, RNAPII-generated RNA at the DSB site has been suggested to specifically promote HR [190]. Supporting this, histone modifications associated with elongating RNAPII has been shown to promote end resection and loading of RAD51 and BRCA1, while it inhibited 53BP1 recruitment [168, 191, 192]. However, damage-induced 53BP1 foci have been shown to require active transcription, as treatment with transcription inhibitor α-amanitin or RNAse A prevented their formation [180, 185]. Several cNHEJ factors form a complex with RNAPII and associate with transcribed genes [143, 193]. It has also been proposed that nascent RNA is applied as a template to facilitate error free NHEJ repair [143]. Taken together, these studies reveal that elongating RNAPII responds to DSBs and may be involved in repair either by itself or indirectly through the production of nascent RNA. However, it remains unclear which circumstances that favour retention of RNAPII at the break site and whether its presence promotes HR, NHEJ or both.

1.4 Replication stress

Replication stress commonly refers to a state where the fork progression is slowed or stalled. There are numerous sources that can cause replication stress (**Figure 6**), where one of the most established ones is DNA lesions [112]. As previously mentioned, DNA damage can occur during normal cell-intrinsic processes or be induced by external sources [78]. Replication fork progression can be locked by lesions that causes significant distortions in the DNA, such as the bulky lesions produced by UV irradiation [194]. During DNA repair, single-stranded nicks and gaps are formed as natural intermediates, which can also contribute to replication stress. Single-stranded nicks and gaps can also form upon release of topological stress by topoisomerases during DNA replication [84]. In addition, replication may stall upon encounter with DNA sequences that are too difficult to replicate, e.g. secondary DNA structures [84, 195]. Replication is also actively blocked in regions such as ribosomal DNA [196]. Impaired fork progression is commonly associated with the formation of stretches of ssDNA. Upon stalling of the DNA polymerase, the replicative helicase will continue to unwind the parental DNA, leading to the formation of ssDNA. If these stretches of ssDNA persist, they are bound by RPA, which initiates the replication stress response. In most cases this response involves the protein kinase ATR [84].

There are numerous factors involved in the process of DNA replication, including the proteins that constitute the replication machinery, free nucleotides, histones and histone chaperones. As the supply of many of these factors can be limited, replication is strictly regulated. If replication is not regulated properly, i.e. if too many origins fire simultaneously, then replication will stall as a consequence of depleted nucleotide pools [84, 197]. The nucleotide pool can also be disturbed by external sources, such as the chemical compound hydroxyurea. Other replication inhibitors form DNA protein adducts (camptothecin), inhibit DNA polymerases (aphidicolin) or interact with DNA to cause DNA crosslinks and bulky lesions (cisplatin) [94]. Fork progression is then blocked upon encounter with these damaged DNA structures or by interfered function of proteins directly involved in replication. Another factor that can interfere with fork progression is transcription, both indirectly through the formation of e.g. secondary DNA structures or directly upon transcription-replication conflicts [84].

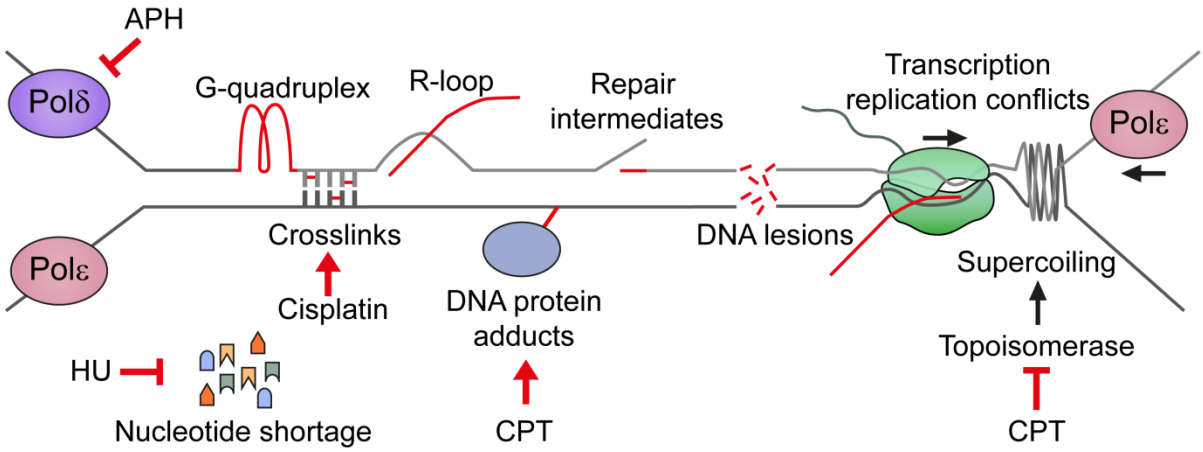

Figure 6: Sources of replication stress. Replication stress is caused by any event that stalls or slows the progression of the replication fork. DNA damage is a common source of replication stress, where different types of lesions in the DNA can threaten the genomic integrity if left unrepaired. During DNA repair, natural intermediates, such as single-stranded nick and gaps can also cause replication stress. Replication inhibitors interfere with normal DNA replication by e.g. inducing nucleotide shortage (HU), inhibition of DNA polymerases (APH), formation of crosslinks and bulky lesions (cisplatin) or by topological stress or formation of DNA protein adducts (CPT). Transcription can indirectly interfere with DNA replication via the formation of R-loops, supercoiling or secondary structures, such as G-quadruplexes, or directly upon conflicts between the transcription and replication machineries. RNA polymerase II is shown as the green protein and nascent RNA is shown in red. See main text for details and references. Adapted from [84, 198]. Abbreviations: HU, hydroxyurea; APH, aphidicolin; CPT, camptothecin; Pol ε/δ, DNA polymerase ε/δ

1.4.1 Transcription replication conflicts

A major threat to genomic stability is conflicts between the transcription and replication machineries (T-R conflicts). As RNA and DNA polymerases share the same template, they may interfere with each other. This is mostly avoided as DNA replication is restricted to S-phase, which allows for uninterrupted transcription in the other cell cycle phases. In S-phase, transcription and replication are spatially separated as they occur in distinct territories in the nucleus [199]. Despite the regulation of these processes in both space and time, T-R conflicts will occasionally occur [5]. Over the past two decades, numerous studies have provided evidence for transcription as a major source of replication stress and genomic instability, which are hallmarks of cancer [5, 6]. Transcription can cause replication stress and genomic instability through e.g. the formation of nucleic acid structures such as R-loops [200, 201]. Other sources of genomic instability induced by transcription are point mutations, transcription associated recombination (TAR) and chromatin rearrangements, where the two latter are dependent on replication [202, 203]. Identifying the mechanisms underlying T-R conflicts and how they are resolved is therefore of great significance.

Directional and temporal coordination of transcription vs. replication

The polymerases of transcription and replication both operate in the 3'-5' direction, which causes replication and transcription to encounter co-directionally. As the RNA polymerase holoenzyme embraces both strands of DNA, transcription can also face replication in a head-on orientation (**Figure 7**). Regardless of the orientation of the encounter, the replisome cannot move past an elongating RNA polymerase [85, 204]. Both orientations will thus lead to a conflict, however, numerous studies performed in bacteria and eukaryotes have shown that the head-on orientation is the most detrimental [200, 202, 205, 206]. Co-directional encounters may cause less severe consequences, as they have been shown in yeast to be resolved by removal or bypass of RNAPII [207, 208]. Of note, head-on encounters have also been proposed to be resolved by displacement of RNAPII from the DNA (in yeast) [209]. Nevertheless, it is unclear whether the replication and transcription machinery actually make contact, as they might cause changes to chromatin and DNA structure that halt their progression prior to a physical encounter.

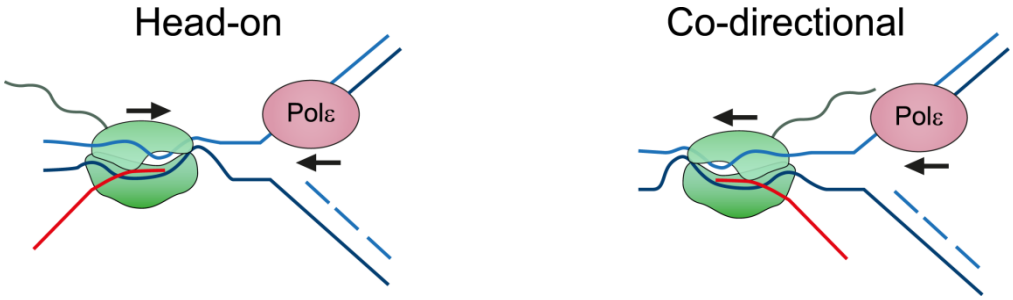

Figure 7: Directional orientation of transcription and replication conflicts. As the RNA polymerase embraces both strands of the DNA, conflicts between the transcription and replication machineries can occur co-directionally or head-on. If RNAPII progresses in the opposite direction than the replication fork, they will encounter in the head-on orientation, while progression in the same direction would lead to co-directional conflicts. RNAPII is shown as the protein in green, while the Pol ε is shown as the pink protein. Newly synthesized RNA is illustrated in red. See main text for details and references. Abbreviations: RNAPII, RNA polymerase II; Pol ε, DNA polymerase ε

In bacteria, genes are often co-oriented so that they can be transcribed in the same direction as the DNA is replicated [210, 211]. Highly transcribed ribosomal DNA (rDNA) in *Saccharomyces cerevisiae* have replication fork barriers that block the progression of replication forks, which consequently prevents encounters with the RNA polymerase [212]. In mammalian cells, replication and transcription seems temporally separated [213]. Genes that replicate early show increased transcription late in S-phase and vice versa [214]. However, this preventative action is limited in certain areas of the genome. For instance, long genes require several cycles to complete transcription and are associated with common fragile sites (CFS), which contain sequences that can impair fork progression. T-R conflicts in long genes thus seems inevitable [215]. Another type of fragile sites, called early-replicated fragile sites (ERFS), is located in highly transcribed genes near replication origins. Conflicts in close proximity to these ERFS can potentially account for their genomic instability [216, 217].

However, the mechanism of how T-R conflicts contribute to the genomic instability of these fragile sites is incompletely understood.

Transcription-associated structures that impact replication

There are several structures generated during transcription that have the potential to halt fork progression (**Figure 8**). For instance, unwinding of the DNA to enable RNA synthesis creates positive supercoiling ahead of the RNA polymerase and negative supercoiling behind [85]. Since DNA is often anchored and therefore not able to resolve such supercoiling by diffusion [218], the torsional stress needs to be resolved by other mechanisms. This is performed by specialized enzymes, DNA topoisomerases, that catalyses breakage of the DNA backbone at either single or both strands to disentangle the torsional stress [86, 87]. Studies in both yeast and humans have shown that topoisomerases are crucial for preventing T-R conflicts [219, 220]. Depletion of topoisomerases leads to accumulation of DNA damage [219] and analyses of replication fork speed by DNA combing revealed that replication stalls upon depletion of topoisomerase type I [220]. Negative supercoiling generated behind the RNA polymerase can lead to the formation of secondary DNA structures, such as hairpins, triplex DNA and G-quadruplexes. These non-B DNA structures have been shown to stall replication forks [221]. In addition, transcription can lead to the formation of RNA-DNA hybrids, also known as R-loops, which can interfere with replication fork progression [85, 222, 223]. As RNA polymerase transcribes the DNA, nascent RNA can reanneal with one of the DNA strands behind the polymerase, causing the non-template strand to displace as single stranded DNA. R-loops occur naturally both during replication and transcription, however, they have also been shown to form aberrantly and can threaten genomic stability [224]. Interestingly, the replisome is involved in regulating the formation of R-loops by reducing their formation in the co-directional orientation, while it promotes those oriented head-on. Deregulated origin firing and replication stress contributes to enhanced head-on T-R conflicts, which leads to the formation of genome-destabilizing R-loops [200]. Both secondary structures and co-transcriptional R-loops can worsen T-R conflicts by creating an additional barrier for the replication fork.

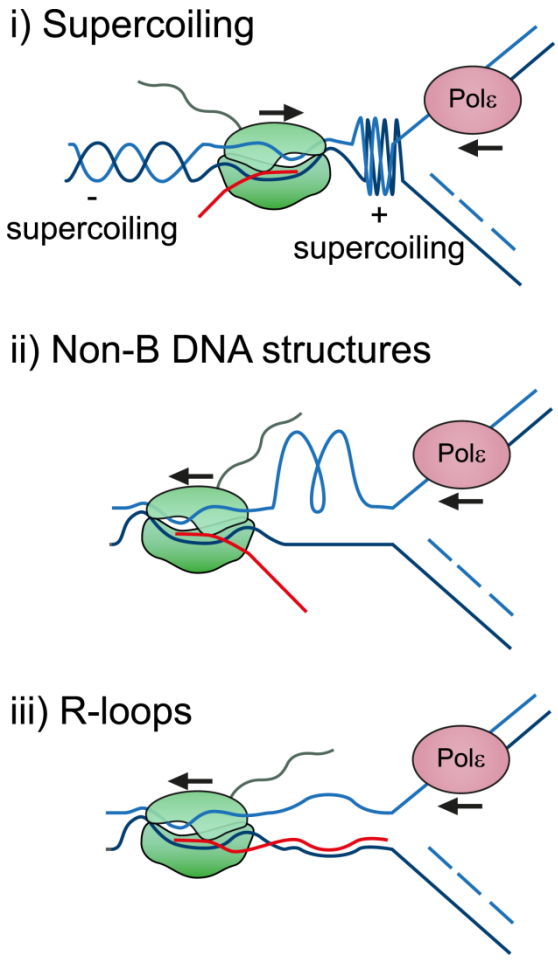

Figure 8: Transcription-associated structures that affect the occurrence of T-R conflicts. i) When RNAPII and the replication fork encounter head-on it can lead to an accumulation of positive (+) DNA supercoiling between them, which would cause the replication fork to stall. ii) Negative (-) DNA supercoiling generated behind the RNAPII can partially unwind to form non-B DNA structures. iii) RNA:DNA hybrids, such as R:loops, are other non-B DNA structures that can block the progression of the replication fork. R-loops are formed when the nascent RNA reanneal to one of the DNA strands. The green protein represents RNAPII, while the Pol ε is shown in pink. Newly synthesized RNA is illustrated in red. See main text for references and details. Adapted from [85]. Abbreviations: RNAPII, RNA polymerase II; Pol ε, DNA polymerase ε.

Destabilization of RNAPII to prevent T-R conflicts

RNA polymerases have an inherent proofreading mechanism, which involves reversed progression and enzymatic removal of the last incorporated nucleotide. This enables the elongating RNAP to restart transcription when progression is blocked by an obstacle or naturally paused during regulation of transcription and RNA metabolism [225]. As the backtracked RNAP is very stable and can potentially block replication fork progression [225], the cell can apply the anti-backtracking factors TFIIS [226, 227] and GreA/GreB [228] to rescue backtracked RNAP and avoid collisions with the replication machinery (**Figure 9**). In addition, destabilized RNAP upon encounter with the replication machinery likely does not pose the same threat to replication progression. Indeed, mutations that reduced the stability of RNAP in transcription complexes inhibited the occurrence of T-R conflicts [229]. T-R conflicts can be resolved by the removal of RNAP from DNA, as shown in bacteria [209]. Upon encounter with DNA lesions, stalled RNAPII is removed by TC-NER or targeted for degradation via a "last resort" pathway, which involves poly-ubiquitylation followed by proteasome-mediated degradation [100, 101]. At the site of conflict, stalled RNAPII has been proposed to be degraded through a mechanism involving the INO80 chromatin remodelling complex [230]. However, the exact mechanism of how RNAPII is targeted for degradation is unclear. Phosphorylation of the CTD has been shown to regulate RNAPII degradation, but there is no clear correlation between the phosphorylation status and whether it promotes degradation or not [231-233]. RNAPII stalling and/or backtracking can be reduced by factors that regulate the transcription rate. One such regulatory factor is the human helicase RECQL5, which has been shown to slow the transcription rate and suppress stalling during transcription to prevent T-R conflicts [234]. RECQL5 is involved is several preventative mechanisms, including inhibition of RNA:DNA hybrid formation. R-loop resolution and proper termination of transcription have been shown to be important in preventing T-R conflicts. In line with this, loss of transcription termination factors, such as the Rho helicase [235] or XRN2 [236] caused replication fork arrest and the formation of DSBs. All these co-transcriptional mechanisms aim to remove the threat posed by stalled RNAP to avoid collisions with the replisome.

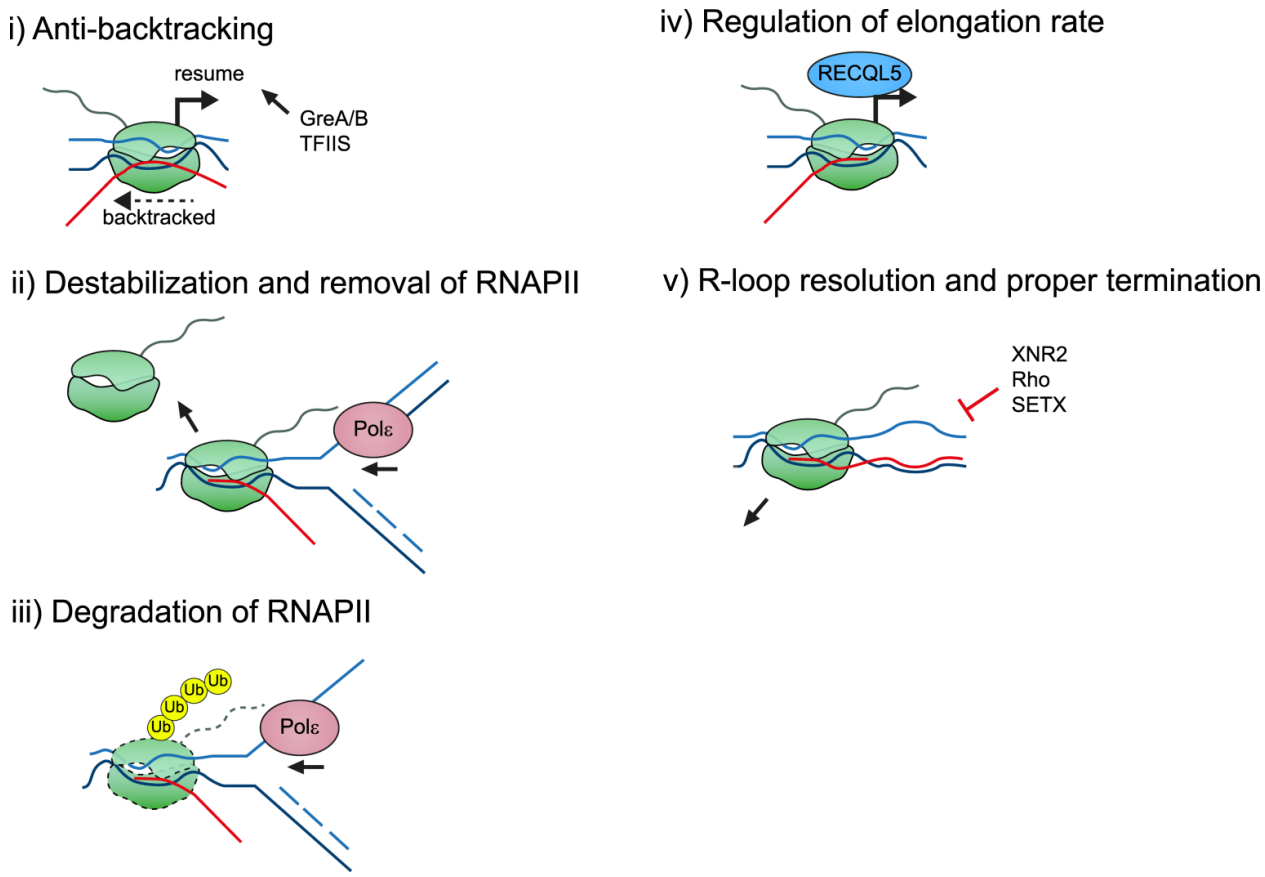

Figure 9: Co-transcriptional mechanisms that act to prevent T-R conflicts. i) Paused RNAPII can be resolved by backtracking, which involves reversed progression into a stable conformation. Anti-backtracking factors, such as TFIIS and GreA/GreB, rescue the backtracked RNAPII to avoid collisions with the replication fork. ii) T-R conflicts are less likely to occur if RNAPII is destabilized upon encounter with the replisome. There are several mechanisms have been proposed to facilitate RNAPII removal from the DNA to suppress T-R conflicts. iii) RNAPII has also been shown to be polyubiquitinated, followed by proteasome-mediated degradation to allow passage of the replisome. iv) Factors that regulate the transcription rate, such as RECQL5, have been shown to suppress T-R conflicts. v) R-loop resolution and proper termination of transcription can also prevent T-R conflicts, and involves factors such as XRN2, Rho and SETX. Nascent RNA is shown in red, while the green and pink proteins represent RNAPII and Pol ε, respectively. See main text for details and references. Figure adapted from [204]. Abbreviations: T-R conflicts, transcription-replication conflicts; RNAPII, RNA polymerase II; Pol ε, DNA polymerase ε; XRN2, 5'-3' exoribonuclease 2, SETX, senataxin

Replication-associated mechanisms to prevent T-R conflicts

As there are co-transcriptional mechanisms that act to prevent T-R conflicts, there are also several replication-associated mechanisms that participate in overcoming such conflicts. In eukaryotic cells, the ATR-mediated S-phase checkpoint resolves T-R conflicts as it promotes release of torsional stress [237], regulates origin firing and fork progression [112], and promotes RNAPII removal [230]. When a replication fork is stalled by transcription complexes, DNA synthesis can resume by several mechanisms. As previously mentioned, a dormant origin in close proximity to the stalled replication fork can be fired to ensure complete DNA synthesis [25]. If the replication fork is persistently stalled, resolution of

topological stress or fork remodelling can promote fork reversal. Once the conflict is resolved, the reversed fork can restart DNA synthesis. However, if the transcription block is not resolved, it can lead to fork breakage and the formation of DSBs or ssDNA gap, which will activate repair mechanisms, such as BIR and HR, to ultimately resolve the T-R conflict [202-204, 238]. Moreover, a recent study proposed that fork breakage triggered by T-R conflicts can be prevented by RAD51-mediated protection of the replication fork [239].

Situations with enhanced T-R conflicts

Factors that alter the activity of transcription or replication increase the risk of their interference. Overexpression of oncogenes and aberrant growth signals causes perturbed replication and deregulated transcriptional activity, which may subsequently lead to T-R conflicts [8, 240]. Replication initiation is strictly regulated by cell cycle and checkpoint signaling pathways, where the timing of origin firing is controlled by the activity of CDK2 and CDK1 in complex with Cyclin E or Cyclin A [21, 22]. Overexpression of the Cyclin E oncogene occurs in a variety of cancers, and is associated with increased origin firing, impaired replication fork progression and DNA damage. Such uncontrolled replication can affect transcription through T-R conflicts. As both CDK and transcription inhibitors were able to rescue the replication phenotype of Cyclin E-overexpressing cells [240], this supports that enhanced origin firing causes more T-R conflicts. Likewise, enhanced transcription may lead to replication effects due to T-R conflicts. Hypertranscription is a trait of many cancers [10], and the MYC oncogene is considered a major driver of hypertranscription [241]. Another oncogene, $HRAS^{V12}$, alters the expression of general transcription factors to enhance the transcriptional activity [8]. This hypertranscription subsequently led to decreased replication fork speed, which was rescued by treatment with transcription inhibitors. T-R conflicts might thus contribute to the oncogene-induced replication stress based on the level of transcription in the regions involved [204].

1.5 Main proteins in the study

1.5.1 PP1

Reversible protein phosphorylation is a main post-translational regulatory mechanism, where phosphate groups are incorporated by kinases and removed by phosphatases [242]. The phosphoprotein phosphatases (PPP) is a serine/threonine-specific family, where Protein Phosphatase 1 (PP1) and 2A (PP2A) account for most of the dephosphorylation events in the cell. As one of the most abundant phosphatases in the cell, PP1 is involved in numerous cellular processes ranging from intermediary metabolism to apoptosis [242, 243]. In mammals, three genes encode the PP1 catalytic isoforms: PP1α, PP1β/δ and PP1γ [244]. The catalytic subunit of PP1 is constructed in a holoenzyme with one or two regulatory subunits and/or targeting subunits. The regulatory subunits determine the catalytic activity and the subcellular localization of the PP1 holoenzyme. PP1 also require a regulatory subunit to obtain specificity as it does not recognize a consensus sequence on their substrates [243, 245].

Nearly 200 PP1-interacting proteins (PIPs) have been identified [243, 246, 247]. Most PIPs can interact with all the PP1 isoforms, while only a few bind to one specific PP1 isoform. The formation of the PP1 holoenzyme relies mainly on an interaction through the RvxF binding motif [243, 246, 247]. As the motif is located away from the catalytic site, the PP1-PIP interaction does not interfere with the PP1 activity. The PP1 binding code is conserved during eukaryotic evolution and is highly specific, as none of the PIPs can bind other members of the PPP family. PIPs compete with each other to bind PP1, however, as there are other PP1 docking motifs than the RvxF they can also bind to the same PP1 molecule. The binding code is highly adaptive as the affinity of the docking motifs is affected by degeneracy and regulatory mechanisms. As the level of PIPs exceeds the amount of PP1 molecules, PP1 is never in a free state where it might dephosphorylate substrates uncontrolled [243, 245].

1.5.2 PNUTS

In the 1990s, PP1 Nuclear Targeting Subunit (PNUTS), also known as PPP1R10, p99 or CAT53, was identified as a regulatory subunit of PP1 [248, 249]. PNUTS, as most PIPs, interacts with PP1 through the RvxF motif [250]. As a RNA-binding protein, PNUTS targets PP1 to specific complexes associated with RNA in the nucleus [250]. Its expression occurs throughout the cell cycle and it has been shown to dissociate from chromatin in mitosis [248]. PNUTS has been proposed to act by inhibiting PP1 activity towards specific substrates, such as pRb and p53 [251-254]. Another substrate of PNUTS is the oncoprotein MYC, where PNUTS-PP1 dephosphorylates MYC to regulate its stability and/or activity [255]. Previous work by our group demonstrated that PNUTS was rapidly and transiently recruited to sites of DNA damage [256], suggesting a role in the DDR. It was also shown that PNUTS depletion

enhanced the G2 checkpoint both in the presence and absence of IR [256]. Normal regulation of the G2 checkpoint was restored upon PNUTS overexpression. In addition, PNUTS depleted cells showed prolonged IR-induced γH2AX, 53BP1 and Rad51 foci at 24h and were hypersensitive to IR-induced cell death [256]. PNUTS interacts with the repair factors Ku70/80 [257] and PARP1, where the latter has been shown to require PNUTS for its recruitment to sites of DNA damage [258]. In line with a role in the DDR, inhibition of PNUTS led to enhanced levels of endogenous DNA damage [256]. It has also been proposed that PNUTS associates with the DNA-PK complex to promote DNA-PK autophosphorylation and activation, which is considered to mediate repair by NHEJ [257].

The only established substrate of PNUTS-PP1 is pRNAPII S5 [259], and depletion of PNUTS causes hyperphosphorylation of the RNAPII CTD [17, 260]. Work by our group showed that PNUTS suppresses ATR signaling via its role in pRNAPII S5 dephosphorylation [17]. As ATR activity is involved in coordinating cell cycle checkpoint, DNA repair and cell death, this contributes to the variety of cellular processes linked to the function of PNUTS [17]. Its ability to bind RNAPII [261] and other factors involved in transcription [262] and RNA processing [263, 264] links PNUTS to the regulation of the transcription cycle. In line with this, a recent study identified PNUTS as a suppressor of the Kaposi's sarcoma-associated herpesvirus (KSHV), which was likely mediated by repressing RNAPII elongation at promoter proximal regions [265]. During transcription elongation, PNUTS-PP1 has been proposed to regulate elongation speed by promoting dephosphorylation of the elongation factor Spt5. Depletion of PNUTS thus accelerates transcription speed and causes distal termination [266]. PNUTS also interacts with termination factors [263, 267], and cells depleted of PNUTS exhibit termination defects [267]. In addition, PNUTS is associated with the splicing machinery, where it forms a trimer with NUAK1 and PP1 to regulate spliceosome activity [264]. Together with Tox4 and WDR82, PNUTS has been shown to form a stable multimeric complex (PTW-PP1 complex) [259]. WDR82 has also been shown to interact with pRNAPII S5 [259, 268, 269], and will be further explored in section 1.5.3. This PTW-PP1 complex has been suggested to regulate chromatin structure and cell cycle progression upon transition into interphase [259]. The role of TOX4 in gene regulation has for long been unclear, however, a recent study proposed a function in promoter proximal pausing and possibly in recycling and re-initiation of RNAPII [270].

In pancreatic and cervical cancer, high expression of PNUTS is considered a positive prognostic marker [271-273]. On the other hand, it has been proposed that PNUTS functions as a proto-oncogene by localizing PTEN to the nucleus in an inactive state [274]. PTEN promotes apoptosis and regulates cell growth [275], and depletion of PNUTS has been shown to cause enhanced apoptosis [274]. As PNUTS is overexpressed in certain cancers, it might contribute to the tumorigenecity of these cancers by inactivating PTEN. In addition, MYC is deregulated in numerous cancers [276], understanding the regulatory axis of PNUTS-MYC, and how it can be implemented in cancer treatment, is thus of great importance.

1.5.3 WDR82

In mammals, WDR82 is a regulatory subunit of the SETD1A/B histone H3-lysine 4 methyltransferase complexes. WDR82 directs and binds SET1 complexes to the transcriptional start sites of active genes by interacting with the SETD1A RNA recognition motif and pRNAPII S5 [268, 277, 278]. Its function as a docking protein is mediated by the seven WD40 domains [259]. These WD40 repeats have a blade-like structure, which together forms a β-propeller shaped platform that enables interaction with other proteins [279, 280].

The yeast homolog of WDR82, Swd2, is a component of two distinct complexes: the SET1/COMPASS methyltransferase and the polyadenylation and cleavage subcomplex APT (associated with Pta1). Methylation of histone 3 on lysine 4 (H3K4me3) by the SET1 methyltransferase is associated with promoter proximal regions and transcription termination at the 3'-end [259, 281-283]. It has been proposed that Swd2 requires PAF1c for recruitment of the SET1/COMPASS methyltransferase to pRNAPII S5 [284]. However, in humans, WDR82 directly binds to pRNAPII S5 and thus mediates the interaction between RNAPII and SET1A/B [268]. As for Swd2, WDR82 also has been implicated in transcription termination. Depletion of WDR82 in mammalian cells caused enhanced pervasive transcription of non-coding RNA [267]. WDR82 recognizes initiating and early elongating RNAPII, where it forms complexes with SET1A/B and PNUTS-PP1 [259, 267] However, the functional output of linking the activity of these two complexes remains unknown. The SET1 complex has been shown to be involved in DNA repair [285, 286], where H3K4 methylation has been proposed to promote recruitment of the repair factor RIF1 to DSBs and suppress end-resection [285]. WDR82 has also been implicated in DNA replication, transcription and DNA repair via its association with the DDB1-Cul4 ubiquitin ligase [287], which ubiquitinates proteins in a broad spectrum of cellular processes [288]. Together with many associated factors of the DDB1-Cul4 ubiquitin ligase (DCAFs), WDR82 binds the ligase via a "WDXR" motif [287] to mediate substrate specificity [288]. WDR82 has also been proposed be involved in the regulation of divergent antisense transcription [289, 290]. Together with ZC3H4 and CK2, WDR82 forms the ZWC complex, which facilitates suppression of antisense transcription by phosphorylating the N-terminal domain of SPT5 [290].

H3K4 methylation and WDR82 are associated with tumour progression. Low expression of both H3K4 and WR82 are associated with poor prognosis in colorectal cancer [291]. Overexpression of WDR82 is considered a favourable prognostic marker in pancreatic cancer and is associated with higher survival [271-273].

1.5.4 CDC73

CDC73, also called Parafibromin, is a subunit of the PAF1c transcription elongation complex, which also includes WDR61, PAF1, LEO1 and CTR9 in humans [292-294]. The recruitment of PAF1c to chromatin is promoted by CDC73 [295] and is additionally stimulated by Spt5 and the activity of the CDKs Bur1 and Kin28, which phosphorylates RNAPII CTD. CDC73 binds to RNAPII directly [296], and the CDC73–phospho-CTD interaction has been shown to be stimulated by phosphorylation on S5 together with either S2 or S7 [297]. Work by our group showed that binding of CDC73 to RNAPII CTD was enhanced by hyperphosphorylated pRNAPII S5 upon PNUTS depletion [17]. In addition, many of the PAF1 components, including CDC73, have been shown to interact with PNUTS [17, 298]. Notably, as for RNAPII, CDC73 has also shown the ability to phase separate [299], however, the importance for its function is still unknown.

Via its interaction with RNAPII, PAF1c regulates different steps of transcription, including promoter-proximal pausing, transcription elongation, histone modifications and mRNA processing. CDC73 has been shown to regulate transcription elongation and 3'mRNA processing [300, 301], as well as promote release from promoter proximal pausing, via its association with the PAF1c [55, 56]. The recruitment of PAF1c by P-TEFb has been suggested to facilitate the release of NELF, as PAF1c and NELF compete for RNAPII binding [58]. PAF1c is also involved in regulating histone modifications [302], as it promotes monoubiquitinylation of H2B and trimethylation of H3K4 via the recruitment of the SET1/COMPASS complex [284, 303, 304]. In yeast, PAF1c has been shown to suppress cryptic transcription [305]. Moreover, PAF1c targets stalled RNAPII for E3 ligase mediated ubiquitylation by facilitating RNAPII CTD phosphorylation by CDK12 [306]. PAF1c has also been proposed to facilitate the removal of RNAPII via its association with INO80 and the checkpoint sensor ATR-ATRIP [230]. This might suggest a role for PAF1c in preventing replication stress and DNA damage, as stalled RNAPII poses a major threat to genomic integrity [6]. Supporting this, CDC73 has been shown to induce local decondensation of chromatin at the break site, via its interaction with SCF/Cullin and INO80/NuA4 chromatin-remodeling complexes, which has been proposed to promote HR [304]. Depletion of CDC73 was found to delay DNA replication and enhance the accumulation of transcription dependent DSBs [307]. Loss of PAF1 components have also been proposed to impair recovery of transcription after UV irradiation, however, PAF1 is not considered to be directly involved in TC-NER [308]. Work by our group showed that CDC73 was required for the enhanced ATR signaling upon PNUTS depletion [17]. Altogether, this demonstrates the versatile functions of CDC73 and the PAF1c.

CDC73 is a tumor suppressor, where low levels of CDC73 causes cellular senescence in cancer cells [309]. Its role as a tumor suppressor has been proposed to be mediated by inhibition of Cyclin D1 and *c-myc*. On the other hand, CDC73 have also been demonstrated to have an oncogenic function by activating Wnt signaling, which is involved in cell growth

and differentiation [310]. *HRPT2*, the gene that encodes CDC73, is inactively mutated in hyperparathyroidism-jaw tumor syndrome [311]. CDC73 mutations are associated with numerous cancers, including carcinomas of the breast [312], renal [313], parathyroid [314], and gastric [315] tissue. Both low and high expression levels of CDC73 have been observed in cancers [316, 317].

2 Aims of study

Overall aim of this work was to explore the interplay between the transcription machinery and the responses to DNA damage and replication stress.

i. In paper I we aimed to further elucidate the replication phenotype seen after PNUTS depletion and to address whether PNUTS-PP1s role in dephosphorylation of RNAPII CTD was interconnected with its role in DNA replication. We also aimed to identify PNUTS interactors that might be involved in this process.

ii. In paper II we wanted to optimize and validate our flow cytometry technique from paper I to detect RNAPII levels on chromatin in individual phases of the cell cycle. With this new technique, we aimed to explore how RNAPII, pRNAPII S5 and pRNAPII S2 levels on chromatin were affected by UV irradiation throughout the cell cycle.

iii. The aim of paper III was to understand how the phosphorylated CTD of RNAPII influences DSB repair, and whether its involvement was dependent on association with RNA or RNAPII CTD-interacting factors

3 Summary of papers

3.1 Paper I

WDR82/PNUTS-PP1 prevents transcription-replication conflicts by promoting RNA polymerase II degradation on chromatin

Previous work by the group showed that PNUTS depletion reduced 5-ethynyl-2'-deoxyuridine (EdU) incorporation and caused cells to accumulate in S-phase [17], suggesting that PNUTS was required for normal DNA replication. The replication effects seen after PNUTS depletion were further explored in paper I, where we observed reduced replication fork speed and slower recovery from thymidine-induced replication block after PNUTS depletion compared to control. The replication phenotype was further characterized as PP1 dependent and verified as PNUTS depletion specific as expression of siRNA resistant mouse PNUTS rescued the phenotype. To find additional factors involved in PNUTS-mediated regulation of replication, we identified PNUTS interactors by SILAC-IP. From the hits, WDR82 was of particular interest as it binds the only established substrate of PNUTS, pRNAPII S5 [259, 268, 269]. Interestingly, WDR82 depletion elicited similar replication phenotype as PNUTS depletion. WDR82 was also shown to facilitate dephosphorylation of pRNAPII S5 by PNUTS-PP1, as WDR82 depletion caused pRNAPII S5 hyperphosphorylation in cell lysates, similarly as for PNUTS depletion. We hypothesized that defective pRNAPII S5 dephosphorylation after depletion of PNUTS/WDR82 altered RNAPII dynamics. To address this, RNAPII levels on chromatin were measured in pre-extracted cells by either western blotting or flow cytometry analysis. Both techniques demonstrated a more stable pRNAPII S5 fraction on chromatin after depletion of PNUTS/WDR82 compared to control cells. We further identified the PAF1c component CDC73, which binds the phosphorylated CTD (phospho-CTD) [297], as necessary for the suppression of replication and the enhanced chromatin retention of RNAPII seen after PNUTS depletion. Next, we noticed that when RNAPII levels on chromatin were reduced after treatment with the transcription inhibitor THZ1, there was not a corresponding increase in soluble RNAPII, suggesting that RNAPII was degraded. We speculated that in the absence of WDR82/PNUTS, CDC73 binding to hyperphosphorylated RNAPII on chromatin was prolonged, where CDC73 shielded RNAPII from degradation. The potential role of PNUTS and WDR82 in promoting RNAPII degradation was addressed with the proteasome inhibitor MG132. Indeed, inhibition of RNAPII degradation greatly enhanced RNAPII chromatin residence time in control cells but less so in cells depleted for PNUTS/WDR82. As enhanced RNAPII retention on chromatin would interfere with replication fork progression, we wondered if the replication phenotype seen after PNUTS/WDR82 depletion could be caused by transcription-replication conflicts (T-R conflicts). Proximity ligation assay revealed increased proximity between RNAPII and the replication component PCNA after depletion of PNUTS. Furthermore, replication fork speed was partially rescued in cells depleted with PNUTS/WDR82 upon treatment with THZ1.

In this paper we provide new insight on how T-R conflicts can be prevented. We propose a model where the dynamic state of RNAPII is controlled by WDR82/PNUTS-PP1 dephosphorylation of RNAPII CTD and association with the phospho-CTD binding protein CDC73. In the absence of proper RNAPII CTD dephosphorylation, such as in the case of PNUTS/WDR82 depletion, CDC73 will continue to bind the phospho-CTD and protect it from degradation. The resulting increase in RNAPII chromatin residence time will promote T-R conflicts. Controlling the CTD phosphorylation status, and thereby maintaining RNAPII in a dynamic state, is thus essential to suppress T-R conflicts.

3.2 Paper II

A novel, rapid and sensitive flow cytometry method reveals degradation of promoter proximal paused RNAPII in the presence and absence of UV

The flow cytometry method from paper I was further optimized and additionally developed to accurately depict RNAPII levels on chromatin in individual phases of the cell cycle. We were able to detect gradually increasing levels of RNAPII throughout the cell cycle from G1 to G2 phase, which was as expected as cells grow and the DNA is duplicated. Based on our results we concluded that our novel flow cytometry method could be used to accurately measure RNAPII levels on chromatin in individual phases of the cell cycle.

Ultraviolet radiation (UV) induces bulky DNA damage that causes arrest of elongating RNAPII [97] and further targets RNAPII for proteasomal degradation [102]. With our novel flow cytometry technique we were able to validate RNAPII degradation at 2h after UV; however, we also discovered that RNAPII levels were actually enhanced at earlier time points. It was specifically the promoter proximal paused form of RNAPII, measured by pRNAPII S5 levels, that was increased. Enhanced promoter proximal pausing correlates with more initiation, suggesting that enhanced initiation is an early response after UV. Moreover, with the proteasome inhibitor MG132, we revealed that elongating RNAPII (pRNAPII S2) was less degraded in S phase after UV, in line with TC-NER specific effects in replicating cells. Interestingly, MG132 enhanced pRNAPII S5 levels both with and without UV, while less so for pRNAPII S2, suggesting that the promoter proximal form of RNAPII was degraded during unperturbed conditions and after UV. These results were unanticipated as elongating RNAPII has been considered to be specifically degraded after UV and promoter proximal paused RNAPII was thought to avoid degradation both in the presence and absence of UV [124, 231]. To address degradation of promoter proximal paused RNAPII, we enhanced promoter proximal pausing with DRB, which prevents release into gene bodies [76], and measured chromatin levels of RNAPII with and without MG132. During unperturbed conditions, reduced RNAPII levels after DRB treatment were completely restored by MG132. As pRNAPII S5 levels were greatly enhanced by MG132 after DRB treatment, this supports that reduced RNAPII levels were caused by degradation of the promoter proximal form. Moreover, if UV specifically targets elongating RNAPII for degradation, then inhibition of productive

elongation with DRB prior to UV treatment would suppress RNAPII degradation. However, DRB treatment prior to UV caused an even larger reduction in RNAPII and pRNAPII S5 levels on chromatin compared to either treatment alone. Chromatin levels of both RNAPII forms were completely restored with MG132. As anticipated, pRNAPII S2 levels were reduced with DRB in combination with UV, however, they were not restored with MG132. This supports our hypothesis that the promoter proximal paused RNAPII is specifically targeted for degradation after UV. When RNAPII progression was inhibited a step prior to promoter proximal pausing, with THZ1 [318, 319], we observed that pRNAPII S5 levels were not further reduced by UV in combination with THZ1. This suggests that UV-induced degradation of RNAPII requires transcription initiation, which further leads to production of new promoter proximal paused RNAPII.

In this paper we developed a new flow cytometry assay that accurately depicts chromatin binding of RNAPII and its phosphorylated forms through the cell cycle. With this technique we revealed that elongating RNAPII becomes more stable in S-phase after UV, which might indicate cell cycle specific effects in the TC-NER. We also propose a modified model for the effects UV has on transcription, as our results shows that the promoter proximal paused form of RNAPII is targeted for degradation both with and without UV. Our results suggest that degradation of promoter proximal paused RNAPII participates in the regulation of the "RNAPII pool", which may further be important for resumption of transcription and cell survival after UV.

3.3 Paper III

The RNA polymerase II C-terminal domain promotes non-homologous end-joining (NHEJ) by recruiting DDX5 and CDC73

In paper II we observed a global reduction in RNAPII levels on chromatin at 2h after UV. Removal of RNAPII from chromatin upon DNA damage is thought to ensure proper DNA repair [175], and to avoid T-R conflicts and other harmful events caused by lesion-stalled RNAPII [5]. We wondered whether RNAPII chromatin association was also reduced after DSBs induced by ionizing radiation (IR). Indeed, chromatin levels of RNAPII were reduced at 2 and 6h after IR, both in G1 and S phases. Interestingly, RNAPII reduction in G1 was partially restored at 6h after IR, while RNAPII levels were further reduced at 6h in S phase. This suggests that RNAPII levels do not strictly correlate with the amount of DSBs, but are also influenced by factors such as DNA replication. Moreover, RNAPII levels were also reduced after IR at 30 and 60 min, which was in contrast to UV where we observed enhanced RNAPII levels at early time points. The reduction of RNAPII after IR was most pronounced for pRNAPII S2, suggesting that IR suppresses transcription elongation. Our results thus support that IR and UV affect transcription differently.

Previous work by the group showed that PNUTS is recruited to sites of DNA damage [256] and in paper I we revealed that PNUTS is required for RNAPII degradation. We thus wondered whether PNUTS is required to suppress RNAPII elongation at sites of IR-induced DNA damage. Indeed, PNUTS depletion suppressed the reduction in RNAPII and pRNAPII S2 levels on chromatin at 30 and 60 min after IR. We wanted to address whether enhanced RNAPII retention after PNUTS depletion affected repair by non-homologous end-joining (NHEJ). Interestingly, with a NHEJ reporter construct we observed that PNUTS depletion did not show reduced but rather enhanced NHEJ repair, suggesting that suppression of RNAPII elongation is not required for NHEJ repair. As PNUTS-PP1 dephosphorylates the CTD of RNAPII [259], we wondered whether such post-translational modifications of the RNAPII CTD could regulate the recruitment of NHEJ factors, as it does for factors involved in transcription and RNA metabolism [40-43]. We manually screened 5 published datasets of phospho-CTD interacting partners for a role in NHEJ, where we identified 16 proteins. As PNUTS is known to associate with RNAPII, we addressed if some of these proteins were in the vicinity of PNUTS. Indeed, our PNUTS BioID screen identified 6 of the NHEJ promoting factors that were found to bind the phospho-CTD. Interestingly, chromatin association was enhanced for several proteins involved in NHEJ after PNUTS depletion, while it was inhibited with the RNAPII CTD kinase inhibitor THZ1. On the other hand, some NHEJ factors showed reduced chromatin association after PNUTS depletion. Moreover, RNA has been proposed to promote chromatin association of NHEJ factors [320, 321]. We wondered whether the enhanced recruitment of NHEJ factors after PNUTS depletion could be caused by increased RNA levels. Indeed, PNUTS depleted cells showed enhanced RNA levels compared to control cells. However, our results suggested that RNA levels did not strictly correlate with the chromatin association of NHEJ factors. We discovered that enhanced chromatin levels of NHEJ factors were dependent on the phospho-CTD binding proteins CDC73 and DDX5. Co-depletion of PNUTS with either CDC73 or DDX5 reduced NHEJ repair frequency. Altogether our results propose a role for the tumor suppressor CDC73 in NHEJ, and we suggest that the phospho-CTD in combination with RNA, CDC73 and DDX5 forms a functional unit that promotes NHEJ. We hypothesized that this functional unit might be a nuclear condensate; however, this has to be further explored.

4 Discussion

4.1 Transcription as a threat to normal DNA replication

Transcription can halt or stall replication fork progression and is considered a major source of replication stress [5, 6]. Encounters between transcription and replication machineries may occur [84, 199], and there are several events that might increase the risk of such encounters (section 1.4.1). Factors that alter the stability of RNAPII or transcription elongation rate might promote T-R conflicts [85]. Notably, it is uncertain whether T-R conflicts are caused by direct contact between the transcription and replication machineries. Several structures generated during transcription have the potential to interfere with fork progression, such as R-loops [85, 222, 223], supercoiling [219, 220] and secondary non-B DNA structures [221]. Enhanced presence of such structures also poses a threat to normal DNA replication.

In paper I we observed that depletion of PNUTS or WDR82 interfered with normal DNA replication, as shown by reduced EdU incorporation and replication fork speed. As PNUTS depletion previously was shown to enhance the formation of R-loops [17], one hypothesis could be that R-loops might be the cause of replication stress. However, overexpression of RNase H1 only partially rescued EdU incorporation and replication fork speed in PNUTS depleted cells. In WDR82 depleted cells, replication fork speed was unaltered upon RNase H1 treatment. R-loops might thus contribute to the replication stress seen after PNUTS depletion, but could not solely explain the replication stress phenotype caused by PNUTS/WDR82 depletion. However, our results rather suggested that the transcription machinery, more specifically RNAPII itself, interfered with replication fork progression.

Upon encounters between transcription and replication, a dynamic state of RNAPII has been proposed to suppress T-R conflicts [85]. Factors that promote RNAPII turnover on chromatin can thus be considered as important for normal DNA replication. In paper I we observed that depletion of PNUTS or WDR82 altered RNAPII dynamics by enhancing RNAPII residence time on chromatin. The enhanced residence time was further discovered to be caused by reduced degradation of RNAPII. Increased stability of RNAPII on chromatin is likely to enhance the threat posed by transcription on normal replication. Supporting this, several studies have proposed that regulated RNAPII stability is important to avoid T-R conflicts [209, 225, 229, 322]. We observed enhanced proximity ligation signal of RNAPII-PCNA after depletion of PNUTS. Treatment with THZ1, which decreased the amount of chromatin bound RNAPII, also partially rescued the reduced replication fork speed caused by depletion of PNUTS. Altogether, our results support previous observations [209, 225, 229, 322], where a dynamic state of RNAPII promotes normal DNA replication.

As PNUTS [17, 259, 260] and WDR82 (paper I) facilitate dephosphorylation of pRNAPII S5, one might wonder if there is a correlation between the phosphorylation status of the RNAPII CTD and RNAPII dynamics. Our results suggested that hyperphosphorylation on pRNAPII S5 caused by PNUTS/WDR82 depletion protected RNAPII from degradation. Similarly, a study in yeast showed that pRNAPII S5 prevented ubiquitylation and degradation of RNAPII [231]. They proposed that dephosphorylation of pRNAPII S5 preceded RNAPII degradation. Enhanced stability of RNAPII on chromatin thus increases the risk of T-R conflicts as the conflict is not easily resolved by RNAPII removal by degradation. Altogether, these results support that PNUTS and WDR82 protect the cell against replication stress by promoting RNAPII turnover on chromatin to suppress T-R conflicts.

4.2 Potential mechanisms to explain the effects of PNUTS and WDR82 on RNAPII dynamics

4.2.1 Regulation of promoter proximal pausing

Promoter proximal pausing is considered an important step in regulation of the transcription rate. Upon premature termination at the promoter proximal pause site, RNAPII has been assumed to be released and recycled for new rounds of transcription [323-326]. However, in paper II we showed that promoter proximal paused RNAPII is targeted for proteasome-mediated degradation. In paper I, depletion of PNUTS/WDR82 was found to protect RNAPII from degradation. One possibility might therefore be that PNUTS/WDR82 promotes degradation of promoter proximal paused RNAPII. As pRNAPII S5 is the substrate of WDR82/PNUTS-PP1, pRNAPII S5 dephosphorylation might be required for degradation of promoter proximal paused RNAPII. Alternatively, PNUTS/WDR82 may suppress release from promoter proximal pausing into productive elongation, and thus promote the presence of the promoter proximal paused form of RNAPII. In paper II we found that pRNAPII S5 was more degraded after treatment with DRB in early S compared to G1-phase in HeLa cells. pRNAPII S5 was also removed to a greater extent in S phase compared to G1 phase after UV treatment. This supports a role for degradation of promoter proximal paused RNAPII in the regulation of T-R conflicts.

Another interesting link between PNUTS and promoter proximal pausing is its proposed role in dephosphorylation of Spt5 [266]. Interestingly, Spt5 has been shown to stabilize promoter proximal paused RNAPII and protect it from degradation [327, 328]. Phosphorylation of Spt5 occurs at the transition from promoter proximal pausing into productive elongation [45]. Spt5 might enhance the release into productive elongation, as phosphorylated Spt5 has been shown to associate with elongation factors, such as the PAF1c [329-331]. Notably, Spt5 has not yet been shown to be a direct substrate of PNUTS *in vitro* and thus needs to be further explored. It is also interesting that co-depletion of CDC73 partially restored RNAPII dynamics and replication fork rates after depletion of PNUTS. One

possibility could be that enhanced association of CDC73 with the phospho-CTD shielded RNAPII from degradation. However, as an elongation factor, CDC73 might also regulate RNAPII dynamics by promoting release from promoter proximal pausing. Indeed, PAF1c has been shown to compete with the pausing factor NELF for association with RNAPII [58], and enhanced CDC73 levels upon PNUTS depletion might likely promote pause release. In line with this, chromatin association of NELF was reduced upon PNUTS depletion (**Figure 10**). The involvement of PNUTS/WDR82 and CDC73 in promoter proximal pausing thus warrants further investigation.

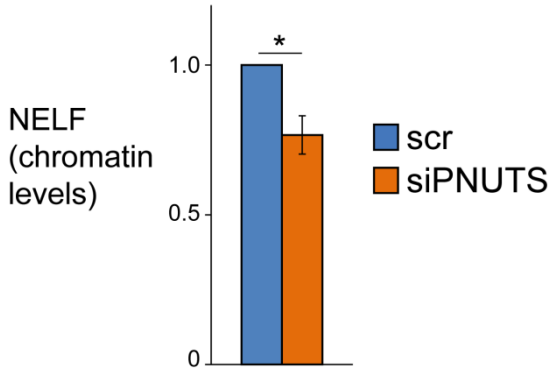

Figure 10: Chromatin levels of NELF. Western blot analysis of chromatin fractions of NELF in HeLa cells 48h after transfection with scramble (scr) or PNUTS (siPNUTS) siRNA. Chromatin levels were normalized to stain free signal and further to scr sample (n=3). Error bars indicate standard error of mean (SEM) and p-value was calculated by the two-tailed Student's one-sample t- test. See materials and methods from paper III for more details.

4.2.2 Regulation of elongation speed

Factors that promote release of RNAPII from the promoter proximal paused state would also determine the rate of RNA synthesis [332]. Supporting this, loss of PAF1 has been shown to negatively affect elongation rates [333]. Rapid promoter proximal pausing and subsequent release is also associated with enhanced levels of gene expression [334, 335]. The potential roles of PNUTS and WDR82 in regulating promoter proximal pausing may contribute to the regulation of RNA synthesis. Upon depletion of PNUTS we observed higher levels of 5-ethynyl-uridine (EU) incorporation (paper III), representing enhanced RNA synthesis. The increase in EU levels caused by PNUTS depletion can be caused by enhanced elongation speed, as the regulatory step of promoter proximal pausing may be disturbed in PNUTS depleted cells. PNUTS-PP1 has also been proposed to regulate elongation speed by promoting dephosphorylation of Spt5. This "sitting duck torpedo" mechanism is based on Spt5 dephosphorylation that causes reduced elongation rate in the termination zone, which further converts RNAPII to a "sitting duck" that is terminated by XRN2 [266]. Accelerated elongation speed in both gene bodies and 3' flanking regions, caused by PNUTS depletion, prolongs the race between RNAPII and XRN2, which ultimately leads to distal termination [266]. PNUTS and WDR82 have been proposed to facilitate proper termination by several

mechanisms. Defective termination and enhanced release from promoter proximal pausing would both contribute to enhanced RNA synthesis, and may thus explain the effects on RNA synthesis seen upon PNUTS depletion.

4.2.3 Regulation of RNAPII termination

In section 4.2.1, PNUTS and WDR82 were proposed to regulate premature termination by promoting degradation of promoter proximal paused RNAPII. Premature termination is important for regulating gene expression, but also to suppress divergent antisense transcription [267]. The role of PNUTS and WDR82 in premature termination during promoter proximal pausing might thus aim to limit antisense transcription. Indeed, depletion of WDR82 or PNUTS has been shown to cause termination defects at active enhancers and promoters, which increased the synthesis of lncRNA [267]. WDR82 has been proposed to regulate antisense transcription via its association with the SET1 methyltransferase [268] or the ZWC complex [290]. PNUTS has not been found in the SET1 [259] or ZWC complexes [289], and our preliminary data suggest that H3K4 methylation is not affected by PNUTS depletion. In line with this, others have proposed that H3K4me3 did not correlate with the termination defect seen upon PNUTS depletion [267]. This might suggest that PNUTS and WDR82 suppress antisense transcription by different mechanisms. In all, these results support a role of PNUTS and WDR82 in promoting premature termination and suppressing antisense transcription.

As the CTD phosphorylation status is likely important during premature termination, one might wonder if termination at the end of genes is equally regulated by the phospho-CTD. Transcription termination factors, such as the RNA splicing machinery and polyadenylation factors (CPF), require pRNAPII S2 for their recruitment to chromatin [40, 60, 336]. One might speculate whether hyperphosphorylation on pRNAPII S5 might interfere with the recruitment of one or several essential transcription factors. Notably, we observed no change in the termination factor XRN2 upon PNUTS depletion, and the RNA splicing factors NONO and SFPQ were rather enhanced. On the other hand, both PNUTS and WDR82 have been shown to directly associate with termination factors in yeast [259, 263, 281-283, 337, 338]. In mammals, the corresponding complexes showed similarities with the ones in yeast [339-341], suggesting that the role of PNUTS/WDR82 in 3' end processing and termination has been conserved from yeast to humans. However, whether PNUTS and WDR82 promote termination by facilitating the recruitment of termination factors has to be further explored. As mentioned above in section 4.2.2, the effects of PNUTS in suppressing elongation rate may also contribute to regulate termination.

All things considered, we have discovered roles for PNUTS and WDR82 in regulating RNAPII dynamics. As PNUTS and WDR82 seem to be involved in several stages of

transcription regulation (**Figure 11**), their contribution to maintaining a dynamic state of RNAPII might be diverse.

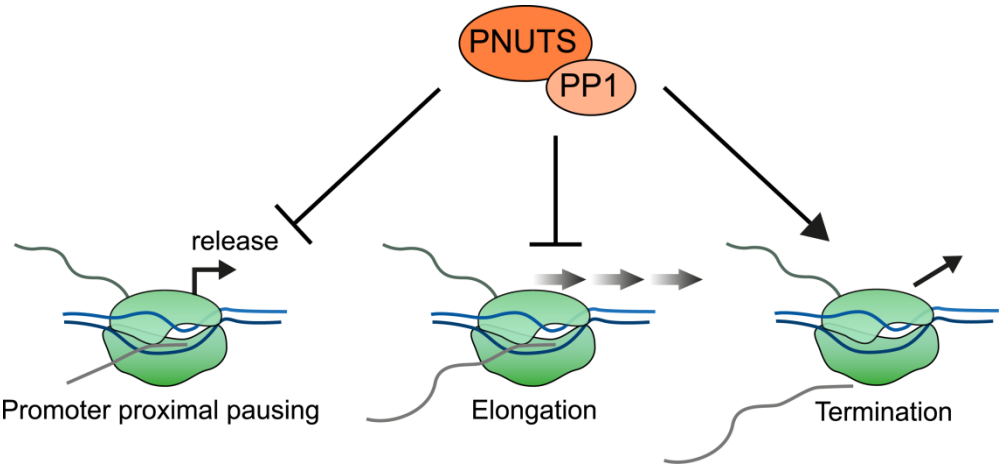

Figure 11: Potential roles of PNUTS-PP1 in transcription regulation.

4.3 The transcription cycle after DNA damage

DNA damage can challenge the progression of transcription upon formation of transcription blocking lesions. Depending on the type of lesion and its location in regards of the transcription machinery, RNAPII progression can be either stalled or fully blocked [342]. In some cases, DNA damage may alter the RNAPII pool, as RNAPII can be removed from the break site by degradation [100-102, 175]. DNA damage is generally considered to inhibit transcription, either locally at the lesion or on a global level [342]. In this section I will elaborate on the transcriptional responses to DNA damage, and how this response differs upon UV- or IR-induced DNA damage.

4.3.1 The transcription response to UV-induced DNA damage

In response to UV-induced bulky lesions, RNAPII stalling at the lesion initiates TC-NER [16]. In most cases, removal of RNAPII from the DNA damage site is considered to promote access of NER factors to the lesion [343]. This might be achieved by release of RNAPII from chromatin [344], backtracking or displacement [345-347], or even degradation of RNAPII [100-102]. UV-mediated degradation was previously considered to target productive elongating RNAPII [97], as this was likely the form of RNAPII that encountered UV-induced lesions. We have shown that the promoter proximal form of RNAPII was specifically targeted for degradation after UV irradiation. This was supported by a recent study, which also observed that promoter proximal paused RNAPII was targeted for UV-mediated degradation [348]. In addition, pRNAPII S5 has been shown to specifically bind to E3 ubiquitin ligase upon UV-induced DNA damage [232]. If only the lesion-stalled RNAPII was affected upon UV irradiation, one might expect a local effect on transcription. The total effect on transcription

would then depend on the number of RNAPII complexes impaired by the different doses of UV irradiation. As we were able to observe reduced RNAPII levels at 2h after UV irradiation by bulk measurements, this suggests a global effect on transcription. This supports the results of numerous studies, where UV irradiation was found to cause a global inhibition of transcription [96, 98, 99, 349]. UV thus also affects transcription elsewhere than the damage site, and our results suggest that this likely involves degradation of promoter proximal paused RNAPII.

UV-induced inhibition of transcription is commonly considered to involve inhibition of transcription initiation [99, 350]. The rate of transcription initiation is likely negatively affected by the reduced RNAPII pool caused by UV-mediated degradation of RNAPII [98]. Interestingly, we observed increased transcription initiation as an early response to UV irradiation. In line with this, RNA-seq analysis showed enhanced RNA synthesis from the TSS at 1h after UV irradiation [351]. As RNAPII stalling is the lesion signal for TC-NER repair [16], enhanced initiation might be an early response upon UV to screen transcriptionally active regions for bulky lesions. Supporting this, UV has been shown to promote the release of RNAPII from promoter proximal pausing into productive elongation [352]. Our results from paper III suggested that enhanced initiation of transcription causes “promoter proximal crowding”, which was relieved by enhanced degradation of promoter proximal paused RNAPII and by promoting release into productive elongation. Of note, a recent study proposed a similar, but slightly different model, where degradation of promoter proximal paused RNAPII after UV required signaling from the lesion-stalled RNAPII [348]. In this model, lesion detection should precede degradation of promoter proximal paused RNAPII. To illustrate this point, the authors used THZ1, which inhibits initiation and thus prevented RNAPII from encountering the lesion. However, if their model was correct, suppressing release from promoter proximal pausing should also prevent encounters between RNAPII and a lesion. In contrast to this, we observed that co-treatment of DRB with UV reduced pRNAPII S5 levels to a greater extent than DRB or UV irradiation alone. Our results rather supports our own hypothesis that increased initiation upon UV irradiation is required for the enhanced degradation of promoter proximal paused RNAPII.

It is increasingly accepted that promoter proximal pausing is important for the transcription machinery to prepare for challenges downstream [45, 323]. In line with this, promoter proximal paused RNAPII was rapidly recovered at low doses of UV irradiation, while lesion-stalled RNAPII remained [348]. It is likely that regulation of the RNAPII pool by degradation of promoter proximal paused RNAPII contributes to transcription recovery after UV irradiation. Inhibition of RNAPII degradation upon UV irradiation has been proposed to cause dysregulation of short gene transcripts, where many are assumed to code for oncoproteins [98]. Regulation of the RNAPII pool and thus transcription activity might prevent the expression of such damage-induced genes for the cell to recover from UV-induced stress.

4.3.2 The transcription response to IR-induced DSBs

Compared to UV, the transcription response to DNA damage caused by IR is less clear. This might be related to the great variety of lesions induced upon IR, including DSBs, SSBs and inter- or intra-strand crosslinks [105, 106, 353]. If one wish to study specifically the effect of DSBs, a transcriptional reporter system, such as in [354], can be used to induce DSBs at specific locations. Notably, the DSBs caused by IR are considered to be complex [106, 132], and might not be replicated by such techniques. As IR is also commonly used in cancer therapy, it is of interest to learn more about the transcription response to IR-induced DNA damage.

DSBs have been shown to arrest RNAPII progression in a manner dependent on the DDR mediators ATM, DNA-PK and PARP1 [170-172]. The DSB response triggers transcriptional silencing at the break site, but also on DSB-flanking genes, which leads to a global inhibition of transcription. Transcription silencing near the DSB has been thought to prevent collisions between transcription and the repair machinery [170]. When DSBs occur within the gene body, transcription silencing has also been proposed to prevent the formation of truncated RNA, which could have unwanted functions [170]. In paper III, we observed that RNAPII levels on chromatin were globally reduced at 2h after IR measured by flow cytometry and western blotting (paper III). pRNAPII S2 levels were especially reduced after IR, most pronounced at 1h, suggesting that IR-induced DNA damage suppresses transcription elongation. This correlates with previous studies where EU incorporation was reduced already at 30 min after IR [175, 176]. The IR-induced reduction in RNAPII and pRNAPII S5 levels was dose-dependent, as 10 Gy caused a greater reduction than 2 Gy. This dose-dependent effect on transcription inhibition would be interesting to explore further. Moreover, we observed that the IR-induced reduction in RNAPII levels was transient, as RNAPII levels were restored at 6h in G1 cells. Supporting this, other studies have shown that the transcriptional activity was restored between 1 to 4h after IR [175, 176]. The observed difference in time required to restore transcription might be dose dependent and cell line specific. As NHEJ repairs 80% of IR-induced breaks within 2h [137], this might partially relieve the global suppression of transcription.

As mentioned in section 1.3.6, suppression of transcription elongation after IR may be mediated by DNA-PK activity, which has been shown to promote degradation of RNAPII in the broken gene [174, 175]. Alternatively, RNAPII may be stalled distant to the DSB in an ATM-dependent manner [173]. PARP1 has also been proposed to cause a global effect on transcription as PARylation and RNAPII mediated recruitment of NELF has been shown to globally suppress transcription by promoting promoter proximal pausing [176, 355]. This NELF-mediated pathway of transcription inhibition has been proposed to involve ATM [176]. Transcription suppression is also thought to be mediated by histone coding and chromatin

remodeling [170, 171, 356]. Both PARP1 and ATM have been shown to edit the histone code following DSB formation to generate a repressive chromatin environment nearby the DSB [170].

In paper III we discovered that PNUTS was required for the global suppression of transcription after IR-induced DNA damage. Chromatin levels of pRNAPII S2 were surprisingly not reduced upon depletion of PNUTS, they were rather enhanced. Total levels of RNAPII were also enhanced, suggesting that the IR-induced global inhibition of transcription was restored. Interestingly, PNUTS has been shown to be rapidly and transiently recruited to sites of DNA damage [256]. As PNUTS may have several functions in the transcription cycle, which were addressed in section 4.2, these might be related to its role in suppressing transcription upon DNA damage. Enhanced release from promoter proximal pausing, elevated elongation speed and suppression of termination might contribute to the restored transcription levels after IR in PNUTS depleted cells. Furthermore, PNUTS has been proposed to regulate DNA-PK activity by promoting DNA-PK phosphorylation at S2056 after DNA damage [257]. However, we observed enhanced levels of pDNA-PK S2056 on chromatin after PNUTS depletion. This was shown by both flow cytometry and western blotting (paper III). Our results thus suggest that PNUTS does not regulate RNAPII degradation after IR via DNA-PK activity. On the other hand, as PNUTS might be associated with the regulation of promoter proximal pausing, it can be considered to suppress transcription via ATM and PARP1. As ATM and PARP1 have been proposed to suppress transcription via NELF [176, 355], reduced levels of PARP1 (paper III) and NELF (**Figure 10**) upon PNUTS depletion might indicate that this mechanism of transcription inhibition is impaired. One possibility is therefore that PNUTS depletion inhibits the global IR-induced suppression of transcription by regulating promoter proximal pausing.

Seen together, these results suggest that both UV and IR might inhibit transcription by regulating promoter proximal pausing. As UV caused enhanced degradation of promoter proximal paused RNAPII, one might wonder if degradation of promoter proximal paused RNAPII is also important after IR. Our preliminary results (data not shown) suggest that promoter proximal paused RNAPII is degraded to a greater extent after co-treatment with DRB and IR compared to either treatment alone, however, this has to be further explored. Furthermore, we want to explore the function of PNUTS in suppressing transcription upon IR, and whether it is related to the activity of the DDR mediators. It would also be of interest to study whether PNUTS has a similar role in transcription regulation upon UV-induced DNA damage.

4.4 RNAPII in DSB repair

Emerging data suggest that RNAPII might have a role in promoting DSB repair [18]. As inhibition of transcription is believed to promote DSB repair, one might wonder why and

how RNAPII would be involved in facilitating repair. In regards of the "why", RNAPII has been proposed to be the ultimate surveyor of genomic integrity, as it continually scans the genome during transcription. Compared to other damage sensors that might have to be recruited to chromatin to initiate repair, numerous RNAPII complexes are already present on chromatin. RNAPII is believed to sense damage by "recognition by proxy", as it stalls upon encounter with a lesion [15-20]. Several types of lesions have been shown to stall RNAPII, including SSBs, crosslinks and bulky lesions [128]. This is exploited in the specialized repair pathway TC-NER, where repair is initiated by stalled RNAPII at bulky UV-lesions [124]. However, upon encounter with DSBs it has been proposed that DDR kinase signaling rather than the break itself causes RNAPII staling [174]. It is thus unclear whether RNAPII stalls locally to the DSBs or in surrounding regions. One might wonder whether RNAPII could be close enough to the DSB to "sense" its presence. As RNAPII has been proposed to block access of repair factors to the break site [170, 172, 175], it might seem unlikely that RNAPII is involved in DSB repair by sensing the DSBs; however, this has to be further explored.

A possible function of RNAPII in DSB repair is by production of DNA-damage response RNAs (DDRNAs) and DSB-induced RNA (diRNA) [179, 180, 185]. These non-coding RNAs have been proposed to promote the recruitment of repair factors [180, 185], but also direct pathway choice [177, 187, 188, 190]. On the other hand, RNAPII-generated RNA has also been shown to promote repair regardless of whether it was synthesized at the break site or not. Indeed, a recent study showed that small Cajal body-specific RNA2 (scaRNA2) directed repair towards HR by inhibiting DNA-PK and competing with the lncRNA LINP1[357], where the latter factor has been shown to promote NHEJ [358]. Pathway choice is also thought to be directed by transcription-associated chromatin modifications, where histone modifications accompanying active transcription have been linked to HR [168, 191, 192, 359, 360]. On the other hand, we and others [143, 180, 185, 193] have seen that transcription also can promote NHEJ. Altogether, RNAPII seems to be involved in DSB repair, however, the exact role of RNAPII and nascent RNA remains to be established, as well as the conditions that favours RNAPII-mediated DSB repair.

4.5 A new role for the phospho-CTD in DSB repair

Interestingly, many DSB repair factors have been found to bind the phospho-CTD (paper III and results not shown). In paper III we discovered that hyperphosphorylation on RNAPII CTD enhanced the recruitment of several of these repair factors to chromatin. The phospho-CTD is commonly known to act as a signaling platform during transcription and mRNA processing, where post-translational modifications of the CTD depicts the recruitment of transcription associated factors [41-43]. We thus hypothesized that the phospho-CTD could have a similar role in DSB repair, more specifically NHEJ. As the chromatin association of many NHEJ repair factors were enhanced by RNAPII CTD hyperphosphorylation in the

absence of damage, this might suggest that selected repair factors travel with RNAPII during elongation. One might speculate that when RNAPII stalls after the induction of DSBs, this might signal to the repair factors to initiate repair.

In paper III, we discovered that pRNAPII S5 levels were important for the recruitment of NHEJ factors, as hyperphosphorylation of pRNAPII S5 caused by PNUTS depletion enhanced their levels on chromatin. This was verified with the CDK7 inhibitor THZ1, which prevents further phosphorylation of serine 5 by CDK7. In paper I we showed that THZ1 suppressed both total RNAPII and pRNAPII S5 levels on chromatin to a larger extent in control cells than in PNUTS depleted cells. Many NHEJ factors followed a similar pattern and showed enhanced stability on chromatin upon PNUTS depletion after THZ1 treatment. A study in yeast showed that aberrant phosphorylation of the CTD reduced resistance to DNA damage [361], further supporting a role of the phospho-CTD in DNA repair. In addition, all key factors of the cNHEJ pathway, such as Ku80, DNA-PK and Ligase IV, have been found in the RNAPII immunocomplex [143, 193]. Of note, a study observed reduced NHEJ repair upon depletion of PNUTS or PP1 [257]. As there are some differences in siRNA, cell lines and techniques used to measure NHEJ repair in their study vs. ours, this might be the cause of our different observations. Our hypothesis is further supported by the observation of enhanced NHEJ frequency upon depletion of WDR82 (**Figure 12**), which similarly causes hyperphosphorylation of pRNAPII S5 as seen for PNUTS depletion (paper I). In paper III, we also showed that loss of phospho-CTD binding factors CDC73 and DDX5 inhibited the enhanced NHEJ frequency seen after PNUTS depletion.

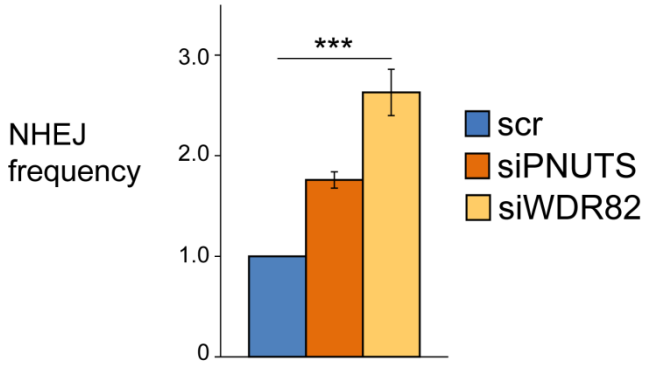

Figure 12: Mean frequency of NHEJ repair measured by percent GFP-positive cells in HeLa cells transfected with the NHEJ reporter construct. Cells were transfected with scramble (scr), PNUTS (siPNUTS) or WDR82 (siWDR82) siRNA at 24h. After 6-24h they were further transfected with the I-SceI-expressing vector and a mCherry-labeled empty vector. The percent of GFP-positive cells relative to the total number of transfected cells (mCherry) was measured after additionally 48h by flow cytometry (n=5). Error bars indicate standard error of mean (SEM) and p-value was calculated by the two-tailed Student's one-sample t- test. See Materials and Methods in paper III for more details.

In paper I we observed that PNUTS depletion caused replication stress, likely by enhancing T-R conflicts. DSBs can form as a consequence of genome destabilizing transcription-associated structures [200, 201, 224] or when the transcription block upon T-R

conflicts remains and leads to fork breakage [202-204, 238]. One possibility is that this could contribute to the enhanced chromatin levels of NHEJ promoting factors seen in paper III. This correlates with Ku80 and DNA-PK chromatin levels, which were only enhanced in S-phase upon PNUTS depletion. On the other hand, DDX5 was clearly enhanced in both G1 and S-phases, arguing for a direct role for the phospho-CTD in its recruitment to chromatin. Moreover, PNUTS depletion causes accumulation of cells in S-phase [17], which would rather be expected to suppress NHEJ as S-phase cells may also rely on HR for their repair. In line with this, HR is considered the preferred pathway to repair one-ended DSBs formed upon collapsed replication forks [107, 108]. The enhanced NHEJ frequency upon PNUTS depletion is thus not likely caused by intrinsic DNA damage. Note that the NHEJ reporter assay measures repair frequency of DSBs specifically induced by the I-SceI restriction enzyme. This suggests that enhanced T-R conflicts upon PNUTS depletion are unlikely to cause the increased NHEJ frequency in this assay. Altogether, our results support a role for the phospho-CTD in DSB repair.

4.5.1 Potential involvement of phase separation in NHEJ repair via the phospho-CTD

In response to DNA damage, many proteins positions at the break site to form local accumulations, known as foci [362]. Such foci can be visualized by immunofluorescence as centers of high signal of fluorescently tagged proteins [363]. Recent studies have shown that liquid-liquid phase separation might drive the accumulation of repair proteins at the DNA lesion [321]. In paper III we proposed a model where the phospho-CTD and RNA form nuclear condensates that may promote NHEJ. The phospho-CTD binding factors CDC73 [299] and DDX5 [364] have also been found to phase separate and are likely to contribute to these nuclear condensates. Several studies have shown that RNAPII form different condensates during the transcription cycle, where the phosphorylation status of RNAPII CTD determines its ability to phase separate with distinct factors involved in transcription [70-72, 77]. Hyperphosphorylated CTD upon PNUTS depletion caused increased NHEJ repair, which might be linked to enhanced formation or increased stability of nuclear condensates. PNUTS depletion has also been proposed to enhance transcription of lncRNAs [267], which promotes the assembly and scaffold biomolecular condensates [77]. 53BP1 has been shown to form biomolecular condensates via its interaction with lncRNA transcribed near the DSB site [183, 365]. In addition, DNA damage-induced 53BP1 foci have been shown to depend on transcription, as treatment with RNase A or α-amanitin prevents their formation [180, 185]. The number of required molecules to process a DSB is unknown and seems to vary for the different repair factors. Some repair factors are clearly many enough at the lesion to be visible as a focus by microscopy [183, 365, 366], while others cannot be detected [367, 368]. If RNAPII and RNA facilitate clustering of repair proteins at the break site, several RNAPII complexes might contribute to locally enhance the concentration of repair factors at a DSB. As DSBs located in actively transcribed regions have been shown to cluster [369], these DSB clusters are likely to involve several RNAPII complexes that might contribute to a high local

pool of repair factors that facilitates their repair. There is still much to explore regarding the role of biomolecular condensates in facilitating DSB repair, and whether RNAPII and nascent RNA are required for their formation.

All things considered, the role of transcription in the response to IR-induced DNA damage seems complex. We have shown that IR-induced DNA damage globally inhibits transcription, which is dependent on PNUTS. On the other hand, we also observe that hyperphosphorylation of the phospho-CTD caused by depletion of PNUTS promotes DSB repair by a NHEJ pathway. Whether this NHEJ pathway is driven by phase separation or not has to be further investigated. It is also unknown whether the recovery of transcription seen upon PNUTS depletion is connected to the phospho-CTD mediated NHEJ after IR. Whether the response to DSBs favors global suppression of transcription, de novo RNAPII-driven RNA synthesis from the break site or RNAPII mediated repair needs to be further explored.

4.6 Interplay between transcription and the responses to DNA damage and replication stress

In the previous sections, transcription has been considered both a threat to genomic integrity, but also a facilitator of DNA repair. We have shown that transcription is globally suppressed upon DNA damage, and that the effects on RNAPII depend on the type of lesion and cell cycle phase. Transcription co-exists on DNA with other basic cellular processes, such as DNA damage and replication [370], and constant crosstalk is required to preserve the genomic integrity (**Figure 13**). The high frequency and constantly recurring behaviour of transcription renders regulatory mechanisms that control transcription likely key to controlling such crosstalk.

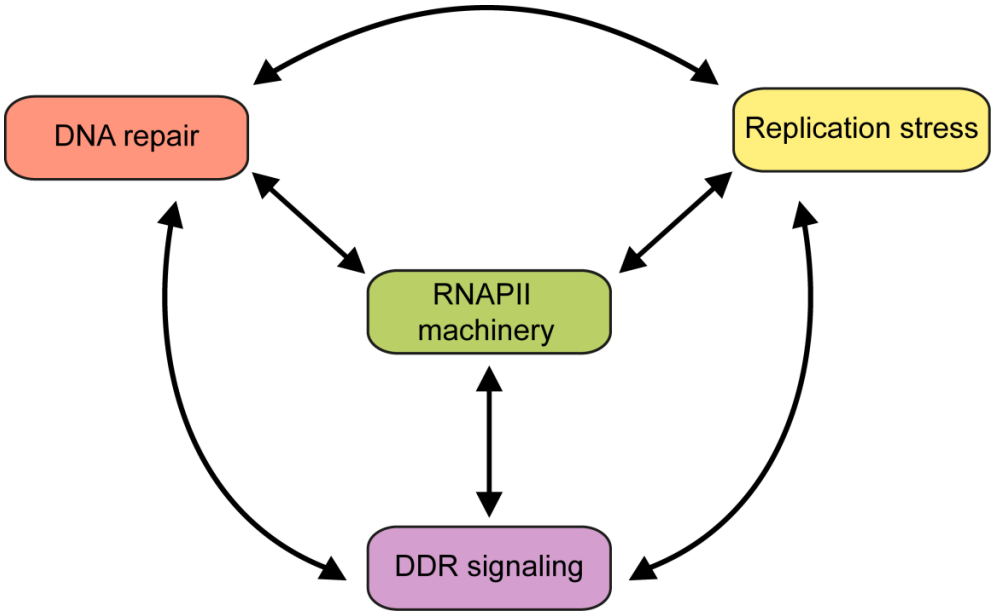

Figure 13: Interplay between RNA polymerase II (RNAPII) machinery, DNA repair, replication stress and DNA damage response (DDR) signaling.

We have shown that a dynamic state of RNAPII is required to suppress replication stress, likely by preventing T-R conflicts (paper I). Factors that regulate RNAPII stability are thus also likely to affect genome stability. Central to the regulation of RNAPII turnover on chromatin are elongation factors. One such factor is CDC73, which as part of PAF1c has been shown to regulate several steps of the transcription cycle (section 4.2), including promoter proximal pausing. We have further shown that promoter proximal pausing is a major step in controlling RNAPII dynamics. Interestingly, promoter proximal pausing is also regulated in response to DNA damage. This correlates with the dual roles of central factors in regulation of promoter proximal pausing, such as CDC73 and NELF, which are also associated with replication stress and DNA repair [176, 304, 307]. Moreover, in section 4.2.3 I addressed whether transcription termination could contribute to the dynamic state of RNAPII. Supporting this, a dual role is also found for many termination factors. For example, the termination factors SENATAXIN [371] and XRN2 [236] have been suggested to suppress replication stress. XRN2 associates with DDX5 to resolve R-loops, and both XRN2 and DDX5 [148] have been linked to the DDR. This supports the importance of transcription factors in regulating the responses to DNA damage and replication stress.

On the other hand, the responses to DNA damage and replication stress can also interfere with transcription. Upon T-R conflicts, transcription can be terminated to allow passage of the replisome (section 1.4.1). Transcription is also affected by DNA damage, as UV- or IR-induced lesions cause a global inhibition of transcription. This global effect on transcription would be expected to have a significant impact on gene expression. Indeed, after IR-induced DNA damage, changes in gene expression have been shown to affect genes involved in radio-resistance [372]. Moreover, DNA damage has been shown to affect the distribution of splicing factors, as well as their expression levels and activity [373]. Several splicing factors are substrates of DDR mediators [114, 373], further linking the interplay between transcription and the DDR. For instance, PAR has been shown to be bound by the splicing factor NONO [145], which has been implicated in both NHEJ and HR [374]. DNA damage induced by IR and UV might also affect splicing indirectly by affecting promoter proximal pausing and elongation speed of RNAPII [349]. Indeed, one proposed mechanism of global transcription inhibition activated upon DNA damage involves the elongation factor NELF [176, 355]. This illustrates that the interplay between transcription and the response to DNA damage goes both ways.

One might consider the phospho-CTD as an ideal platform for crosstalk. It is known that modifications of the phospho-CTD regulate binding of factors involved in transcription and RNA splicing [41-43]. We have now shown that CTD modifications can also regulate the recruitment of central factors of DNA repair and DNA damage signaling (paper III). Of note, hyperphosphorylation of the RNAPII CTD was found to promote binding of factors associated with both NHEJ (paper III) and HR (results not shown). Moreover, the phospho-CTD has been

proposed to facilitate the formation of biomolecular condensates with factors associated with transcription and RNA metabolism [70-72]. The phosphorylation status was shown to determine which factors that phase-separated with RNAPII [72, 75, 76]. In paper III, we proposed that phospho-CTD–driven phase separation might also promote NHEJ. PNUTS is an important regulator of the phospho-CTD, and our work suggests that it has roles within transcription, replication stress and DNA repair. Altogether, this supports that the phospho-CTD could be a platform for the interplay between the transcription machinery and the responses to DNA damage and replication stress.

4.7 The use of flow cytometry to study transcription

During this work we have developed a novel method to study the transcription cycle. We have thoroughly verified that our flow cytometry technique accurately detects levels of RNAPII on chromatin in individual phases of the cell cycle. In this section I will consider the advantages and disadvantages with this technique. Moreover, I will consider how it may contribute to the analysis of transcription compared to other available techniques.

One major advantage with flow cytometry is the possibility of simultaneous analysis of multiple parameters. This enabled us to identify individual cell cycle phases, either based on DNA content alone or in combination with EdU. Incorporation of EdU allowed us to separate S-phase cells from cells in G1 and G2 phases with similar DNA content. Flow cytometry thus enables cell cycle analysis without the need to synchronize cells. Other available sequencing or chromatin fractionation techniques are based on cell lysates made from pooled cells and thus rely on cell synchronization to study cell cycle effects. Cell synchronization methods are mostly based on chemical agents that inhibit building blocks and central factors of DNA synthesis to arrest cell cycle progression at specific stages [375]. Some of these agents have been shown to cause unwanted effects, such as replication stress or changes to transcription [375]. Moreover, synchronization methods can also be limited by statistical significance as they may not provide a sufficient amount of cells in the cell cycle phase of interest [375]. As flow cytometry enables rapid measurements of thousands of cells, it ensures quantitative analysis of cell cycle specific effects. In addition, all cell cycle phases can be identified in the same experiment by flow cytometry, which allows for direct comparison of RNAPII levels between the individual cell cycle phases.

Flow cytometry multiplexing also enables normalization of RNAPII levels by including barcoding. As sample-to-sample variation in antibody staining could be a major limitation upon RNAPII analysis, normalization ensures quantitative comparison of RNAPII modifications. By including fluorescent cell barcoding, non-treated cells can be mixed with all samples prior to antibody staining. This allows for direct normalization of each sample to non-treated cells. Some techniques do not easily allow for barcoding, such as microscopy,

where all samples are normalized to a separate non-treated sample. Such normalization procedure does not exclude sample-to-sample variation upon antibody staining. Sequencing techniques, such as ChIP-seq, can achieve normalization by "spike-in" of exogenous chromatin [376-378], which resembles the concept of barcoding in flow cytometry. However, the "spike-in" procedure is likely to add to the complexity and cost of ChIP-seq. Flow cytometry, on the other hand, offers a quick and easy barcoding step that ensures normalization of RNAPII levels. Moreover, flow cytometry offers the possibility of conducting large experiments, as one can include additional samples without a significant cost effect.

Flow cytometry can also be applied to study RNA synthesis by measuring EU incorporation. RNA lifetime and turnover can be addressed by measuring RNA synthesis per unit of time. With our technique we discovered that PNUTS depletion enhanced RNA synthesis. As EU incorporation measures RNAPI, RNAPII and RNAPIII synthesis of RNA, and does not identify the different types of RNA, the specificity of these results should be validated. Moreover, we do not know if enhanced RNA levels are caused by enhanced elongation speed, enhanced transcription of regions less transcribed during normal conditions or if specific genes are more transcribed. Such information could be provided by nascent RNA sequencing techniques [379]. Furthermore, as PNUTS has been proposed to regulate antisense transcription [267], it would have been interesting to explore whether enhanced transcription of lncRNA upon PNUTS depletion was involved in mediating DNA repair. Nascent RNA sequencing techniques thus could have provided key information for the transcription coupled DSB repair phenotype seen upon PNUTS depletion.

One major limitation with flow cytometry in analysis of transcription is that it measures bulk changes in RNAPII levels. Bulk measurements of chromatin associated RNAPII does not discern whether RNAPII is bound to promoters, gene bodies, enhancers etc. As post-translational modifications of RNAPII are regulated during the transcription cycle [60], this can be used to discern different phases of the transcription cycle. However, although pRNAPII S5 is mainly associated with promoter proximal pausing, it is also found in gene-internal regions and at splice sites [44]. To overcome these limitations we used RNAPII inhibiting drugs that block progression of transcription at specific steps. With DRB, which inhibits release into elongation [76], we were able to determine that promoter proximal paused RNAPII was indeed targeted for degradation after UV. Similar conclusions were reached by FRAP analysis of GFP-RNAPII and ChIP-seq in another study [348]. This shows that transcription inhibitors can be used to address transcription cycle specific effects on RNAPII chromatin levels obtained by flow cytometry. Moreover, sequence specific effects might not cause large enough differences in RNAPII levels in a cell, and therefore might not be detected by flow cytometry. Flow cytometry can thus only measure effects that cause a global change in RNAPII levels. In regards of paper III, it would be interesting to address whether the DNA repair response seen after PNUTS depletion is specific to break sites located in active transcriptional regions. Spatial or sequence specific information could have

been provided by microscopy or sequence and chromatin fractionation techniques, respectively.

In all, our flow cytometry technique provides rapid, quantitative and sensitive information on cell cycle specific effects on RNAPII or EU levels in single cells. We have shown that it can be used to study the interplay between the transcription machinery and the responses to DNA damage and replication stress. Microscopy or sequencing and chromatin fractionation techniques may be used to verify our results, as well as provide spatial and sequence specific information.

4.8 Implications for cancer and cancer treatment

Radiotherapy and many chemotherapeutic drugs aim to kill cancer cells by inducing DNA damage. Cancer cells are associated with high levels of replication stress, which can be caused by oncogenes, deficiencies in the DNA damage response or changes to transcription [198]. The survival of cancer cells is thus dependent on the DNA damage and replication stress responses. This can be exploited in cancer treatment, which is demonstrated by the implementation of chemotherapeutic agents that induce replication stress in cancer therapy [380]. As the ATR-CHK1 signaling cascade has an essential role in protecting against replication stress, inhibitors of ATR, CHK1 and WEE1 are possible agents for enhancing the stress exerted on replication [380, 381]. The high level of replication stress in cancer has been proposed to sensitize cancer cells to such agents. Moreover, replication stress can also be targeted by DNA damage inhibitors, such as inhibitors of PARP1 [382, 383]. Inhibition of PARP1 induces replication stress by multiple mechanisms, including attenuation of HR activity by decreasing the levels of central HR factors [123]. Pathway choice between NHEJ and HR is of great importance in cancer cells as their high proliferative capacity causes enhanced population of cells in S and G2 phases. Factors that regulate pathway choice can thus be targeted in cancer treatment or be used as biomarkers to predict the efficacy of treatment. It is therefore of great interest to explore factors and pathways involved in replication stress and DNA damage.

Transcription is emerging as a central player in the response to replication stress. As there are several factors involved in the interplay between transcription and the response to replication stress, transcription can be targeted to enhance replication stress in cancer. Some cancers experience elevated transcription rate, termed hypertranscription, which leads to high levels of replication stress [10]. Overexpression of oncogenes has been linked to the high transcription levels in cancer [10], where the MYC family is specifically of interest. MYC is overexpressed in numerous cancers [276], and its role in hypertranscription is regulated by superenhancers and CDK7 [384]. As the transcription inhibitor THZ1 inhibits CDK7, it has been shown to target MYC dependency in cancers [11-13, 384]. Triple-negative

breast cancer has also been shown to be highly dependent on CDK7, where THZ1 treatment blocked tumor growth [14]. The relevance of transcription inhibitors is also illustrated by that loss of CDK12 and CDK13 activity caused HR deficiency and sensitized cancer cells to PARP inhibitors [385-387]. Many of the genes that are more transcribed in cancer cells encode for factors that contribute to treatment resistance. This has been shown after IR, where many of the affected genes contributed to radio-resistance [372]. In such cases, inhibitors that globally suppress transcription can be used to improve treatment outcome. Indeed, inhibition of transcription pausing with THZ1 in combination with IR caused a complete block of tumor growth compared to IR treatment alone [372]. Altogether, this supports that transcription can be targeted to improve cancer treatment and that transcription associated mechanisms or factors may be used as biomarkers for therapeutic agents that act by inducing replication stress.

During our work we have identified several factors and conditions that may potentially be relevant to determine treatment efficacy, but that might also be exploited in cancer treatment. PNUTS and WDR82 were found to be central factors in suppressing replication stress (paper I). Low levels of PNUTS or WDR82 might thus sensitize cancer cells to replication-stress inducing agents. As overexpression of PNUTS or WDR82 is considered favorable prognostic markers in some cancers [271-273], this might be related to their role in suppressing replication stress and alleviating the aggressiveness of such cancers. Moreover, PNUTS is involved in the regulation of MYC stability by suppressing c-Myc protein degradation [388]. Targeting PNUTS expression in MYCN amplified cancers can thus improve treatment prognosis. Moreover, hyperphosphorylation of the RNAPII CTD caused by PNUTS depletion was found to promote NHEJ repair (paper III). It was proposed that the phospho-CTD might promote repair by driving the formation of DSB repair condensates. As several co-occurring transcription cycles may be connected across actively transcribing regions by the formation of biomolecular condensates, targeting oncogenic transcription cycles may thus affect several transcription cycles connected by phase separation. This may potentially be exploited in cancer therapy by targeting the formation of such condensates or developing inhibitors that are specifically incorporated into biomolecular condensates. Furthermore, enhanced RNAPII CTD phosphorylation was accompanied by hypertranscription in Ewing Sarcoma cells [389]. Hypertranscription or defective PNUTS may thus promote the sensitivity to DDR inhibitors. Other factors that are potentially relevant for cancer treatment are CDC73 (section 1.5.4) and DDX5 [390]. CDC73 is a tumor suppressor [309], but has been shown to have oncogenic traits in some cases [310]. Our results suggest that CDC73 is important for promoting replication stress after PNUTS depletion (paper I), but that it also participates in the phospho-CTD mediated DSB repair (paper III). As CDC73 is mutated in several cancers [311-315], its exact function in the responses to replication stress and DNA damage needs to be further explored. Another phospho-CTD binding protein, DDX5, was also found to promote DSB repair upon PNUTS depletion (paper III). Its role in transcription termination [148] suggests that DDX5 also might suppress replication stress. DDX5 has been shown to be

up-regulated in cancer [390], where high levels negatively correlated with disease progression. CDC73 and DDX5 might thus also be potential biomarkers for treatment efficacy.

5 Concluding remarks

We have discovered that RNAPII dynamics is required for maintaining normal DNA replication and have provided new insight into regulation of the transcription cycle with and without DNA damage. Moreover, our results suggest a direct role for the phospho-CTD in NHEJ repair upon DNA double-stranded breaks induced by ionizing radiation. Altogether, our results support that the RNAPII machinery plays a central role in DNA replication and repair.

6 Reference list

1. Gaillard, H., T. García-Muse and A. Aguilera, *Replication stress and cancer.* Nature Reviews Cancer, 2015. 15(5): p. 276-289.
2. Forment, J.V. and M.J. O'Connor, *Targeting the replication stress response in cancer.* Pharmacology & therapeutics, 2018. 188: p. 155-167.
3. Pilié, P.G., C. Tang, G.B. Mills and T.A. Yap, *State-of-the-art strategies for targeting the DNA damage response in cancer.* Nature reviews Clinical oncology, 2019. 16(2): p. 81-104.
4. Aunan, J.R., W.C. Cho and K. Søreide, *The biology of aging and cancer: a brief overview of shared and divergent molecular hallmarks.* Aging and disease, 2017. 8(5): p. 628.
5. Gómez-González, B. and A. Aguilera, *Transcription-mediated replication hindrance: a major driver of genome instability.* Genes & development, 2019. 33(15-16): p. 1008-1026.
6. Gaillard, H. and A. Aguilera, *Transcription as a threat to genome integrity.* Annual review of biochemistry, 2016. 85: p. 291-317.
7. Cao, S., J.R. Wang, S. Ji, P. Yang, M.D. Montierth*, et al.*, *Tumor cell total mRNA expression shapes the molecular and clinical phenotype of cancer.* bioRxiv, 2021: p. 2020.09. 30.306795.
8. Kotsantis, P., L.M. Silva, S. Irmscher, R.M. Jones, L. Folkes*, et al.*, *Increased global transcription activity as a mechanism of replication stress in cancer.* Nature communications, 2016. 7(1): p. 1-13.
9. Lavado, A., J.Y. Park, J. Pare, D. Finkelstein, H. Pan*, et al.*, *The Hippo pathway prevents YAP/TAZ-driven hypertranscription and controls neural progenitor number.* Developmental cell, 2018. 47(5): p. 576-591. e8.
10. Bowry, A., R.D. Kelly and E. Petermann, *Hypertranscription and replication stress in cancer.* Trends in Cancer, 2021. 7(9): p. 863-877.
11. Veo, B., E. Danis, A. Pierce, D. Wang, S. Fosmire*, et al.*, *Transcriptional control of DNA repair networks by CDK7 regulates sensitivity to radiation in MYC-driven medulloblastoma.* Cell Reports, 2021. 35(4): p. 109013.
12. Christensen, C.L., N. Kwiatkowski, B.J. Abraham, J. Carretero, F. Al-Shahrour*, et al.*, *Targeting transcriptional addictions in small cell lung cancer with a covalent CDK7 inhibitor.* Cancer cell, 2014. 26(6): p. 909-922.
13. Chipumuro, E., E. Marco, C.L. Christensen, N. Kwiatkowski, T. Zhang*, et al.*, *CDK7 inhibition suppresses super-enhancer-linked oncogenic transcription in MYCN-driven cancer.* Cell, 2014. 159(5): p. 1126-1139.
14. Wang, Y., T. Zhang, N. Kwiatkowski, B.J. Abraham, T.I. Lee*, et al.*, *CDK7-dependent transcriptional addiction in triple-negative breast cancer.* Cell, 2015. 163(1): p. 174-186.
15. Gaul, L. and J.Q. Svejstrup, *Transcription-coupled repair and the transcriptional response to UV-Irradiation.* DNA repair, 2021. 107: p. 103208.
16. Lindsey-Boltz, L.A. and A. Sancar, *RNA polymerase: the most specific damage recognition protein in cellular responses to DNA damage?* Proceedings of the National Academy of Sciences, 2007. 104(33): p. 13213-13214.
17. Landsverk, H.B., L.E. Sandquist, S.C. Sridhara, G.E. Rødland, J.C. Sabino*, et al.*, *Regulation of ATR activity via the RNA polymerase II associated factors CDC73 and PNUTS-PP1.* Nucleic acids research, 2019. 47(4): p. 1797-1813.
18. Lesage, E., T. Clouaire and G. Legube, *Repair of DNA double-strand breaks in RNAPI-and RNAPII-transcribed loci.* DNA repair, 2021. 104: p. 103139.
19. Montaldo, N.P., D.L. Bordin, A. Brambilla, M. Rösinger, S.L. Fordyce Martin*, et al.*, *Alkyladenine DNA glycosylase associates with transcription elongation to coordinate DNA repair with gene expression.* Nature communications, 2019. 10(1): p. 1-13.

20. Enoiu, M., J. Jiricny and O.D. Schärer, *Repair of cisplatin-induced DNA interstrand crosslinks by a replication-independent pathway involving transcription-coupled repair and translesion synthesis.* Nucleic acids research, 2012. 40(18): p. 8953-8964.
21. Vermeulen, K., D.R. Van Bockstaele and Z.N. Berneman, *The cell cycle: a review of regulation, deregulation and therapeutic targets in cancer.* Cell proliferation, 2003. 36(3): p. 131-149.
22. Schafer, K., *The cell cycle: a review.* Veterinary pathology, 1998. 35(6): p. 461-478.
23. Dimitrova, D.S., T.A. Prokhorova, J.J. Blow, I.T. Todorov and D.M. Gilbert, *Mammalian nuclei become licensed for DNA replication during late telophase.* Journal of cell science, 2002. 115(1): p. 51-59.
24. Sclafani, R. and T. Holzen, *Cell cycle regulation of DNA replication.* Annual review of genetics, 2007. 41: p. 237.
25. Yekezare, M., B. Gómez-González and J.F. Diffley, *Controlling DNA replication origins in response to DNA damage–inhibit globally, activate locally.* Journal of cell science, 2013. 126(6): p. 1297-1306.
26. Takisawa, H., S. Mimura and Y. Kubota, *Eukaryotic DNA replication: from pre-replication complex to initiation complex.* Current opinion in cell biology, 2000. 12(6): p. 690-696.
27. Grant, G.D. and J.G. Cook, *The temporal regulation of S phase proteins during G 1.* DNA Replication, 2017: p. 335-369.
28. Marchal, C., J. Sima and D.M. Gilbert, *Control of DNA replication timing in the 3D genome.* Nature Reviews Molecular Cell Biology, 2019. 20(12): p. 721-737.
29. Raghuraman, M., E.A. Winzeler, D. Collingwood, S. Hunt, L. Wodicka*, et al.*, *Replication dynamics of the yeast genome.* science, 2001. 294(5540): p. 115-121.
30. Heller, R.C., S. Kang, W.M. Lam, S. Chen, C.S. Chan*, et al.*, *Eukaryotic origin-dependent DNA replication in vitro reveals sequential action of DDK and S-CDK kinases.* Cell, 2011. 146(1): p. 80-91.
31. Kang, S., M.-S. Kang, E. Ryu and K. Myung, *Eukaryotic DNA replication: Orchestrated action of multi-subunit protein complexes.* Mutation Research/Fundamental and Molecular Mechanisms of Mutagenesis, 2018. 809: p. 58-69.
32. Boos, D. and P. Ferreira, *Origin firing regulations to control genome replication timing.* Genes, 2019. 10(3): p. 199.
33. Bryant, J.A. and S.J. Aves, *Initiation of DNA replication: functional and evolutionary aspects.* Annals of botany, 2011. 107(7): p. 1119-1126.
34. Parsons, G.G. and C.A. Spencer, *Mitotic repression of RNA polymerase II transcription is accompanied by release of transcription elongation complexes.* Molecular and Cellular Biology, 1997. 17(10): p. 5791-5802.
35. Liang, K., A.R. Woodfin, B.D. Slaughter, J.R. Unruh, A.C. Box*, et al.*, *Mitotic transcriptional activation: clearance of actively engaged Pol II via transcriptional elongation control in mitosis.* Molecular cell, 2015. 60(3): p. 435-445.
36. Jiang, Y., M. Liu, C.A. Spencer and D.H. Price, *Involvement of transcription termination factor 2 in mitotic repression of transcription elongation.* Molecular cell, 2004. 14(3): p. 375-386.
37. Sharp, J.A., C. Perea-Resa, W. Wang and M.D. Blower, *Cell division requires RNA eviction from condensing chromosomes.* Journal of Cell Biology, 2020. 219(11).
38. Clancy, S., *RNA functions.* Nature Education, 2008. 1(1): p. 102.
39. Chapman, R.D., M. Heidemann, C. Hintermair and D. Eick, *Molecular evolution of the RNA polymerase II CTD.* Trends in Genetics, 2008. 24(6): p. 289-296.
40. Harlen, K.M. and L.S. Churchman, *The code and beyond: transcription regulation by the RNA polymerase II carboxy-terminal domain.* Nature reviews Molecular cell biology, 2017. 18(4): p. 263-273.
41. Egloff, S., M. Dienstbier and S. Murphy, *Updating the RNA polymerase CTD code: adding gene-specific layers.* Trends in Genetics, 2012. 28(7): p. 333-341.
42. Custódio, N. and M. Carmo-Fonseca, *Co-transcriptional splicing and the CTD code.* Critical reviews in biochemistry and molecular biology, 2016. 51(5): p. 395-411.

43. Bentley, D.L., *Coupling mRNA processing with transcription in time and space.* Nature Reviews Genetics, 2014. 15(3): p. 163-175.
44. Nojima, T., T. Gomes, A.R.F. Grosso, H. Kimura, M.J. Dye*, et al.*, *Mammalian NET-seq reveals genome-wide nascent transcription coupled to RNA processing.* Cell, 2015. 161(3): p. 526-540.
45. Core, L. and K. Adelman, *Promoter-proximal pausing of RNA polymerase II: a nexus of gene regulation.* Genes & development, 2019. 33(15-16): p. 960-982.
46. Luse, D.S., *The RNA polymerase II preinitiation complex: through what pathway is the complex assembled?* Transcription, 2014. 5(1): p. e27050.
47. Jeronimo, C. and F. Robert, *Kin28 regulates the transient association of Mediator with core promoters.* Nature structural & molecular biology, 2014. 21(5): p. 449-455.
48. Nakamura, A. and G. Seydoux, *Less is more: specification of the germline by transcriptional repression.* 2008.
49. Rougvie, A.E. and J.T. Lis, *The RNA polymerase II molecule at the 5' end of the uninduced hsp70 gene of D. melanogaster is transcriptionally engaged.* Cell, 1988. 54(6): p. 795-804.
50. Strobl, L.J. and D. Eick, *Hold back of RNA polymerase II at the transcription start site mediates down-regulation of c-myc in vivo.* The EMBO Journal, 1992. 11(9): p. 3307-3314.
51. Tome, J.M., N.D. Tippens and J.T. Lis, *Single-molecule nascent RNA sequencing identifies regulatory domain architecture at promoters and enhancers.* Nature genetics, 2018. 50(11): p. 1533-1541.
52. Wen, Y. and A.J. Shatkin, *Transcription elongation factor hSPT5 stimulates mRNA capping.* Genes & development, 1999. 13(14): p. 1774-1779.
53. Komarnitsky, P., E.-J. Cho and S. Buratowski, *Different phosphorylated forms of RNA polymerase II and associated mRNA processing factors during transcription.* Genes & development, 2000. 14(19): p. 2452-2460.
54. Shandilya, J. and S.G. Roberts, *The transcription cycle in eukaryotes: from productive initiation to RNA polymerase II recycling.* Biochimica et Biophysica Acta (BBA)-Gene Regulatory Mechanisms, 2012. 1819(5): p. 391-400.
55. Chen, F.X., A.R. Woodfin, A. Gardini, R.A. Rickels, S.A. Marshall*, et al.*, *PAF1, a molecular regulator of promoter-proximal pausing by RNA polymerase II.* Cell, 2015. 162(5): p. 1003-1015.
56. Yu, M., W. Yang, T. Ni, Z. Tang, T. Nakadai*, et al.*, *RNA polymerase II–associated factor 1 regulates the release and phosphorylation of paused RNA polymerase II.* Science, 2015. 350(6266): p. 1383-1386.
57. Wang, Z., A. Song, H. Xu, S. Hu, B. Tao*, et al.*, *Coordinated regulation of RNA polymerase II pausing and elongation progression by PAF1.* Science Advances, 2022. 8(13): p. eabm5504.
58. Vos, S.M., L. Farnung, M. Boehning, C. Wigge, A. Linden*, et al.*, *Structure of activated transcription complex Pol II–DSIF–PAF–SPT6.* Nature, 2018. 560(7720): p. 607-612.
59. Ardehali, M.B., J. Yao, K. Adelman, N.J. Fuda, S.J. Petesch*, et al.*, *Spt6 enhances the elongation rate of RNA polymerase II in vivo.* The EMBO journal, 2009. 28(8): p. 1067-1077.
60. Heidemann, M., C. Hintermair, K. Voß and D. Eick, *Dynamic phosphorylation patterns of RNA polymerase II CTD during transcription.* Biochimica et Biophysica Acta (BBA)-Gene Regulatory Mechanisms, 2013. 1829(1): p. 55-62.
61. Proudfoot, N.J., *Transcriptional termination in mammals: Stopping the RNA polymerase II juggernaut.* Science, 2016. 352(6291): p. aad9926.
62. Rosonina, E., S. Kaneko and J.L. Manley, *Terminating the transcript: breaking up is hard to do.* Genes & development, 2006. 20(9): p. 1050-1056.
63. West, S., N. Gromak and N.J. Proudfoot, *Human 5'→ 3' exonuclease Xrn2 promotes transcription termination at co-transcriptional cleavage sites.* Nature, 2004. 432(7016): p. 522-525.

64. Cossa, G., P.K. Parua, M. Eilers and R.P. Fisher, *Protein phosphatases in the RNAPII transcription cycle: erasers, sculptors, gatekeepers, and potential drug targets.* Genes & Development, 2021. 35(9-10): p. 658-676.
65. Contreras, X., M. Benkirane and R. Kiernan, *Premature termination of transcription by RNAP II: the beginning of the end.* Transcription, 2013. 4(2): p. 72-76.
66. Jensen, T.H., A. Jacquier and D. Libri, *Dealing with pervasive transcription.* Molecular cell, 2013. 52(4): p. 473-484.
67. Eaton, J.D. and S. West, *Termination of transcription by RNA polymerase II: BOOM!* Trends in Genetics, 2020. 36(9): p. 664-675.
68. Boehning, M., C. Dugast-Darzacq, M. Rankovic, A.S. Hansen, T. Yu*, et al.*, *RNA polymerase II clustering through carboxy-terminal domain phase separation.* Nature structural & molecular biology, 2018. 25(9): p. 833-840.
69. Boija, A., I.A. Klein, B.R. Sabari, A. Dall'Agnese, E.L. Coffey*, et al.*, *Transcription factors activate genes through the phase-separation capacity of their activation domains.* Cell, 2018. 175(7): p. 1842-1855. e16.
70. Guo, Y.E., J.C. Manteiga, J.E. Henninger, B.R. Sabari, A. Dall'Agnese*, et al.*, *Pol II phosphorylation regulates a switch between transcriptional and splicing condensates.* Nature, 2019. 572(7770): p. 543-548.
71. Lu, H., D. Yu, A.S. Hansen, S. Ganguly, R. Liu*, et al.*, *Phase-separation mechanism for C-terminal hyperphosphorylation of RNA polymerase II.* Nature, 2018. 558(7709): p. 318-323.
72. Max, T., M. Søgaard and J.Q. Svejstrup, *Hyperphosphorylation of the C-terminal repeat domain of RNA polymerase II facilitates dissociation of its complex with mediator.* Journal of Biological Chemistry, 2007. 282(19): p. 14113-14120.
73. Banani, S.F., H.O. Lee, A.A. Hyman and M.K. Rosen, *Biomolecular condensates: organizers of cellular biochemistry.* Nature reviews Molecular cell biology, 2017. 18(5): p. 285-298.
74. Li, P., S. Banjade, H.-C. Cheng, S. Kim, B. Chen*, et al.*, *Phase transitions in the assembly of multivalent signalling proteins.* Nature, 2012. 483(7389): p. 336-340.
75. Kwon, I., M. Kato, S. Xiang, L. Wu, P. Theodoropoulos*, et al.*, *Phosphorylation-regulated binding of RNA polymerase II to fibrous polymers of low-complexity domains.* Cell, 2013. 155(5): p. 1049-1060.
76. Yamaguchi, Y., H. Shibata and H. Handa, *Transcription elongation factors DSIF and NELF: promoter-proximal pausing and beyond.* Biochimica Et Biophysica Acta (BBA)-Gene Regulatory Mechanisms, 2013. 1829(1): p. 98-104.
77. Guo, Q., X. Shi and X. Wang, *RNA and liquid-liquid phase separation.* Non-coding RNA Research, 2021. 6(2): p. 92-99.
78. Ciccia, A. and S.J. Elledge, *The DNA damage response: making it safe to play with knives.* Molecular cell, 2010. 40(2): p. 179-204.
79. Jackson, S.P. and J. Bartek, *The DNA-damage response in human biology and disease.* Nature, 2009. 461(7267): p. 1071-1078.
80. Lindahl, T., *Instability and decay of the primary structure of DNA.* nature, 1993. 362(6422): p. 709-715.
81. Ashton, N.W., E. Bolderson, L. Cubeddu, K.J. O'Byrne and D.J. Richard, *Human single-stranded DNA binding proteins are essential for maintaining genomic stability.* BMC molecular biology, 2013. 14(1): p. 1-20.
82. Pfeiffer, P., W. Goedecke and G. Obe, *Mechanisms of DNA double-strand break repair and their potential to induce chromosomal aberrations.* Mutagenesis, 2000. 15(4): p. 289-302.
83. Kuzminov, A., *Single-strand interruptions in replicating chromosomes cause double-strand breaks.* Proceedings of the National Academy of Sciences, 2001. 98(15): p. 8241-8246.
84. Zeman, M.K. and K.A. Cimprich, *Causes and consequences of replication stress.* Nature cell biology, 2014. 16(1): p. 2-9.
85. García-Muse, T. and A. Aguilera, *Transcription–replication conflicts: how they occur and how they are resolved.* Nature reviews Molecular cell biology, 2016. 17(9): p. 553-563.

86. Champoux, J.J., *DNA topoisomerases: structure, function, and mechanism.* Annual review of biochemistry, 2001. 70(1): p. 369-413.
87. Wang, J.C., *Cellular roles of DNA topoisomerases: a molecular perspective.* Nature reviews Molecular cell biology, 2002. 3(6): p. 430-440.
88. Cristini, A., M. Géraud and O. Sordet, *Chapter Five - Transcription-associated DNA breaks and cancer: A matter of DNA topology*, in *International Review of Cell and Molecular Biology*, U. Weyemi and L. Galluzzi, Editors. 2021, Academic Press. p. 195-240.
89. Williams, G.M. and A.M. Jeffrey, *Oxidative DNA damage: endogenous and chemically induced.* Regulatory Toxicology and Pharmacology, 2000. 32(3): p. 283-292.
90. Ray, P.D., B.-W. Huang and Y. Tsuji, *Reactive oxygen species (ROS) homeostasis and redox regulation in cellular signaling.* Cellular signalling, 2012. 24(5): p. 981-990.
91. Srinivas, U.S., B.W. Tan, B.A. Vellayappan and A.D. Jeyasekharan, *ROS and the DNA damage response in cancer.* Redox biology, 2019. 25: p. 101084.
92. Chatterjee, N. and G.C. Walker, *Mechanisms of DNA damage, repair, and mutagenesis.* Environmental and molecular mutagenesis, 2017. 58(5): p. 235-263.
93. Cannan, W.J., B.P. Tsang, S.S. Wallace and D.S. Pederson, *Nucleosomes suppress the formation of double-strand DNA breaks during attempted base excision repair of clustered oxidative damages.* Journal of Biological Chemistry, 2014. 289(29): p. 19881-19893.
94. Vesela, E., K. Chroma, Z. Turi and M. Mistrik, *Common chemical inductors of replication stress: focus on cell-based studies.* Biomolecules, 2017. 7(1): p. 19.
95. McGregor, W.G. *DNA repair, DNA replication, and UV mutagenesis*. in *Journal of Investigative Dermatology Symposium Proceedings*. 1999. Elsevier.
96. Dhuppar, S., S. Roy and A. Mazumder, *γH2AX in the S phase after UV irradiation corresponds to DNA replication and does not report on the extent of DNA damage.* Molecular and cellular biology, 2020. 40(20): p. e00328-20.
97. Lans, H., J.H. Hoeijmakers, W. Vermeulen and J.A. Marteijn, *The DNA damage response to transcription stress.* Nature reviews Molecular cell biology, 2019. 20(12): p. 766-784.
98. Vidaković, A.T., R. Mitter, G.P. Kelly, M. Neumann, M. Harreman*, et al.*, *Regulation of the RNAPII pool is integral to the DNA damage response.* Cell, 2020. 180(6): p. 1245-1261. e21.
99. Williamson, L., M. Saponaro, S. Boeing, P. East, R. Mitter*, et al.*, *UV irradiation induces a non-coding RNA that functionally opposes the protein encoded by the same gene.* Cell, 2017. 168(5): p. 843-855. e13.
100. Wilson, M.D., M. Harreman and J.Q. Svejstrup, *Ubiquitylation and degradation of elongating RNA polymerase II: the last resort.* Biochimica et Biophysica Acta (BBA)-Gene Regulatory Mechanisms, 2013. 1829(1): p. 151-157.
101. Wilson, M.D., M. Harreman, M. Taschner, J. Reid, J. Walker*, et al.*, *Proteasome-mediated processing of Def1, a critical step in the cellular response to transcription stress.* Cell, 2013. 154(5): p. 983-995.
102. Ratner, J.N., B. Balasubramanian, J. Corden, S.L. Warren and D.B. Bregman, *Ultraviolet radiation-induced ubiquitination and proteasomal degradation of the large subunit of RNA polymerase II: implications for transcription-coupled DNA repair.* Journal of Biological Chemistry, 1998. 273(9): p. 5184-5189.
103. Ward, J.F., *DNA damage produced by ionizing radiation in mammalian cells: identities, mechanisms of formation, and reparability.* Progress in nucleic acid research and molecular biology, 1988. 35: p. 95-125.
104. Ward, J., *The yield of DNA double-strand breaks produced intracellularly by ionizing radiation: a review.* International journal of radiation biology, 1990. 57(6): p. 1141-1150.
105. Ma, W., C.J. Halweg, D. Menendez and M.A. Resnick, *Differential effects of poly (ADP-ribose) polymerase inhibition on DNA break repair in human cells are revealed with Epstein–Barr virus.* Proceedings of the National Academy of Sciences, 2012. 109(17): p. 6590-6595.
106. Olive, P.L., *The role of DNA single-and double-strand breaks in cell killing by ionizing radiation.* Radiation research, 1998. 150(5s): p. S42-S51.

107. Stinson, B.M. and J.J. Loparo, *Repair of DNA double-strand breaks by the nonhomologous end joining pathway.* Annual Review of Biochemistry, 2021. 90: p. 137-164.
108. Rothkamm, K., I. Kruger, L.H. Thompson and M. Löbrich, *Pathways of DNA double-strand break repair during the mammalian cell cycle.* Molecular and cellular biology, 2003. 23(16): p. 5706-5715.
109. Zhou, B.-B.S. and S.J. Elledge, *The DNA damage response: putting checkpoints in perspective.* Nature, 2000. 408(6811): p. 433-439.
110. Blackford, A.N. and S.P. Jackson, *ATM, ATR, and DNA-PK: The Trinity at the Heart of the DNA Damage Response.* Molecular cell, 2017. 66(6): p. 801-817.
111. Löbrich, M. and P.A. Jeggo, *Harmonising the response to DSBs: a new string in the ATM bow.* DNA repair, 2005. 4(7): p. 749-759.
112. Cimprich, K.A. and D. Cortez, *ATR: an essential regulator of genome integrity.* Nature reviews Molecular cell biology, 2008. 9(8): p. 616-627.
113. Maréchal, A. and L. Zou, *DNA damage sensing by the ATM and ATR kinases.* Cold Spring Harbor perspectives in biology, 2013. 5(9): p. a012716.
114. Matsuoka, S., B.A. Ballif, A. Smogorzewska, E.R. McDonald III, K.E. Hurov*, et al.*, *ATM and ATR substrate analysis reveals extensive protein networks responsive to DNA damage.* science, 2007. 316(5828): p. 1160-1166.
115. Gell, D. and S.P. Jackson, *Mapping of protein-protein interactions within the DNA-dependent protein kinase complex.* Nucleic acids research, 1999. 27(17): p. 3494-3502.
116. Singleton, B., M. Torres-Arzayus, S. Rottinghaus, G. Taccioli and P. Jeggo, *The C terminus of Ku80 activates the DNA-dependent protein kinase catalytic subunit.* Molecular and cellular biology, 1999. 19(5): p. 3267-3277.
117. Falck, J., J. Coates and S.P. Jackson, *Conserved modes of recruitment of ATM, ATR and DNA-PKcs to sites of DNA damage.* Nature, 2005. 434(7033): p. 605-611.
118. Carson, C.T., R.A. Schwartz, T.H. Stracker, C.E. Lilley, D.V. Lee*, et al.*, *The Mre11 complex is required for ATM activation and the G2/M checkpoint.* The EMBO journal, 2003. 22(24): p. 6610-6620.
119. Lee, J.-H. and T.T. Paull, *ATM activation by DNA double-strand breaks through the Mre11-Rad50-Nbs1 complex.* Science, 2005. 308(5721): p. 551-554.
120. Zou, L. and S.J. Elledge, *Sensing DNA damage through ATRIP recognition of RPA-ssDNA complexes.* Science, 2003. 300(5625): p. 1542-1548.
121. Schreiber, V., F. Dantzer, J.-C. Ame and G. De Murcia, *Poly (ADP-ribose): novel functions for an old molecule.* Nature reviews Molecular cell biology, 2006. 7(7): p. 517-528.
122. Langelier, M.-F. and J.M. Pascal, *PARP-1 mechanism for coupling DNA damage detection to poly (ADP-ribose) synthesis.* Current opinion in structural biology, 2013. 23(1): p. 134-143.
123. Ray Chaudhuri, A. and A. Nussenzweig, *The multifaceted roles of PARP1 in DNA repair and chromatin remodelling.* Nature reviews Molecular cell biology, 2017. 18(10): p. 610-621.
124. Noe Gonzalez, M., D. Blears and J.Q. Svejstrup, *Causes and consequences of RNA polymerase II stalling during transcript elongation.* Nature Reviews Molecular Cell Biology, 2021. 22(1): p. 3-21.
125. Ljungman, M. and F. Zhang, *Blockage of RNA polymerase as a possible trigger for UV light-induced apoptosis. Oncogene 13, 823-831.* Oncogene, 1996. 13: p. 823-31.
126. Derheimer, F.A., H.M. O'Hagan, H.M. Krueger, S. Hanasoge, M.T. Paulsen*, et al.*, *RPA and ATR link transcriptional stress to p53.* Proceedings of the National Academy of Sciences, 2007. 104(31): p. 12778-12783.
127. Williams, A.B. and B. Schumacher, *p53 in the DNA-damage-repair process.* Cold Spring Harbor perspectives in medicine, 2016. 6(5): p. a026070.
128. Jia, N., C. Guo, Y. Nakazawa, D. van den Heuvel, M.S. Luijsterburg*, et al.*, *Dealing with transcription-blocking DNA damage: repair mechanisms, RNA polymerase II processing and human disorders.* DNA repair, 2021. 106: p. 103192.

129. Lindahl, T. and D. Barnes. *Repair of endogenous DNA damage*. in *Cold Spring Harbor symposia on quantitative biology*. 2000. Cold Spring Harbor Laboratory Press.
130. Ljungman, M. and D.P. Lane, *Transcription—guarding the genome by sensing DNA damage.* Nature Reviews Cancer, 2004. 4(9): p. 727-737.
131. Vermeulen, W. and M. Fousteri, *Mammalian transcription-coupled excision repair.* Cold Spring Harbor perspectives in biology, 2013. 5(8): p. a012625.
132. Lomax, M., L. Folkes and P. O'neill, *Biological consequences of radiation-induced DNA damage: relevance to radiotherapy.* Clinical oncology, 2013. 25(10): p. 578-585.
133. Chapman, J.R., M.R. Taylor and S.J. Boulton, *Playing the end game: DNA double-strand break repair pathway choice.* Molecular cell, 2012. 47(4): p. 497-510.
134. Löbrich, M., A. Shibata, A. Beucher, A. Fisher, M. Ensminger*, et al.*, *γH2AX foci analysis for monitoring DNA double-strand break repair: strengths, limitations and optimization.* Cell cycle, 2010. 9(4): p. 662-669.
135. Brandsma, I. and D.C. van Gent, *Pathway choice in DNA double strand break repair: observations of a balancing act.* Genome integrity, 2012. 3(1): p. 1-10.
136. Beucher, A., J. Birraux, L. Tchouandong, O. Barton, A. Shibata*, et al.*, *ATM and Artemis promote homologous recombination of radiation-induced DNA double-strand breaks in G2.* The EMBO journal, 2009. 28(21): p. 3413-3427.
137. Rothkamm, K. and M. Löbrich, *Evidence for a lack of DNA double-strand break repair in human cells exposed to very low x-ray doses.* Proceedings of the National Academy of Sciences, 2003. 100(9): p. 5057-5062.
138. Deriano, L. and D.B. Roth, *Modernizing the nonhomologous end-joining repertoire: alternative and classical NHEJ share the stage.* Annual review of genetics, 2013. 47(1): p. 433-55.
139. Huertas, P., F. Cortés-Ledesma, A.A. Sartori, A. Aguilera and S.P. Jackson, *CDK targets Sae2 to control DNA-end resection and homologous recombination.* Nature, 2008. 455(7213): p. 689-692.
140. Jazayeri, A., J. Falck, C. Lukas, J. Bartek, G.C. Smith*, et al.*, *ATM-and cell cycle-dependent regulation of ATR in response to DNA double-strand breaks.* Nature cell biology, 2006. 8(1): p. 37-45.
141. Ira, G., A. Pellicioli, A. Balijja, X. Wang, S. Fiorani*, et al.*, *DNA end resection, homologous recombination and DNA damage checkpoint activation require CDK1.* Nature, 2004. 431(7011): p. 1011-1017.
142. Mladenov, E., S. Magin, A. Soni and G. Iliakis. *DNA double-strand-break repair in higher eukaryotes and its role in genomic instability and cancer: Cell cycle and proliferation-dependent regulation*. in *Seminars in cancer biology*. 2016. Elsevier.
143. Chakraborty, A., N. Tapryal, T. Venkova, N. Horikoshi, R.K. Pandita*, et al.*, *Classical non-homologous end-joining pathway utilizes nascent RNA for error-free double-strand break repair of transcribed genes.* Nature communications, 2016. 7(1): p. 1-12.
144. Kakarougkas, A. and P. Jeggo, *DNA DSB repair pathway choice: an orchestrated handover mechanism.* The British journal of radiology, 2014. 87(1035): p. 20130685.
145. Krietsch, J., M.-C. Caron, J.-P. Gagne, C. Ethier, J. Vignard*, et al.*, *PARP activation regulates the RNA-binding protein NONO in the DNA damage response to DNA double-strand breaks.* Nucleic acids research, 2012. 40(20): p. 10287-10301.
146. Jaafar, L., Z. Li, S. Li and W.S. Dynan, *SFPQ• NONO and XLF function separately and together to promote DNA double-strand break repair via canonical nonhomologous end joining.* Nucleic acids research, 2017. 45(4): p. 1848-1859.
147. Shamanna, R.A., M. Hoque, A. Lewis-Antes, E.I. Azzam, D. Lagunoff*, et al.*, *The NF90/NF45 complex participates in DNA break repair via nonhomologous end joining.* Molecular and cellular biology, 2011. 31(23): p. 4832-4843.

148. Yu, Z., S.Y. Mersaoui, L. Guitton-Sert, Y. Coulombe, J. Song*, et al.*, *DDX5 resolves R-loops at DNA double-strand breaks to promote DNA repair and avoid chromosomal deletions.* NAR cancer, 2020. 2(3): p. zcaa028.
149. Chang, C., P. Chu, P. Wu, M. Yu, J. Lee*, et al.*, *PHRF1 promotes genome integrity by modulating non-homologous end-joining.* Cell Death & Disease, 2015. 6(4): p. e1716-e1716.
150. Chapman, J.R., P. Barral, J.-B. Vannier, V. Borel, M. Steger*, et al.*, *RIF1 is essential for 53BP1-dependent nonhomologous end joining and suppression of DNA double-strand break resection.* Molecular cell, 2013. 49(5): p. 858-871.
151. Dang, T.T. and J.C. Morales, *XRN2 Links RNA: DNA hybrid resolution to double strand break repair pathway choice.* Cancers, 2020. 12(7): p. 1821.
152. Hu, W., L. Lei, X. Xie, L. Huang, Q. Cui*, et al.*, *Heterogeneous nuclear ribonucleoprotein L facilitates recruitment of 53BP1 and BRCA1 at the DNA break sites induced by oxaliplatin in colorectal cancer.* Cell Death & Disease, 2019. 10(8): p. 550.
153. Morales, J.C., P. Richard, A. Rommel, F.J. Fattah, E.A. Motea*, et al.*, *Kub5-Hera, the human Rtt103 homolog, plays dual functional roles in transcription termination and DNA repair.* Nucleic acids research, 2014. 42(8): p. 4996-5006.
154. Hansen, R.K., A. Mund, S.L. Poulsen, M. Sandoval, K. Klement*, et al.*, *SCAI promotes DNA double-strand break repair in distinct chromosomal contexts.* Nature cell biology, 2016. 18(12): p. 1357-1366.
155. Smeenk, G., W.W. Wiegant, J.A. Marteijn, M.S. Luijsterburg, N. Sroczynski*, et al.*, *Poly (ADP-ribosyl) ation links the chromatin remodeler SMARCA5/SNF2H to RNF168-dependent DNA damage signaling.* Journal of cell science, 2013. 126(4): p. 889-903.
156. Ramsden, D.A., J. Carvajal-Garcia and G.P. Gupta, *Mechanism, cellular functions and cancer roles of polymerase-theta-mediated DNA end joining.* Nature Reviews Molecular Cell Biology, 2022. 23(2): p. 125-140.
157. Deriano, L., T.H. Stracker, A. Baker, J.H. Petrini and D.B. Roth, *Roles for NBS1 in alternative nonhomologous end-joining of V (D) J recombination intermediates.* Molecular cell, 2009. 34(1): p. 13-25.
158. Mansour, W.Y., T. Rhein and J. Dahm-Daphi, *The alternative end-joining pathway for repair of DNA double-strand breaks requires PARP1 but is not dependent upon microhomologies.* Nucleic Acids Research, 2010. 38(18): p. 6065-6077.
159. Lee-Theilen, M., A.J. Matthews, D. Kelly, S. Zheng and J. Chaudhuri, *CtIP promotes microhomology-mediated alternative end joining during class-switch recombination.* Nature structural & molecular biology, 2011. 18(1): p. 75-79.
160. Mateos-Gomez, P.A., F. Gong, N. Nair, K.M. Miller, E. Lazzerini-Denchi*, et al.*, *Mammalian polymerase ϑ promotes alternative NHEJ and suppresses recombination.* Nature, 2015. 518(7538): p. 254-257.
161. Luedeman, M.E., S. Stroik, W. Feng, A.J. Luthman, G.P. Gupta*, et al.*, *Poly (ADP) ribose polymerase promotes DNA polymerase theta-mediated end joining by activation of end resection.* Nature communications, 2022. 13(1): p. 1-10.
162. Bothmer, A., D.F. Robbiani, N. Feldhahn, A. Gazumyan, A. Nussenzweig*, et al.*, *53BP1 regulates DNA resection and the choice between classical and alternative end joining during class switch recombination.* Journal of Experimental Medicine, 2010. 207(4): p. 855-865.
163. Escribano-Díaz, C., A. Orthwein, A. Fradet-Turcotte, M. Xing, J.T. Young*, et al.*, *A cell cycle-dependent regulatory circuit composed of 53BP1-RIF1 and BRCA1-CtIP controls DNA repair pathway choice.* Molecular cell, 2013. 49(5): p. 872-883.
164. Zimmermann, M., F. Lottersberger, S.B. Buonomo, A. Sfeir and T. de Lange, *53BP1 regulates DSB repair using Rif1 to control 5' end resection.* Science, 2013. 339(6120): p. 700-704.
165. Chapman, J.R., A.J. Sossick, S.J. Boulton and S.P. Jackson, *BRCA1-associated exclusion of 53BP1 from DNA damage sites underlies temporal control of DNA repair.* Journal of cell science, 2012. 125(15): p. 3529-3534.

166. Isobe, S.-Y., K. Nagao, N. Nozaki, H. Kimura and C. Obuse, *Inhibition of RIF1 by SCAI allows BRCA1-mediated repair.* Cell reports, 2017. 20(2): p. 297-307.
167. Batenburg, N.L., J.R. Walker, S.M. Noordermeer, N. Moatti, D. Durocher*, et al.*, *ATM and CDK2 control chromatin remodeler CSB to inhibit RIF1 in DSB repair pathway choice.* Nature communications, 2017. 8(1): p. 1-17.
168. Aymard, F., B. Bugler, C.K. Schmidt, E. Guillou, P. Caron*, et al.*, *Transcriptionally active chromatin recruits homologous recombination at DNA double-strand breaks.* Nature structural & molecular biology, 2014. 21(4): p. 366-374.
169. Shibata, A., S. Conrad, J. Birraux, V. Geuting, O. Barton*, et al.*, *Factors determining DNA double-strand break repair pathway choice in G2 phase.* The EMBO journal, 2011. 30(6): p. 1079-1092.
170. Machour, F.E. and N. Ayoub, *Transcriptional regulation at DSBs: mechanisms and consequences.* Trends in Genetics, 2020. 36(12): p. 981-997.
171. Ui, A., N. Chiba and A. Yasui, *Relationship among DNA double-strand break (DSB), DSB repair, and transcription prevents genome instability and cancer.* Cancer science, 2020. 111(5): p. 1443-1451.
172. Min, S., J.-H. Ji, Y. Heo and H. Cho, *Transcriptional regulation and chromatin dynamics at DNA double-strand breaks.* Experimental & Molecular Medicine, 2022: p. 1-8.
173. Shanbhag, N.M., I.U. Rafalska-Metcalf, C. Balane-Bolivar, S.M. Janicki and R.A. Greenberg, *ATM-dependent chromatin changes silence transcription in cis to DNA double-strand breaks.* Cell, 2010. 141(6): p. 970-981.
174. Pankotai, T., C. Bonhomme, D. Chen and E. Soutoglou, *DNAPKcs-dependent arrest of RNA polymerase II transcription in the presence of DNA breaks.* Nature structural & molecular biology, 2012. 19(3): p. 276-282.
175. Caron, P., T. Pankotai, W.W. Wiegant, M.A. Tollenaere, A. Furst*, et al.*, *WWP2 ubiquitylates RNA polymerase II for DNA-PK-dependent transcription arrest and repair at DNA breaks.* Genes & development, 2019. 33(11-12): p. 684-704.
176. Awwad, S.W., E.R. Abu-Zhayia, N. Guttmann-Raviv and N. Ayoub, *NELF-E is recruited to DNA double-strand break sites to promote transcriptional repression and repair.* EMBO reports, 2017. 18(5): p. 745-764.
177. D'Alessandro, G. and F.d.A. di Fagagna, *Transcription and DNA damage: holding hands or crossing swords?* Journal of molecular biology, 2017. 429(21): p. 3215-3229.
178. Wei, W., Z. Ba, M. Gao, Y. Wu, Y. Ma*, et al.*, *A role for small RNAs in DNA double-strand break repair.* Cell, 2012. 149(1): p. 101-112.
179. Michelini, F., S. Pitchiaya, V. Vitelli, S. Sharma, U. Gioia*, et al.*, *Damage-induced lncRNAs control the DNA damage response through interaction with DDRNAs at individual double-strand breaks.* Nature cell biology, 2017. 19(12): p. 1400-1411.
180. Francia, S., F. Michelini, A. Saxena, D. Tang, M. De Hoon*, et al.*, *Site-specific DICER and DROSHA RNA products control the DNA-damage response.* Nature, 2012. 488(7410): p. 231-235.
181. Sharma, S., R. Anand, X. Zhang, S. Francia, F. Michelini*, et al.*, *MRE11-RAD50-NBS1 complex is sufficient to promote transcription by RNA polymerase II at double-strand breaks by melting DNA ends.* Cell reports, 2021. 34(1): p. 108565.
182. D'Alessandro, G., D.R. Whelan, S.M. Howard, V. Vitelli, X. Renaudin*, et al.*, *BRCA2 controls DNA: RNA hybrid level at DSBs by mediating RNase H2 recruitment.* Nature communications, 2018. 9(1): p. 1-17.
183. Pessina, F., F. Giavazzi, Y. Yin, U. Gioia, V. Vitelli*, et al.*, *Functional transcription promoters at DNA double-strand breaks mediate RNA-driven phase separation of damage-response factors.* Nature cell biology, 2019. 21(10): p. 1286-1299.
184. Ohle, C., R. Tesorero, G. Schermann, N. Dobrev, I. Sinning*, et al.*, *Transient RNA-DNA hybrids are required for efficient double-strand break repair.* Cell, 2016. 167(4): p. 1001-1013. e7.

185. Francia, S., M. Cabrini, V. Matti, A. Oldani and F. d'Adda di Fagagna, *DICER, DROSHA and DNA damage response RNAs are necessary for the secondary recruitment of DNA damage response factors.* Journal of cell science, 2016. 129(7): p. 1468-1476.
186. Vítor, A.C., S.C. Sridhara, J.C. Sabino, A.I. Afonso, A.R. Grosso*, et al.*, *Single-molecule imaging of transcription at damaged chromatin.* Science advances, 2019. 5(1): p. eaau1249.
187. Unfried, J.P., M. Marín-Baquero, Á. Rivera-Calzada, N. Razquin, E.M. Martín-Cuevas*, et al.*, *Long noncoding RNA NIHCOLE promotes ligation efficiency of DNA double-strand breaks in hepatocellular carcinoma.* Cancer research, 2021. 81(19): p. 4910-4925.
188. Thapar, R., J.L. Wang, M. Hammel, R. Ye, K. Liang*, et al.*, *Mechanism of efficient double-strand break repair by a long non-coding RNA.* Nucleic acids research, 2020. 48(19): p. 10953-10972.
189. Marnef, A. and G. Legube, *R-loops as Janus-faced modulators of DNA repair.* Nature cell biology, 2021. 23(4): p. 305-313.
190. Gómez-Cabello, D., G. Pappas, D. Aguilar-Morante, C. Dinant and J. Bartek, *CtIP-dependent nascent RNA expression flanking DNA breaks guides the choice of DNA repair pathway.* Nature communications, 2022. 13(1): p. 1-15.
191. Pfister, S.X., S. Ahrabi, L.-P. Zalmas, S. Sarkar, F. Aymard*, et al.*, *SETD2-dependent histone H3K36 trimethylation is required for homologous recombination repair and genome stability.* Cell reports, 2014. 7(6): p. 2006-2018.
192. Tang, J., N.W. Cho, G. Cui, E.M. Manion, N.M. Shanbhag*, et al.*, *Acetylation limits 53BP1 association with damaged chromatin to promote homologous recombination.* Nature structural & molecular biology, 2013. 20(3): p. 317-325.
193. Maldonado, E., R. Shiekhattar, M. Sheldon, H. Cho, R. Drapkin*, et al.*, *A human RNA polymerase II complex associated with SRB and DNA-repair proteins.* Nature, 1996. 381(6577): p. 86-89.
194. Cox, M.M., *Recombinational DNA repair of damaged replication forks in Escherichia coli.* Annu. Rev. Genet, 2001. 35: p. 35-82.
195. Woodford, K.J., K. Usdin and M.N. Weitzmann, *DNA secondary structures and the evolution of hypervariable tandem arrays.* Journal of Biological Chemistry, 1997. 272(14): p. 9517-9523.
196. Brewer, B.J., D. Lockshon and W.L. Fangman, *The arrest of replication forks in the rDNA of yeast occurs independently of transcription.* Cell, 1992. 71(2): p. 267-276.
197. Beck, H., V. Nähse-Kumpf, M.S.Y. Larsen, K.A. O'Hanlon, S. Patzke*, et al.*, *Cyclin-dependent kinase suppression by WEE1 kinase protects the genome through control of replication initiation and nucleotide consumption.* Molecular and cellular biology, 2012. 32(20): p. 4226-4236.
198. da Costa, A.A., D. Chowdhury, G.I. Shapiro, A.D. D'Andrea and P.A. Konstantinopoulos, *Targeting replication stress in cancer therapy.* Nature Reviews Drug Discovery, 2022: p. 1-21.
199. Wei, X., J. Samarabandu, R.S. Devdhar, A.J. Siegel, R. Acharya*, et al.*, *Segregation of transcription and replication sites into higher order domains.* Science, 1998. 281(5382): p. 1502-1505.
200. Hamperl, S., M.J. Bocek, J.C. Saldivar, T. Swigut and K.A. Cimprich, *Transcription-replication conflict orientation modulates R-loop levels and activates distinct DNA damage responses.* Cell, 2017. 170(4): p. 774-786. e19.
201. Lang, K.S., A.N. Hall, C.N. Merrikh, M. Ragheb, H. Tabakh*, et al.*, *Replication-transcription conflicts generate R-loops that orchestrate bacterial stress survival and pathogenesis.* Cell, 2017. 170(4): p. 787-799. e18.
202. Prado, F. and A. Aguilera, *Impairment of replication fork progression mediates RNA polII transcription-associated recombination.* The EMBO journal, 2005. 24(6): p. 1267-1276.
203. Gottipati, P., T.N. Cassel, L. Savolainen and T. Helleday, *Transcription-associated recombination is dependent on replication in Mammalian cells.* Molecular and cellular biology, 2008. 28(1): p. 154-164.
204. Hamperl, S. and K.A. Cimprich, *Conflict resolution in the genome: how transcription and replication make it work.* Cell, 2016. 167(6): p. 1455-1467.

205. Liu, B. and B.M. Alberts, *Head-on collision between a DNA replication apparatus and RNA polymerase transcription complex.* Science, 1995. 267(5201): p. 1131-1137.
206. Srivatsan, A., A. Tehranchi, D.M. MacAlpine and J.D. Wang, *Co-orientation of replication and transcription preserves genome integrity.* PLoS genetics, 2010. 6(1): p. e1000810.
207. Liu, B., M. Lie Wong, R.L. Tinker, E.P. Geiduschek and B.M. Alberts, *The DNA replication fork can pass RNA polymerase without displacing the nascent transcript.* Nature, 1993. 366(6450): p. 33-39.
208. Pomerantz, R.T. and M. O'Donnell, *The replisome uses mRNA as a primer after colliding with RNA polymerase.* Nature, 2008. 456(7223): p. 762-766.
209. Pomerantz, R.T. and M. O'Donnell, *Direct restart of a replication fork stalled by a head-on RNA polymerase.* Science, 2010. 327(5965): p. 590-592.
210. Merrikh, H., Y. Zhang, A.D. Grossman and J.D. Wang, *Replication–transcription conflicts in bacteria.* Nature Reviews Microbiology, 2012. 10(7): p. 449-458.
211. Guy, L. and C.-A.H. Roten, *Genometric analyses of the organization of circular chromosomes: a universal pressure determines the direction of ribosomal RNA genes transcription relative to chromosome replication.* Gene, 2004. 340(1): p. 45-52.
212. Ivessa, A.S., J.-Q. Zhou and V.A. Zakian, *The Saccharomyces Pif1p DNA helicase and the highly related Rrm3p have opposite effects on replication fork progression in ribosomal DNA.* Cell, 2000. 100(4): p. 479-489.
213. Gilbert, D.M., *Replication timing and transcriptional control: beyond cause and effect.* Current opinion in cell biology, 2002. 14(3): p. 377-383.
214. Meryet-Figuiere, M., B. Alaei-Mahabadi, M.M. Ali, S. Mitra, S. Subhash*, et al.*, *Temporal separation of replication and transcription during S-phase progression.* Cell Cycle, 2014. 13(20): p. 3241-3248.
215. Helmrich, A., M. Ballarino and L. Tora, *Collisions between replication and transcription complexes cause common fragile site instability at the longest human genes.* Molecular cell, 2011. 44(6): p. 966-977.
216. Barlow, J.H., R.B. Faryabi, E. Callén, N. Wong, A. Malhowski*, et al.*, *Identification of early replicating fragile sites that contribute to genome instability.* Cell, 2013. 152(3): p. 620-632.
217. Mortusewicz, O., P. Herr and T. Helleday, *Early replication fragile sites: where replication–transcription collisions cause genetic instability.* The EMBO journal, 2013. 32(4): p. 493-495.
218. Bermejo, R., M.S. Lai and M. Foiani, *Preventing replication stress to maintain genome stability: resolving conflicts between replication and transcription.* Molecular cell, 2012. 45(6): p. 710-718.
219. Bermejo, R., Y. Doksani, T. Capra, Y.-M. Katou, H. Tanaka*, et al.*, *Top1-and Top2-mediated topological transitions at replication forks ensure fork progression and stability and prevent DNA damage checkpoint activation.* Genes & development, 2007. 21(15): p. 1921-1936.
220. Tuduri, S., L. Crabbé, C. Conti, H. Tourrière, H. Holtgreve-Grez*, et al.*, *Topoisomerase I suppresses genomic instability by preventing interference between replication and transcription.* Nature cell biology, 2009. 11(11): p. 1315-1324.
221. Zhao, J., A. Bacolla, G. Wang and K.M. Vasquez, *Non-B DNA structure-induced genetic instability and evolution.* Cellular and molecular life sciences, 2010. 67(1): p. 43-62.
222. Gan, W., Z. Guan, J. Liu, T. Gui, K. Shen*, et al.*, *R-loop-mediated genomic instability is caused by impairment of replication fork progression.* Genes & development, 2011. 25(19): p. 2041-2056.
223. Hegazy, Y.A., C.M. Fernando and E.J. Tran, *The balancing act of R-loop biology: The good, the bad, and the ugly.* Journal of Biological Chemistry, 2020. 295(4): p. 905-913.
224. Aguilera, A. and T. García-Muse, *R loops: from transcription byproducts to threats to genome stability.* Molecular cell, 2012. 46(2): p. 115-124.
225. Nudler, E., *RNA polymerase backtracking in gene regulation and genome instability.* Cell, 2012. 149(7): p. 1438-1445.

226. Izban, M.G. and D.S. Luse, *The RNA polymerase II ternary complex cleaves the nascent transcript in a 3'----5'direction in the presence of elongation factor SII.* Genes & development, 1992. 6(7): p. 1342-1356.
227. Dutta, A., V. Babbarwal, J. Fu, D. Brunke-Reese, D.M. Libert*, et al.*, *Ccr4-Not and TFIIS function cooperatively to rescue arrested RNA polymerase II.* Molecular and cellular biology, 2015. 35(11): p. 1915-1925.
228. Borukhov, S., V. Sagitov and A. Goldfarb, *Transcript cleavage factors from E. coli.* Cell, 1993. 72(3): p. 459-466.
229. Baharoglu, Z., R. Lestini, S. Duigou and B. Michel, *RNA polymerase mutations that facilitate replication progression in the rep uvrD recF mutant lacking two accessory replicative helicases.* Molecular microbiology, 2010. 77(2): p. 324-336.
230. Poli, J., C.-B. Gerhold, A. Tosi, N. Hustedt, A. Seeber*, et al.*, *Mec1, INO80, and the PAF1 complex cooperate to limit transcription replication conflicts through RNAPII removal during replication stress.* Genes & development, 2016. 30(3): p. 337-354.
231. Somesh, B.P., J. Reid, W.-F. Liu, T.M.M. Søgaard, H. Erdjument-Bromage*, et al.*, *Multiple mechanisms confining RNA polymerase II ubiquitylation to polymerases undergoing transcriptional arrest.* Cell, 2005. 121(6): p. 913-923.
232. Yasukawa, T., T. Kamura, S. Kitajima, R.C. Conaway, J.W. Conaway*, et al.*, *Mammalian Elongin A complex mediates DNA-damage-induced ubiquitylation and degradation of Rpb1.* The EMBO journal, 2008. 27(24): p. 3256-3266.
233. McKay, B.C., F. Chen, S.T. Clarke, H.E. Wiggin, L.M. Harley*, et al.*, *UV light-induced degradation of RNA polymerase II is dependent on the Cockayne's syndrome A and B proteins but not p53 or MLH1.* Mutation Research/DNA Repair, 2001. 485(2): p. 93-105.
234. Saponaro, M., T. Kantidakis, R. Mitter, G.P. Kelly, M. Heron*, et al.*, *RECQL5 controls transcript elongation and suppresses genome instability associated with transcription stress.* Cell, 2014. 157(5): p. 1037-1049.
235. Washburn, R.S. and M.E. Gottesman, *Transcription termination maintains chromosome integrity.* Proceedings of the National Academy of Sciences, 2011. 108(2): p. 792-797.
236. Morales, J.C., P. Richard, P.L. Patidar, E.A. Motea, T.T. Dang*, et al.*, *XRN2 links transcription termination to DNA damage and replication stress.* PLoS genetics, 2016. 12(7): p. e1006107.
237. Bermejo, R., T. Capra, R. Jossen, A. Colosio, C. Frattini*, et al.*, *The replication checkpoint protects fork stability by releasing transcribed genes from nuclear pores.* Cell, 2011. 146(2): p. 233-246.
238. Gómez-González, B., I. Felipe-Abrio and A. Aguilera, *The S-phase checkpoint is required to respond to R-loops accumulated in THO mutants.* Molecular and cellular biology, 2009. 29(19): p. 5203-5213.
239. Bhowmick, R., M. Lerdrup, S.A. Gadi, G.G. Rossetti, M.I. Singh*, et al.*, *RAD51 protects human cells from transcription-replication conflicts.* Molecular Cell, 2022. 82(18): p. 3366-3381. e9.
240. Jones, R., O. Mortusewicz, I. Afzal, M. Lorvellec, P. Garcia*, et al.*, *Increased replication initiation and conflicts with transcription underlie Cyclin E-induced replication stress.* Oncogene, 2013. 32(32): p. 3744-3753.
241. Zatzman, M., F. Fuligni, R. Ripsman, T. Suwal, F. Comitani*, et al.*, *Widespread hypertranscription in aggressive human cancers.* Science Advances, 2022. 8(47): p. eabn0238.
242. DePaoli-Roach, A.A., *Chapter 88 - Protein Phosphatase 1 Binding Proteins*, in *Handbook of Cell Signaling (Second Edition)*, R.A. Bradshaw and E.A. Dennis, Editors. 2010, Academic Press: San Diego. p. 689-697.
243. Bollen, M., W. Peti, M.J. Ragusa and M. Beullens, *The extended PP1 toolkit: designed to create specificity.* Trends in biochemical sciences, 2010. 35(8): p. 450-458.
244. e Silva, E.d.C., C.A. Fox, C.C. Ouimet, E. Gustafson, S.J. Watson*, et al.*, *Differential expression of protein phosphatase 1 isoforms in mammalian brain.* Journal of Neuroscience, 1995. 15(5): p. 3375-3389.

245. Heroes, E., B. Lesage, J. Görnemann, M. Beullens, L. Van Meervelt*, et al.*, *The PP1 binding code: a molecular-lego strategy that governs specificity.* The FEBS journal, 2013. 280(2): p. 584-595.
246. Hendrickx, A., M. Beullens, H. Ceulemans, T. Den Abt, A. Van Eynde*, et al.*, *Docking motif-guided mapping of the interactome of protein phosphatase-1.* Chemistry & biology, 2009. 16(4): p. 365-371.
247. Meiselbach, H., H. Sticht and R. Enz, *Structural analysis of the protein phosphatase 1 docking motif: molecular description of binding specificities identifies interacting proteins.* Chemistry & biology, 2006. 13(1): p. 49-59.
248. Allen, P.B., Y.-G. Kwon, A.C. Nairn and P. Greengard, *Isolation and characterization of PNUTS, a putative protein phosphatase 1 nuclear targeting subunit.* Journal of Biological Chemistry, 1998. 273(7): p. 4089-4095.
249. Kreivi, J.-P., L. Trinkle-Mulcahy, C.E. Lyon, N.A. Morrice, P. Cohen*, et al.*, *Purification and characterisation of p99, a nuclear modulator of protein phosphatase 1 activity.* FEBS letters, 1997. 420(1): p. 57-62.
250. Kim, Y.-M., T. Watanabe, P.B. Allen, Y.-M. Kim, S.-J. Lee*, et al.*, *PNUTS, a protein phosphatase 1 (PP1) nuclear targeting subunit: characterization of its PP1-and RNA-binding domains and regulation by phosphorylation.* Journal of Biological Chemistry, 2003. 278(16): p. 13819-13828.
251. Graña, X., *Downregulation of the phosphatase nuclear targeting subunit (PNUTS) triggers pRB dephosphorylation and apoptosis in pRB positive tumor cell lines.* Cancer biology & therapy, 2008. 7(6): p. 842-844.
252. De Leon, G., T.C. Sherry and N.A. Krucher, *Reduced expression of PNUTS leads to activation of Rb-phosphatase and caspase-mediated apoptosis.* Cancer biology & therapy, 2008. 7(6): p. 833-841.
253. Udho, E., V.C. Tedesco, A. Zygmunt and N.A. Krucher, *PNUTS (phosphatase nuclear targeting subunit) inhibits retinoblastoma-directed PP1 activity.* Biochemical and biophysical research communications, 2002. 297(3): p. 463-467.
254. Lee, S., C. Lim, J. Min, J. Lee, Y. Kim*, et al.*, *Protein phosphatase 1 nuclear targeting subunit is a hypoxia inducible gene: its role in post-translational modification of p53 and MDM2.* Cell Death & Differentiation, 2007. 14(6): p. 1106-1116.
255. Wei, Y., C. Redel, A. Ahlner, A. Lemak, I. Johansson-Åkhe*, et al.*, *The MYC oncoprotein directly interacts with its chromatin cofactor PNUTS to recruit PP1 phosphatase.* Nucleic Acids Research, 2022. 50(6): p. 3505-3522.
256. Landsverk, H.B., F. Mora-Bermúdez, O.J. Landsverk, G. Hasvold, S. Naderi*, et al.*, *The protein phosphatase 1 regulator PNUTS is a new component of the DNA damage response.* EMBO reports, 2010. 11(11): p. 868-875.
257. Zhu, S., L.A. Fisher, T. Bessho and A. Peng, *Protein phosphatase 1 and phosphatase 1 nuclear targeting subunit-dependent regulation of DNA-dependent protein kinase and non-homologous end joining.* Nucleic acids research, 2017. 45(18): p. 10583-10594.
258. Wang, F., S. Zhu, L.A. Fisher, L. Wang, N.J. Eurek*, et al.*, *Phosphatase 1 Nuclear Targeting Subunit Mediates Recruitment and Function of Poly (ADP-Ribose) Polymerase 1 in DNA RepairPNUTS Coordinates with PARP1 in DNA Repair.* Cancer research, 2019. 79(10): p. 2526-2535.
259. Lee, J.-H., J. You, E. Dobrota and D.G. Skalnik, *Identification and characterization of a novel human PP1 phosphatase complex.* Journal of Biological Chemistry, 2010. 285(32): p. 24466-24476.
260. Xing, Z., A. Lin, C. Li, K. Liang, S. Wang*, et al.*, *lncRNA directs cooperative epigenetic regulation downstream of chemokine signals.* Cell, 2014. 159(5): p. 1110-1125.
261. Jerebtsova, M., S.A. Klotchenko, T.O. Artamonova, T. Ammosova, K. Washington*, et al.*, *Mass spectrometry and biochemical analysis of RNA polymerase II: targeting by protein phosphatase-1.* Molecular and cellular biochemistry, 2011. 347(1): p. 79-87.

262. Lee, S.-J., J.-K. Lee, Y.-S. Maeng, Y.-M. Kim and Y.-G. Kwon, *Langerhans cell protein 1 (LCP1) binds to PNUTS in the nucleus: implications for this complex in transcriptional regulation.* Experimental & molecular medicine, 2009. 41(3): p. 189-200.
263. Vanoosthuyse, V., P. Legros, S.J. van der Sar, G. Yvert, K. Toda*, et al.*, *CPF-associated phosphatase activity opposes condensin-mediated chromosome condensation.* PLoS genetics, 2014. 10(6): p. e1004415.
264. Cossa, G., I. Roeschert, F. Prinz, A. Baluapuri, R.S. Vidal*, et al.*, *Localized inhibition of protein phosphatase 1 by NUAK1 promotes spliceosome activity and reveals a MYC-sensitive feedback control of transcription.* Molecular cell, 2020. 77(6): p. 1322-1339. e11.
265. Devlin, A.M., A. Shukla, J.C. Ruiz, S.D. Barnes, A. Govindan*, et al.*, *The PNUTS-PP1 complex acts as an intrinsic barrier to herpesvirus KSHV gene expression and replication.* Nature Communications, 2022. 13(1): p. 1-17.
266. Cortazar, M.A., R.M. Sheridan, B. Erickson, N. Fong, K. Glover-Cutter*, et al.*, *Control of RNA Pol II speed by PNUTS-PP1 and Spt5 dephosphorylation facilitates termination by a "Sitting Duck Torpedo" mechanism.* Molecular cell, 2019. 76(6): p. 896-908. e4.
267. Austenaa, L.M., I. Barozzi, M. Simonatto, S. Masella, G. Della Chiara*, et al.*, *Transcription of mammalian cis-regulatory elements is restrained by actively enforced early termination.* Molecular cell, 2015. 60(3): p. 460-474.
268. Lee, J.-H. and D.G. Skalnik, *Wdr82 is a C-terminal domain-binding protein that recruits the Setd1A Histone H3-Lys4 methyltransferase complex to transcription start sites of transcribed human genes.* Molecular and cellular biology, 2008. 28(2): p. 609-618.
269. Ciurciu, A., L. Duncalf, V. Jonchere, N. Lansdale, O. Vasieva*, et al.*, *PNUTS/PP1 regulates RNAPII-mediated gene expression and is necessary for developmental growth.* PLoS genetics, 2013. 9(10): p. e1003885.
270. Liu, Z., A. Wu, Z. Wu, T. Wang, Y. Pan*, et al.*, *TOX4 facilitates promoter-proximal pausing and C-terminal domain dephosphorylation of RNA polymerase II in human cells.* Communications Biology, 2022. 5(1): p. 300.
271. Gendoo, D., M. Zon, V. Sandhu, V.S. Manem, N. Ratanasirigulchai*, et al.*, *MetaGxData: clinically annotated breast, ovarian and pancreatic cancer datasets and their use in generating a multi-cancer gene signature.* Scientific reports, 2019. 9(1): p. 1-14.
272. Uhlen, M., C. Zhang, S. Lee, E. Sjöstedt, L. Fagerberg*, et al.*, *A pathology atlas of the human cancer transcriptome.* Science, 2017. 357(6352): p. eaan2507.
273. Hu, D., D. Ansari, K. Pawłowski, Q. Zhou, A. Sasor*, et al.*, *Proteomic analyses identify prognostic biomarkers for pancreatic ductal adenocarcinoma.* Oncotarget, 2018. 9(11): p. 9789.
274. Kavela, S., S.R. Shinde, R. Ratheesh, K. Viswakalyan, M.D. Bashyam*, et al.*, *PNUTS functions as a proto-oncogene by sequestering PTEN.* Cancer research, 2013. 73(1): p. 205-214.
275. Stambolic, V., A. Suzuki, J.L. De La Pompa, G.M. Brothers, C. Mirtsos*, et al.*, *Negative regulation of PKB/Akt-dependent cell survival by the tumor suppressor PTEN.* Cell, 1998. 95(1): p. 29-39.
276. Dang, C.V., *MYC on the path to cancer.* Cell, 2012. 149(1): p. 22-35.
277. Lee, J.-H. and D.G. Skalnik, *CpG-binding protein (CXXC finger protein 1) is a component of the mammalian Set1 histone H3-Lys4 methyltransferase complex, the analogue of the yeast Set1/COMPASS complex.* Journal of Biological Chemistry, 2005. 280(50): p. 41725-41731.
278. Lee, J.-H., C.M. Tate, J.-S. You and D.G. Skalnik, *Identification and characterization of the human Set1B histone H3-Lys4 methyltransferase complex.* Journal of Biological Chemistry, 2007. 282(18): p. 13419-13428.
279. Wall, M.A., D.E. Coleman, E. Lee, J.A. Iñiguez-Lluhi, B.A. Posner*, et al.*, *The structure of the G protein heterotrimer Giα1ß1γ2.* Cell, 1995. 83(6): p. 1047-1058.
280. Xu, C. and J. Min, *Structure and function of WD40 domain proteins.* Protein & cell, 2011. 2(3): p. 202-214.

281. Nedea, E., X. He, M. Kim, J. Pootoolal, G. Zhong*, et al.*, *Organization and function of APT, a subcomplex of the yeast cleavage and polyadenylation factor involved in the formation of mRNA and small nucleolar RNA 3'-ends.* Journal of Biological Chemistry, 2003. 278(35): p. 33000-33010.
282. Dichtl, B., R. Aasland and W. Keller, *Functions for S. cerevisiae Swd2p in 3' end formation of specific mRNAs and snoRNAs and global histone 3 lysine 4 methylation.* Rna, 2004. 10(6): p. 965-977.
283. Cheng, H., X. He and C. Moore, *The essential WD repeat protein Swd2 has dual functions in RNA polymerase II transcription termination and lysine 4 methylation of histone H3.* Molecular and cellular biology, 2004. 24(7): p. 2932-2943.
284. Krogan, N.J., J. Dover, A. Wood, J. Schneider, J. Heidt*, et al.*, *The Paf1 complex is required for histone H3 methylation by COMPASS and Dot1p: linking transcriptional elongation to histone methylation.* Molecular cell, 2003. 11(3): p. 721-729.
285. Bayley, R., V. Borel, R.J. Moss, E. Sweatman, P. Ruis*, et al.*, *H3K4 methylation by SETD1A/BOD1L facilitates RIF1-dependent NHEJ.* Molecular Cell, 2022. 82(10): p. 1924-1939. e10.
286. Constantin, D. and C. Widmann, *ASH2L drives proliferation and sensitivity to bleomycin and other genotoxins in Hodgkin's lymphoma and testicular cancer cells.* Cell Death & Disease, 2020. 11(11): p. 1019.
287. Higa, L.A., M. Wu, T. Ye, R. Kobayashi, H. Sun*, et al.*, *CUL4–DDB1 ubiquitin ligase interacts with multiple WD40-repeat proteins and regulates histone methylation.* Nature cell biology, 2006. 8(11): p. 1277-1283.
288. Lee, J. and P. Zhou, *DCAFs, the missing link of the CUL4-DDB1 ubiquitin ligase.* Molecular cell, 2007. 26(6): p. 775-780.
289. Austenaa, L.M., V. Piccolo, M. Russo, E. Prosperini, S. Polletti*, et al.*, *A first exon termination checkpoint preferentially suppresses extragenic transcription.* Nature structural & molecular biology, 2021. 28(4): p. 337-346.
290. Park, K., J. Zhong, J.S. Jang, J. Kim, H.-J. Kim*, et al.*, *ZWC complex-mediated SPT5 phosphorylation suppresses divergent antisense RNA transcription at active gene promoters.* Nucleic Acids Research, 2022. 50(7): p. 3835-3851.
291. Liu, H., Y. Li, J. Li, Y. Liu and B. Cui, *H3K4me3 and Wdr82 are associated with tumor progression and a favorable prognosis in human colorectal cancer.* Oncology Letters, 2018. 16(2): p. 2125-2134.
292. Mueller, C.L. and J.A. Jaehning, *Ctr9, Rtf1, and Leo1 are components of the Paf1/RNA polymerase II complex.* Molecular and cellular biology, 2002. 22(7): p. 1971-1980.
293. Krogan, N.J., M. Kim, S.H. Ahn, G. Zhong, M.S. Kobor*, et al.*, *RNA polymerase II elongation factors of Saccharomyces cerevisiae: a targeted proteomics approach.* Molecular and cellular biology, 2002. 22(20): p. 6979-6992.
294. Zhu, B., S.S. Mandal, A.-D. Pham, Y. Zheng, H. Erdjument-Bromage*, et al.*, *The human PAF complex coordinates transcription with events downstream of RNA synthesis.* Genes & development, 2005. 19(14): p. 1668-1673.
295. Amrich, C.G., C.P. Davis, W.P. Rogal, M.K. Shirra, A. Heroux*, et al.*, *Cdc73 subunit of Paf1 complex contains C-terminal Ras-like domain that promotes association of Paf1 complex with chromatin.* Journal of Biological Chemistry, 2012. 287(14): p. 10863-10875.
296. Shi, X., M. Chang, A.J. Wolf, C.-H. Chang, A.A. Frazer-Abel*, et al.*, *Cdc73p and Paf1p are found in a novel RNA polymerase II-containing complex distinct from the Srbp-containing holoenzyme.* Molecular and cellular biology, 1997. 17(3): p. 1160-1169.
297. Qiu, H., C. Hu, N.A. Gaur and A.G. Hinnebusch, *Pol II CTD kinases Bur1 and Kin28 promote Spt5 CTR-independent recruitment of Paf1 complex.* The EMBO journal, 2012. 31(16): p. 3494-3505.

298. Hein, M.Y., N.C. Hubner, I. Poser, J. Cox, N. Nagaraj*, et al.*, *A human interactome in three quantitative dimensions organized by stoichiometries and abundances.* Cell, 2015. 163(3): p. 712-723.
299. Lacroix, E. and T.E. Audas, *Keeping up with the condensates: The retention, gain, and loss of nuclear membrane-less organelles.* Frontiers in Molecular Biosciences, 2022. 9.
300. Rozenblatt-Rosen, O., T. Nagaike, J.M. Francis, S. Kaneko, K.A. Glatt*, et al.*, *The tumor suppressor Cdc73 functionally associates with CPSF and CstF 3' mRNA processing factors.* Proceedings of the National Academy of Sciences, 2009. 106(3): p. 755-760.
301. Nordick, K., M.G. Hoffman, J.L. Betz and J.A. Jaehning, *Direct interactions between the Paf1 complex and a cleavage and polyadenylation factor are revealed by dissociation of Paf1 from RNA polymerase II.* Eukaryotic cell, 2008. 7(7): p. 1158-1167.
302. Jaehning, J.A., *The Paf1 complex: Platform or player in RNA polymerase II transcription?* Biochimica et Biophysica Acta (BBA) - Gene Regulatory Mechanisms, 2010. 1799(5): p. 379-388.
303. Wood, A., J. Schneider, J. Dover, M. Johnston and A. Shilatifard, *The Paf1 complex is essential for histone monoubiquitination by the Rad6-Bre1 complex, which signals for histone methylation by COMPASS and Dot1p.* Journal of Biological Chemistry, 2003. 278(37): p. 34739-34742.
304. Herr, P., C. Lundin, B. Evers, D. Ebner, C. Bauerschmidt*, et al.*, *A genome-wide IR-induced RAD51 foci RNAi screen identifies CDC73 involved in chromatin remodeling for DNA repair.* Cell discovery, 2015. 1(1): p. 1-16.
305. Chu, Y., R. Simic, M.H. Warner, K.M. Arndt and G. Prelich, *Regulation of histone modification and cryptic transcription by the Bur1 and Paf1 complexes.* The EMBO journal, 2007. 26(22): p. 4646-4656.
306. Sanchez, G., J. Barbier, C. Elie, R. Kiernan and S. Rouquier, *PAF1 facilitates RNA polymerase II ubiquitination by the Elongin A complex through phosphorylation by CDK12.* bioRxiv, 2020.
307. Endres, T., D. Solvie, J.B. Heidelberger, V. Andrioletti, A. Baluapuri*, et al.*, *Ubiquitylation of MYC couples transcription elongation with double-strand break repair at active promoters.* Molecular Cell, 2021. 81(4): p. 830-844. e13.
308. van den Heuvel, D., C.G. Spruijt, R. González-Prieto, A. Kragten, M.T. Paulsen*, et al.*, *A CSB-PAF1C axis restores processive transcription elongation after DNA damage repair.* Nature communications, 2021. 12(1): p. 1-19.
309. Jia, Q., H. Nie, X. Wan, H. Fu, F. Yang*, et al.*, *Down-regulation of cancer-associated gene CDC73 contributes to cellular senescence.* Biochemical and biophysical research communications, 2018. 499(4): p. 809-814.
310. Takahashi, A., R. Tsutsumi, I. Kikuchi, C. Obuse, Y. Saito*, et al.*, *SHP2 tyrosine phosphatase converts parafibromin/Cdc73 from a tumor suppressor to an oncogenic driver.* Molecular cell, 2011. 43(1): p. 45-56.
311. Carpten, J., C. Robbins, A. Villablanca, L. Forsberg, S. Presciuttini*, et al.*, *HRPT2, encoding parafibromin, is mutated in hyperparathyroidism–jaw tumor syndrome.* Nature genetics, 2002. 32(4): p. 676-680.
312. Selvarajan, S., L.H. Sii, A. Lee, G. Yip, B.H. Bay*, et al.*, *Parafibromin expression in breast cancer: a novel marker for prognostication?* Journal of clinical pathology, 2008. 61(1): p. 64-67.
313. Zhao, J., A. Yart, S. Frigerio, A. Perren, P. Schraml*, et al.*, *Sporadic human renal tumors display frequent allelic imbalances and novel mutations of the HRPT2 gene.* Oncogene, 2007. 26(23): p. 3440-3449.
314. Shattuck, T.M., S. Välimäki, T. Obara, R.D. Gaz, O.H. Clark*, et al.*, *Somatic and germ-line mutations of the HRPT2 gene in sporadic parathyroid carcinoma.* New England Journal of Medicine, 2003. 349(18): p. 1722-1729.
315. Zheng, H.-c., H. Takahashi, X.-h. Li, T. Hara, S. Masuda*, et al.*, *Downregulated parafibromin expression is a promising marker for pathogenesis, invasion, metastasis and prognosis of gastric carcinomas.* Virchows Archiv, 2008. 452(2): p. 147-155.

316. Zhang, C., D. Kong, M.-H. Tan, D.L. Pappas Jr, P.-F. Wang*, et al.*, *Parafibromin inhibits cancer cell growth and causes G1 phase arrest.* Biochemical and biophysical research communications, 2006. 350(1): p. 17-24.
317. Zheng, H.-C., B.-C. Gong and S. Zhao, *The clinicopathological and prognostic significances of CDC73 expression in cancers: a bioinformatics analysis.* Oncotarget, 2017. 8(56): p. 95270.
318. Steurer, B., R.C. Janssens, B. Geverts, M.E. Geijer, F. Wienholz*, et al.*, *Live-cell analysis of endogenous GFP-RPB1 uncovers rapid turnover of initiating and promoter-paused RNA Polymerase II.* Proceedings of the National Academy of Sciences, 2018. 115(19): p. E4368-E4376.
319. Nilson, K.A., J. Guo, M.E. Turek, J.E. Brogie, E. Delaney*, et al.*, *THZ1 reveals roles for Cdk7 in co-transcriptional capping and pausing.* Molecular cell, 2015. 59(4): p. 576-587.
320. Britton, S., J. Coates and S.P. Jackson, *A new method for high-resolution imaging of Ku foci to decipher mechanisms of DNA double-strand break repair.* Journal of Cell Biology, 2013. 202(3): p. 579-595.
321. Fijen, C. and E. Rothenberg, *The evolving complexity of DNA damage foci: RNA, condensates and chromatin in DNA double-strand break repair.* DNA repair, 2021. 105: p. 103170.
322. Felipe-Abrio, I., J. Lafuente-Barquero, M.L. García-Rubio and A. Aguilera, *RNA polymerase II contributes to preventing transcription-mediated replication fork stalls.* The EMBO journal, 2015. 34(2): p. 236-250.
323. Kamieniarz-Gdula, K. and N.J. Proudfoot, *Transcriptional control by premature termination: a forgotten mechanism.* Trends in Genetics, 2019. 35(8): p. 553-564.
324. Cugusi, S., R. Mitter, G.P. Kelly, J. Walker, Z. Han*, et al.*, *Heat shock induces premature transcript termination and reconfigures the human transcriptome.* Molecular Cell, 2022. 82(8): p. 1573-1588. e10.
325. Beckedorff, F., E. Blumenthal, L. Ferreira daSilva, Y. Aoi, P.R. Cingaram*, et al.*, *The human integrator complex facilitates transcriptional elongation by endonucleolytic cleavage of nascent transcripts.* Cell reports, 2020. 32(3): p. 107917.
326. Erickson, B., R.M. Sheridan, M. Cortazar and D.L. Bentley, *Dynamic turnover of paused Pol II complexes at human promoters.* Genes & development, 2018. 32(17-18): p. 1215-1225.
327. Aoi, Y., Y.-h. Takahashi, A.P. Shah, M. Iwanaszko, E.J. Rendleman*, et al.*, *SPT5 stabilization of promoter-proximal RNA polymerase II.* Molecular cell, 2021. 81(21): p. 4413-4424. e5.
328. Hu, S., L. Peng, C. Xu, Z. Wang, A. Song*, et al.*, *SPT5 stabilizes RNA polymerase II, orchestrates transcription cycles, and maintains the enhancer landscape.* Molecular Cell, 2021. 81(21): p. 4425-4439. e6.
329. Wier, A.D., M.K. Mayekar, A. Héroux, K.M. Arndt and A.P. VanDemark, *Structural basis for Spt5-mediated recruitment of the Paf1 complex to chromatin.* Proceedings of the National Academy of Sciences, 2013. 110(43): p. 17290-17295.
330. Mayekar, M.K., R.G. Gardner and K.M. Arndt, *The recruitment of the Saccharomyces cerevisiae Paf1 complex to active genes requires a domain of Rtf1 that directly interacts with the Spt4-Spt5 complex.* Molecular and cellular biology, 2013. 33(16): p. 3259-3273.
331. Chen, J.J., J. Mbogning, M.A. Hancock, D. Majdpour, M. Madhok*, et al.*, *Spt5 phosphorylation and the Rtf1 Plus3 domain promote Rtf1 function through distinct mechanisms.* Molecular and Cellular Biology, 2020. 40(15): p. e00150-20.
332. Adelman, K. and J.T. Lis, *Promoter-proximal pausing of RNA polymerase II: emerging roles in metazoans.* Nature Reviews Genetics, 2012. 13(10): p. 720-731.
333. Hou, L., Y. Wang, Y. Liu, N. Zhang, I. Shamovsky*, et al.*, *Paf1C regulates RNA polymerase II progression by modulating elongation rate.* Proceedings of the National Academy of Sciences, 2019. 116(29): p. 14583-14592.
334. Gressel, S., B. Schwalb and P. Cramer, *The pause-initiation limit restricts transcription activation in human cells.* Nature communications, 2019. 10(1): p. 1-12.

335. Vihervaara, A., D.B. Mahat, M.J. Guertin, T. Chu, C.G. Danko*, et al.*, *Transcriptional response to stress is pre-wired by promoter and enhancer architecture.* Nature communications, 2017. 8(1): p. 1-16.
336. Gu, B., D. Eick and O. Bensaude, *CTD serine-2 plays a critical role in splicing and termination factor recruitment to RNA polymerase II in vivo.* Nucleic acids research, 2013. 41(3): p. 1591-1603.
337. Dichtl, B., D. Blank, M. Ohnacker, A. Friedlein, D. Roeder*, et al.*, *A role for SSU72 in balancing RNA polymerase II transcription elongation and termination.* Molecular cell, 2002. 10(5): p. 1139-1150.
338. He, X., A.U. Khan, H. Cheng, D.L. Pappas, M. Hampsey*, et al.*, *Functional interactions between the transcription and mRNA 3′ end processing machineries mediated by Ssu72 and Sub1.* Genes & development, 2003. 17(8): p. 1030-1042.
339. Shi, Y., D.C. Di Giammartino, D. Taylor, A. Sarkeshik, W.J. Rice*, et al.*, *Molecular architecture of the human pre-mRNA 3′ processing complex.* Molecular cell, 2009. 33(3): p. 365-376.
340. van Nuland, R., A.H. Smits, P. Pallaki, P.W. Jansen, M. Vermeulen*, et al.*, *Quantitative dissection and stoichiometry determination of the human SET1/MLL histone methyltransferase complexes.* Molecular and cellular biology, 2013. 33(10): p. 2067-2077.
341. Malovannaya, A., R.B. Lanz, S.Y. Jung, Y. Bulynko, N.T. Le*, et al.*, *Analysis of the human endogenous coregulator complexome.* Cell, 2011. 145(5): p. 787-799.
342. Wang, J., M. Muste Sadurni and M. Saponaro, *RNAPII response to transcription-blocking DNA lesions in mammalian cells.* The FEBS journal, 2022.
343. Borsos, B.N., H. Majoros and T. Pankotai, *Emerging roles of post-translational modifications in nucleotide excision repair.* Cells, 2020. 9(6): p. 1466.
344. Chiou, Y.-Y., J. Hu, A. Sancar and C.P. Selby, *RNA polymerase II is released from the DNA template during transcription-coupled repair in mammalian cells.* Journal of Biological Chemistry, 2018. 293(7): p. 2476-2486.
345. Epshtein, V., V. Kamarthapu, K. McGary, V. Svetlov, B. Ueberheide*, et al.*, *UvrD facilitates DNA repair by pulling RNA polymerase backwards.* Nature, 2014. 505(7483): p. 372-377.
346. Kokic, G., F.R. Wagner, A. Chernev, H. Urlaub and P. Cramer, *Structural basis of human transcription–DNA repair coupling.* Nature, 2021. 598(7880): p. 368-372.
347. Gregersen, L.H. and J.Q. Svejstrup, *The cellular response to transcription-blocking DNA damage.* Trends in Biochemical Sciences, 2018. 43(5): p. 327-341.
348. Steurer, B., R.C. Janssens, M.E. Geijer, F. Aprile-Garcia, B. Geverts*, et al.*, *DNA damage-induced transcription stress triggers the genome-wide degradation of promoter-bound Pol II.* Nature Communications, 2022. 13(1): p. 3624.
349. Muñoz, M.J., M.S.P. Santangelo, M.P. Paronetto, M. de la Mata, F. Pelisch*, et al.*, *DNA damage regulates alternative splicing through inhibition of RNA polymerase II elongation.* Cell, 2009. 137(4): p. 708-720.
350. van den Heuvel, D., Y. van der Weegen, D.E. Boer, T. Ogi and M.S. Luijsterburg, *Transcription-coupled DNA repair: from mechanism to human disorder.* Trends in Cell Biology, 2021. 31(5): p. 359-371.
351. Liakos, A., D. Konstantopoulos, M.D. Lavigne and M. Fousteri, *Continuous transcription initiation guarantees robust repair of all transcribed genes and regulatory regions.* Nature Communications, 2020. 11(1): p. 916.
352. Lavigne, M.D., D. Konstantopoulos, K.Z. Ntakou-Zamplara, A. Liakos and M. Fousteri, *Global unleashing of transcription elongation waves in response to genotoxic stress restricts somatic mutation rate.* Nature Communications, 2017. 8(1): p. 2076.
353. Huang, R.-X. and P.-K. Zhou, *DNA damage response signaling pathways and targets for radiotherapy sensitization in cancer.* Signal transduction and targeted therapy, 2020. 5(1): p. 60.

354. Shanbhag, N.M., I.U. Rafalska-Metcalf, C. Balane-Bolivar, S.M. Janicki and R.A. Greenberg, *An ATM-dependent transcriptional silencing program is transmitted through chromatin in cis to DNA double strand breaks.* Cell, 2010. 141(6): p. 970.
355. Polo, S.E., *Switching genes to silent mode near DNA double-strand breaks.* EMBO reports, 2017. 18(5): p. 659-660.
356. Clouaire, T. and G. Legube, *A snapshot on the cis chromatin response to DNA double-strand breaks.* Trends in Genetics, 2019. 35(5): p. 330-345.
357. Bergstrand, S., E.M. O'Brien, C. Coucoravas, D. Hrossova, D. Peirasmaki*, et al.*, *Small Cajal body-associated RNA 2 (scaRNA2) regulates DNA repair pathway choice by inhibiting DNA-PK.* Nature communications, 2022. 13(1): p. 1015.
358. Wang, X., H. Liu, L. Shi, X. Yu, Y. Gu*, et al.*, *LINP1 facilitates DNA damage repair through non-homologous end joining (NHEJ) pathway and subsequently decreases the sensitivity of cervical cancer cells to ionizing radiation.* Cell cycle, 2018. 17(4): p. 439-447.
359. Ouyang, J., L. Lan and L. Zou, *Regulation of DNA break repair by transcription and RNA.* Science China Life Sciences, 2017. 60: p. 1081-1086.
360. Clouaire, T., V. Rocher, A. Lashgari, C. Arnould, M. Aguirrebengoa*, et al.*, *Comprehensive mapping of histone modifications at DNA double-strand breaks deciphers repair pathway chromatin signatures.* Molecular cell, 2018. 72(2): p. 250-262. e6.
361. Winsor, T.S., B. Bartkowiak, C.B. Bennett and A.L. Greenleaf, *A DNA damage response system associated with the phosphoCTD of elongating RNA polymerase II.* PloS one, 2013. 8(4): p. e60909.
362. Rothkamm, K., S. Barnard, J. Moquet, M. Ellender, Z. Rana*, et al.*, *DNA damage foci: Meaning and significance.* Environmental and molecular mutagenesis, 2015. 56(6): p. 491-504.
363. Penninckx, S., E. Pariset, E. Cekanaviciute and S.V. Costes, *Quantification of radiation-induced DNA double strand break repair foci to evaluate and predict biological responses to ionizing radiation.* NAR cancer, 2021. 3(4): p. zcab046.
364. Harel, I., Y.R. Chen, I. Ziv, P.P. Singh, P.N. Negredo*, et al.*, *Identification of protein aggregates in the aging vertebrate brain with prion-like and phase separation properties.* Biorxiv, 2022: p. 2022.02. 26.482115.
365. Kilic, S., A. Lezaja, M. Gatti, E. Bianco, J. Michelena*, et al.*, *Phase separation of 53 BP 1 determines liquid-like behavior of DNA repair compartments.* The EMBO journal, 2019. 38(16): p. e101379.
366. Miné-Hattab, J., S. Liu and A. Taddei, *Repair Foci as Liquid Phase Separation: Evidence and Limitations.* Genes, 2022. 13(10): p. 1846.
367. Polo, S.E. and S.P. Jackson, *Dynamics of DNA damage response proteins at DNA breaks: a focus on protein modifications.* Genes & development, 2011. 25(5): p. 409-433.
368. Bekker-Jensen, S., C. Lukas, R. Kitagawa, F. Melander, M.B. Kastan*, et al.*, *Spatial organization of the mammalian genome surveillance machinery in response to DNA strand breaks.* The Journal of cell biology, 2006. 173(2): p. 195-206.
369. Aymard, F., M. Aguirrebengoa, E. Guillou, B.M. Javierre, B. Bugler*, et al.*, *Genome-wide mapping of long-range contacts unveils clustering of DNA double-strand breaks at damaged active genes.* Nature structural & molecular biology, 2017. 24(4): p. 353-361.
370. Svejstrup, J.Q., *The interface between transcription and mechanisms maintaining genome integrity.* Trends in biochemical sciences, 2010. 35(6): p. 333-338.
371. Alzu, A., R. Bermejo, M. Begnis, C. Lucca, D. Piccini*, et al.*, *Senataxin associates with replication forks to protect fork integrity across RNA-polymerase-II-transcribed genes.* Cell, 2012. 151(4): p. 835-846.
372. Yuan, K., H. Liu, C. Yu, N. Zhang, Y. Meng*, et al.*, *Elevated pausing of RNA Polymerase II underlies acquired resistance to ionizing radiation.* 2021.
373. Shkreta, L. and B. Chabot, *The RNA splicing response to DNA damage.* Biomolecules, 2015. 5(4): p. 2935-2977.

374. Li, S., W.W. Kuhne, A. Kulharya, F.Z. Hudson, K. Ha*, et al.*, *Involvement of p54 (nrb), a PSF partner protein, in DNA double-strand break repair and radioresistance.* Nucleic acids research, 2009. 37(20): p. 6746-6753.
375. Ligasová, A. and K. Koberna, *Strengths and weaknesses of cell synchronization protocols based on inhibition of DNA synthesis.* International Journal of Molecular Sciences, 2021. 22(19): p. 10759.
376. Orlando, D.A., M.W. Chen, V.E. Brown, S. Solanki, Y.J. Choi*, et al.*, *Quantitative ChIP-Seq normalization reveals global modulation of the epigenome.* Cell reports, 2014. 9(3): p. 1163-1170.
377. Bonhoure, N., G. Bounova, D. Bernasconi, V. Praz, F. Lammers*, et al.*, *Quantifying ChIP-seq data: a spiking method providing an internal reference for sample-to-sample normalization.* Genome research, 2014. 24(7): p. 1157-1168.
378. Egan, B., C.-C. Yuan, M.L. Craske, P. Labhart, G.D. Guler*, et al.*, *An alternative approach to ChIP-Seq normalization enables detection of genome-wide changes in histone H3 lysine 27 trimethylation upon EZH2 inhibition.* PloS one, 2016. 11(11): p. e0166438.
379. Wissink, E.M., A. Vihervaara, N.D. Tippens and J.T. Lis, *Nascent RNA analyses: tracking transcription and its regulation.* Nature Reviews Genetics, 2019. 20(12): p. 705-723.
380. Sørensen, C.S. and R.G. Syljuåsen, *Safeguarding genome integrity: the checkpoint kinases ATR, CHK1 and WEE1 restrain CDK activity during normal DNA replication.* Nucleic acids research, 2012. 40(2): p. 477-486.
381. Dobbelstein, M. and C.S. Sørensen, *Exploiting replicative stress to treat cancer.* Nature reviews Drug discovery, 2015. 14(6): p. 405-423.
382. Gralewska, P., A. Gajek, A. Marczak, M. Mikuła, J. Ostrowski*, et al.*, *PARP inhibition increases the reliance on ATR/CHK1 checkpoint signaling leading to synthetic lethality—an alternative treatment strategy for epithelial ovarian cancer cells independent from HR effectiveness.* International journal of molecular sciences, 2020. 21(24): p. 9715.
383. Liao, H., F. Ji, T. Helleday and S. Ying, *Mechanisms for stalled replication fork stabilization: new targets for synthetic lethality strategies in cancer treatments.* EMBO reports, 2018. 19(9): p. e46263.
384. Tee, A.E., O.C. Ciampa, M. Wong, J.I. Fletcher, A. Kamili*, et al.*, *Combination therapy with the CDK7 inhibitor and the tyrosine kinase inhibitor exerts synergistic anticancer effects against MYCN-amplified neuroblastoma.* International journal of cancer, 2020. 147(7): p. 1928-1938.
385. Dubbury, S.J., P.L. Boutz and P.A. Sharp, *CDK12 regulates DNA repair genes by suppressing intronic polyadenylation.* Nature, 2018. 564(7734): p. 141-145.
386. Quereda, V., S. Bayle, F. Vena, S.M. Frydman, A. Monastyrskyi*, et al.*, *Therapeutic targeting of CDK12/CDK13 in triple-negative breast cancer.* Cancer cell, 2019. 36(5): p. 545-558. e7.
387. Vervoort, S.J., J.R. Devlin, N. Kwiatkowski, M. Teng, N.S. Gray*, et al.*, *Targeting transcription cycles in cancer.* Nature Reviews Cancer, 2022. 22(1): p. 5-24.
388. Dingar, D., W.B. Tu, D. Resetca, C. Lourenco, A. Tamachi*, et al.*, *MYC dephosphorylation by the PP1/PNUTS phosphatase complex regulates chromatin binding and protein stability.* Nature communications, 2018. 9(1): p. 3502.
389. Gorthi, A., J.C. Romero, E. Loranc, L. Cao, L.A. Lawrence*, et al.*, *EWS–FLI1 increases transcription to cause R-loops and block BRCA1 repair in Ewing sarcoma.* Nature, 2018. 555(7696): p. 387-391.
390. Secchi, M., C. Lodola, A. Garbelli, S. Bione and G. Maga, *DEAD-box RNA helicases DDX3X and DDX5 as oncogenes or oncosuppressors: a network perspective.* Cancers, 2022. 14(15): p. 3820.

Appendix

I

Cell Reports

Article

WDR82/PNUTS-PP1 Prevents Transcription-Replication Conflicts by Promoting RNA Polymerase II Degradation on Chromatin

Graphical Abstract

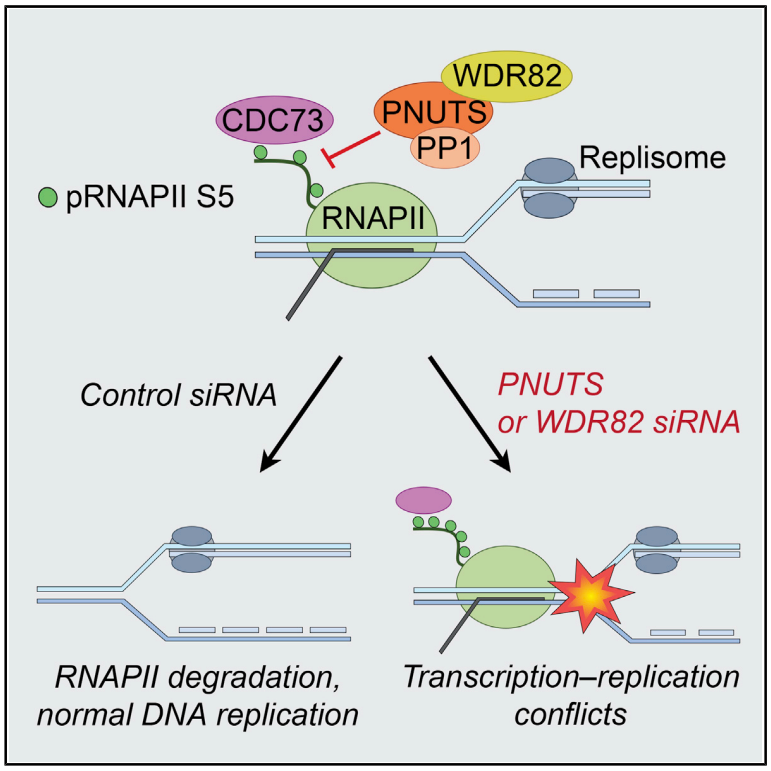

Authors

Helga B. Landsverk, Lise E. Sandquist, Lilli T.E. Bay, ..., Eva Petermann, Laura Trinkle-Mulcahy, Randi G. Syljuåsen

Correspondence

helga.bjarnason.landsverk@rr-research.no (H.B.L.), randi.syljuasen@rr-research.no (R.G.S.)

In Brief

Landsverk et al. show that the RNAPII S5 phosphatase complex WDR82/PNUTS-PP1 suppresses replication stress. WDR82/PNUTS-PP1 promotes degradation of RNAPII on chromatin, thereby reducing the residence time of RNAPII. Their results suggest that proper dephosphorylation of RNAPII is needed to prevent conflicts between transcription and replication.

Highlights

- RNAPII S5 phosphatase PNUTS-PP1 promotes RNAPII turnover on chromatin
- Depletion of PNUTS leads to transcription-replication conflicts
- WDR82 shows similar effects on RNAPII turnover and replication stress as PNUTS
- CDC73 prevents RNAPII degradation and promotes replication stress after PNUTS depletion

Landsverk et al., 2020, Cell Reports *33*, 108469
December 1, 2020
https://doi.org/10.1016/j.celrep.2020.108469

CellPress

Cell Reports

CellPress
OPEN ACCESS

Article

WDR82/PNUTS-PP1 Prevents Transcription-Replication Conflicts by Promoting RNA Polymerase II Degradation on Chromatin

Helga B. Landsverk,[1,7,*] Lise E. Sandquist,[1,7] Lilli T.E. Bay,[1,7] Barbara Steurer,[2] Coen Campsteijn,[5] Ole J.B. Landsverk,[6] Jurgen A. Marteijn,[2] Eva Petermann,[3] Laura Trinkle-Mulcahy,[4] and Randi G. Syljuåsen[1,8,*]

[1]Department of Radiation Biology, Institute for Cancer Research, Norwegian Radium Hospital, Oslo University Hospital, 0379 Oslo, Norway
[2]Department of Molecular Genetics, Oncode Institute, Erasmus MC, University Medical Center Rotterdam, 3015 GE Rotterdam, the Netherlands
[3]Institute of Cancer and Genomic Sciences, College of Medical and Dental Sciences, University of Birmingham, Birmingham B15 2TT, UK
[4]Department of Cellular and Molecular Medicine and Ottawa Institute of Systems Biology, University of Ottawa, Ottawa, ON K1H 8M5, Canada
[5]Department of Molecular Medicine, Institute of Basic Medical Sciences, University of Oslo, 0372 Oslo, Norway
[6]Department of Pathology, Oslo University Hospital, 0372 Oslo, Norway
[7]These authors contributed equally
[8]Lead Contact
*Correspondence: helga.bjarnason.landsverk@rr-research.no (H.B.L.), randi.syljuasen@rr-research.no (R.G.S.)
https://doi.org/10.1016/j.celrep.2020.108469

SUMMARY

Transcription-replication (T-R) conflicts cause replication stress and loss of genome integrity. However, the transcription-related processes that restrain such conflicts are poorly understood. Here, we demonstrate that the RNA polymerase II (RNAPII) C-terminal domain (CTD) phosphatase protein phosphatase 1 (PP1) nuclear targeting subunit (PNUTS)-PP1 inhibits replication stress. Depletion of PNUTS causes lower EdU uptake, S phase accumulation, and slower replication fork rates. In addition, the PNUTS binding partner WDR82 also promotes RNAPII-CTD dephosphorylation and suppresses replication stress. RNAPII has a longer residence time on chromatin after depletion of PNUTS or WDR82. Furthermore, the RNAPII residence time is greatly enhanced by proteasome inhibition in control cells but less so in PNUTS- or WDR82-depleted cells, indicating that PNUTS and WDR82 promote degradation of RNAPII on chromatin. Notably, reduced replication is dependent on transcription and the phospho-CTD binding protein CDC73 after depletion of PNUTS/WDR82. Altogether, our results suggest that RNAPII-CTD dephosphorylation is required for the continuous turnover of RNAPII on chromatin, thereby preventing T-R conflicts.

INTRODUCTION

Faithful DNA replication is essential to maintain genome integrity during cell division. However, problems during DNA replication (i.e., replication stress) can arise from many sources (Gaillard et al., 2015). Replication stress contributes to cancer development (Forment and O'Connor, 2018; Gaillard et al., 2015) and may also be exploited in clinical therapy to selectively kill cancer cells (Forment and O'Connor, 2018; Sørensen and Syljuåsen, 2012). Identification of the molecular mechanisms underlying replication stress is therefore of great significance.

Transcription-replication (T-R) conflicts are a major source of replication stress (Gómez-González and Aguilera, 2019). Sharing the same template, RNA and DNA polymerases may interfere with each other, and such interference (i.e., T-R conflicts) can cause replication stress and genome instability (Gaillard and Aguilera, 2016; Gómez-González and Aguilera, 2019). Interestingly, T-R conflicts are enhanced by oncogenic RAS and CYCLIN E and the breast-cancer-inducing hormone estrogen (Jones et al., 2013; Kotsantis et al., 2016; Stork et al., 2016) and may thus also be involved in cancer development. T-R conflicts can create replication stress by transcription-induced chromatin alterations or topological stress (Gómez-González and Aguilera, 2019). Furthermore, transcription can lead to formation of nucleic acid structures such as R-loops, which can cause both replication stress and genome instability (Hamperl et al., 2017; Lang et al., 2017). R-loops are thus a characteristic of T-R conflicts, and overexpression of RNaseH1, which degrades the RNA strand in RNA-DNA hybrids, can promote replication fork progression in cells with replication stress caused by T-R conflicts (Hodroj et al., 2017; Klusmann et al., 2018; Kotsantis et al., 2016).

RNA polymerase II (RNAPII) pervasively transcribes the genome (Jensen et al., 2013) and has a high potential for creating a physical barrier for DNA replication by itself (Gómez-González and Aguilera, 2019). Indeed, the bacterial replisome pauses upon encountering bacterial RNA polymerase (RNAP) in a head-on conflict (Liu and Alberts, 1995). Furthermore, the

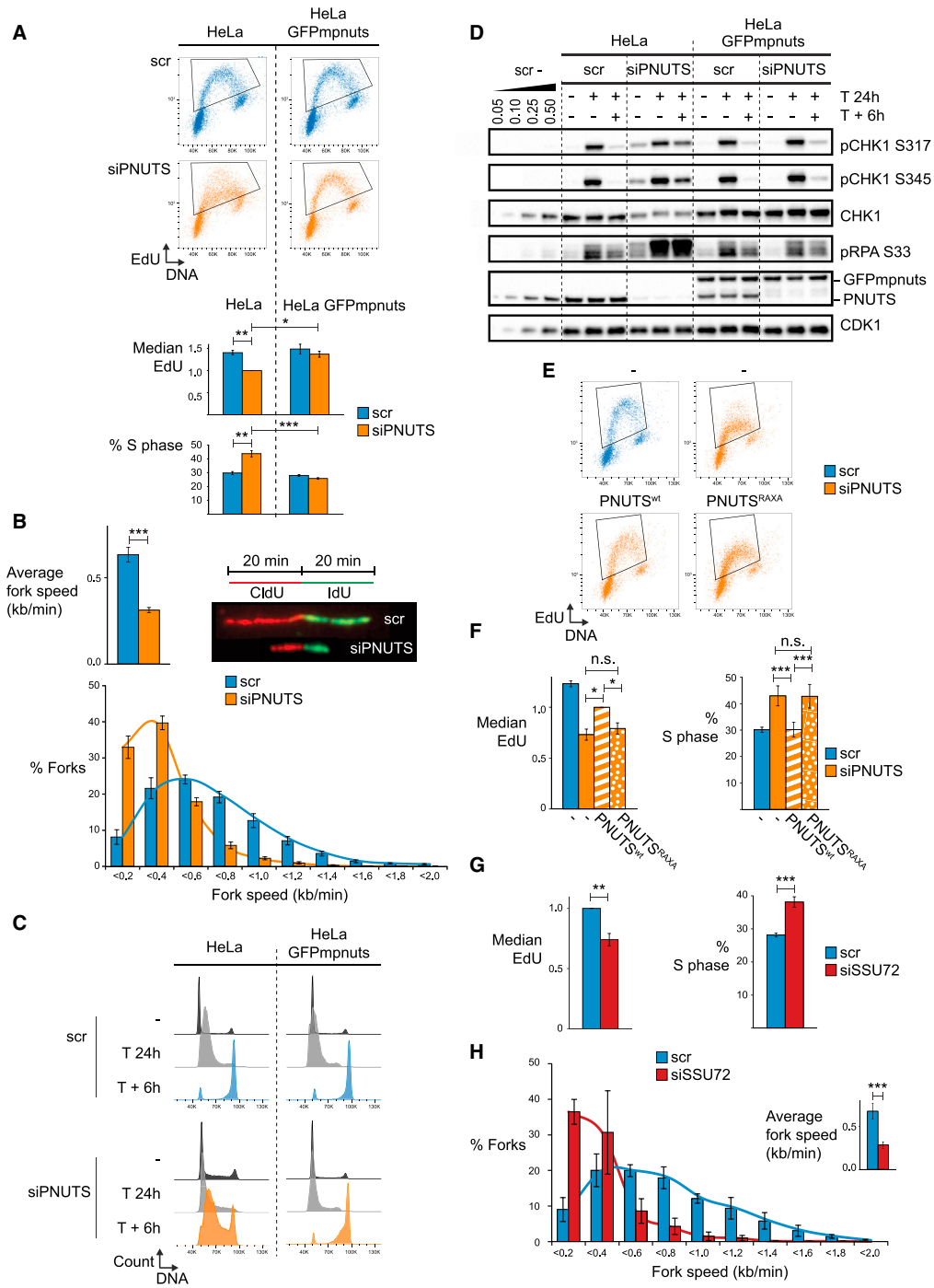

Figure 1. The pRNAPII S5 Phosphatase PNUTS-PP1 Promotes DNA Replication

(A) Flow cytometry analysis of EdU incorporation in HeLa cells or HeLa bacterial artificial chromosome (BAC) clones stably expressing EGFP mouse pnuts (HeLa GFPmpnuts) at 72 h after transfection with siRNA targeting human PNUTS (siPNUTS) or control siRNA (scr). Bottom charts show mean median EdU levels and percentage of cells in S phase (indicated by regions in scatterplots) (n = 3). p value for percentage of cells in S phase was determined by the two-tailed Student's one-sample t test.

(B) DNA fiber analysis of HeLa cells 48 h after transfection with scr or siPNUTS. Representative images of obtained fibers, mean replication fork speed, and distributions of replication fork speed are shown (n = 6). p value was determined by the Wilcoxon signed rank test.

(C) Flow cytometry analysis of HeLa and HeLa GFPmpnuts cells transfected as in (A) and stained with Hoechst 33258. Indicated samples were treated with thymidine (T) for 24 h (T 24 h). In T + 6 h samples, thymidine was removed, and fresh media was added for 6 h.

(legend continued on next page)

transcription-coupled repair factor Mfd and the accessory helicases Rep and UvrD promote replication in bacteria by displacing stalled RNAP (Hawkins et al., 2019; Pomerantz and O'Donnell, 2010). In addition, RNAPII mutants in yeast, which promote the retention of RNAPII on chromatin, display impaired replication fork progression and enhanced genome instability (Felipe-Abrio et al., 2015). These findings imply that a dynamic association of RNAPII with chromatin is required to prevent T-R conflicts. However, at least in human cells, the factors involved remain poorly understood.

During the transcription cycle, RNAPII becomes post-transcriptionally modified in its C-terminal domain (CTD), which is a large unstructured domain consisting of 52 heptapeptide repeats in humans (Harlen and Churchman, 2017). The modifications of the CTD regulate its association with factors involved in initiation, elongation, RNA processing, and termination (Bentley, 2014; Custódio and Carmo-Fonseca, 2016). The most well-known modifications of the CTD are phosphorylation on serine (S)2 (pRNAPII S2) and S5 (pRNAPII S5). Though previously thought to be primarily associated with promoter proximal regions, pRNAPII S5 is also found in gene-internal regions and is particularly enriched on paused RNAPII at splice sites (Nojima et al., 2015). pRNAPII S2 is low at promoter-proximal regions and is associated with elongation and termination (Ahn et al., 2004; Harlen and Churchman, 2017). The CTD also responds to stress such as UV DNA damage, when it becomes extensively hyperphosphorylated (Rockx et al., 2000). Whether the CTD is involved in replication stress is not known. However, several CTD binding proteins are required for resistance to the replication stress inducer doxorubicin (Winsor et al., 2013), indicating such a connection.

Protein phosphatase 1 (PP1) is a major serine threonine phosphatase whose specificity is mediated by regulatory proteins (Boens et al., 2013). PP1 nuclear targeting subunit (PNUTS) is an abundant nuclear PP1 regulatory protein (Kreivi et al., 1997), and its only established substrate is S5 in the CTD of RNAPII (pRNAPII S5) (Ciurciu et al., 2013; Lee et al., 2010). We previously found that PNUTS is involved in the G2 checkpoint and ataxia telangiectasia and Rad3 related (ATR) signaling (Landsverk et al., 2010, 2019). Our results suggested that ATR can be activated via the CTD of RNAPII (Landsverk et al., 2019). Here, we present evidence that PNUTS-PP1-mediated dephosphorylation of RNAPII CTD suppresses T-R conflicts by promoting degradation of RNAPII on chromatin, thus reducing its residence time. Furthermore, we show that WDR82, a major PNUTS interacting partner, shows similar effects. The phenotypes of PNUTS and WDR82 depletion on both replication and the RNAPII residence time on chromatin are dependent on the phospho-CTD binding protein CDC73, a component of the PAF1 transcription elongation complex. Altogether, our results provide insight into how regulation of the transcription machinery contributes to suppression of T-R conflicts in human cells.

RESULTS

PNUTS-PP1 Is Required for DNA Replication under Normal and Stressed Conditions

In our previous work, we observed an increased fraction of cells in S phase and reduced 5-ethynyl-2′-deoxyuridine (EdU) incorporation after small interfering RNA (siRNA)-mediated depletion of PNUTS in HeLa cells, suggesting PNUTS is required for normal DNA replication (Landsverk et al., 2019). These effects were specifically caused by depletion of PNUTS, as they were rescued in cells expressing mouse GFPpnuts (GFPmpnuts) (Figure 1A), which is not affected by human PNUTS siRNA (PNUTS blot in Figure 1D). In addition, PNUTS depletion strongly reduced replication fork rates compared to control siRNA transfected cells (Figure 1B). A higher fraction of S phase cells after depletion of PNUTS was also observed in U2OS cells (Figure S1A). Moreover, PNUTS depletion induced slower recovery from thymidine-induced replication stalling, as more cells transfected with control siRNA had reached the G2/M transition 6 h after release from thymidine than cells transfected with PNUTS siRNA (Figure 1C). The reduced recovery from thymidine-induced replication stalling was also observed in U2OS cells (Figure S1B) and was a specific effect after PNUTS depletion (Figure 1C). Interestingly, a screen searching for factors necessary for recovery from hydroxyurea (HU)-induced replication stalling identified PNUTS among the candidate hits (Sirbu et al., 2013). In line with a role after HU, more PNUTS-depleted cells accumulated in S phase after HU treatment than control siRNA transfected cells (Figure S1C). Consistent with our own previous findings (Landsverk et al., 2019), enhanced ATR signaling was observed after PNUTS siRNA transfection, as measured by increased phosphorylation of CHK1 on S317 and S345 and RPA32 on S33 (Figures 1D and S1D). ATR signaling after depletion of PNUTS was further enhanced by thymidine and was also rescued by GFPmpnuts (Figures 1D and S1D). Moreover, the higher ATR signaling in PNUTS-depleted cells correlated with reduced recovery from replication stalling and a higher percentage of cells with high levels of the DNA damage marker γH2AX at 6 h after release from thymidine block (Figures 1C, 1D, and S1E). To address whether the high ATR activity after depletion of PNUTS was responsible for the effects on replication, we added the ATR inhibitor VE822 (Fokas et al., 2012). Neither EdU uptake nor replication fork rate was reversed by VE822 (Figures S1F and S1G),

(D) Western blot of experiment as in (C).
(E) Flow cytometry analysis as in (A) of HeLa cells 48 h after transfection with scr or siPNUTS. EGFP PNUTS ($PNUTS^{wt}$) or PP1-binding deficient EGFP PNUTS ($PNUTS^{RAXA}$) were transfected at 24 h post-siRNA transfection.
(F) Mean median EdU incorporation or percentage of S phase cells from experiments as in (E) (n = 3).
(G) Mean median EdU incorporation and percentage of cells in S phase from experiments as in (A) of HeLa cells transfected with scr or siRNA targeting SSU72 (siSSU72) (n = 4).
(H) DNA fiber analysis of HeLa cells 48 h after transfection with scr or siSSU72. Average replication fork speed and distributions of replication fork speed are shown. (n = 3). p value was determined by the two-tailed Student's one-sample t test.
Error bars represent SEM. See also Figure S1.

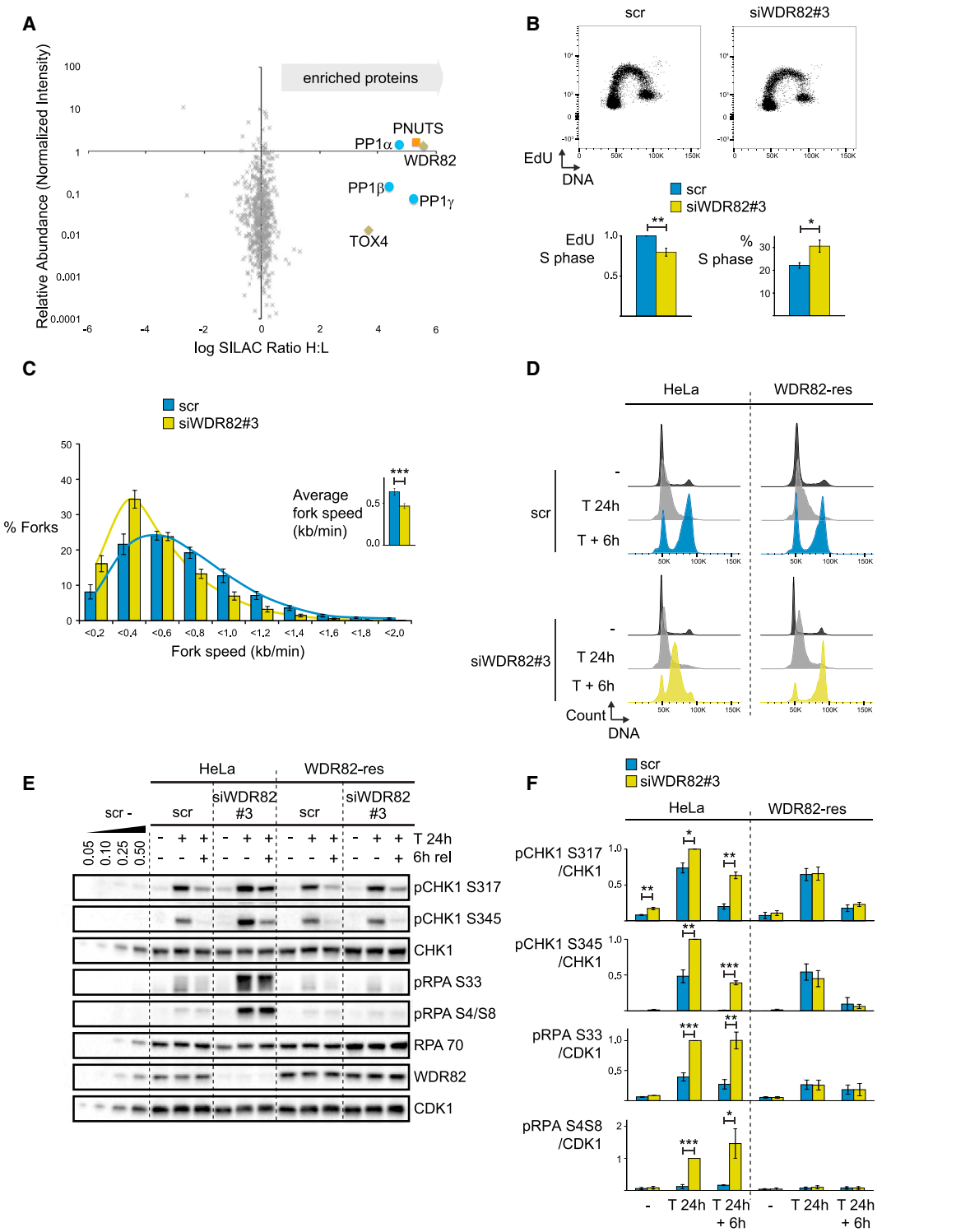

Figure 2. WDR82, a Major PNUTS Interaction Partner, Also Promotes DNA Replication

(A) HeLa cells were isotopically labeled by growth in SILAC media and transiently transfected with PNUTS-EGFP or empty EGFP. After 24 h, lysates were prepared and mixed at a 1:1 ratio. Complexes containing EGFP were isolated, separated by 1D SDS-PAGE, trypsin digested, and analyzed by liquid chromatography-tandem mass spectrometry (LC-MS/MS). Proteins were identified and SILAC ratios and relative abundance quantified using MaxQuant.

(B) Flow cytometry analysis (as in Figure 1A) at 72 h after transfection with scr or siRNA against WDR82 (siWDR82#3) (n = 5).

(legend continued on next page)

suggesting ATR activity is not the main cause of the suppressed replication after depletion of PNUTS. We further addressed whether PP1 was involved by overexpressing a siRNA-resistant PP1 binding deficient mutant (EGFP PNUTS^{RAXA}). While wild-type PNUTS (EGFP PNUTS^{wt}) partially rescued the lower EdU uptake and completely rescued the enhanced S phase fraction after depletion of endogenous PNUTS, EGFP PNUTS^{RAXA} did not (Figures 1E and 1F). The dependency on PP1 suggested that reduced pRNAPII S5 dephosphorylation might be causing the effects of PNUTS depletion on replication. Supporting this, depletion of another pRNAPII S5 phosphatase, SSU72 (Krishnamurthy et al., 2004), also reduced EdU incorporation and replication fork speed and enhanced the S phase fraction (Figures 1G, 1H, and S3B). Together, these findings show that PNUTS-PP1 is required for normal replication fork progression and suggest it does so by dephosphorylating pRNAPII S5.

WDR82, a PNUTS Interaction Partner, Is Also Required for DNA Replication under Normal and Stressed Conditions

To search for additional PNUTS binding partners that might contribute to the role of PNUTS-PP1 in DNA replication, we performed stable isotope labeling of amino acids in cell culture (SILAC) immunoprecipitation (IP) of PNUTS EGFP followed by mass spectrometry (Figure 2A). This method allows the identification of high confidence protein interactions, as it enables subtraction of background and bait interactions (Trinkle-Mulcahy, 2012). The major PNUTS interaction partners identified were WDR82, TOX4 and the PP1 isoforms; PP1α, PP1β, and PP1γ (Figure 2A; Table S1). The PNUTS/TOX4/WDR82 (PTW)-PP1 complex has also been reported by others (Lee et al., 2010). We verified the interactions by coIP using EGFP-tagged PNUTS, mpnuts, TOX4, WDR82, PP1α, PP1β, and PP1γ (Figures S2A–S2E; data not shown). Consistent with PNUTS acting as a scaffolding protein in the PTW-PP1 complex (Lee et al., 2010), depletion of WDR82 did not reduce association of EGFP mpnuts with PP1γ or TOX4 (Figure S2D), and PP1 binding was not required for the association between PNUTS and WDR82 or TOX4 (Figures S2A and S2C). As WDR82 binds directly to pRNAPII S5 (Lee and Skalnik, 2008), we addressed whether WDR82 might also play a role in DNA replication. Indeed, siRNA-mediated depletion of WDR82 reduced EdU incorporation and increased the fraction of cells in S phase compared to control siRNA transfected cells (Figure 2B). Supporting that PNUTS and WDR82 are acting in the same pathway, co-depletion of WDR82 with PNUTS did not show additive effects on EdU uptake or the S phase fraction (Figures S3A and S3B). Depletion of WDR82 also reduced replication fork speed, reduced recovery from replication stalling, and enhanced ATR signaling with and without thymidine (Figures 2C–2F, S2F, and S2G). The effects on recovery from replication stalling and ATR signaling were specific for WDR82, as they were rescued by siRNA-resistant WDR82 (Figures 2D–2F, S2F, and S2G). Enhanced ATR signaling was also observed with two additional siRNA oligonucleotides (Figures S2H and S2I). Furthermore, WDR82 depletion caused higher accumulation in S phase after HU and more RPA loading and higher levels of γH2AX and pRPA S4S8 24 h after thymidine (Figures 2E, 2F , and S3C–S3E), suggesting WDR82 is required to prevent DNA damage and promotes cell survival during replication stress. Supporting this, WDR82 depletion reduced cell survival after hydroxyurea treatment (Figure S3F).

WDR82 Facilitates pRNAPII S5 Dephosphorylation by PNUTS-PP1 in Live Cells

We further addressed whether WDR82 plays a role in dephosphorylation of pRNAPII S5. Indeed, WDR82 depletion specifically enhanced levels of pRNAPII S5 (Figures 3A, 3B, and S2I). Previously, we used the CDK7 inhibitor THZ1 to show that PNUTS-PP1 plays a major role in pRNAPII S5 dephosphorylation during replication stress (Landsverk et al., 2019). Remarkably, we obtained similar results with WDR82. While pRNAPII S5 was reduced after THZ1 treatment in control siRNA transfected cells, it was not reduced in cells transfected with WDR82 siRNA (Figures 3C and 3D), supporting a role for WDR82 in pRNAPII S5 dephosphorylation. To further explore this, we performed an *in vitro* dephosphorylation assay. Using RNAPII bound to GFPmpnuts as a substrate, we confirmed that pRNAPII S5 is a direct substrate for PNUTS-PP1 (Figures 3E and 3F; Ciurciu et al., 2013; Lee et al., 2010). pRNAPII S5 was selectively dephosphorylated compared to pRNAPII S2 (Figures 3E and 3F), showing that PNUTS-PP1 displays specificity for pRNAPII S5 versus pRNAPII S2 *in vitro*. Furthermore, PP1 was the phosphatase involved, as calyculin A, a PP1 inhibitor (Swingle et al., 2007), inhibited pRNAPII S5 dephosphorylation (Figure 3E). Though depletion of WDR82 reduced the amount of WDR82 in the GFPmpnuts pull-downs, the rate of pRNAPII S5 dephosphorylation was unaltered compared to controls (Figures 3E and 3G). Thus, though WDR82 is required for pRNAPII S5 dephosphorylation in live cells, it may not be required for its dephosphorylation *in vitro*. Alternatively, the small remaining amount of WDR82 (Figure 3E) may be sufficient for *in vitro* dephosphorylation of pRNAPII S5. Supporting a requirement for WDR82 in mediating RNAPII dephosphorylation in live cells, a higher amount of RNAPII relative to GFPmpnuts was pulled down from WDR82-depleted versus control siRNA transfected cells (Figure 3E, time 0 min, and Figure 3H). Moreover, the amount of RNAPII relative to PP1γ was also higher (Figure 3E, time 0 min, and Figure 3I). This is reminiscent of the increased interaction between pRNAPII S5 with a hypoactive PNUTS-PP1 fusion mutant observed in pull-downs from HEK293T cells (Wu et al., 2018) and is thus highly consistent with a dephosphorylation defect.

(C) DNA fiber analysis of HeLa cells 48 h after transfection with scr or siWDR82#3 as in Figure 1B. p value was determined by the Wilcoxon signed rank test (n = 6).
(D) Flow cytometry analysis (as in Figure 1C) of HeLa or HeLa cells stably expressing siRNA-resistant WDR82 (WDR82-res) 72 h after transfection with scr or siWDR82#3.
(E) Western blot of experiment as in (D).
(F) Mean results from experiments as in (E) (n = 3).
Error bars represent SEM. See also Figures S2 and S3 and Table S1.

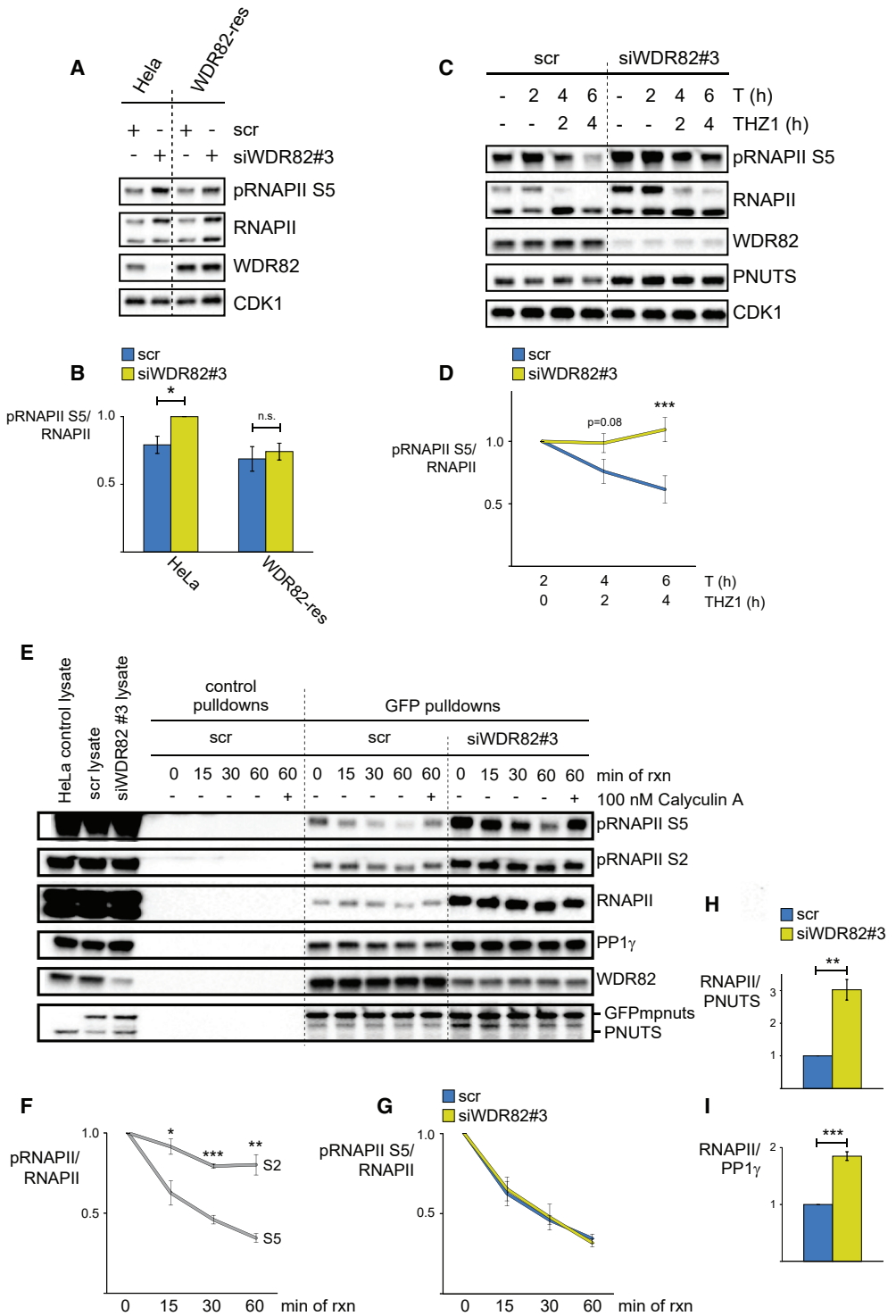

Figure 3. WDR82 Facilitates pRNAPII S5 Dephosphorylation by PNUTS-PP1 in Live Cells

(A) Western blot of HeLa or WDR82-res cells 72 h after siRNA transfection with scr or siWDR82#3.

(B) Mean pRNAPII S5 versus RNAPII from experiments as in (A). p values were determined by the two-tailed Student's one-sample t test (n = 7).

(C) Western blot analysis of scr or siWDR82#3 transfected HeLa cells treated with thymidine (T) for 2, 4, and 6 h. THZ1 was added 2 h after thymidine treatment.

(D) Mean fold changes of pRNAPII S5 relative to RNAPII for THZ1 and thymidine samples relative to the T 2 h sample from experiments as in (C) (n = 8). Statistical significance was determined from fold changes in scr versus siWDR82#3 samples at indicated time points.

(legend continued on next page)

Depletion of PNUTS or WDR82 Enhances the Residence Time of Phosphorylated RNAPII on Chromatin

T-R conflicts can occur due to enhanced retention of RNAPII on chromatin (Chakraborty et al., 2018; Felipe-Abrio et al., 2015; Poli et al., 2016). Thus, one hypothesis might be that defective pRNAPII S5 dephosphorylation could lead to alterations in the dynamics of RNAPII, causing T-R conflicts. We addressed this by fluorescence recovery after photobleaching (FRAP) analysis of GFP RNAPII in MRC5 cells (Steurer et al., 2018). PNUTS depletion caused a larger immobile fraction of GFP RNAPII (Figure 4A), indicating a larger fraction of RNAPII complexes were stably chromatin bound. Of note, the levels of GFP RNAPII were lower after PNUTS depletion compared to control siRNA transfected cells (Figure S4A). We further explored this by assessing the chromatin residence time of transcriptionally engaged RNAPII. To do so, we measured the decrease in RNAPII chromatin binding after THZ1 treatment, which prevents *de novo* transcription initiation (Steurer et al., 2018) and pRNAPII S5 phosphorylation (Kwiatkowski et al., 2014). Supporting inhibition of *de novo* transcription initiation by THZ1, a reduction of chromatin-bound RNAPII was observed both in PNUTS-depleted and in control siRNA transfected cells after THZ1 treatment during thymidine-induced replication stress (Figures 4B and 4C). However, RNAPII on chromatin was less reduced in cells depleted of PNUTS (reduced by 42%) compared to control siRNA transfected cells (reduced by 72%) (Figures 4B and 4C), consistent with higher residence time of chromatin-bound RNAPII. Furthermore, pRNAPII S5 was also less reduced in PNUTS-depleted cells after THZ1 treatment (Figure 4B and 4D). These results were further extended by high-precision flow cytometry analysis of detergent-extracted cells, which confirmed the higher residence time of pRNAPII S5 on chromatin with THZ1 after PNUTS depletion, both in the presence and absence of thymidine (Figures 4E, 4G, 4H, S4B, S4D, and S4F). Furthermore, similar results for pRNAPII S5 were found in WDR82-depleted cells (Figures 4E, 4G, 4H, S4B, and S4D). Notably, flow cytometry also allowed the distinction between G1 and S phases of the cell cycle based on DNA content, and for pRNAPII S5, similar effects were observed in both phases (Figures 4H and S4D). Using an antibody that recognizes the N terminus of RNAPII, we confirmed that levels of total RNAPII were reduced by THZ1 on chromatin in PNUTS and WDR82 depleted and in control siRNA transfected cells (Figures 4F, 4I, S4C, and S4E). Moreover, though the differences were smaller than with pRNAPII S5, total RNAPII chromatin loading was significantly less reduced by THZ1 after depletion of PNUTS or WDR82, at least in G1 phase (Figure 4I). These results show that RNAPII has a higher residence time on chromatin after depletion of PNUTS or WDR82. We reasoned that this was likely caused by defective dephosphorylation of pRNAPII S5. Supporting this, while EGFP PNUTS^{wt} partially rescued the lower reduction in chromatin binding of pRNAPII S5 and RNAPII after THZ1 in PNUTS siRNA transfected cells, EGFP PNUTS^{RAXA} rescued less (Figures 4J, 4K, S4G, and S4H). Furthermore, depletion of SSU72 also suppressed the reduction in pRNAPII S5 and RNAPII on chromatin after THZ1 (Figure 4L). As depletion of two different pRNAPII S5 phosphatases show similar effects, these results suggest that defective dephosphorylation of pRNAPII S5 underlies the enhanced residence time of RNAPII on chromatin.

CDC73 Is Required to Enhance the Residence Time of Phosphorylated RNAPII on Chromatin and for Suppression of Replication after Depletion of PNUTS or WDR82

We previously found that CDC73, a component of the PAF1 transcription elongation complex which binds the phospho-CTD (Qiu et al., 2012), was required for high ATR activity after depletion of PNUTS (Landsverk et al., 2019). To address whether it also plays a role in the replication phenotypes and the enhanced RNAPII-residence time on chromatin, we co-depleted CDC73 with PNUTS. Co-depletion of CDC73 partially reversed the enhanced residence time of RNAPII on chromatin, as RNAPII and pRNAPII S5 were more reduced after THZ1 in cells co-depleted of CDC73 and PNUTS compared to cells transfected with PNUTS siRNA alone (Figures 5A–5F and S5A–S5C). Co-depletion of CDC73 with PNUTS also partially reversed the slower replication fork rate and EdU uptake in PNUTS depleted cells, while depletion of CDC73 alone did not alter the replication fork rate compared to control siRNA transfected cells (Figures 5G, 5H, S5D, and S5E). Moreover, the enhanced EdU uptake upon co-depletion of CDC73 with PNUTS was a specific effect of the CDC73 siRNA, as it was rescued in cells expressing siRNA-resistant CDC73 (Figures 5H, S5D, and S5E). Co-depletion of CDC73 also reversed the effects on replication after depletion of WDR82, as it suppressed the enhanced accumulation of cells in S phase after a low dose of hydroxyurea observed in cells depleted of WDR82 alone (Figure S5F). Together, these results show CDC73 is required for the prolonged residence time of phosphorylated RNAPII on chromatin and for suppression of replication after depletion of PNUTS and WDR82.

Enhanced Chromatin Retention of RNAPII Is Due to Reduced Degradation on Chromatin after Depletion of PNUTS or WDR82

During the chromatin extractions, we noticed that though the levels of RNAPII decreased on chromatin with THZ1, they did not increase in the corresponding soluble fractions (Figures 6A and 6B). This indicated that RNAPII was being degraded at or

(E) Western blot of a phosphatase assay using RNAPII pulled down with GFPmpnuts as substrate. HeLa GFPmpnuts or HeLa cells (used for control pull-downs) were harvested 72 h after transfection with scr or siWDR82#3. Isolated GFP complexes were incubated at 30°C for the indicated times in the presence or absence of 100 nM calyculin A.

(F) Mean fold changes of pRNAPII/RNAPII for S2 and S5 relative to the t = 0 min sample from (E) in complexes from cells transfected with scr. Statistical significance was determined from fold changes of pRNAPII S2/RNAPII versus pRNAPII S5/RNAPII at indicated time points (n = 3).

(G) As in (F) except showing fold changes of pRNAPII S5/RNAPII in complexes from cells transfected with scr and siWDR82#3.

(H) Mean RNAPII relative to GFPmpnuts in complexes from cells transfected with scr or siWDR82#3 as in (E) at t = 0 min. (n = 3).

(I) As in (H) except showing RNAPII relative to PP1γ.

p values in (H) and (I) were determined by the two-tailed Student's one-sample t test. Error bars represent SEM.

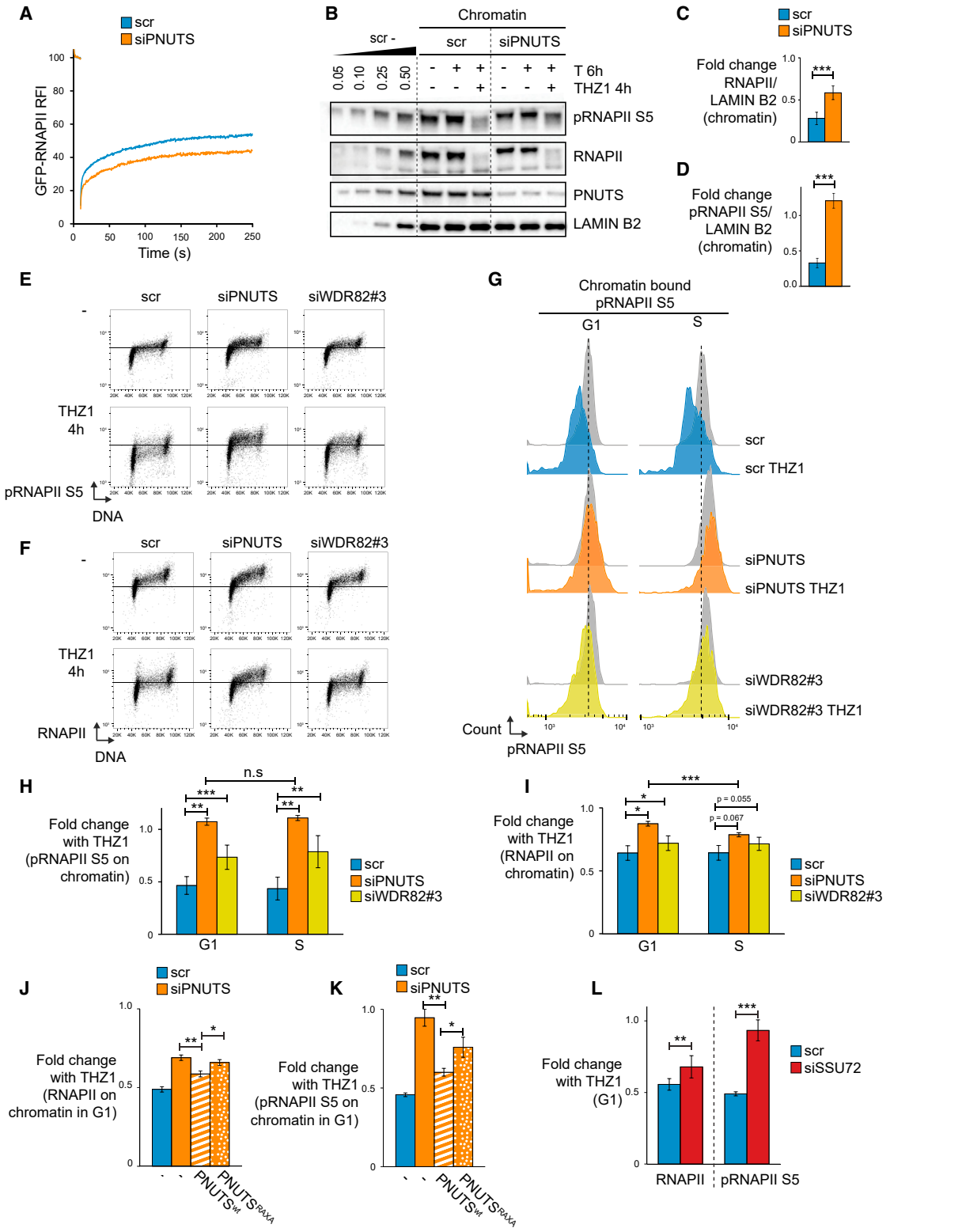

(legend on next page)

in the close vicinity of chromatin during THZ1 treatment. To further address this, we measured the chromatin residence time of RNAPII and pRNAPII S5 after THZ1 treatment with the proteasome inhibitor MG132. Remarkably, in the presence of MG132, the levels of pRNAPII S5 and RNAPII were substantially less reduced by THZ1 in control siRNA transfected cells in both G1 and S phase (Figures 6C–6E). This is consistent with extensive proteasome-mediated degradation of chromatin-bound RNAPII during THZ1 treatment. In contrast, MG132 had a much smaller effect on the levels of RNAPII and pRNAPII S5 in PNUTS-depleted cells (Figures 6C–6G), indicating less proteasome-mediated degradation of chromatin-bound RNAPII. Similar effects were observed after depletion of WDR82 and SSU72 (Figures 6C–6G). Moreover, co-depletion of CDC73 with PNUTS partially reversed the reduced effects of MG132 on RNAPII and pRNAPII S5 levels in cells depleted of PNUTS alone (Figure S5G). Altogether, these results strongly suggest pRNAPII S5 dephosphorylation by WDR82/PNUTS-PP1 is promoting degradation of RNAPII on chromatin, thereby reducing RNAPII residence time.

Phosphorylated RNAPII Promotes T-R Conflicts after Depletion of PNUTS or WDR82

So far, our results were consistent with defective pRNAPII S5 dephosphorylation stabilizing RNAPII by suppressing its degradation on chromatin, and thus enhancing T-R conflicts after depletion of PNUTS or WDR82. To further test this hypothesis, we performed a proximity ligation assay (PLA) with RNAPII and the replication factor proliferating cell nuclear antigen (PCNA) by high-precision flow cytometry (Figures 7A, S6A, and S6B). Supporting more T-R conflicts after depletion of PNUTS, a higher RNAPII-PCNA PLA signal in S phase was observed in PNUTS-depleted cells compared to control cells (Figure 7A). A higher PLA signal could also be observed by fluorescence microscopy (Figure S6C). As we had previously observed increased amounts of R-loops after depletion of PNUTS (Landsverk et al., 2019), we addressed whether R-loops might be involved in the effects on replication. Consistent with T-R conflicts, overexpression of RNaseH1 partially rescued the reduced EdU incorporation and fork rate after depletion of PNUTS (Figures 7B and 7C). In contrast, overexpression of RNaseH1 reduced EdU incorporation and fork rate in control siRNA transfected cells (Figures 7B and 7C). R-loops are thus likely contributing to the reduced replication after depletion of PNUTS. On the other hand, overexpression of RNaseH1 did not rescue the reduced fork rate in cells depleted of WDR82 (Figure 7C). To address whether the higher stability of RNAPII on chromatin might contribute to suppression of replication, we performed the fiber assay after inhibition of *de novo* transcription initiation by THZ1. Remarkably, THZ1 enhanced replication fork rates after depletion of PNUTS and WDR82 (Figure 7D), strongly supporting an involvement of T-R conflicts via the longer residence time of RNAPII on chromatin. In contrast, in control siRNA transfected cells, THZ1 slightly reduced fork rates (Figure 7D). Note that THZ1 treatment had a greater effect on rescuing the reduced fork rates after depletion of WDR82 than PNUTS (Figure 7D). Indeed, this may reflect the difference in severity of the effects after depletion PNUTS versus WDR82 on replication and RNAPII residence time. Altogether, our results strongly support the hypothesis that dephosphorylation of pRNAPII S5 by WDR82/PNUTS-PP1 suppresses the residence of time RNAPII on chromatin by promoting its degradation, thus preventing T-R conflicts and counteracting replication stress (Figure 7E).

DISCUSSION

Replication stress is common in cancer cells and can be caused by T-R conflicts (Gaillard and Aguilera, 2016; Gaillard et al., 2015). The mechanisms that regulate transcription to prevent T-R conflicts have until now remained obscure. In this work, we describe a pathway involving a main signaling platform of transcription, namely the CTD, that promotes degradation of RNAPII on chromatin and counteracts replication stress. Our work identifies an important role for RNAPII-CTD dephosphorylation in suppressing replication stress during normal transcription. As reduced dephosphorylation of the CTD prevented proteasome-mediated degradation of RNAPII and caused

Figure 4. Depletion of PNUTS or WDR82 Enhances the Residence Time of Phosphorylated RNAPII on Chromatin

(A) FRAP analysis of GFP-RNAPII knockin MRC5 cells transfected with siPNUTS or scr. GFP-RNAPII was bleached in a narrow strip spanning the nucleus. Fluorescence recovery was measured every 0.4 s for 4 min, background corrected, and normalized to prebleach fluorescence intensity. Mean values of n = 32 cells from three independent experiments are shown.

(B) Western blot analysis of chromatin fractions from cells at 48 h after transfection with scr or siPNUTS. Thymidine was added at 6 h and THZ1 at 4 h prior to harvest. LAMIN B2 was used as loading control for chromatin fractions.

(C) Mean fold changes of RNAPII/LAMIN B2 with THZ1 and thymidine relative to thymidine alone in (B) (n = 6).

(D) As in (C) except showing pRNAPII S5/LAMIN B2.

(E) Flow cytometry analysis showing levels of pRNAPII S5 on chromatin versus DNA content 48 h after transfection with scr, siPNUTS, or siWDR82#3 with and without THZ1 (THZ1 4 h). The black line is to ease visual interpretation.

(F) As in (E) except showing levels of RNAPII on chromatin relative to DNA content.

(G) Histograms showing distribution of pRNAPII S5 levels on chromatin in G1 and S phase in individual cells from same experiment as in (E). The dotted line is provided to ease visual interpretation.

(H) Mean fold changes of pRNAPII S5 on chromatin in THZ1-treated relative to nontreated cells in G1 and S phases from experiments as in (E) (n = 3).

(I) As in (H) except showing fold changes in total RNAPII levels.

(J) Mean fold changes of RNAPII on chromatin in THZ1-treated relative to nontreated cells in G1, 48 h after transfection with scr and siPNUTS, and 42 h after transfection with $PNUTS^{wt}$ or $PNUTS^{RAXA}$ (n = 3).

(K) As in (J) except showing pRNAPII S5.

(L) As in (H) and (I), 42 h after transfection with scr and siSSU72 (n = 4).

In this figure, all p values were determined by the two-tailed Student's one-sample t test. Error bars represent SEM. See also Figure S4.

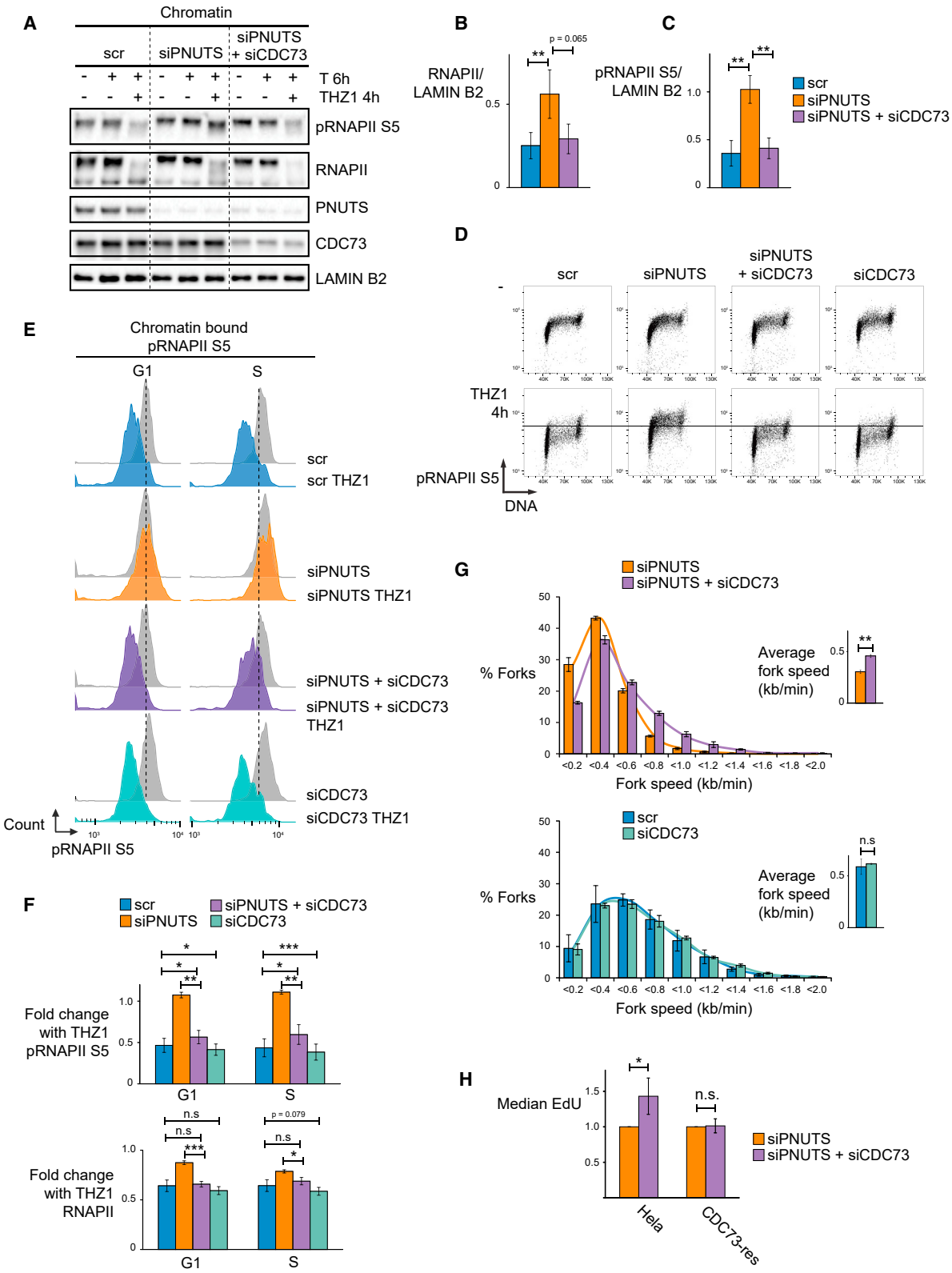

(legend on next page)

replication stress, our results suggest that continuous turnover of RNAPII on chromatin is required to prevent T-R conflicts.

Our results support previous studies suggesting that increased retention of RNAPII on chromatin can cause replication stress and that RNAPII can be removed by degradation during T-R conflicts (Felipe-Abrio et al., 2015; Poli et al., 2016). Our results show that this applies also in human cells and identify several factors involved in regulation of RNAPII turnover to prevent T-R conflicts, namely WDR82/PNUTS-PP1 and pRNAPII S5. A previous study in yeast showed pRNAPII S5 prevented ubiquitinylation and degradation of RNAPII (Somesh et al., 2005), suggesting that the inhibitory role of pRNAPII S5 in RNAPII degradation may be conserved. On the other hand, previous studies in human cells showed that the phosphorylated CTD was associated with increased RNAPII degradation (McKay et al., 2001) and pRNAPII S5 was specifically bound to E3 ubiquitin ligase after DNA damage (Yasukawa et al., 2008). Thus, in human cells, there are likely multiple pathways for RNAPII degradation. In line with this, the stability of RNAPII on chromatin was reduced in S phase compared to G1 phase and pRNAPII S5 was reduced in S phase by addition of thymidine after depletion of PNUTS, but not in control siRNA transfected cells (Figures 4I and S4F). High pressure to remove RNAPII during T-R collisions in PNUTS-depleted cells in S phase may thus promote alternative pathways for RNAPII removal from chromatin.

Though more work is required to understand the conditions under which WDR82/PNUTS-PP1-dependent RNAPII degradation occurs, the following points of evidence suggest it involves elongating RNAPII. First, RNAPII bound to PNUTS was phosphorylated on S2 (Figure 3E), which is associated with elongation. Supporting this, PNUTS colocalizes with pRNAPII S2 in flies and human cells (Ciurciu et al., 2013; Verheyen et al., 2015) and was found throughout the gene body by chromatin IP (ChIP) analysis in human cells (Cortazar et al., 2019). Furthermore, after THZ1 treatment of PNUTS-depleted human cells, phosphorylation of both RNAPII S5 and S2 was prolonged (Landsverk et al., 2019), suggesting that the lack of pRNAPII S5 dephosphorylation might also inhibit dephosphorylation of pRNAPII S2 or, more likely, degradation of S2-phosphorylated elongating RNAPII. Moreover, PNUTS was recently found to be a global decelerator of RNAPII elongation that promotes termination (Austenaa et al., 2015; Cortazar et al., 2019) and WDR82 also has a similar role in termination (Austenaa et al., 2015). Interestingly, termination factors have previously been found to play a role in counteracting replication stress and genome instability, leading to the hypothesis that transcription termination counteracts T-R conflicts (Gómez-González and Aguilera, 2019). Therefore, the more stable, chromatin-bound, phosphorylated RNAPII fraction after depletion of PNUTS or WDR82 may in part represent elongating RNAPII that has failed to terminate and is unable to be removed by degradation.

Notably, transcription termination factors are also connected to R-loop metabolism (Santos-Pereira and Aguilera, 2015). One way termination factors may prevent replication stress could therefore be to remove hazardous R-loops (Santos-Pereira and Aguilera, 2015). As depletion of PNUTS causes R-loops (Landsverk et al., 2019), the enhanced replication stress may therefore be related to R-loops. Supporting this, we found that overexpression of RNaseH1 partially rescued the reduced EdU uptake and fork rate after depletion of PNUTS. On the other hand, while THZ1 completely rescued the fork rate in cells depleted of WDR82, overexpression of RNaseH1 did not. Thus, R-loops may contribute to the reduced replication when pRNAPII S5 dephosphorylation is suppressed by depletion of PNUTS but is unlikely to be the main underlying cause.

CDC73, a tumor suppressor, is a component of the PAF1 transcription elongation complex, which includes WDR61, CDC73, PAF1, LEO1, and CTR9 in humans. Interactions between CDC73, WDR61, and CTR9 with PNUTS have previously been identified (Hein et al., 2015; Landsverk et al., 2019), and CDC73 and WDR61 were putative hits in our SILAC IP (Table S1), suggesting the whole or parts of the PAF complex may functionally interact with WDR82/PNUTS-PP1. Here, we show that CDC73 is required for suppression of replication following depletion of PNUTS or WDR82. CDC73 binding to the phospho-CTD is stimulated by diphosphorylation on S5/S2 or S5/S7 (Qiu et al., 2012). Moreover, CDC73 binds more to RNAPII after depletion of PNUTS (Landsverk et al., 2019). CDC73 may thus partially shield RNAPII from other pRNAPII S5 phosphatases and/or from the proteasome machinery itself. Interestingly, in yeast, CDC73 and the PAF1 complex were required for Mec1 dependent removal of RNAPII during replication stress (Poli et al., 2016), suggesting interspecies differences or multiple pathways for RNAPII degradation.

Here we show that WDR82 and PNUTS counteract replication stress and find several lines of evidence connecting this to their

Figure 5. Co-depletion of CDC73 Reverses Enhanced Residence Time of RNAPII on Chromatin and Replication Effects after Depletion of PNUTS or WDR82

(A) Western blot analysis of chromatin fractions from cells transfected with scr, siPNUTS, or siPNUTS and siRNA against CDC73 (siCDC73) at 48 h after siRNA transfection. Thymidine was added at 6 h and THZ1 at 4 h prior to harvest.

(B and C) Mean fold changes of RNAPII/LAMIN B2 (B) or pRNAPII S5/LAMIN B2 (C) with THZ1 and thymidine relative to thymidine alone from experiments as in (A) (n = 3). p values were determined by the two-tailed Student's one-sample t test.

(D) Flow cytometry analysis of pRNAPII S5 on chromatin in extracted cells 48 h after transfection with scr, siPNUTS, siCDC73, and siPNUTS and siCDC73 with or without THZ1 for 4 h (THZ1 4 h). The black line is shown to ease visual interpretation.

(E) Distribution of pRNAPII S5 levels on chromatin in G1 and S phase in cells from same experiment as in (D).

(F) Mean fold changes of pRNAPII S5 and RNAPII on chromatin in THZ1-treated versus nontreated cells in G1 and S phases. (n = 3). p values were determined by the two-tailed Student's one-sample t test.

(G) DNA fiber analysis performed in HeLa cells 48 h after transfection with scr, siPNUTS, siCDC73, and siPNUTS and siCDC73. Mean distributions of replication fork speed, as well as replication fork speed, are shown (n = 3). p values were determined by the Wilcoxon signed rank test.

(H) Mean median EdU incorporation in HeLa or HeLa cells stably expressing siRNA-resistant CDC73 (CDC73-res) 72 h after siRNA transfection with siPNUTS or siPNUTS and siCDC73 from experiments as shown in Figure S5D. p values were determined by the two-tailed Student's one-sample t test (n = 4).

Error bars represent SEM. See also Figure S5.

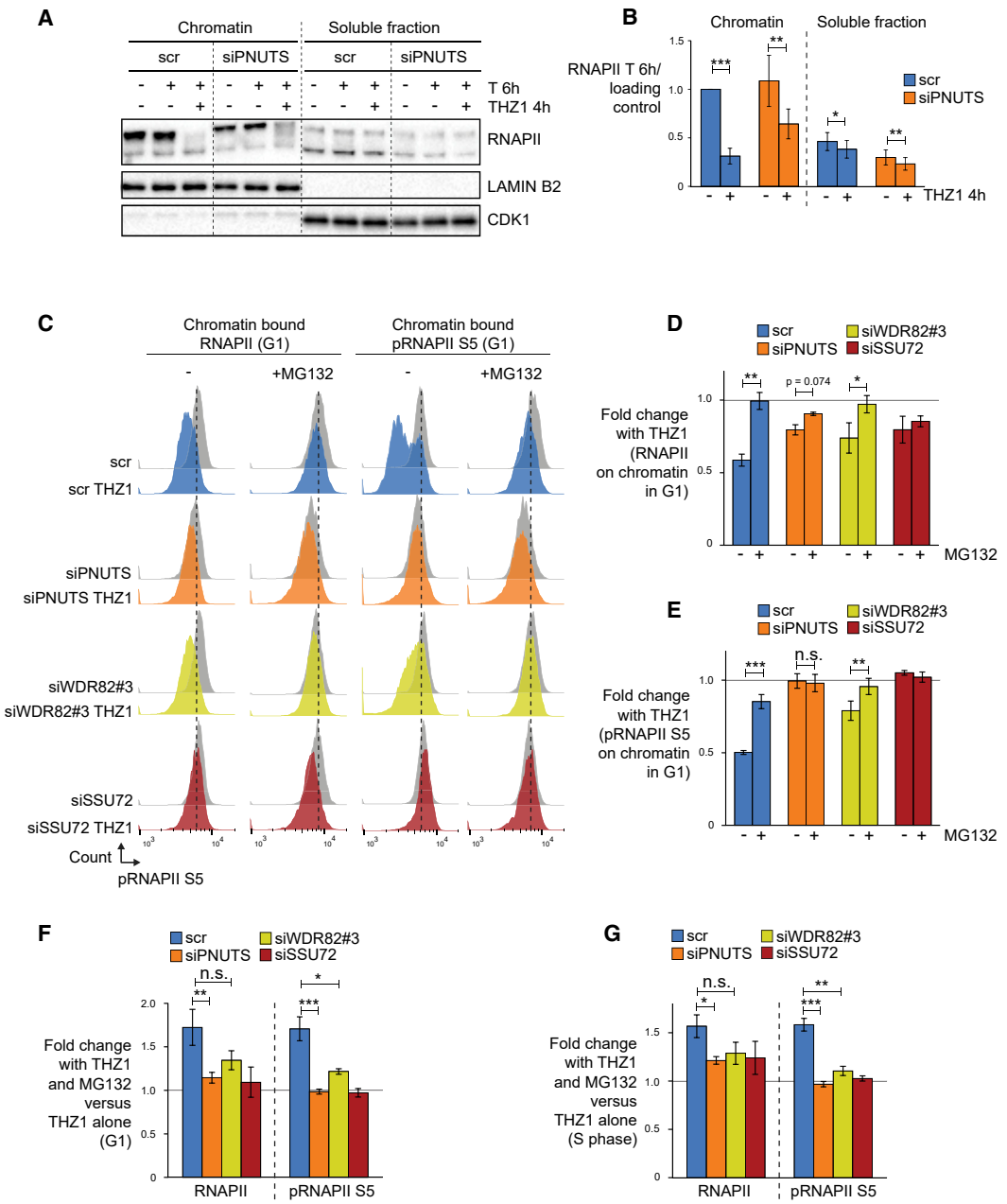

Figure 6. Enhanced RNAPII Chromatin Residence Time Is Caused by Less Proteasome-Mediated Degradation on Chromatin after Depletion of PNUTS or WDR82

(A) Western blot analysis of chromatin and soluble fractions 48 h after transfection with scr or siPNUTS. Thymidine was added at 6 h and THZ1 at 4 h prior to harvest. LAMIN B2 and CDK1 were used as loading controls for chromatin and soluble fractions, respectively.

(B) Mean levels of RNAPII/LAMIN B2 and RNAPII/CDK1 from experiments as in (A) (n = 5). p values were determined by the two-tailed Student's one-sample t test.

(C) Distribution of RNAPII and pRNAPII S5 levels on chromatin in G1 cells 48 h after transfection with scr, siPNUTS, siWDR82#3, and siSSU72 with and without THZ1 and MG132 (4 h).

(D) Mean fold changes from (C) of RNAPII on chromatin in THZ1-treated relative to nontreated cells with and without MG132 in G1 phase (n = 3, except for siSSU72, where n = 2).

(E) As in (D) but showing fold changes of pRNAPII S5.

(F) Effect of MG132 on fold changes after THZ1, as determined by the fold change with MG132 divided by the fold change without MG132 from (D) and (E). If this value is above 1, then MG132 stabilizes pRNAPII S5 and/or RNAPII on chromatin. Data are presented as mean ± SEM (n = 3, except for siSSU72, where n = 2).

(G) As in (F) but in S phase.

p values in (D)–(G) were determined by the two-tailed Student's one-sample t test. Error bars represent SEM.

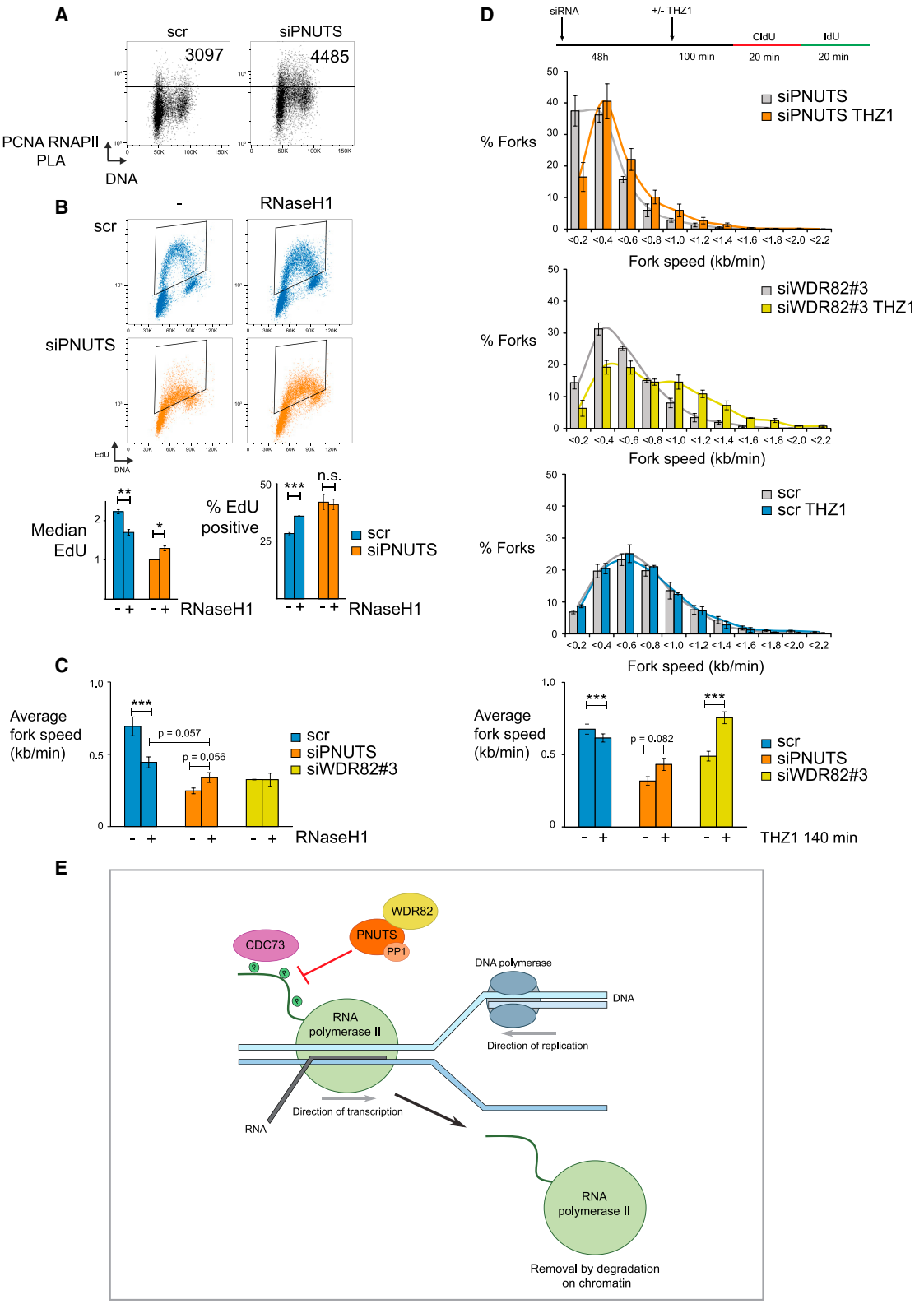

(legend on next page)

roles in RNAPII CTD dephosphorylation. By using a PP1 binding deficient mutant of PNUTS, we show that PP1 is required for the effects of PNUTS on DNA replication and RNAPII residence time (Figures 1E, 1F, 4J, and 4K). Furthermore, depletion of SSU72, a different RNAPII S5 phosphatase, gave similar effects as depletion of PNUTS and WDR82 on DNA replication and RNAPII chromatin stability (Figures 1G, 1H, and 6C–6G), strongly supporting that RNAPII S5 is the relevant substrate for WDR82/PNUTS-PP1. In line with this, co-depletion of the phospho-CTD binding protein CDC73 (Qiu et al., 2012) with PNUTS, suppressed the effects on RNAPII chromatin binding and DNA replication (Figures 5, S5A–S5E, and S5G). Moreover, addition of a transcription inhibitor that prevents *de novo* RNAPII initiation or overexpression of RNaseH1 to remove R-loops partially reversed the replication stress phenotype (Figures 7B–7D). Interestingly, low expression of WDR82 was associated with poor prognosis in colorectal cancer (Liu et al., 2018), but the underlying molecular explanation was unknown. Furthermore, high expression of WDR82 correlated with higher survival in pancreatic cancer, and high expression of PNUTS is a favorable prognostic marker in pancreatic and cervical cancer (Gendoo et al., 2019; Hu et al., 2018; Uhlen et al., 2017). Replication stress is frequently found in pancreatic and colorectal cancers (Manic et al., 2018; Wallez et al., 2018) and can also be induced by human papillomavirus infection, the main cause of cervical cancer (Moody, 2019). Therefore, in light of our results, we propose that PNUTS and WDR82 may prevent tumor aggressiveness by suppressing replication stress.

STAR★METHODS

Detailed methods are provided in the online version of this paper and include the following:

- KEY RESOURCES TABLE
- RESOURCE AVAILABILITY
  - Lead Contact
  - Materials Availability
  - Data and Code Availability
- EXPERIMENTAL MODEL AND SUBJECT DETAILS
- METHOD DETAILS
  - Chemicals and treatments
  - siRNA and DNA transfections
  - Western blotting and antibodies
  - Flow cytometry analysis
  - Chromatin fractionation for western blotting
  - Chromatin fractionation for flow cytometry
  - Proximity ligation assay for flow cytometry
  - Proximity ligation assay by microscopy
  - DNA Fiber assay
  - GFP pulldowns and SILAC experiment
  - Mass spectrometry and data analysis
  - Phosphatase assay
  - Live cell imaging
  - Immunofluorescence
  - Clonogenic survival assay
  - Prognostic data
- QUANTIFICATION AND STATISTICAL ANALYSIS

SUPPLEMENTAL INFORMATION

Supplemental Information can be found online at https://doi.org/10.1016/j.celrep.2020.108469.

ACKNOWLEDGMENTS

We thank the Flow Cytometry Core Facility and Core Facility for Advanced Light Microscopy at the Oslo University Hospital for helpful assistance and Beata Grallert for generating the CDC73 siRNA-resistant cell line. We are grateful for funds from the Norwegian Research Council (275918), the South-Eastern Norway Regional Health Authority (2014035 and 2013017), and the Norwegian Cancer Society (3367910).

AUTHOR CONTRIBUTIONS

H.B.L., L.E.S., and L.T.E.B. conducted most of the experiments. L.T.-M. performed SILAC mass spectrometry (MS) proteomics. B.S. and J.A.M. performed FRAP analysis. C.C. and L.E.S. constructed cells stably expressing siRNA-resistant WDR82. E.P. provided the DNA fiber assay technique and gave expert advice. O.J.B.L. performed initial experiments regarding WDR82. L.E.S., L.T.E.B., L.T.-M., B.S., J.A.M., H.B.L., and R.G.S. planned experiments and analyzed results. H.B.L. and R.G.S. conceived and supervised the study and wrote most of the paper. All authors contributed to editing the manuscript text.

DECLARATIONS OF INTEREST

The authors declare no competing interests.

Received: May 1, 2020
Revised: October 5, 2020
Accepted: November 10, 2020
Published: December 1, 2020

Figure 7. Replication-Transcription Collisions Suppress DNA Replication after Depletion of PNUTS or WDR82

(A) Flow cytometry proximity ligation assay (PLA) analysis showing proximity of RNAPII and PCNA in HeLa cells 72 h after siRNA transfection with scr or siPNUTS. Values in flow cytometry scatterplots show median PLA levels in S phase cells (within the region shown in Figure S6B). The black line is used to ease visual interpretation, as more dots (single cells) are above this line in PNUTS siRNA transfected cells than in control siRNA transfected cells.

(B) Flow cytometry analysis showing EdU incorporation 72 h after transfection with siPNUTS or scr and 48 h after transfection with EGFP-RNaseH1. Samples were stained and analyzed as in Figure 1A. Mean median EdU incorporation and percentage of cells in S phase are shown. (n = 3).

(C) Average replication fork speed from DNA fiber analysis in HeLa cells 48 h after transfection with scr, siPNUTS, or siWDR82#3 and 24 h after transfection with EGFP-RNase H1. p values were determined by the two-tailed Student's one-sample t test.

(D) DNA fiber analysis in HeLa cells at 48 h after siRNA transfection. THZ1 was added for 100 min before and during DNA fiber labeling (total 140 min). Mean replication fork speed and distributions of replication fork speed are shown (n = 3). p values were determined by the two-tailed Student's one-sample t test.

(E) Model for how WDR82/PNUTS-PP1 counteracts T-R collisions. Under regular conditions, WDR82/PNUTS-PP1 contributes to turnover of RNAPII on chromatin by dephosphorylating pRNAPII S5 in a timely manner, thus allowing RNAPII degradation and removal and preventing T-R conflicts. After depletion of PNUTS/WDR82, CDC73 binds to phosphorylated RNAPII and prevents RNAPII degradation, thus creating T-R conflicts. See main text for details.

Error bars represent SEM. See also Figure S6.

REFERENCES

Ahn, S.H., Kim, M., and Buratowski, S. (2004). Phosphorylation of serine 2 within the RNA polymerase II C-terminal domain couples transcription and 3′ end processing. Mol. Cell *13*, 67–76.

Andersen, J.S., Lyon, C.E., Fox, A.H., Leung, A.K., Lam, Y.W., Steen, H., Mann, M., and Lamond, A.I. (2002). Directed proteomic analysis of the human nucleolus. Curr. Biol. *12*, 1–11.

Austenaa, L.M., Barozzi, I., Simonatto, M., Masella, S., Della Chiara, G., Ghisletti, S., Curina, A., de Wit, E., Bouwman, B.A., de Pretis, S., et al. (2015). Transcription of mammalian cis-regulatory elements is restrained by actively enforced early termination. Mol. Cell *60*, 460–474.

Bentley, D.L. (2014). Coupling mRNA processing with transcription in time and space. Nat. Rev. Genet. *15*, 163–175.

Beullens, M., Stalmans, W., and Bollen, M. (1998). The biochemical identification and characterization of new species of protein phosphatase 1. Methods Mol. Biol. *93*, 145–155.

Bjursell, G., and Reichard, P. (1973). Effects of thymidine on deoxyribonucleoside triphosphate pools and deoxyribonucleic acid synthesis in Chinese hamster ovary cells. J. Biol. Chem. *248*, 3904–3909.

Boens, S., Szekér, K., Van Eynde, A., and Bollen, M. (2013). Interactor-guided dephosphorylation by protein phosphatase-1. Methods Mol. Biol. *1053*, 271–281.

Campeau, E., Ruhl, V.E., Rodier, F., Smith, C.L., Rahmberg, B.L., Fuss, J.O., Campisi, J., Yaswen, P., Cooper, P.K., and Kaufman, P.D. (2009). A versatile viral system for expression and depletion of proteins in mammalian cells. PLoS ONE *4*, e6529.

Chakraborty, P., Huang, J.T.J., and Hiom, K. (2018). DHX9 helicase promotes R-loop formation in cells with impaired RNA splicing. Nat. Commun. *9*, 4346.

Ciurciu, A., Duncalf, L., Jonchere, V., Lansdale, N., Vasieva, O., Glenday, P., Rudenko, A., Vissi, E., Cobbe, N., Alphey, L., and Bennett, D. (2013). PNUTS/PP1 regulates RNAPII-mediated gene expression and is necessary for developmental growth. PLoS Genet. *9*, e1003885.

Cortazar, M.A., Sheridan, R.M., Erickson, B., Fong, N., Glover-Cutter, K., Brannan, K., and Bentley, D.L. (2019). Control of RNA Pol II speed by PNUTS-PP1 and Spt5 dephosphorylation facilitates termination by a "sitting duck torpedo" mechanism. Mol. Cell *76*, 896–908.e4.

Custódio, N., and Carmo-Fonseca, M. (2016). Co-transcriptional splicing and the CTD code. Crit. Rev. Biochem. Mol. Biol. *51*, 395–411.

Dull, T., Zufferey, R., Kelly, M., Mandel, R.J., Nguyen, M., Trono, D., and Naldini, L. (1998). A third-generation lentivirus vector with a conditional packaging system. J. Virol. *72*, 8463–8471.

Felipe-Abrio, I., Lafuente-Barquero, J., García-Rubio, M.L., and Aguilera, A. (2015). RNA polymerase II contributes to preventing transcription-mediated replication fork stalls. EMBO J. *34*, 236–250.

Fokas, E., Prevo, R., Pollard, J.R., Reaper, P.M., Charlton, P.A., Cornelissen, B., Vallis, K.A., Hammond, E.M., Olcina, M.M., Gillies McKenna, W., et al. (2012). Targeting ATR in vivo using the novel inhibitor VE-822 results in selective sensitization of pancreatic tumors to radiation. Cell Death Dis. *3*, e441.

Forment, J.V., and O'Connor, M.J. (2018). Targeting the replication stress response in cancer. Pharmacol. Ther. *188*, 155–167.

Gaillard, H., and Aguilera, A. (2016). Transcription as a threat to genome integrity. Annu. Rev. Biochem. *85*, 291–317.

Gaillard, H., García-Muse, T., and Aguilera, A. (2015). Replication stress and cancer. Nat. Rev. Cancer *15*, 276–289.

Gendoo, D.M.A., Zon, M., Sandhu, V., Manem, V.S.K., Ratanasirigulchai, N., Chen, G.M., Waldron, L., and Haibe-Kains, B. (2019). MetaGxData: clinically annotated breast, ovarian and pancreatic cancer datasets and their use in generating a multi-cancer gene signature. Sci. Rep. *9*, 8770.

Gómez-González, B., and Aguilera, A. (2019). Transcription-mediated replication hindrance: a major driver of genome instability. Genes Dev. *33*, 1008–1026.

Hahn, M.A., Dickson, K.A., Jackson, S., Clarkson, A., Gill, A.J., and Marsh, D.J. (2012). The tumor suppressor CDC73 interacts with the ring finger proteins RNF20 and RNF40 and is required for the maintenance of histone 2B monoubiquitination. Hum. Mol. Genet. *21*, 559–568.

Håland, T.W., Boye, E., Stokke, T., Grallert, B., and Syljuåsen, R.G. (2015). Simultaneous measurement of passage through the restriction point and MCM loading in single cells. Nucleic Acids Res. *43*, e150.

Hamperl, S., Bocek, M.J., Saldivar, J.C., Swigut, T., and Cimprich, K.A. (2017). Transcription-replication conflict orientation modulates R-loop levels and activates distinct DNA damage responses. Cell *170*, 774–786.e719.

Harlen, K.M., and Churchman, L.S. (2017). The code and beyond: transcription regulation by the RNA polymerase II carboxy-terminal domain. Nat. Rev. *18*, 263–273.

Hawkins, M., Dimude, J.U., Howard, J.A.L., Smith, A.J., Dillingham, M.S., Savery, N.J., Rudolph, C.J., and McGlynn, P. (2019). Direct removal of RNA polymerase barriers to replication by accessory replicative helicases. Nucleic Acids Res. *47*, 5100–5113.

Hein, M.Y., Hubner, N.C., Poser, I., Cox, J., Nagaraj, N., Toyoda, Y., Gak, I.A., Weisswange, I., Mansfeld, J., Buchholz, F., et al. (2015). A human interactome in three quantitative dimensions organized by stoichiometries and abundances. Cell *163*, 712–723.

Hodroj, D., Recolin, B., Serhal, K., Martinez, S., Tsanov, N., Abou Merhi, R., and Maiorano, D. (2017). An ATR-dependent function for the Ddx19 RNA helicase in nuclear R-loop metabolism. EMBO J. *36*, 1182–1198.

Hu, D., Ansari, D., Pawłowski, K., Zhou, Q., Sasor, A., Welinder, C., Kristl, T., Bauden, M., Rezeli, M., Jiang, Y., et al. (2018). Proteomic analyses identify prognostic biomarkers for pancreatic ductal adenocarcinoma. Oncotarget *9*, 9789–9807.

Jackson, D.A., and Pombo, A. (1998). Replicon clusters are stable units of chromosome structure: evidence that nuclear organization contributes to the efficient activation and propagation of S phase in human cells. J. Cell Biol. *140*, 1285–1295.

Jensen, T.H., Jacquier, A., and Libri, D. (2013). Dealing with pervasive transcription. Mol. Cell *52*, 473–484.

Jones, R.M., Mortusewicz, O., Afzal, I., Lorvellec, M., García, P., Helleday, T., and Petermann, E. (2013). Increased replication initiation and conflicts with transcription underlie Cyclin E-induced replication stress. Oncogene *32*, 3744–3753.

Klusmann, I., Wohlberedt, K., Magerhans, A., Teloni, F., Korbel, J.O., Altmeyer, M., and Dobbelstein, M. (2018). Chromatin modifiers Mdm2 and RNF2 prevent RNA:DNA hybrids that impair DNA replication. Proc. Natl. Acad. Sci. USA *115*, E11311–E11320.

Kotsantis, P., Silva, L.M., Irmscher, S., Jones, R.M., Folkes, L., Gromak, N., and Petermann, E. (2016). Increased global transcription activity as a mechanism of replication stress in cancer. Nat. Commun. *7*, 13087.

Kreivi, J.P., Trinkle-Mulcahy, L., Lyon, C.E., Morrice, N.A., Cohen, P., and Lamond, A.I. (1997). Purification and characterisation of p99, a nuclear modulator of protein phosphatase 1 activity. FEBS Lett. *420*, 57–62.

Krishnamurthy, S., He, X., Reyes-Reyes, M., Moore, C., and Hampsey, M. (2004). Ssu72 Is an RNA polymerase II CTD phosphatase. Mol. Cell *14*, 387–394.

Kwiatkowski, N., Zhang, T., Rahl, P.B., Abraham, B.J., Reddy, J., Ficarro, S.B., Dastur, A., Amzallag, A., Ramaswamy, S., Tesar, B., et al. (2014). Targeting transcription regulation in cancer with a covalent CDK7 inhibitor. Nature *511*, 616–620.

Landsverk, H.B., Mora-Bermúdez, F., Landsverk, O.J., Hasvold, G., Naderi, S., Bakke, O., Ellenberg, J., Collas, P., Syljuåsen, R.G., and Küntziger, T. (2010). The protein phosphatase 1 regulator PNUTS is a new component of the DNA damage response. EMBO Rep. *11*, 868–875.

Landsverk, H.B., Sandquist, L.E., Sridhara, S.C., Rødland, G.E., Sabino, J.C., de Almeida, S.F., Grallert, B., Trinkle-Mulcahy, L., and Syljuåsen, R.G. (2019). Regulation of ATR activity via the RNA polymerase II associated factors CDC73 and PNUTS-PP1. Nucleic Acids Res. *47*, 1797–1813.

Lang, K.S., Hall, A.N., Merrikh, C.N., Ragheb, M., Tabakh, H., Pollock, A.J., Woodward, J.J., Dreifus, J.E., and Merrikh, H. (2017). Replication-transcription conflicts generate R-loops that orchestrate bacterial stress survival and pathogenesis. Cell *170*, 787–799.e18.

Lee, J.H., and Skalnik, D.G. (2008). Wdr82 is a C-terminal domain-binding protein that recruits the Setd1A Histone H3-Lys4 methyltransferase complex to transcription start sites of transcribed human genes. Mol. Cell. Biol. *28*, 609–618.

Lee, J.H., You, J., Dobrota, E., and Skalnik, D.G. (2010). Identification and characterization of a novel human PP1 phosphatase complex. J. Biol. Chem. *285*, 24466–24476.

Liu, B., and Alberts, B.M. (1995). Head-on collision between a DNA replication apparatus and RNA polymerase transcription complex. Science *267*, 1131–1137.

Liu, H., Li, Y., Li, J., Liu, Y., and Cui, B. (2018). H3K4me3 and Wdr82 are associated with tumor progression and a favorable prognosis in human colorectal cancer. Oncol. Lett. *16*, 2125–2134.

Manic, G., Signore, M., Sistigu, A., Russo, G., Corradi, F., Siteni, S., Musella, M., Vitale, S., De Angelis, M.L., Pallocca, M., et al. (2018). CHK1-targeted therapy to deplete DNA replication-stressed, p53-deficient, hyperdiploid colorectal cancer stem cells. Gut *67*, 903–917.

McKay, B.C., Chen, F., Clarke, S.T., Wiggin, H.E., Harley, L.M., and Ljungman, M. (2001). UV light-induced degradation of RNA polymerase II is dependent on the Cockayne's syndrome A and B proteins but not p53 or MLH1. Mutat. Res. *485*, 93–105.

Moody, C.A. (2019). Impact of replication stress in human papillomavirus pathogenesis. J. Virol. *93*, e01012–e01017.

Mortensen, P., Gouw, J.W., Olsen, J.V., Ong, S.E., Rigbolt, K.T., Bunkenborg, J., Cox, J., Foster, L.J., Heck, A.J., Blagoev, B., et al. (2010). MSQuant, an open source platform for mass spectrometry-based quantitative proteomics. J. Proteome Res. *9*, 393–403.

Nojima, T., Gomes, T., Grosso, A.R.F., Kimura, H., Dye, M.J., Dhir, S., Carmo-Fonseca, M., and Proudfoot, N.J. (2015). Mammalian NET-seq reveals genome-wide nascent transcription coupled to RNA processing. Cell *161*, 526–540.

Poli, J., Gerhold, C.B., Tosi, A., Hustedt, N., Seeber, A., Sack, R., Herzog, F., Pasero, P., Shimada, K., Hopfner, K.P., and Gasser, S.M. (2016). Mec1, INO80, and the PAF1 complex cooperate to limit transcription replication conflicts through RNAPII removal during replication stress. Genes Dev. *30*, 337–354.

Pomerantz, R.T., and O'Donnell, M. (2010). Direct restart of a replication fork stalled by a head-on RNA polymerase. Science *327*, 590–592.

Prévost, M., Chamousset, D., Nasa, I., Freele, E., Morrice, N., Moorhead, G., and Trinkle-Mulcahy, L. (2013). Quantitative fragmentome mapping reveals novel, domain-specific partners for the modular protein RepoMan (recruits PP1 onto mitotic chromatin at anaphase). Mol. Cell. Proteomics *12*, 1468–1486.

Qiu, H., Hu, C., Gaur, N.A., and Hinnebusch, A.G. (2012). Pol II CTD kinases Bur1 and Kin28 promote Spt5 CTR-independent recruitment of Paf1 complex. EMBO J. *31*, 3494–3505.

Rockx, D.A., Mason, R., van Hoffen, A., Barton, M.C., Citterio, E., Bregman, D.B., van Zeeland, A.A., Vrieling, H., and Mullenders, L.H. (2000). UV-induced inhibition of transcription involves repression of transcription initiation and phosphorylation of RNA polymerase II. Proc. Natl. Acad. Sci. USA *97*, 10503–10508.

Santos-Pereira, J.M., and Aguilera, A. (2015). R loops: new modulators of genome dynamics and function. Nat. Rev. Genet. *16*, 583–597.

Schneider, C.A., Rasband, W.S., and Eliceiri, K.W. (2012). NIH Image to ImageJ: 25 years of image analysis. Nat. Methods *9*, 671–675.

Sirbu, B.M., McDonald, W.H., Dungrawala, H., Badu-Nkansah, A., Kavanaugh, G.M., Chen, Y., Tabb, D.L., and Cortez, D. (2013). Identification of proteins at active, stalled, and collapsed replication forks using isolation of proteins on nascent DNA (iPOND) coupled with mass spectrometry. J. Biol. Chem. *288*, 31458–31467.

Somesh, B.P., Reid, J., Liu, W.F., Søgaard, T.M., Erdjument-Bromage, H., Tempst, P., and Svejstrup, J.Q. (2005). Multiple mechanisms confining RNA polymerase II ubiquitylation to polymerases undergoing transcriptional arrest. Cell *121*, 913–923.

Sørensen, C.S., and Syljuåsen, R.G. (2012). Safeguarding genome integrity: the checkpoint kinases ATR, CHK1 and WEE1 restrain CDK activity during normal DNA replication. Nucleic Acids Res. *40*, 477–486.

Steurer, B., Janssens, R.C., Geverts, B., Geijer, M.E., Wienholz, F., Theil, A.F., Chang, J., Dealy, S., Pothof, J., van Cappellen, W.A., et al. (2018). Live-cell analysis of endogenous GFP-RPB1 uncovers rapid turnover of initiating and promoter-paused RNA polymerase II. Proc. Natl. Acad. Sci. USA *115*, E4368–E4376.

Stork, C.T., Bocek, M., Crossley, M.P., Sollier, J., Sanz, L.A., Chédin, F., Swigut, T., and Cimprich, K.A. (2016). Co-transcriptional R-loops are the main cause of estrogen-induced DNA damage. eLife *5*, e17548.

Swingle, M., Ni, L., and Honkanen, R.E. (2007). Small-molecule inhibitors of ser/thr protein phosphatases: specificity, use and common forms of abuse. Methods Mol. Biol. *365*, 23–38.

Timson, J. (1975). Hydroxyurea. Mutat. Res. *32*, 115–132.

Trinkle-Mulcahy, L. (2012). Resolving protein interactions and complexes by affinity purification followed by label-based quantitative mass spectrometry. Proteomics *12*, 1623–1638.

Trinkle-Mulcahy, L., Ajuh, P., Prescott, A., Claverie-Martin, F., Cohen, S., Lamond, A.I., and Cohen, P. (1999). Nuclear organisation of NIPP1, a regulatory subunit of protein phosphatase 1 that associates with pre-mRNA splicing factors. J. Cell Sci. *112*, 157–168.

Trinkle-Mulcahy, L., Andersen, J., Lam, Y.W., Moorhead, G., Mann, M., and Lamond, A.I. (2006). Repo-Man recruits PP1 gamma to chromatin and is essential for cell viability. J. Cell Biol. *172*, 679–692.

Uhlen, M., Zhang, C., Lee, S., Sjöstedt, E., Fagerberg, L., Bidkhori, G., Benfeitas, R., Arif, M., Liu, Z., Edfors, F., et al. (2017). A pathology atlas of the human cancer transcriptome. Science *357*, eaan2507.

Verheyen, T., Görnemann, J., Verbinnen, I., Boens, S., Beullens, M., Van Eynde, A., and Bollen, M. (2015). Genome-wide promoter binding profiling of protein phosphatase-1 and its major nuclear targeting subunits. Nucleic Acids Res. *43*, 5771–5784.

Wallez, Y., Dunlop, C.R., Johnson, T.I., Koh, S.B., Fornari, C., Yates, J.W.T., Bernaldo de Quirós Fernández, S., Lau, A., Richards, F.M., and Jodrell, D.I. (2018). The ATR inhibitor AZD6738 synergizes with gemcitabine *in vitro* and *in vivo* to induce pancreatic ductal adenocarcinoma regression. Mol. Cancer Ther. *17*, 1670–1682.

Winsor, T.S., Bartkowiak, B., Bennett, C.B., and Greenleaf, A.L. (2013). A DNA damage response system associated with the phosphoCTD of elongating RNA polymerase II. PLoS ONE *8*, e60909.

Wu, D., De Wever, V., Derua, R., Winkler, C., Beullens, M., Van Eynde, A., and Bollen, M. (2018). A substrate-trapping strategy for protein phosphatase PP1 holoenzymes using hypoactive subunit fusions. J. Biol. Chem. *293*, 15152–15162.

Yasukawa, T., Kamura, T., Kitajima, S., Conaway, R.C., Conaway, J.W., and Aso, T. (2008). Mammalian Elongin A complex mediates DNA-damage-induced ubiquitylation and degradation of Rpb1. EMBO J. *27*, 3256–3266.

STAR★METHODS

KEY RESOURCES TABLE

REAGENT or RESOURCE	SOURCE	IDENTIFIER
Antibodies		
CDC73 (Lot #2)	Bethyl Laboratories	Cat#A300-170A; RRID:AB_309449
CDK1 (Clone 17)	Santa Cruz Biotechnology	Cat#sc-54; RRID:AB_627224
CHK1 (Clone DCS-310)	Santa Cruz Biotechnology	Cat#sc-56291; RRID:AB_1121554
CldU (rat anti-bromodeoxyuridine) (Clone BU1/75 (ICR1))	Abcam	Cat#ab74545; RRID:AB_1523224
CldU and IdU (mouse anti-bromodeoxuridine) (Clone B44)	BD Biosciences	Cat#B44; RRID:AB_2313824
GFP (Clones 7.1 and 13.1)	Sigma Aldrich	Cat#11814460001; RRID:AB_390913
γH2AX (Clone jbw301)	Millipore	Cat#05-636; RRID:AB_309864
γTUBULIN (Clone GTU-88)	Sigma Aldrich	Cat#T6557; RRID:AB_477584
LAMIN B (Clone D8P3U)	Cell Signaling Technology	Cat#12255; RRID:AB_2797859
MCM7 (Clone DCS-141)	Santa Cruz Biotechnology	Cat#sc-65469; RRID:AB_1125698
PCNA (Lot #GR3240364-1)	Abcam	Cat#ab18197; RRID:AB_444313
phosphoCHK1 S317 (Lot #12)	Cell Signaling Technology	Cat#2344; RRID:AB_331488
phosphoCHK1 S345 (Lot #18)	Cell Signaling Technology	Cat#2341; RRID:AB_330023
phosphoRNAPII S2 (Clone 3E10)	Millipore	Cat#04-1571; RRID:AB_10627998
phosphoRNAPII S5 (Clone 3E8)	Millipore	Cat#04-1572; RRID:AB_11213421
phosphoRPA32 S33 (Lot #7)	Bethyl Laboratories	Cat#A300-246A; RRID:AB_2180847
phosphoRPA32 S4S8 (Lot #6)	Bethyl Laboratories	A300-245A; RRID:AB_210547
PNUTS (Clone 47)	BD Biosciences	Cat#611060; RRID:AB_398373
PP1γ (Clone C-19)	Santa Cruz Biotechnology	Cat#sc-6108; RRID:AB_2168091
RNAPII C terminus (Clone 1PB-7C2)	Proteogenics	Cat#PTGX-PB-7C2; RRID:AB_2847823
RNAPII N terminus (Clone D8L4Y)	Cell Signaling Technology	Cat#14958; RRID:AB_2687876
RNAPII N terminus (Clone F-12)	Santa Cruz Biotechnology	Cat#sc-55492; RRID:AB_630203
RPA70 (Lot #3)	Cell Signaling Technology	Cat#2267; RRID:AB_2180506
TOX4 (Lot #G1915)	Santa Cruz Biotechnology	Cat#sc-102139; RRID:AB_2206288
WDR82 (Clone D2I3B)	Cell Signaling Technology	Cat#99715; RRID:AB_2800319
WDR82 (Lot #A1212)	Santa Cruz Biotechnology	Cat#sc-103325; RRID:AB_10838774
Chemicals, Peptides, and Recombinant Proteins		
Thymidine	Sigma Aldrich	CAS: 50-89-5
Hydroxyurea	Sigma Aldrich	CAS: 127-07-1
5-Chloro-2′-deoxyuridine	Sigma Aldrich	CAS: 50-90-8
5-Iodo-2′-deoxyuridine	Sigma Aldrich	CAS: 54-42-2
GFP-Trap_Dynabeads	Chromotek	Cat#gtm-20
Complete EDTA-free Protease Inhibitor Cocktail	Merck	Cat#5892791001
PhosSTOP phosphatase inhibitors	Merck	Cat#4906837001
Benzonase	Merck	Cat#70664-3
Calyculin A	Sigma Aldrich	CAS: 101932-71-2
THZ1	ApexBio	CAS: 1604810-83-4
EdU	Thermo Fisher	CAS: 61135-33-9
Pacific Blue Succinimidyl Ester	Thermo Fisher	CAS: 215868-33-0
Alexa Fluor 647 NHS Ester (Succinimidyl Ester)	Thermo Fisher	Cat#A20006

(*Continued on next page*)

Continued

REAGENT or RESOURCE	SOURCE	IDENTIFIER
Formalin solution	Sigma Aldrich	Cat#HT5011
VE822	Selleckchem	CAS: 1232416-25-9
MG132	Sigma Aldrich	CAS: 133407-82-6
Critical Commercial Assays		
Click-iT Plus EdU Alexa Fluor 594 Flow Cytometry Assay Kit	Thermo Fisher	Cat#C10646
Click-iT Plus EdU Alexa Fluor 488 Flow Cytometry Assay Kit	Thermo Fisher	Cat#C10633
Duolink flowPLA Detection Kit - Orange	Sigma Aldrich	Cat#DUO94003
Duolink *In Situ* Detection Reagents Red	Sigma Aldrich	Cat#DUO92008
Duolink *In Situ* PLA Probe Anti-Mouse MINUS	Sigma Aldrich	Cat#DUO92004
Duolink *In Situ* PLA Probe Anti-Mouse PLUS	Sigma Aldrich	Cat#DUO92002
Experimental Models: Cell Lines		
HeLa (human female adenocarcinoma epithelial cells)	Landsverk et al., 2019	N/A
U2OS (human female osteosarcoma epithelial cells)	Landsverk et al., 2019	N/A
GFP- POLR2A knockin MRC5 SV40 cells (Human male fetal lung, SV40 transformed fibroblast cells)	Steurer et al., 2018	N/A
HeLa GFP mpnuts (HeLa BAC clones stably expressing GFP mouse pnuts)	Hyman laboratory	N/A
HeLa CDC73-res cells (HeLa cells stably expressing siRNA resistant untagged wildtype CDC73)	This paper	N/A
HeLa WDR82-res cells (HeLa cells stably expressing siRNA resistant unagged wildtype WDR82)	This paper	N/A
Oligonucleotides		
Scr (scrambled control siRNA) GGUUUCUGUCAAAUGCAAACGGCUU	Landsverk et al., 2010	Stealth siRNA
siRNA targeting sequence: PNUTS (siPNUTS) GCAAUAGUCAGGAGCGAUA	Thermo Fisher (Landsverk et al., 2019)	Silencer select s328
siCDC73 AAACAAGGUUGUCAACGAGAA	Hahn et al., 2012	N/A
siRNA targeting sequence: WDR82 (siWDR82 #1) CUACCUUUAAGAUGCAGUA	Sigma-Aldrich	SASI_Hs02_00358014
siRNA targeting sequence: WDR82 (siWDR82 #2) CCUUUAAGAUGCAGUAUGA	Sigma-Aldrich	SASI_Hs02_00358015
siRNA targeting sequence: WDR82 (siWDR82 #3) CAAAAUAGACGAUACUAUU	Thermo Fisher	Silencer select s58697
siRNA targeting sequence: SSU72 (siSSU72) GGAGCUUCCUGUUGUUCAU	Sigma-Aldrich (Landsverk et al., 2019)	SASI_Hs01_00024012
Recombinant DNA		
pEGFP PNUTS	Landsverk et al., 2019	N/A
pEGFP PNUTS (V399A, W401A)	Landsverk et al., 2019	N/A
pEGFP-RNaseH1	Landsverk et al., 2019	N/A
pPNUTS EGFP	Landsverk et al., 2010	N/A

(*Continued on next page*)

Continued

REAGENT or RESOURCE	SOURCE	IDENTIFIER
pEGFP WDR82	This paper	N/A
pEGFP TOX4	This paper	N/A
Software and Algorithms		
ImageJ	Schneider et al., 2012	https://imagej.nih.gov/ij/
FlowJo 10.6.0	BD Biosciences	N/A
Image Lab	BioRad	N/A
MS-Quant	Mortensen et al., 2010	http://msquant.sourceforge.net
Axiovision 4.8.2	Carl Zeiss	N/A
FACS Diva	BD Biosciences	N/A

RESOURCE AVAILABILITY

Lead Contact

Further information and requests for resources and reagents should be directed to and will be fulfilled by the Lead Contact, Randi Syljuåsen (randi.syljuasen@rr-research.no).

Materials Availability

All reagents generated in this study are available upon request to the Lead Contact.

Data and Code Availability

The published article includes all datasets generated or analyzed during this study (Table S1).

EXPERIMENTAL MODEL AND SUBJECT DETAILS

Human female cervical cancer HeLa Kyoto and female osteosarcoma U2OS cells were grown at 37°C in Dulbecco's modified Eagle's medium (DMEM) and human male SV40 transformed fetal lung fibroblast MRC5 cells were grown in DMEM: Nutrient Mixture F-12 supplemented with antibiotics and 10% fetal bovine serum, at 37°C; 20% O_2, and 5% CO_2 in a humidified incubator. Throughout the manuscript, HeLa Kyoto (HeLa) cells were used unless otherwise stated. The cell lines, with exception of the MRC5 cells, were authenticated by short tandem repeat profiling using Powerplex 16 (Promega) and regularly tested for mycoplasma contamination. HeLa BAC cells stably expressing EGFP mouse pnuts were a generous gift from the laboratory of Tony Hyman. MRC5 cells with knockin GFP POLR2A (Referred to in text as GFP RNAPII) were previously described (Steurer et al., 2018). To generate the untagged CDC73-res cell lines, siRNA resistant CDC73 was cloned as previously described (Landsverk et al., 2019). HeLa cells were transduced and cells carrying the transgene were selected with 0.5 μg/ml puromycin. For the WDR82-res cell lines, the weak PGK promoter was used for transgene expression to achieve low expression levels. Third generation Lentivirus was generated using procedures and plasmids as previously described (Campeau et al., 2009). Briefly, an untagged siRNA-resistant WDR82 allele was cloned into Gateway ENTRY plasmids using standard molecular biology techniques. From these vectors, Lentiviral transfer vectors were generated by recombination into lentiviral destination vectors (vectors derived from Addgene plasmid #19068 and pCDH-EF1α-MCS-IRES-PURO (SystemBiosciences, inc.)) using Gateway LR reactions. VSV-G pseudotyped lentiviral particles were packaged using a third generation packaging system (Dull et al., 1998) (Addgene plasmids # 12251, 12253, 12259). HeLa Kyoto cells were then transduced with low virus titers (MOI $\leq$ 1) and stable expressing populations were generated by antibiotic selection.

METHOD DETAILS

Chemicals and treatments

Thymidine (Sigma Aldrich) was used at 2 mM, Hydroxyurea (Sigma Aldrich) at 100 μM, CDK7-inhibitor THZ1 (ApexBio) at 1 μM, EdU (Thermo Fisher) at 2 μM, VE822 (Selleckchem) at 500 nM and MG132 (Sigma Aldrich) at 50 μM. Note that thymidine, like hydroxyurea (Timson, 1975), suppresses replication by inhibiting deoxyribonucleotide synthesis (Bjursell and Reichard, 1973).

siRNA and DNA transfections

Wild-type and RAXA(V399A,W401A) full-length pEGFP PNUTS, pEGFP RNaseH1 and pEGFP NIPP1 have been previously described (Landsverk et al., 2019; Trinkle-Mulcahy et al., 1999). For the SILAC IP, PNUTS EGFP lacking the seven C-terminal aminoacids was used (Landsverk et al., 2010). The WDR82 gene was synthesized from geneart and cloned into pEGFP-C1. During gene synthesis, the encoded amino acid sequence was kept constant, but the nucleotide sequence was altered to enhance genesynthesis, resulting in

siRNA resistance against siWDR82#3. TOX4 was ordered from Open Biosystems (*Homo sapiens* MGC verified FL cDNA, Clone ID: 3880134, Accession: BC013689), and cloned into pEGFP-C1 (Clontech), using EcoRI/SalI restriction sites and the following primers: FWD_EcoRI:

GATCGAATTCTATGGAGTTTCCCGGAGGAAATG and REV_SalI:

GATCGTCGACTTTCACAAACACCACTGTGTTTG. Sequences of siRNA oligonucleotides can be found in the Key Resources Table. siRNA was transfected using Oligofectamine or RNAimax (Life technologies), and plasmid DNA with Fugene HD (Promega) or Attractene (QIAGEN). Experiments were performed 65–72 h after siRNA transfection unless otherwise stated.

Western blotting and antibodies

Quantitative western blotting was performed as previously described (Landsverk et al., 2019). Briefly, cells were resuspended in ice-cold TX-100 buffer (100 mM NaCl, 50 mM Tris pH 7.5, 2 mM $MgCl_2$, 0.5% TX-100) containing 100 U/ml Benzonase (Sigma-Aldrich), Complete EDTA-free Protease Inhibitor Cocktail (Merck) and PhosSTOP phosphatase inhibitors (Merck). After 24 h incubation at 4°C, Lane Marker Reducing Sample Buffer (Pierce Biotechnologies) was added and samples were boiled (95°C, 5 min). Criterion TGX gels (BioRad) and nitrocellulose membranes (BioRad) were used for separation and transfer. Antibodies used are found in Key Resources Table. Blots were imaged in a Chemidoc MP (BioRad) using chemiluminescence substrates (Supersignal west pico, dura or femto; Thermo Scientific). Quantifications were performed and images processed in Image Lab 4.1 (BioRad) software. Range of detection was verified by including a dilution series of one of the samples and excluding saturated signals. The resulting standard curve allowed accurate quantification. To blot for total protein after detection of a phosphorylated protein, membranes were stripped using ReBlot Plus Mild Antibody Stripping Solution (Millipore).

Flow cytometry analysis

For analysis of EdU incorporation, cells were labeled for 1 h with 2 μM EdU (Thermo Fisher) and fixed in 70% ethanol or, when GFP fluorescence was simultaneously monitored, formalin solution (Sigma Aldrich). EdU was labeled with the Click-iT Plus EdU Alexa Fluor 488 or 594 Flow Cytometry Assay Kits (Thermo Fisher), and DNA with FxCycle Far Red (Thermo Fisher) or Hoechst 33258 (Thermo Fisher). EdU positive cells (shown in black region in Figure 1A) were defined as S phase cells, and median EdU levels were measured within these. When GFP fluorescence was simultaneously monitored, GFP positive cells were selected prior to further analysis. In most of the flow cytometry experiments, with exception of those involving RPA loading, γH2AX or DNA profiles alone, barcoding was performed as previously described (Håland et al., 2015), using either Pacific blue or Alexa Fluor 647 Succinimidyl Ester, to eliminate variation in antibody/EdU staining between the individual samples. Briefly, samples were incubated with dilutions in the range of 0.001 – 0.1 ng/μL Pacific blue Succinimidyl Ester (Thermo Fisher) or 0,002 μg/μL Alexa Fluor 647 Succinimidyl Ester (Thermo Fisher) in PBS for 30 min prior to staining. The barcoded cells were added to the other cells prior to labeling, thus acting as an internal standard which were separated by gating during analysis. Flow cytometry analysis of γH2AX staining and RPA loading was performed as previously described (Håland et al., 2015; Landsverk et al., 2019). Briefly, for measuring RPA loading, the cells were treated with 750 μL low salt extraction buffer (0.1% Igepal CA-630, 10 mM NaCl, 5 mM $MgCl_2$, 0.1 mM PMSF, 10 mM Potassium phosphate buffer (pH 7.4)) for 5 min on ice, fixed by adding 250 μL formalin (Sigma Aldrich) and incubation was continued for 1 h on ice. For γH2AX labeling, cells were fixed directly in ice cold 70% ethanol. The samples were next incubated with primary (anti-RPA70 or anti-γH2AX) and secondary antibodies (Alexa Flour 488 and 647), diluted in flow buffer (0.1% Igepal CA-630, 6.5 mM Na2HPO4, 1.5 mM KH2PO4, 2.7 mM KCl, 137 mM NaCl, 0.5 mM ethylenediaminetetraacetic acid (pH7.5)) containing 4% non-fat milk, and stained with the DNA-stains Hoechst 33258 or FxCycle. Note that in the rescue experiments with CDC73 (Figure 5H), depletions of CDC73 and PNUTS were verified by western blotting (Figure S5E). Samples were analyzed in a LSRII flow cytometer (BD Biosciences) and processed in FACSDiva and FlowJo software (Both BD Biosciences).

Chromatin fractionation for western blotting

For chromatin fractionation of western blotting samples, cells were harvested, isolated by centrifugation and washed in PBS. To release non-chromatin bound factors, the cell pellet was resuspended in ice-cold chromatin extraction buffer (20 mM HEPES (pH 7.9), 1.5 mM $MgCl_2$, 50 mM NaCl, 300 mM Sucrose, 0.5% TX-100, Complete EDTA-free Protease Inhibitor Cocktail (Merck), PhosSTOP phosphatase inhibitors (Merck) and 20 μM MG132 (Sigma Aldrich)) and incubated for 10 min at 4°C with gentle mixing (300 rpm). Soluble and chromatin bound fractions were separated by centrifugation. The pellet containing chromatin bound factors was washed once in chromatin extraction buffer, followed by chromatin digestion for 2 h at 4°C with gentle mixing (300 rpm) in chromatin extraction buffer containing 100 U/mL Benzonase (Sigma Aldrich). Lane Marker Reducing Sample Buffer (Pierce Biotechnologies) was added to both soluble and chromatin bound fraction samples, and the samples were boiled for 5 min at 95°C prior to analysis by quantitative western blotting. Final volumes of soluble versus chromatin bound fractions were kept equal, so they could be directly compared. Notably, as we included a dilution curve in the western blots after chromatin fractionation, in our study this method was superior for determining absolute values.

Chromatin fractionation for flow cytometry

For flow cytometry analysis of chromatin bound RNAPII, cell pellets were resuspended in 100 μL chromatin extraction buffer for 5 min on ice. The cells were fixed by addition of formalin solution (Sigma Aldrich) directly to the cell suspension at a ratio of 10:1 of formalin

versus chromatin extraction buffer, and incubated at room temperature for 10 min. Cells were then washed once in PBS and barcoded and labeled as above (see γH2AX and RPA staining) with antibodies to RNAPII and pRNAPII S5 with the following modifications. One barcoded (with Pacific blue or Alexa Fluor 647) control sample of non-treated, non-extracted HeLa cells was added to all the individual samples. This provided an internal control both for extraction efficiency and for normalization, resulting in highly accurate quantifications. In addition, a secondary antibody control was included in each experiment, where primary antibody staining was omitted, allowing subtraction of background due to secondary antibody staining. Note that for the experiments involving MG132, the rescue experiments with EGFP PNUTS^{wt} and EGFP PNUTS^{RAXA}, and the experiments with siSSU72, chromatin extraction buffer with 140 mM NaCl was used. The higher NaCl concentration enhanced the differences in RNAPII and pRNAPII S5 chromatin binding between THZ1 treated and non-treated samples. In the rescue experiments with EGFP PNUTS^{wt} and EGFP PNUTS^{RAXA}, efficient knockdown of endogenous PNUTS was verified by western blotting and equal expression of the GFP constructs was verified by GFP expression by flow cytometry (Figures S4G and S4H).

Proximity ligation assay for flow cytometry

The proximity ligation assay (PLA) for flow cytometry (Duolink flowPLA Detection Kit – Orange (Sigma Aldich)) was performed in accordance to the manufacturer's instructions with the following modifications. At 72 h after siRNA transfection, HeLa cells were harvested, counted (8 × 10^5 cells per condition were used per 100 μL Duolink reaction volume) and fixed in 70% ethanol for 24 h or more at −20°C. Next, cells were barcoded with Pacific Blue, mixed and split into different tubes: one stained with both antibodies (anti-PCNA and anti-RNAPII) and both PLA probes, both antibodies and only one PLA probe, only one of the antibodies, but both PLA probes, or unstained (For overview see Figure S6A). Cells were blocked for 5 min in flow buffer (0.1% Igepal CA-630, 6.5 mM Na_2HPO_4, 1.5 mM KH_2PO_4, 2.7 mM KCl, 137 mM NaCl, 0.5 mM EDTA (pH7.5)), containing 4% (w/v) non-fat milk, and incubated with antibodies diluted in blocking buffer at 4°C overnight. After this, cells were washed once with 500 μL PBS with 1% FBS and incubated with pre-mixed PLA probe anti-rabbit minus and PLA probe anti-mouse plus diluted in PLA blocking buffer for 1 h at 37°C. The subsequent steps were carried out in accordance to manufacturer's instructions using 100 min amplification time and 30 min detection time. Finally, the cells were resuspended in PBS containing 1 μl/ml FxCycle Red (Thermo Fisher) and 50 μl/ml Ribonuclease A (QIAGEN). The cells were then analyzed in a LSRII flow cytometer (BD Biosciences) and processed in FACSDiva and FlowJo software (Both BD Biosciences).

Proximity ligation assay by microscopy

For detection of proximity between RNAPII and PCNA using the proximity ligation assay for immunofluoresence microscopy, HeLa cells were pre-extracted in detergent buffer (20 mM HEPES, pH 7.4; 50 mM NaCl; 1.5 mM MgCl2: 300 mM sucrose; 0.05% Triton X-100) for 5 min on ice prior to fixation with formalin. Coverslips were stained with anti-RNAPII (1PB 7C2, Proteogenix) and anti- PCNA (Abcam) in PBS-AT (PBS with 0.5% Triton X-100 and 1% BSA) overnight. The subsequent steps in proximal ligation assay were carried out with Duolink *In Situ* Orange Kit Mouse/Rabbit (Sigma Aldrich) in accordance to manufacturer's instructions (100 min amplification time). Cells were examined with a Zeiss LSM 880 confocal microscope (Carl Zeiss MicroImaging GmbH, Jena, Germany) equipped with an Ar-Laser Multiline (458/488/514 nm), a DPSS-561 10 (561 nm), a Laser diode 405-30 CW (405 nm), and a HeNe-laser (633 nm). The objective used was a Zeiss C-Apochromat 40x NA/1.2 W DICIII.

DNA Fiber assay

HeLa cells were pulse labeled with 25 μM 5-Chloro-2′-deoxyuridine (CldU) (Sigma Aldrich) followed by 250 μM 5-Iodo-2′-deoxyuridine (IdU) (Sigma Aldrich) for 20 min each. After labeling, cells were harvested and resuspended in ice-cold PBS. DNA fiber spreads were prepared by spotting 2 μL of cells (5 × 10^5 cells per mL in PBS) onto microscope slides (SuperFrost, Thermo Scientific), followed by lysis with 7 μL of 0.5% SDS, 200 mM Tris-HCl pH 7.4 and 50 mM EDTA for 5-7 min before spreading. DNA spreads were fixed in methanol/acetic acid (3:1). Prior to immunodetection, slides were treated with 2.5 M HCl for 1 h and 15 min. The slides were further incubated with rat anti-bromodeoxyuridine and mouse anti-bromodeoxyuridine for 1 h to detect CldU and IdU labeled tracts, respectively. Subsequently, slides were fixed in formalin solution for 10 min to increase staining intensity and further incubated with anti-rat IgG AlexaFluor 568 and anti-mouse IgG AlexaFluor 488 (Molecular Probes, 1:500) for 2 h. Slides were mounted with Fluoroshield (Sigma). Images were acquired with an AxioImager Z1 ApoTome microscope system (Carl Zeiss, Jena, DE) using a 63x (1.4 numerical aperture) oil lens, a AxioCam Mrm camera and the Axiovision 4.8.2 (Carl Zeiss) software. Images were analyzed using ImageJ (Schneider et al., 2012). In each independent experiment, at least 250 fibers were measured per condition. Replication track lengths were calculated using the conversion factor 1 μM = 2.59 kb (Jackson and Pombo, 1998).

GFP pulldowns and SILAC experiment

For SILAC GFP pulldowns, cells were grown for six cell divisions in DMEM containing L-arginine and L-lysine or L-arginine $^{13}C_6$ and L-lysine 4,4,5,5-D4 (Life Technologies). 24 h prior to harvesting, labeled cells were transiently transfected with EGFP alone or PNUTS EGFP. Nuclei were harvested, and GFP pulldowns performed as previously described with some modifications (Trinkle-Mulcahy et al., 2006). To increase efficiency of extraction of chromatin bound proteins, nuclei were resuspended in a high salt (500 mM NaCl) RIPA buffer for the sonication step and the resulting lysates diluted with NaCl-free RIPA buffer to a final concentration of 150 mM NaCl. Equal amounts of lysate (by total protein concentration) were mixed 1:1 and EGFP-tagged proteins isolated using

the GFP-Trap_A affinity matrix (Chromotek). Beads were washed and combined and proteins eluted for gel separation and trypsin digestion as previously described (Prévost et al., 2013). GFP pulldowns followed by western blotting were performed as the SILAC GFP pulldowns, but with the following modifications. Cells grown in regular medium were transiently transfected with EGFP PNUTS^{wt}, EGFP PNUTS^{RAXA}, EGFP TOX4, EGFP WDR82 or EGFP NIPP1 24 h prior to harvest. The cells were spun down and re-suspended directly in ice-cold high salt RIPA buffer (500 mM NaCl) and sonicated. The resulting lysates were diluted as above to 150 mM NaCl, and lysate volumes were adjusted to contain an equal amount of protein prior to isolation of EGFP-tagged proteins with GFP-Trap_Dynabeads (ChromoTek). The beads were washed five times in RIPA buffer (150 mM NaCl), diluted in 1x Lane Marker Reducing Sample Buffer (Pierce Biotechnologies) and were boiled (95°C, 5 min) prior to analysis by western blotting.

Mass spectrometry and data analysis

High-resolution mass spectrometric analysis was performed as described previously (Andersen et al., 2002) using a LTQ-FT-ICR mass spectrometer (Thermo Finnigan). Protein ratios were calculated for each arginine and lysine-containing peptide as the peak area of L-arginine $^{13}C_6$ and L-lysine 4,4,5,5-D4 divided by the peak area of L-arginine and L-lysine for each single scan mass spectrum. Peptide ratios for all arginine and lysine -containing peptides sequenced for each protein were averaged. The open source software MS-Quant was used to extract information from the Mascot HTML database search files (Matrix Science) and to evaluate the certainty in peptide identification and in peptide abundance ratio.

Phosphatase assay

Phosphatase assay was based on the method of Beullens et al. (Beullens et al., 1998) with modifications detailed below. RNAPII in isolated GFPpnuts complexes were used as substrate, and isolated as in the GFP pulldowns above with the following modifications. HeLa or HeLa GFPmpnuts were transfected with scr or siWDR82#3 and harvested after 72 h. Cells were resuspended in ice-cold TX-100 buffer (100 mM NaCl, 50 mM Tris pH 7.5, 2 mM $MgCl_2$, 0.5% TX-100) containing 100 U/ml Benzonase (Merck), Complete EDTA-free Protease Inhibitor Cocktail (Merck), PhosSTOP phosphatase inhibitors (Merck) and 50 μM MG132 (Sigma Aldrich). Lysates were precleared and GFPmpnuts complexes were isolated with GFP-Trap_Dynabeads (Chromotek). GFPmpnuts complexes were washed three times with TX-100 buffer containing 400 mM NaCl, and two times with PP1 buffer (20 mM Tris, 0.5 mM DTT, 1 mM MnCl2, 0.025% Tween-20, Complete EDTA-free Protease Inhibitor Cocktail and 50 μM MG132). Complexes were resuspended in PP1 buffer, aliquoted and placed at 30°C with gentle mixing (300 rpm) for the indicated times. Reactions were stopped by addition of PhosSTOP phosphatase inhibitors (Merck) and Lane Marker Reducing Sample Buffer (Pierce Biotechnologies), and samples were boiled prior to analysis by western blotting.

Live cell imaging

Live-cell imaging was performed on a Leica SP5 confocal laser scanning microscope with a HCX PL APO CS 63 ×, 1.40-NA oil-immersion lens. Images were recorded with a 488-nm Argon laser and a 500- to 600-nm bandpass filter. For FRAP, at pixel size 24.6 × 24.6 μM, a strip of 512 × 32 pixels spanning the nucleus was imaged every 400 ms with 400 Hz. Twenty-five frames were recorded before the bleach pulse. The average, background-corrected fluorescence intensity of frames 10–20 of these prebleach measurements were used to calculate the prebleach fluorescence intensity. GFP fluorescence in the strip was bleached for one frame with 100% laser power. The recovery of fluorescence was monitored for 4 min (600 frames) within and outside the strip, background-corrected, and normalized to pre-bleach fluorescence intensity.

Immunofluorescence

For detection of chromatin loaded RPA70 and γH2AX by immunofluorescence, HeLa cells were pre-extracted in detergent buffer (20 mM HEPES, pH 7.4; 50 mM NaCl; 1.5 mM MgCl2: 300 mM sucrose; 0.05% Triton X-100) for 5 min on ice prior to fixation with formalin solution (Sigma Aldrich). Coverslips were stained with anti-RPA70 and anti- γH2AX in PBS-AT (PBS with 0.5% Triton X-100 and 1% BSA), followed by anti-mouse Alexa Fluor 568 and anti-rabbit Alexa Fluor 488 (Thermo Fisher). Imaging and analysis was as previously described (Landsverk et al., 2019).

Clonogenic survival assay

For the clonogenic survival assay 200 HeLa cells were seeded in 6 cm culture dishes (BD Biosciences) with medium containing no drug or 50 μM or 100μM of hydroxyurea (Sigma Aldrich). On day 13 after seeding, 500 μL fresh medium was added to the dishes and the cells were cultured for an additional 6 days (19 days in total), fixed in 70% ethanol and stained with methylene blue. Colonies of 50 or more cells were counted as survivors. Survival fractions were calculated in each experiment as the average cloning efficiency (from 3 parallel dishes) after treatment with hydroxyurea, divided by the average cloning efficiency for non-treated cells.

Prognostic data

Prognostic data for PNUTS (PPP1R10) was found at the Human Protein Atlas available from http://www.proteinatlas.org

QUANTIFICATION AND STATISTICAL ANALYSIS

All experiments, except when otherwise stated, were performed three times or more. Error bars represent standard error of mean (SEM). P values were determined by the two-tailed student's two sample t test unless otherwise stated, and were determined using Microsoft Excel, except the Wilcoxon test, which was performed using Sigmaplot. *n* refers to number of independent experiments, except in Figure 4A, when it refers to number of cells analyzed. * < 0.05, ** < 0.01, *** < 0.001

Cell Reports, Volume *33*

Supplemental Information

WDR82/PNUTS-PP1 Prevents Transcription-Replication Conflicts by Promoting RNA Polymerase II Degradation on Chromatin

Helga B. Landsverk, Lise E. Sandquist, Lilli T.E. Bay, Barbara Steurer, Coen Campsteijn, Ole J.B. Landsverk, Jurgen A. Marteijn, Eva Petermann, Laura Trinkle-Mulcahy, and Randi G. Syljuåsen

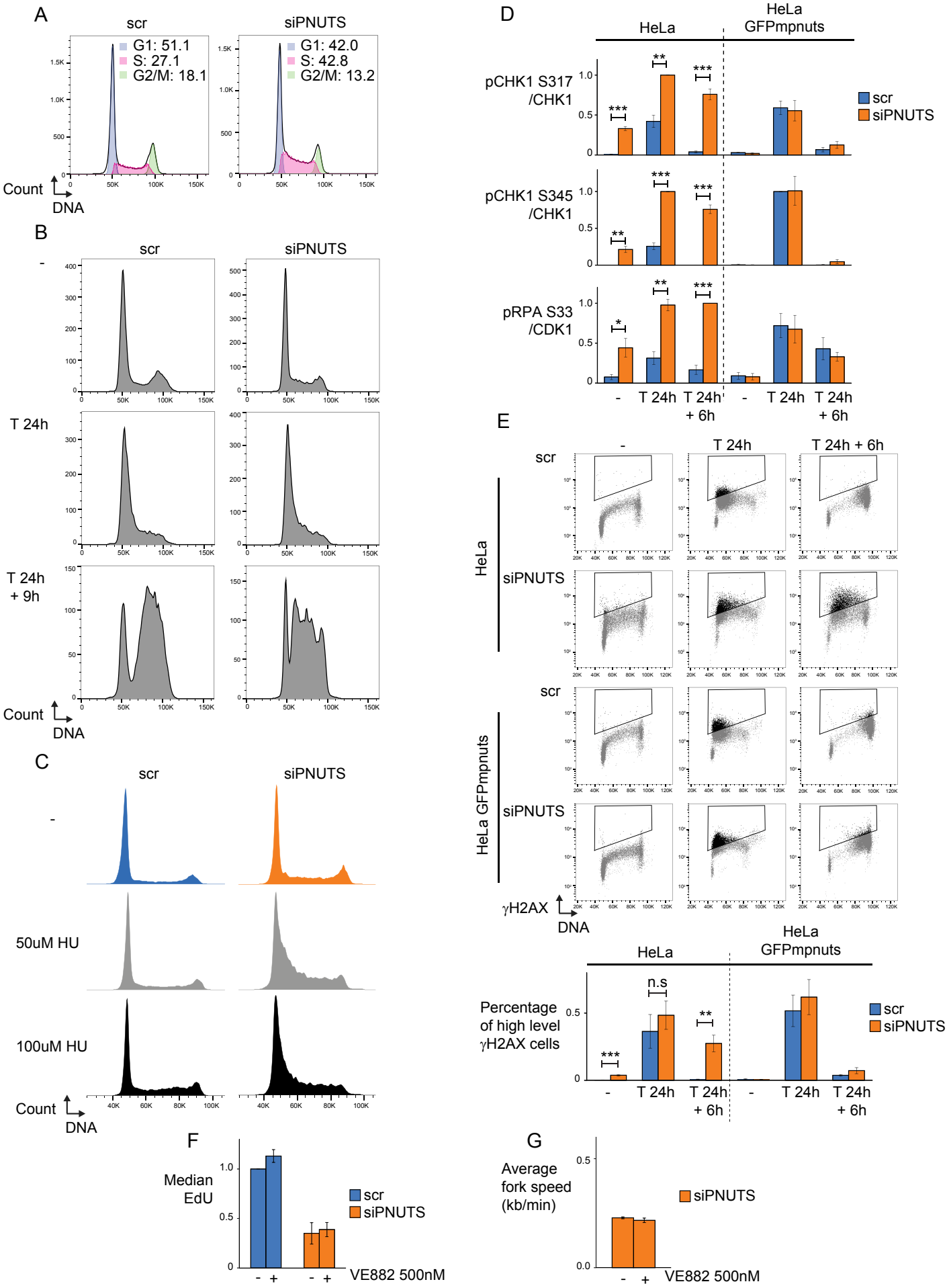
A
scr
siPNUTS
G1: 51.1
S: 27.1
G2/M: 18.1
G1: 42.0
S: 42.8
G2/M: 13.2
Count
DNA
B
scr
siPNUTS
-
T 24h
T 24h
+ 9h
Count
DNA
C
scr
siPNUTS
-
50uM HU
100uM HU
Count
DNA
D
HeLa
HeLa
GFPmpnuts
pCHK1 S317
/CHK1
pCHK1 S345
/CHK1
pRPA S33
/CDK1
scr
siPNUTS
-
T 24h
T 24h
+ 6h
E
-
T 24h
T 24h + 6h
scr
siPNUTS
HeLa
HeLa GFPmpnuts
γH2AX
DNA
HeLa
HeLa
GFPmpnuts
Percentage
of high level
γH2AX cells
n.s
scr
siPNUTS
F
Median
EdU
scr
siPNUTS
VE882 500nM
G
Average
fork speed
(kb/min)
siPNUTS
VE882 500nM

Figure S1. PNUTS prevents replication stress, related to Figure 1. A) Cell cycle analysis using the Watson model on DNA histograms from flow cytometry analysis of U2OS cells 72 h after transfection with siPNUTS or scr. % cells in G1, S and G2/M phases are from a representative experiment. (*n*=3). **B)** Flow cytometry analysis of U2OS cells 72 h after transfection with siPNUTS or scr. Prior to harvest, indicated samples were treated with thymidine for 24 h (T 24 h) , and released with fresh medium for 9 h (T 24 h + 9 h). **C)** Flow cytometry analysis showing DNA profiles 72 h after siRNA transfection and 24 h after treatment with 50 or 100 µM HU. **D)** Mean values from experiments as in Figure 1D). Error bars: ± SEM (*n*=3). **E)** Top: Flow cytometry analysis showing γH2AX staining versus DNA content in HeLa and HeLa GFPmpnuts cells 72 h after transfection with scr or siPNUTS. Selected samples were treated with thymidine for 24 h (T 24 h). To the indicated samples, thymidine was washed away and replaced with fresh media 6 h prior to harvest (T 24 h + 6 h). Regions with darker dots indicate cells with high levels of γH2AX. Bottom: percentage of cells with high levels of γH2AX from experiments as presented above. Mean results are shown. Error bars: ± SEM (*n*=4). **F)** Mean median EdU incorporation from flow cytometry analysis of cells 72 h after transfection with scr or siPNUTS and with and without 500 nM VE822 for 1h. Error bars: ± SEM (*n*=4). **G)** Average fork speed from fiber analysis of cells 48 h after siPNUTS transfection with and without 500 nM VE822 during labelling (40 min). Error bars: ± SEM (*n*=2).

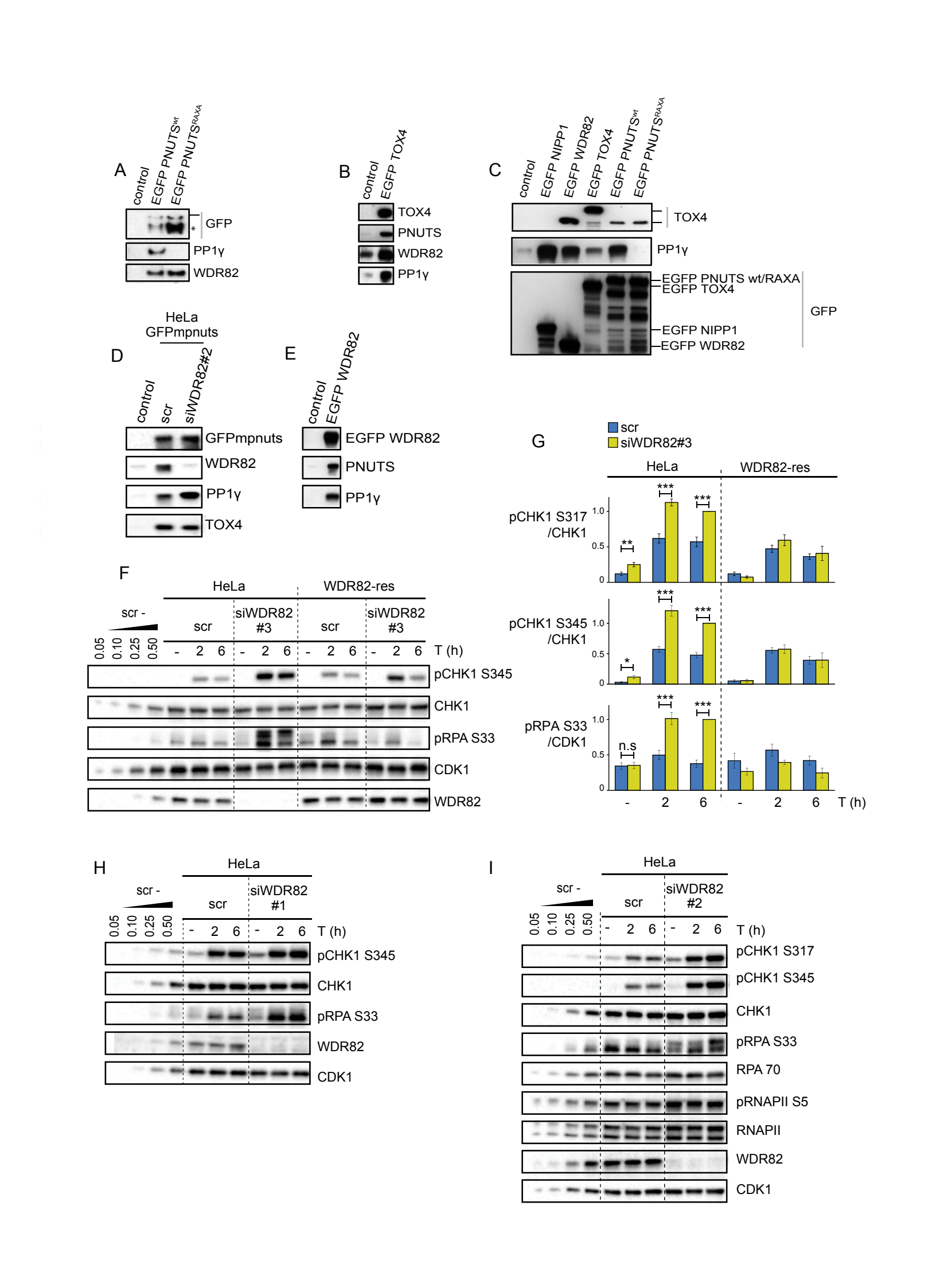
A
control
EGFP PNUTS^wt
EGFP PNUTS^RAXA
GFP
PP1γ
WDR82
B
control
EGFP TOX4
TOX4
PNUTS
WDR82
PP1γ
C
control
EGFP NIPP1
EGFP WDR82
EGFP TOX4
EGFP PNUTS^wt
EGFP PNUTS^RAXA
TOX4
PP1γ
EGFP PNUTS wt/RAXA
EGFP TOX4
EGFP NIPP1
EGFP WDR82
GFP
HeLa
GFPmpnuts
D
control
scr
siWDR82#2
GFPmpnuts
WDR82
PP1γ
TOX4
E
control
EGFP WDR82
EGFP WDR82
PNUTS
PP1γ
G
scr
siWDR82#3
HeLa
WDR82-res
pCHK1 S317 /CHK1
pCHK1 S345 /CHK1
pRPA S33 /CDK1
n.s
T (h)
F
HeLa
WDR82-res
scr -
scr
siWDR82 #3
0.05
0.10
0.25
0.50
T (h)
pCHK1 S345
CHK1
pRPA S33
CDK1
WDR82
H
HeLa
scr -
scr
siWDR82 #1
T (h)
pCHK1 S345
CHK1
pRPA S33
WDR82
CDK1
I
HeLa
scr -
scr
siWDR82 #2
T (h)
pCHK1 S317
pCHK1 S345
CHK1
pRPA S33
RPA 70
pRNAPII S5
RNAPII
WDR82
CDK1

Figure S2. PNUTS/TOX4/WDR82-PP1 complex interactions, and suppression of ATR signaling by WDR82, related to Figure 2. A) Western blot of GFP pulldowns from HeLa cells 24 h after transfection with wild type EGFP PNUTS or PP1-binding deficient EGFP PNUTS (RAXA). Control pulldowns were performed on lysates from nontransfected HeLa cells (control). **B)** Western blot of experiment performed as in A), but after transfection with EGFP TOX4. **C)** Experiment performed as in A and B) and in addition after transfection with EGFP WDR82 and EGFP NIPP1. EGFP NIPP1 was used as a control, which binds to PP1γ, but not to TOX4. **D)** Western blot of GFP pulldowns from HeLa GFPmpnuts cells 72 h after siRNA transfection with scr or siWDR82 #2. Control pulldowns were performed in lysates from regular HeLa cells. **E)** Western blot of experiment performed as in A), but after transfection with EGFP WDR82. **F)** Western blot of HeLa and WDR82-res cells transfected with scr or siWDR82#3 harvested at 72 h with or without 2 or 6 h thymidine treatment. **G)** Average values from experiments as in F). Error bars: ± SEM (*n*=3). **H)** Western blot performed as in F), in HeLa cells transfected with siWDR82#1. **I)** Western blot performed as in F), in HeLa cells transfected with siWDR82#2.

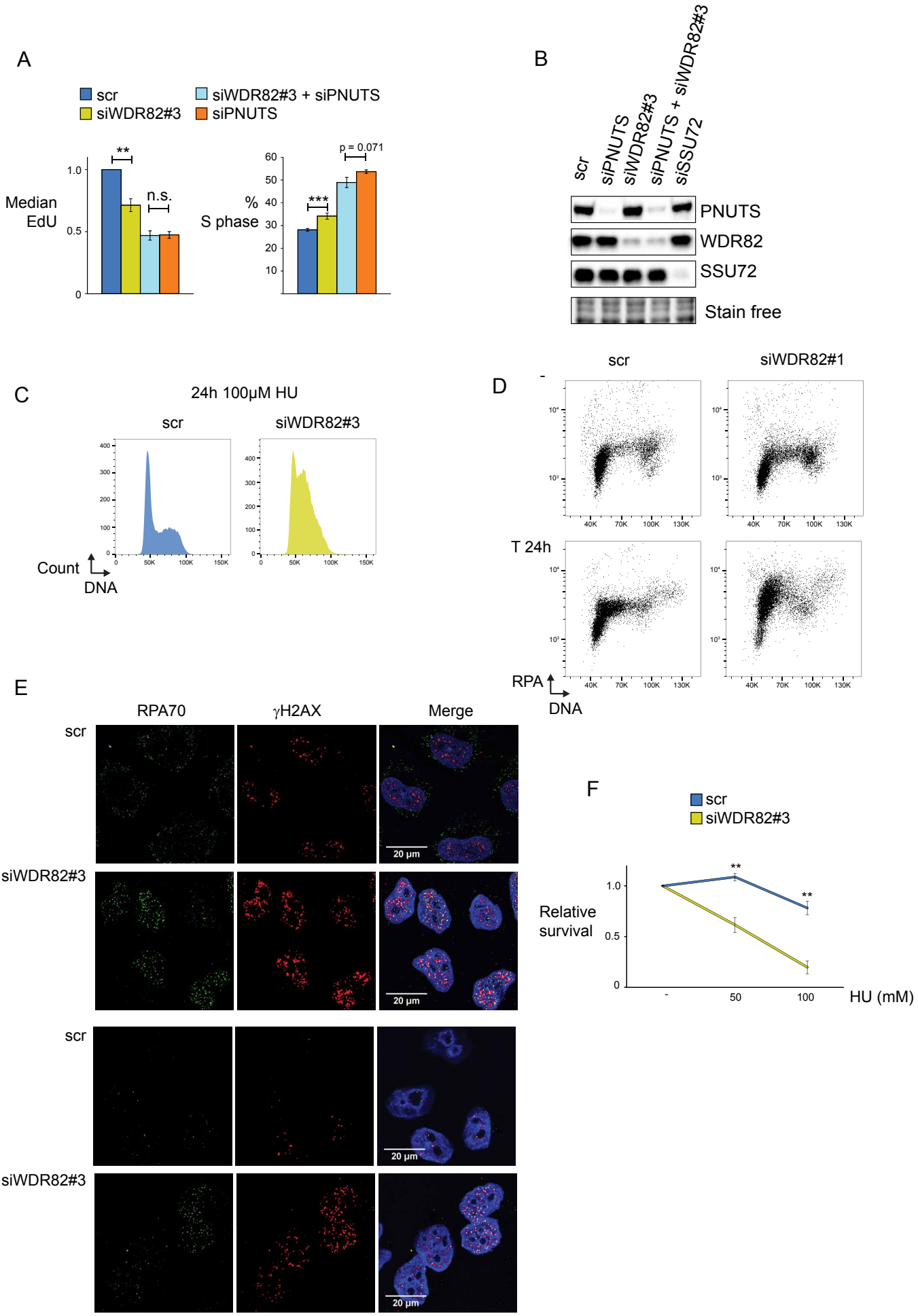
A
scr
siWDR82#3
siWDR82#3 + siPNUTS
siPNUTS
Median EdU
**
n.s.
1.0
0.5
0
% S phase
p = 0.071
***
60
50
40
30
20
10
B
scr
siPNUTS
siWDR82#3
siPNUTS + siWDR82#3
siSSU72
PNUTS
WDR82
SSU72
Stain free
C
24h 100µM HU
scr
siWDR82#3
Count
DNA
D
scr
siWDR82#1
T 24h
RPA
DNA
E
RPA70
γH2AX
Merge
scr
siWDR82#3
T 24h
T 24h + 6h
20 µm
F
scr
siWDR82#3
Relative survival
HU (mM)
50
100

Figure S3. WDR82 suppresses replication stress, related to Figure 2. A) Average median EdU incorporation from flow cytometry analysis of cells 48 h after transfection with scr, siWDR82, siWDR82 and siPNUTS and siPNUTS alone. The two-tailed Student's one sample *t*-test was used for significance testing. Error bars: ± SEM (*n*=4). **B)** Western blot showing levels of PNUTS,WDR82 and SSU72 depletion in experiments such as A) and Figure 1G. Total protein was used as loading control, as detected with stain-free technology (BioRad). **C)** DNA histograms from flow cytometry analysis of HeLa cells 72 h after transfection with scr or siWDR82#3. Prior to harvest, cells were treated with 100 µM HU for 24 h. **D)** Flow cytometry analysis showing RPA70 chromatin loading in HeLa cells 72 h after transfection with siWDR82#1, with or without thymidine for 24 h. **E)** Immunofluorescence analysis of extracted cells 72 h after transfected with scr, siWDR82#3 using antibodies to RPA70 and γH2AX. Thymidine was added for 24 h (T 24 h), and indicated cells were released by fresh medium 6 h prior to harvest (T 24 h + 6 h). **F)** Clonogenic survival assays showing relative survival of scr and siWDR82#3 transfected cells as a function of HU dose. Average data are shown. Error bars: ± SEM (*n*=3).

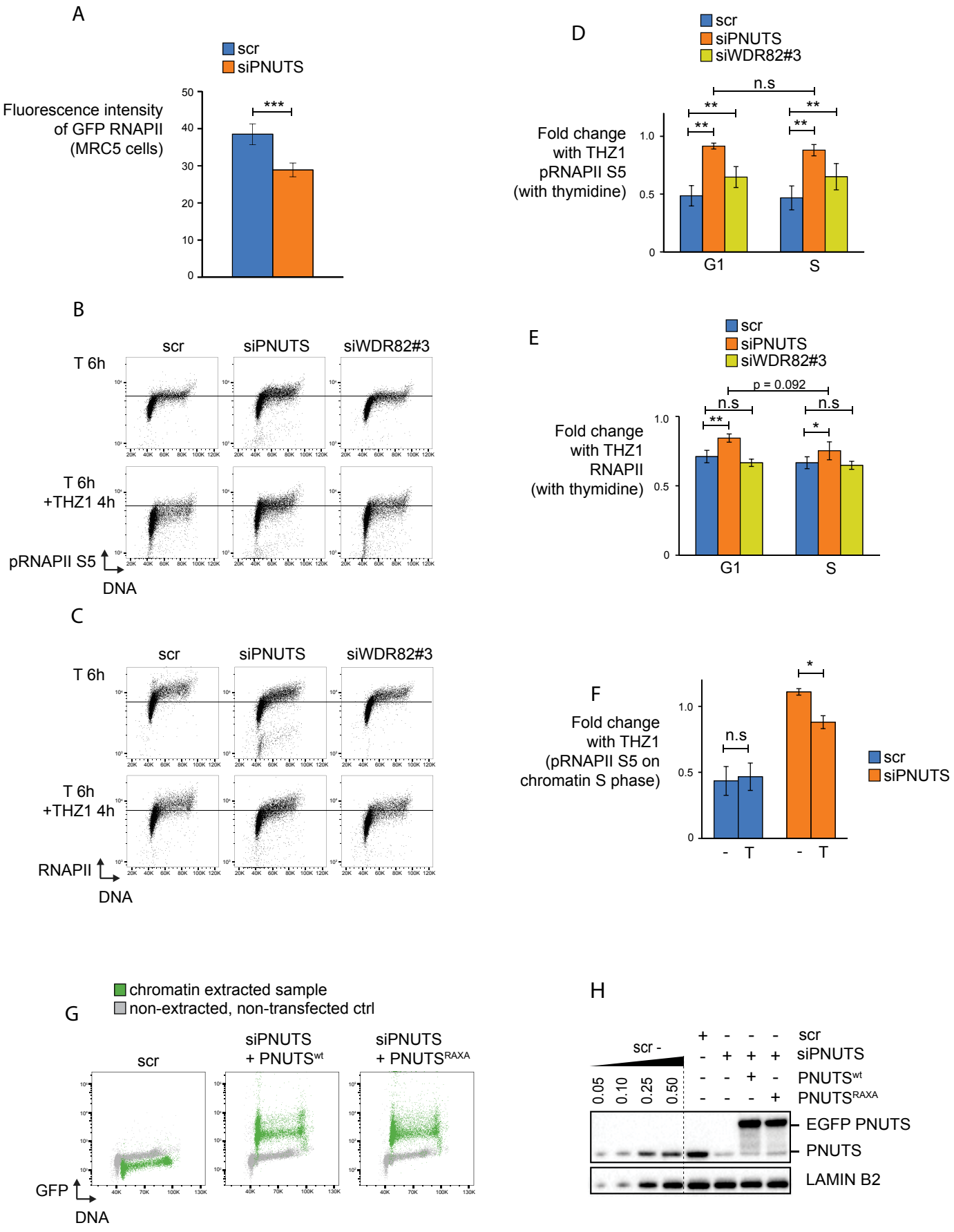
A
scr
siPNUTS
Fluorescence intensity
of GFP RNAPII
(MRC5 cells)
***
B
scr
siPNUTS
siWDR82#3
T 6h
T 6h
+THZ1 4h
pRNAPII S5
DNA
C
scr
siPNUTS
siWDR82#3
T 6h
T 6h
+THZ1 4h
RNAPII
DNA
D
scr
siPNUTS
siWDR82#3
n.s
Fold change
with THZ1
pRNAPII S5
(with thymidine)
G1
S
E
scr
siPNUTS
siWDR82#3
p = 0.092
n.s
Fold change
with THZ1
RNAPII
(with thymidine)
G1
S
F
Fold change
with THZ1
(pRNAPII S5 on
chromatin S phase)
n.s
scr
siPNUTS
G
chromatin extracted sample
non-extracted, non-transfected ctrl
scr
siPNUTS
+ PNUTSwt
siPNUTS
+ PNUTSRAXA
GFP
DNA
H
scr -
0.05
0.10
0.25
0.50
scr
siPNUTS
PNUTSwt
PNUTSRAXA
EGFP PNUTS
PNUTS
LAMIN B2

Figure S4. Depletion of PNUTS and WDR82 enhances the residence time of RNAPII on chromatin in S phase, related to Figure 4. A) Average fluorescence intensity of GFP RNAPII in MRC5 cells 48 h after transfection with scr or siPNUTS. **B)** Flow cytometry analysis showing chromatin loading of pRNAPII S5 versus DNA content in extracted HeLa cells 48 h after transfection with scr, siPNUTS or siWDR82#3. Samples were treated with thymidine for 6 h prior to harvest (T 6 h) with or without THZ1 for the last 4 h (T 6 h + THZ1 4 h). **C)** As in B) except showing RNAPII relative to DNA content. **D)** Average fold changes of pRNAPII S5 on chromatin with THZ1 from experiments as in B) in G1 and S phase of the cell cycle. P-values were determined by the two-tailed Student's one sample *t*-test. Error bars: ± SEM (*n*=3). **E)** Average fold changes of RNAPII on chromatin with THZ1 from experiments as in C) in G1 and S phase of the cell cycle. P-values were determined by the two-tailed Student's one sample *t*-test. Error bars: ± SEM (*n*=3). **F)** Average fold changes of pRNAPII S5 on chromatin in S phase in scr or siPNUTS transfected cells with THZ1 alone (-), or with THZ1 in the presence of thymidine (T). Note that these results are presented separately in D) and in Figure 4H. P-values were determined by the Wilcoxon signed rank test. Error bars: ± SEM (*n*=3). **G)** Flow cytometry analysis showing GFP intensity versus DNA content in cells 48 h after transfection with scr or siPNUTS and 42 h after transfection with EGFP PNUTS^{wt} (PNUTS^{wt}) or EGFP PNUTS^{RAXA} (PNUTS^{RAXA}). Barcoded, non-extracted and non-transfected control cells are shown in grey and chromatin extracted samples are shown in green. **H)** Western blot showing depletion of endogenous PNUTS and expression of PNUTS^{wt} and PNUTS^{RAXA} in cells transfected as in G. Note that PNUTS^{wt} and PNUTS^{RAXA} migrate slower, due to the presence of the GFP tag.

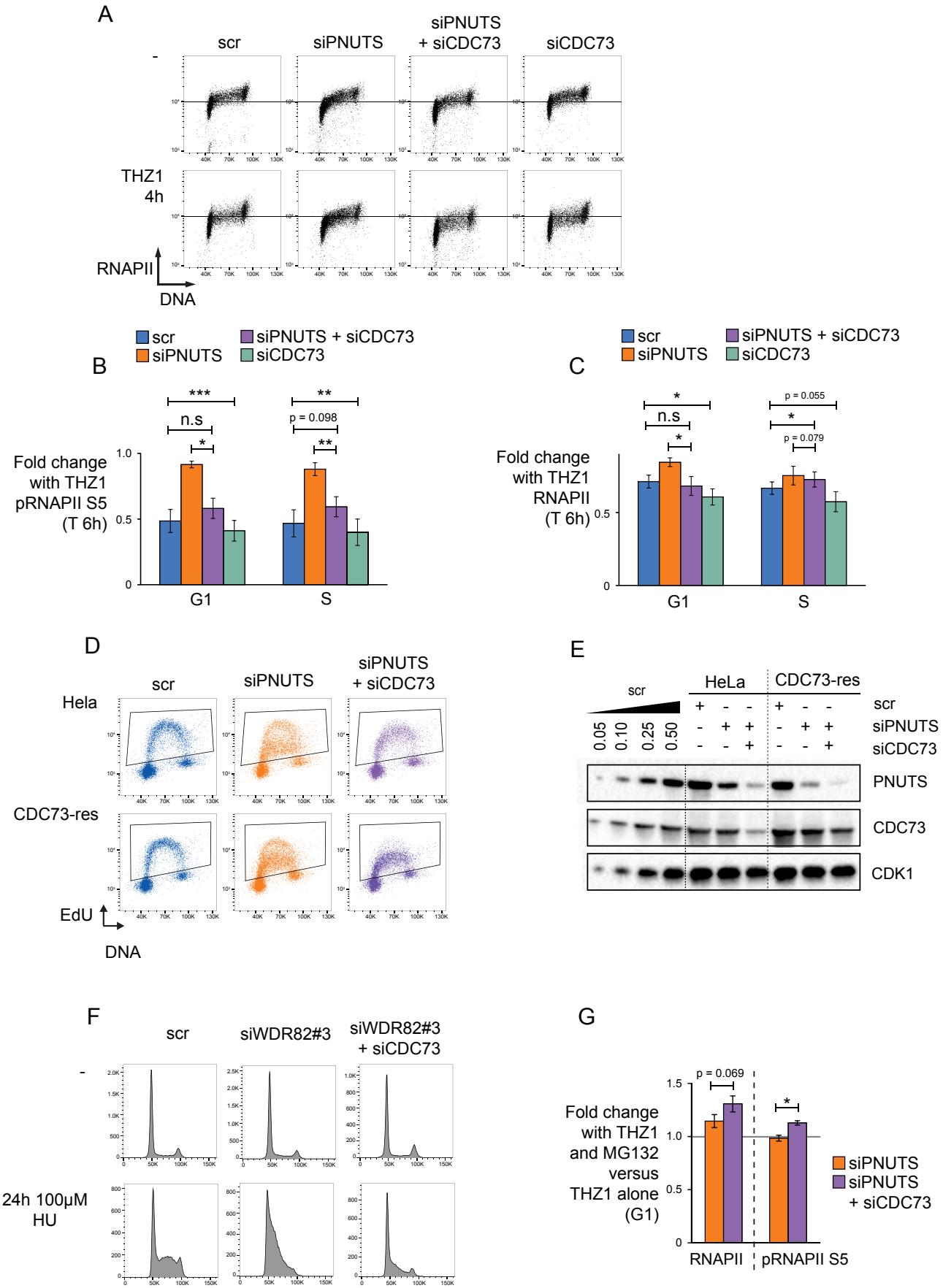
A
scr
siPNUTS
siPNUTS + siCDC73
siCDC73
-
THZ1 4h
RNAPII
DNA
B
scr
siPNUTS
siPNUTS + siCDC73
siCDC73
***
n.s
*
**
p = 0.098
**
Fold change with THZ1 pRNAPII S5 (T 6h)
1.0
0.5
0
G1
S
C
scr
siPNUTS
siPNUTS + siCDC73
siCDC73
*
n.s
*
p = 0.055
*
p = 0.079
Fold change with THZ1 RNAPII (T 6h)
0.5
0
G1
S
D
scr
siPNUTS
siPNUTS + siCDC73
Hela
CDC73-res
EdU
DNA
E
scr
HeLa
CDC73-res
0.05
0.10
0.25
0.50
scr
siPNUTS
siCDC73
PNUTS
CDC73
CDK1
F
scr
siWDR82#3
siWDR82#3 + siCDC73
-
24h 100μM HU
G
p = 0.069
*
Fold change with THZ1 and MG132 versus THZ1 alone (G1)
1.5
1.0
0.5
0
siPNUTS
siPNUTS + siCDC73
RNAPII
pRNAPII S5

Figure S5. Co-depletion of CDC73 reverses the enhanced residence time of RNAPII on chromatin and replication stress after depletion of PNUTS or WDR82, related to Figures 5 and 6. A) Flow cytometry analysis showing RNAPII on chromatin versus DNA content in extracted HeLa cells 48 h after transfection with scr, siPNUTS, siPNUTS and siCDC73 or siCDC73 with or without THZ1 for 4 h. **B)** Average fold changes from experiments as in A) but in addition cells were treated with thymidine for 6 h in the presence and absence of THZ1 for the last 4 h. Fold changes were determined in G1 and S phases by the ratio of pRNAPII S5 on chromatin with THZ1 and thymidine vs thymidine alone. P-values were determined by the two-tailed Student's one sample *t*-test. Error bars: ± SEM (*n*=3). **C)** As in B) except with RNAPII. **D)** Flow cytometry analysis from a representative experiment as in Figure 5H, showing EdU incorporation in HeLa or CDC73-res cells 72 h after siRNA transfection with scr, siPNUTS or siPNUTS and siCDC73. **E)** Western blot showing levels of PNUTS and CDC73 depletions from same experiment as in D). **F)** Flow cytometry analysis showing DNA profiles of HeLa cells 72 h after transfection with scr, siWDR82#3 or siWDR82#3 and siCDC73, with or without 100 µM HU for 24 h. **G)** Effect of MG132 on fold changes after THZ1, as determined by the fold change after THZ1 with MG132 divided by the fold change without MG132, in cells transfected with siPNUTS or siPNUTS and siCDC73 in G1 phase. If this value is above 1, MG132 stabilizes pRNAPII S5 and/or RNAPII on chromatin. P-values were determined by the two-tailed Student's one sample *t*-test. Error bars: ± SEM (*n*=3).

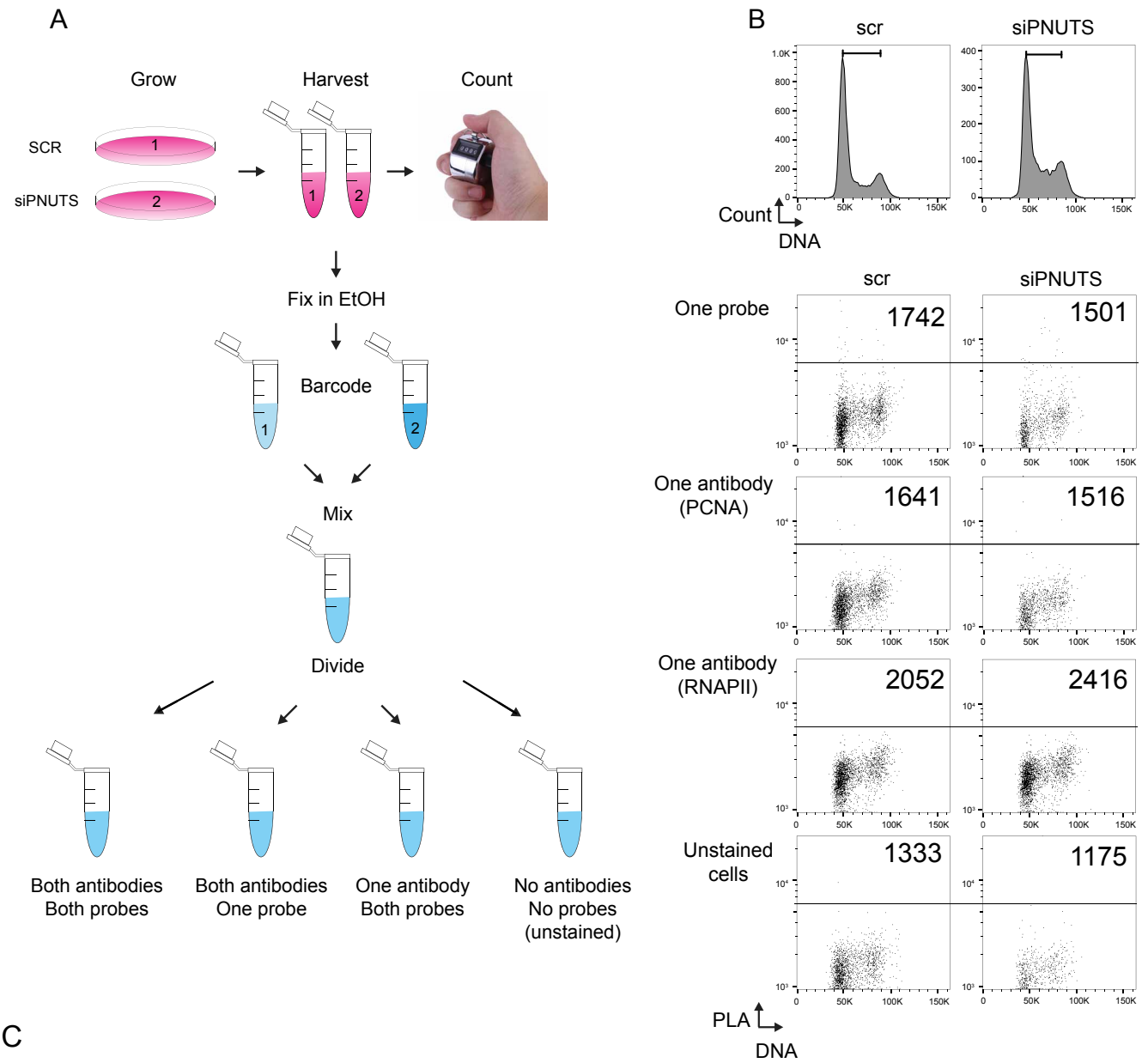
A
Grow
Harvest
Count
SCR
siPNUTS
1
2
Fix in EtOH
Barcode
Mix
Divide
Both antibodies
Both probes
Both antibodies
One probe
One antibody
Both probes
No antibodies
No probes
(unstained)
B
scr
siPNUTS
Count
DNA
One probe
1742
1501
One antibody
(PCNA)
1641
1516
One antibody
(RNAPII)
2052
2416
Unstained
cells
1333
1175
PLA
DNA

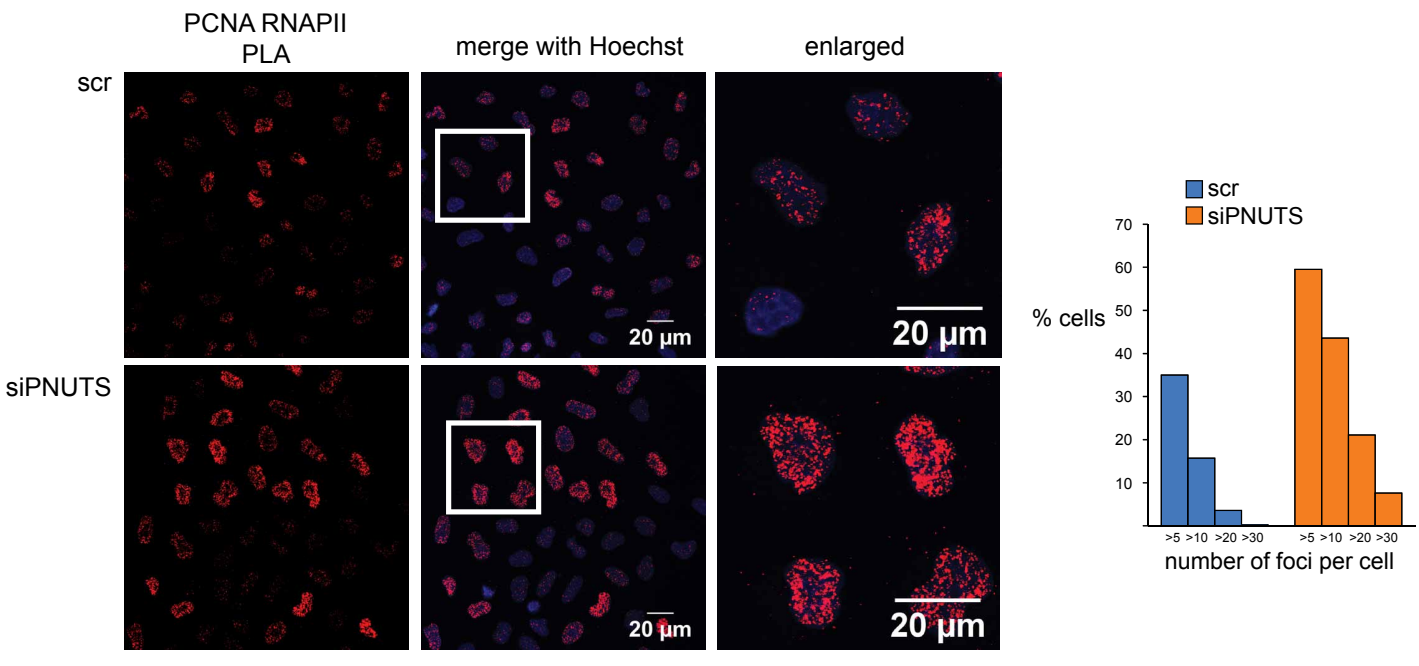
C
PCNA RNAPII
PLA
merge with Hoechst
enlarged
scr
siPNUTS
20 µm
20 µm
20 µm
20 µm
scr
siPNUTS
% cells
70
60
50
40
30
20
10
>5 >10 >20 >30
>5 >10 >20 >30
number of foci per cell

Figure S6. Depletion of PNUTS promotes T-R conflicts, related to Figure 7. A) Overview of PLA assay. **B)** Flow cytometry analysis showing top: DNA profiles. The S phase region used for quantifications in Figure 7A) is indicated by the black gate and includes cells with DNA content between the G1 peak (at ~50K) and the G2 peak (at ~90K). Bottom: PLA signal versus DNA content scatter plots showing the different controls used for the experiment in Figure 7A): only one probe, but both antibodies, both probes, but only one antibody for either PCNA and RNAPII, and unstained cells. The black line is used to ease visual interpretation and is set equally as in Figure 7A. Note that all the cells in the controls are located well below this line. **C)** Microscopy images of one representative RNAPII-PCNA PLA assay in HeLa cells 72 h after transfection with scr and siPNUTS. Values to the right show quantifications from the same experiment, of % cells with the indicated number of foci per cell. >250 cells were counted per siRNA oligonucleotide condition.

II

Nucleic Acids Research, 2022 **1**
https://doi.org/10.1093/nar/gkac434

A novel, rapid and sensitive flow cytometry method reveals degradation of promoter proximal paused RNAPII in the presence and absence of UV

Lilli T.E. Bay, Randi G. Syljuåsen and Helga B. Landsverk*

Department of Radiation Biology, Institute for Cancer Research, Norwegian Radium Hospital, Oslo University Hospital, 0379 Oslo, Norway

Received December 21, 2021; Revised April 08, 2022; Editorial Decision April 26, 2022; Accepted May 11, 2022

ABSTRACT

RNA polymerase II (RNAPII) is emerging as an important factor in DNA damage responses, but how it responds to genotoxic stress is not fully understood. We have developed a rapid and sensitive flow cytometry method to study chromatin binding of RNAPII in individual human cells through the cell cycle. Indicating enhanced transcription initiation at early timepoints, levels of RNAPII were increased at 15–30min after UV-induced DNA damage. This was particularly evident for the S5 phosphorylated form of RNAPII (pRNAPII S5), which is typically associated with promoter proximal pausing. Furthermore, degradation of pRNAPII S5 frequently occurs, as its levels on chromatin were strongly enhanced by the proteasome inhibitor MG132 with and without UV. Remarkably, inhibiting pause release with 5,6-dichloro-1-beta-ribo-furanosyl benzimidazole (DRB) further promoted UV-induced degradation of pRNAPII S5, suggesting enhanced initiation may lead to a phenomenon of 'promoter proximal crowding' resulting in premature termination via degradation of RNAPII. Moreover, pRNAPII S2 levels on chromatin were more stable in S phase of the cell cycle 2h after UV, indicating cell cycle specific effects. Altogether our results demonstrate a useful new method and suggest that degradation of promoter proximal RNAPII plays an unanticipated large role both during normal transcription and after UV.

INTRODUCTION

RNA polymerase II (RNAPII) transcribes DNA into mRNA and several non-coding RNAs (1). In addition, RNAPII plays a central role in the response to DNA damage. Cells are exposed to various forms of DNA damage from both endogenous and exogenous sources, and RNAPII is involved in detection, repair and signaling following such events (2–8). Understanding how RNAPII responds to DNA damage is therefore important to fully understand the DNA damage signaling and repair pathways, which are critical in human conditions such as cancer, neurodegenerative diseases, immune deficiencies, metabolic syndromes, ageing and infertility (9). DNA damage produced by ultraviolet radiation (UV) arrests the progression of elongating RNAPII (10). This arrest initiates transcription-coupled nucleotide excision repair (TC-NER) (2) and leads to a potent inhibition of transcription at the global level (11). Transcription resumption is required for cell survival after UV (12). Another global change to RNAPII after UV is its proteasome-mediated degradation (13). Elongating RNAPII is thought to be degraded as a 'last resort' mechanism to remove RNAPII when a block to transcription cannot be dealt with either by repair or bypass (14). However, whether degradation of other forms of RNAPII occurs after UV is not known.

The basal RNAPII transcription cycle includes recruitment and formation of the preinitiation complex at the promoter region, promoter release and stalling after ∼50 nts at the promoter proximal pause site, release from pausing into productive elongation, and finally termination. Release from promoter proximal pausing into productive elongation is considered a main rate-limiting step of transcription (15). In addition, premature termination from the promoter proximal pause site or during productive elongation is common and limits pervasive transcription (16–18). Terminating RNAPII is thought to be recycled for new rounds of transcription (19). In its C-terminal domain (CTD), RPB1 (hereafter referred to as RNAPII), the largest subunit of RNAPII, contains a large non-structured domain, which in humans is made up of 52 heptapeptide aminoacid repeats that can undergo extensive post-transcriptional modifications. These modifications are involved in all stages of the transcription cycle and in RNA metabolism (20). The most studied modifications are phosphorylation of serine 5 (pRNAPII S5) and serine 2 (pRNAPII S2). While pRNAPII S5 is high in pro-

*To whom correspondence should be addressed. Tel: +47 22781462; Fax: +47 22781495; Email: heblan@rr-research.no

moter proximal regions, pRNAPII S2 is associated with productive elongation (20). Global levels of pRNAPII S5 and pRNAPII S2 can therefore be used as markers for the promoter proximal and productively elongating fractions respectively. Proteasome-mediated degradation of RNAPII occurs even in the absence of DNA damage, and is thought to positively affect the rate of transcription by removing stalled RNAPII complexes (21). As pRNAPII S5 was shown to strongly inhibit ubiquitination and proteasome mediated degradation, promoter proximal paused RNAPII has been assumed to be refractory to degradation (21). On the other hand, binding between a E3 ubiquitin ligase complex and pRNAPII S5 was enhanced after UV (22), suggesting pRNAPII S5 may play multiple roles in RNAPII degradation after UV.

Cell cycle progression is highly regulated by RNAPII-mediated transcription, as transcription of specific cell cycle genes is required for transition from one cell cycle phase into the other (23). Conversely, the cell cycle regulates RNAPII. This is evident in mitosis, when most of RNAPII and many transcription associated proteins are lost from chromatin through a process known as mitotic inhibition of transcription (24–26). RNAPII is also regulated by replication during S phase. Sharing the same template, RNAPII can create a physical barrier for DNA replication (27). Resulting transcription–replication conflicts (T–R conflicts) can cause replication stress, and are actively suppressed by evicting RNAPII from chromatin (28), by its degradation on chromatin (29). In line with a negative role for T–R conflicts in regulation of transcription, the level of transcription of a specific gene is lower during its time of replication (30). Promoter proximal sites also tend to be under-replicated during S phase, indicating that the presence of RNAPII at the promoter proximal region creates a hindrance for DNA replication (30). Moreover, UV affects the cell cycle as it strongly suppresses DNA replication (31) and activates cell cycle checkpoints (32). Nevertheless, it is not known how UV impacts RNAPII levels on chromatin through the cell cycle.

Techniques to study the RNAPII transcription cycle after UV include chromatin immunoprecipitation followed by sequencing (ChIP-seq) (33,34), GRO-seq (11) or nascent RNA-seq (34), chromatin fractionation followed by western blotting (35) or mass spectrometry (36) and live cell microscopy of endogenous GFP-RNAPII (37,38). These complementary techniques have provided major insights into the effect of UV on RNAPII-mediated transcription. However, although sequencing or chromatin fractionation techniques can give high resolution sequence information and/or quantitative data, they have so far been based on cell lysates made from a large number of pooled cells. To study cell cycle effects with these methods, cells must therefore be synchronized, which, depending on the synchronization method, may induce replication stress or changes to transcription. On the other hand, live cell microscopy gives spatial information and single cell resolution, but is limited in the number of cells analyzed, and does not easily allow the analysis of modifications on RNAPII. There is therefore a need for additional methods to study RNAPII chromatin levels in individual cells. Here, we describe a new rapid, quantitative and sensitive flow cytometry method to study RNAPII chromatin binding in individual cells through the cell cycle. Using this method we show that promoter proximal paused RNAPII is subject to proteasome-mediated degradation in the presence and absence of UV-induced DNA damage. Moreover, productively elongating RNAPII becomes more stable in S phase after UV, in line with TC-NER specific effects in replicating cells. Finally, as pRNAPII S5 was more removed in early S phase compared to G1 phase after suppression of release into productive elongation by 5,6-dichloro-1-beta-ribo-furanosyl benzimidazole (DRB), this suggests T–R conflicts are likely dealt with by degrading promoter proximal RNAPII.

MATERIALS AND METHODS

Cell culture

Human female cervical cancer HeLa Kyoto cells were cultivated in Dulbecco's modified Eagle's medium (DMEM) and human male SV40-transformed fetal lung fibroblast MRC5 and human non-transformed retinal pigment epithelial (RPE) cells were cultivated in DMEM:Nutrient Mixture F-12 at 37°C in a humidified environment with 20% O_2 and 5% CO_2. Both mediums were supplemented with 10% fetal bovine serum (VWR, Biowest) and 1% Penicillin/Streptomycin (ThermoFisher Scientific). HeLa Kyoto (HeLa) cells were used throughout the manuscript unless otherwise stated.

Chemicals and treatments

UV- irradiation was performed with an UVC crosslinker (UV Stratalinker 2400 (Stratagene)) at 20 J/m^2. DRB (Sigma Aldrich) was used at 100 μM, EdU (Thermo Fisher) at 1 μM, CDK7-inhibitor THZ1 (ApexBio) at 1 μM, MG132 (Sigma Aldrich) at 50 μM, and Nocodazole (Sigma Aldrich) at 1 μg/ml.

Western blotting—chromatin fractionation and antibodies

Cells were harvested and washed with PBS. To release soluble factors, the cell pellet was resuspended in ice-cold chromatin extraction buffer (20 mM HEPES (pH 7.9), 1.5 mM $MgCl_2$, 140 mM NaCl, 300 mM Sucrose, 0.5% TX-100, Complete EDTA-free Protease Inhibitor Cocktail (Merck), PhosSTOP phosphatase inhibitors (Merck) and 20 μM MG132 (Sigma Aldrich). The cell pellet was incubated in the extraction buffer for 5min at 4°C with gentle mixing (300 rpm), and soluble and chromatin bound fractions were separated by centrifugation. The chromatin bound pellet was washed once in extraction buffer, followed by chromatin digestion with 100 U/ml benzonase (Sigma Aldrich) in extraction buffer for 2h at 4°C with gentle mixing (300 rpm). Both soluble and chromatin bound fractions were added Lane Marker Reducing Sample Buffer (Pierce Biotechnologies) and boiled at 95°C prior to analysis by quantitative western blotting. The final volumes of chromatin bound and soluble fractions were kept equal to allow comparison of the two fractions. Criterion TGX Stain-free gels (Bio-Rad) and nitrocellulose membranes (BioRad) were used for separation and transfer respectively. Criterion Stain-free imager was activated in a Chemidoc MP (BioRad) prior to

transfer. Antibodies used were: total RNAPII (F-12, Santa Cruz Biotechnologies), pRNAPII S5 (3E8) and pRNAPII S2 (3E10) (Sigma Aldrich). Total protein levels obtained from stain-free signal on membranes were used as loading control. Blots were imaged using chemiluminescence substrates (Supersignal west pico, dura or femto from Thermo Scientific). The Image Lab 4.1 (BioRad) software was used for quantifications and processing of images. Saturated signals were excluded. For accurate quantifications, a dilution curve of one of the samples was included. Membranes were stripped using ReBlot Plus Mild Antibody Stripping Solution (Millipore) in order to allow a new round of blotting for proteins.

Isolation of mitotic cells

For analysis of mitotic cells, cells were synchronized by 1 μg/ml nocodazole treatment 16h prior to harvest. The mitotic fraction was further isolated through mitotic shake off by gently tapping the dish in order to loosen mitotic cells. Cells floating in the medium were next transferred to a tube and isolated by centrifugation. For western blotting, cells were counted and cell number was adjusted in order to directly compare chromatin association of RNAPII in mitosis vs interphase. Chromatin fractionation was performed as described above.

Chromatin fractionation for flow cytometry

To release unbound factors, isolated cell pellets were resuspended in 100 μl chromatin extraction buffer for 5min on ice. For the experiments performed to optimize extraction strength, different concentrations of NaCl in the chromatin extraction buffer were tested: 50, 140, 180, 220, 280 mM, for all other experiments, 140 mM NaCl was used. Following extraction, cells were fixed by addition of 900 μl 10% formalin solution (Sigma Aldrich), and left at room temperature for 10min. Cells were then resuspended in PBS, followed by barcoding and antibody staining as described below.

Flow cytometry analysis

In all flow cytometry experiments, antibody staining and barcoding was performed as previously described (29,39). Flow cytometry analysis was performed on a LSRII flow cytometer (BD Biosciences) using Diva and FlowJo software. 10 000 cells or more were analyzed per sample, per experiment, including barcoding cells.

In brief, non-treated HeLa cells were incubated with 0.002 μg/μl Alexa Fluor 647 Succinimidyl Ester (Thermo Fisher) in PBS for 30min prior to antibody staining. In most experiments the barcoded control consisted of extracted cells, with the exception of the salt concentration optimization experiments where the barcoded control was non-extracted. Barcoding was quenched by addition of PBS with 5% fetal bovine serum (FBS (Biowest)). Thereafter, the barcoded cells were distributed equally among all the samples prior to staining as described below. For co-staining with pH3S10 and RNAPII, pRNAPII S5 or pRNAPII S2, cells were incubated with primary (anti-pH3S10 (Millipore) and anti-RNAPII (D8L4Y, Cell Signaling Technology)), anti-pRNAPII S5 (3E8) or anti-pRNAPII S2 (3E10) (Sigma Aldrich) and secondary antibodies (anti-mouse Alexa Fluor 568 and anti-rabbit (RNAPII) or anti-rat Alexa Fluor 488 (pRNAPII S5 and pRNAPII S2) Thermo Fisher), diluted in flow buffer (0.1% Igepal CA-630, 6.5 mM Na_2HPO_4, 1.5 mM KH_2PO_4, 2.7 mM KCl, 137 mM NaCl, 0.5 mM ethylenediaminetetraacetic acid (pH 7.5)) containing 4% non-fat milk. Samples were next stained with the DNA-stain Hoechst 33258 (1.5 μg/ml (Sigma Aldrich)) in flow buffer and analyzed by flow cytometry. As endogenous RNAPII was tagged with GFP, for MRC5 cells, staining for anti-pRNAPII S5, S2 or anti-pH3S10 was followed by anti-rat or mouse Alexa Fluor 568. For experiments with EdU incorporation, cells were labeled with 1 μM EdU for 1h prior to further 2h treatment with UV or inhibitors, resulting in a maximal EdU incorporation of 3h. The relatively long incubation with EdU was to ensure that all cells that had gone from G1 into S during the course of the treatments were correctly gated as EdU positive S phase cells. On the other hand, the long EdU incubation may have caused some cells gated as late S to actually be G2 cells that had stopped replicating during the course of the treatment. After EdU incorporation and treatments, samples were harvested and subjected to chromatin fractionation for flow cytometry (see above), barcoded (as described above) and labeled with primary (anti-RNAPII (D8L4Y, Cell Signaling Technology), anti-pRNAPII S5 (3E8) or anti-pRNAPII S2 (3E10) (Sigma Aldrich)) and secondary antibodies (Alexa Fluor 488, anti-rabbit for RNAPII and anti-rat for pRNAPII S5 and S2 (Thermo Fisher)). Following this, EdU was labeled with the Click-iT Plus EdU Alexa Fluor 594 Flow Cytometry Assay Kit (Thermo Fisher), and DNA was stained with Hoechst 33258 (1.5 μg/ml(Sigma Aldrich)) in flow buffer. The rationale for gating of the cell cycle phases was the following (See also Figure 1F). G1 cells were negative for EdU, and had a G1 DNA content. Early S phase cells had close to G1 DNA content but were EdU positive. Mid S had an intermediary DNA content and were EdU positive. Late S phase cells had approximately a G2 DNA content, but were EdU positive. G2 cells were EdU negative and had a G2 DNA content. Mitotic cells formed the small population below the G2 cells (see Figure 1F—this was verified by low RNAPII staining (results not shown)) and were not included in the analysis of 'G2 cells'.

Immunofluorescence analysis

RNAPII loading was measured by immunofluorescence microcopy in either non-extracted or chromatin-extracted HeLa cells. For detection of chromatin-bound RNAPII, cells were incubated in chromatin extraction buffer for 5min on ice prior to 12min fixation with formalin solution (Sigma Aldrich) at room temperature. Coverslips were stained with anti-pH3S10 (Millipore) in combination with either anti-RNAPII (D8L4Y, Cell Signaling Technology), anti-pRNAPII S5 (3E8) or anti-pRNAPII S2 (3E10) (Sigma Aldrich) in PBS-AT (PBS with 0.5% Triton X-100 and 1% BSA), followed by anti-mouse Alexa Fluor 568 and anti-rabbit Alexa Fluor 488 (for RNAPII) or anti-rat Alexa Fluor 488 (for pRNAPII S5 and S2) (Thermo Fisher). DNA was stained with Hoechst 33342 (Sigma Aldrich) and cover-

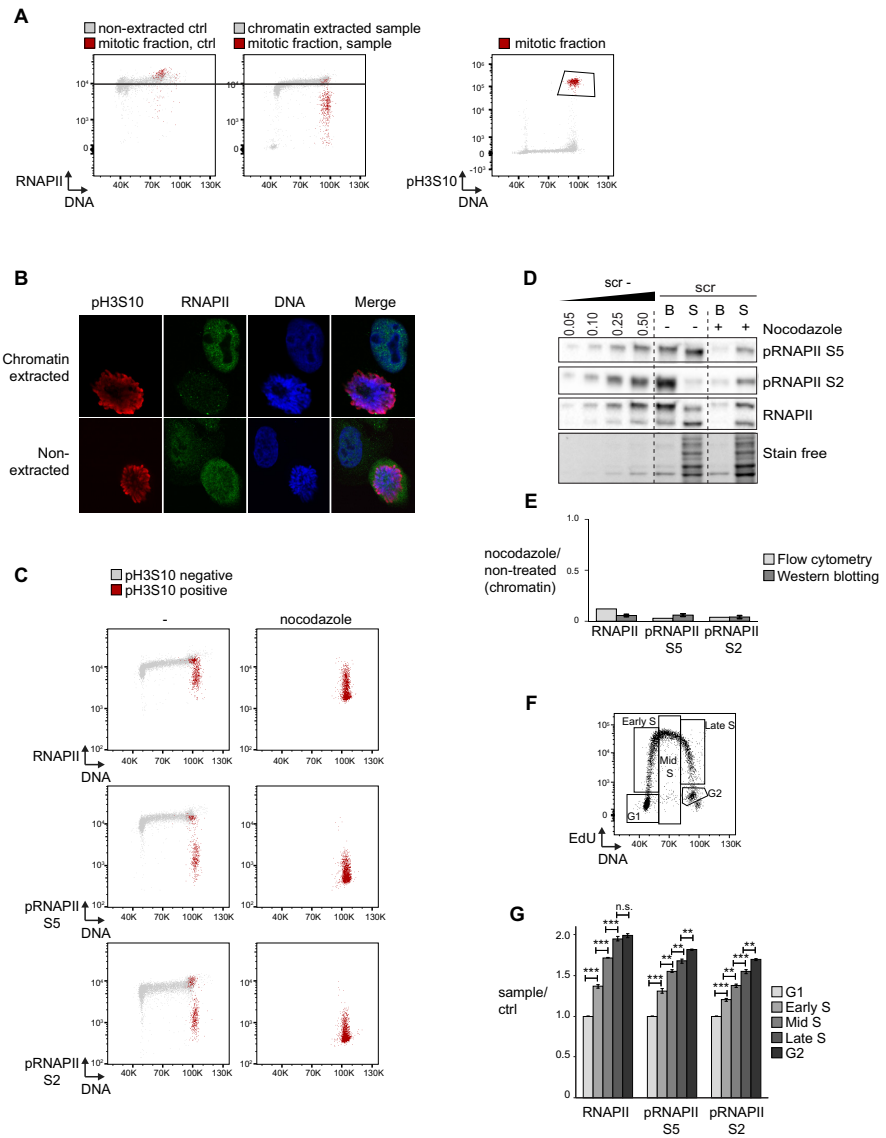

Figure 1. A new method to accurately measure RNAPII chromatin loading in individual cells through the cell cycle. (**A**) Flow cytometry scatter plots showing chromatin extracted (140 mM NaCl) or non-extracted cells labeled with antibodies against the N-terminal domain of RNAPII and the mitotic marker phosphorylated histone H3 on Serine 10 (pH3S10) relative to DNA content. The mitotic cells were gated as shown in the pH3S10 plot to the right, and shown in red in the RNAPII plots to the left. RNAPII staining was lost from chromatin in mitosis in the chromatin extracted, but not in the non-extracted cells. (**B**) Immunofluorescence analysis of chromatin extracted (140 mM NaCl) or non-extracted cells using antibodies to RNAPII and pH3S10. DNA was stained with Hoechst 33342. (**C**) Flow cytometry scatter plots of chromatin extracted non-treated (−) and nocodazole synchronized (nocodazole) HeLa cells. Non-treated cells were barcoded and mixed with mitotic cells synchronized by mitotic shake off after nocodazole treatment for 16h. Samples were stained with antibodies against total RNAPII, or phosphorylated serine 2 or 5 on the carboxyterminal domain of RNAPII combined with antibodies against pH3S10 and separated during analysis. pH3S10 negative cells are shown in grey and pH3S10 positive cells are shown in red in the respective non-treated and nocodazole synchronized cells. Note that, as expected, all the cells were pH3S10 positive in the nocodazole synchronized condition, and thus there are no observable pH3S10 negative cells. (**D**) Western blot analysis of chromatin bound (B) and soluble (S) fractions after extraction of non-treated and nocodazole synchronized cells as in (C). Cells were counted prior to extraction, and equal amounts of cells were loaded per lane. Stain free signal (BioRad Technologies), indicating total protein loading, was used as loading control. (**E**) Median chromatin levels of RNAPII, pRNAPII S5 and pRNAPII S2 in nocodazole treated sample divided by median chromatin levels in the non-treated ctrl (grey + red), obtained by flow cytometry analysis as in (C), compared to chromatin levels obtained in similar samples by western blotting as in (D). Notably, levels in dilution curve (as in (D)) were used for accurate quantification by western blot. ($n = 3$ for western blot samples). (**F**) Flow cytometry scatter plot of EdU incorporation relative to DNA content in HeLa cells. 1 μM EdU was added 3h prior to harvest. The cell cycle phases G1, early S, mid S, late S and G2 were determined based on EdU levels versus DNA content as shown. (**G**) Mean median RNAPII, pRNAPII S5 and pRNAPII S2 chromatin levels in individual phases of the cell cycle in HeLa cells. Alexa Fluor 647 barcoded, chromatin extracted control cells (that were not EdU treated) were added to each individual sample prior to staining. These were separated from the sample cells during analysis (Supplementary Figure S1B). Thereafter, median RNAPII, pRNAPII S5 and pRNAPII S2 levels in individual cell cycle phases were normalized to median levels in the barcoding cells to minimize sample to sample variation. Furthermore, each cell cycle phase was compared to G1, which was set to 1 ($n = 3$) *P*-values were determined by the two-tailed one sample *Student's* t-test. Error bars represent SEM.

slips were mounted onto a microscopy slide using Prolong Diamond (Thermo Fisher). Imaging and analysis was performed as previously described (29).

RESULTS

A new method to accurately measure RNAPII chromatin loading in individual cells through the cell cycle

To optimize a flow cytometry method accurately determining RNAPII levels on chromatin in individual cells through the cell cycle, we took advantage of the loss of RNAPII from chromatin in mitosis (40). To visualize mitotic cells, we co-stained RNAPII with the mitotic marker phosphorylated Histone H3 on Serine 10 (pH3S10). Chromatin extraction was performed using a mild detergent (0.5% TX-100) with various NaCl concentrations (Supplementary Figure S1A). Barcoding with non-extracted control HeLa cells was used as an internal standard for accurate quantifications and to determine extraction strength (Supplementary Figure S1A, B). As expected, mitotic cells clearly showed lower RNAPII staining after extraction with 140 mM NaCl and above (Figure 1A and Supplementary Figure S1A). However, in non-extracted cells, RNAPII levels in mitotic cells were similar to interphase cells with a G2 DNA content (Figure 1A). Notably, some of the extracted pH3S10 positive cells had high RNAPII staining (Figure 1A, C and Supplementary Figure S1A). The high RNAPII staining in a fraction of the pH3S10 positive cells remained even after extraction with increasing NaCl concentrations (Supplementary Figure S1A), showing it was not due to insufficiently strong extraction conditions. High pH3S10 levels thus likely occurs prior to loss of RNAPII from chromatin at the G2 to M transition. We chose to continue our experimental work with 140 mM NaCl, as it is close to physiological conditions and the chromatin levels of RNAPII were clearly lower in the mitotic fraction (Figure 1A). Analysis of the GFP signal in MRC5 cells expressing knock-in GFP tagged RNAPII (38) verified that the pattern of RNAPII antibody staining corresponded to endogenous RNAPII levels (Supplementary Figure S1C). The mitotic vs interphase RNAPII staining pattern after extraction with detergent and 140 mM NaCl was also confirmed by immunofluorescence microscopy (Figure 1B). To validate that the flow cytometry technique could be used to accurately quantify RNAPII levels on chromatin, we compared RNAPII levels in nocodazole-synchronized mitotic cells measured by flow cytometry versus quantitative western blotting. Similar levels of RNAPII on chromatin were observed using the two techniques (Figure 1C–E). Antibodies against pRNAPII S5 and pRNAPII S2 also showed low chromatin staining of mitotic cells (Figure 1C and Supplementary Figure S1D, E) and similar chromatin levels were found using flow cytometry vs quantitative western blotting (Figure 1C–E). As RNAPII is involved in S phase specific events, such as T–R conflicts, we next addressed whether we could measure RNAPII chromatin levels in finely separated cell cycle transitions by including EdU incorporation to mark replicating cells. Gradually increasing RNAPII, pRNAPII S5 and pRNAPII S2 levels could be detected in cells from G1 to early-, mid- and late S and G2 phases (Figure 1F, G). The increasing levels of RNAPII on chromatin through the cell cycle were expected, as the cells grow and the DNA is duplicated. Of note, we also assessed chromatin bound RNAPII and pRNAPII S5 in a previous study (29), but in that work we did not include cell cycle analysis and did not fully optimize and validate the method. Based on the results shown here, we conclude that our novel flow cytometry method can be used to accurately measure RNAPII levels on chromatin in individual cells through the cell cycle.

Initiation is likely enhanced at early timepoints after UV irradiation

Using our new technique, we addressed changes in RNAPII levels on chromatin after UV irradiation. Higher levels of all forms of RNAPII were observed at early timepoints (15 and 30min) after UV in HeLa cells, especially in G1 phase of the cell cycle (Figure 2A–D and Supplementary Figure S2A). This effect was most pronounced for pRNAPII S5 (Figure 2B–D), in line with enhanced initiation causing more promoter proximal pausing at early timepoints after UV. Higher levels of pRNAPII S5 were also observed at 30min after UV in RPE cells (Figure 2E). Moreover, slightly higher levels of pRNAPII S2 could also be observed at 30min after UV in HeLa cells (Figure 2D), consistent with accompanying increased productive elongation. At 2h after UV, RNAPII and pRNAPII S5 were reduced, but pRNAPII S2 remained high in HeLa cells (Figure 2B–D). In this cell line, pRNAPII S2 is thus more long-lived than pRNAPII S5 after UV. Furthermore, chromatin binding of pRNAPII S5 was clearly lower in S phase compared to G1 and G2 phases at 2h after UV in HeLa cells (Figure 2F). Less pronounced cell cycle effects were observed at 15 and 30min, although the pRNAPII S5 levels again were slightly lower in S phase compared to G1 (Supplementary Figure S2B, C). pRNAPII S5 may therefore be more removed in S phase after UV in HeLa cells. The latter is likely a cell line dependent effect as pRNAPII S5 was not lower in S versus G1 phase after UV in RPE cells (Supplementary Figure S2D,E). On the other hand, levels of pRNAPII S2 were higher in S versus G1 phase 2h after UV in both HeLa and RPE cells (Figure 2F and Supplementary Figure S2D), indicating the productively elongating fraction may become more stable in S phase after UV. Higher stability of pRNAPII S2 in S phase at 2h after UV was also observed in MRC5 cells (Supplementary Figure S2F). Enhanced initiation causing more promoter proximal pausing at early timepoints, and higher stability of the elongating RNAPII fraction in S phase, thus likely represent general phenomena after UV.

pRNAPII S5 is degraded on chromatin in the presence and absence of UV

To address whether cell cycle phase differences in RNAPII chromatin binding after UV might be caused by changes in RNAPII degradation on chromatin, we added the proteasome inhibitor MG132. RNAPII and pRNAPII S5 levels were enhanced on chromatin after MG132 (Figure 3A–C) in an unperturbed cell cycle in HeLa cells, as previously observed (29). Enhanced levels of pRNAPII S5 on chromatin after treatment with MG132 were also observed in RPE cells (Figure 3D). pRNAPII S2 levels were less enhanced by

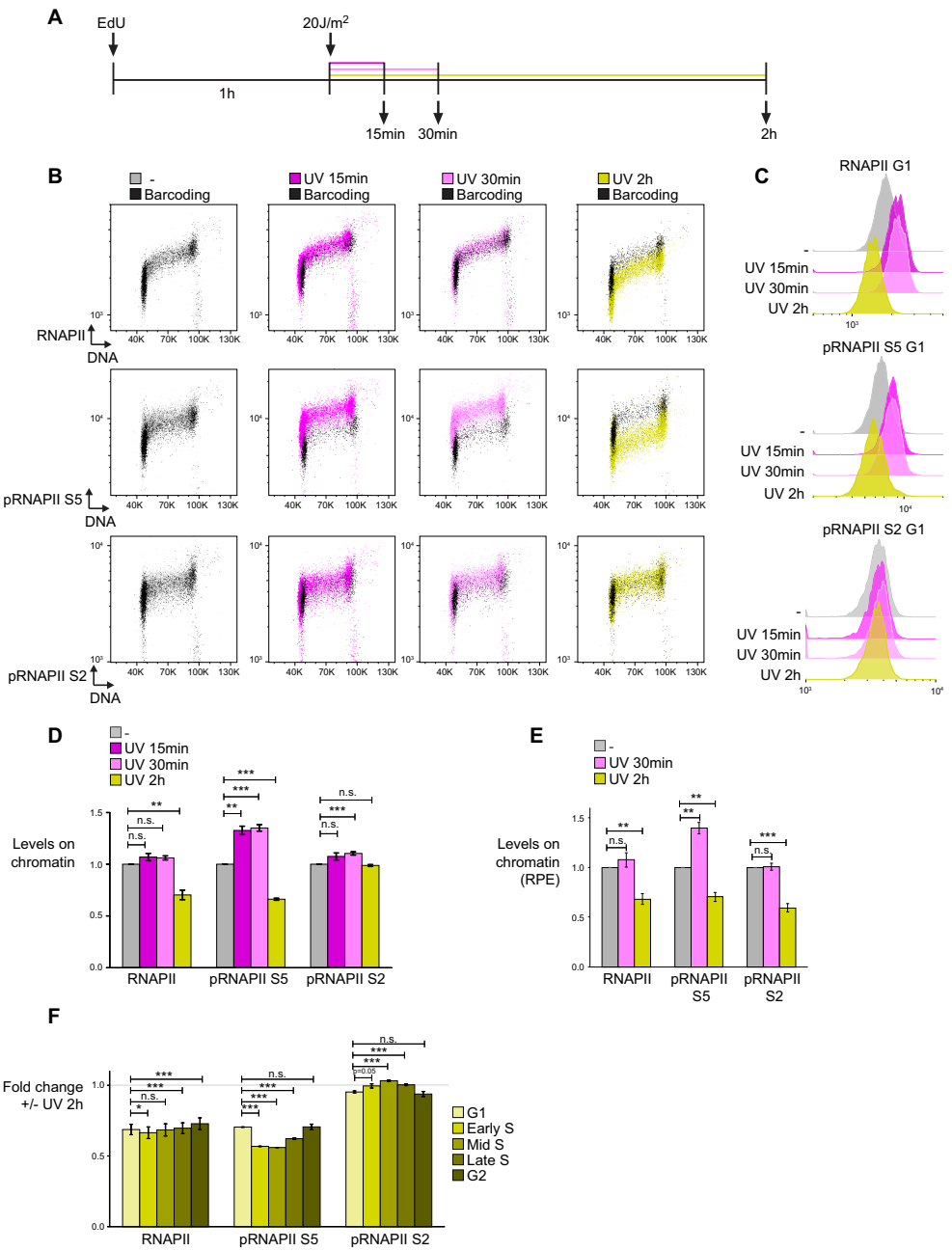

Figure 2. Initiation is likely enhanced at early timepoints after UV irradiation. (**A**) Overview of experimental set up. EdU was added to HeLa cells 1h prior to UV irradiation with 20 J/m^2. Samples were harvested, extracted and fixed for flow cytometry analysis at 15min, 30min and 2h after UV. Non-UV irradiated cell samples were harvested together with the UV 2h cell samples. (**B**) Flow cytometry scatter plots showing levels of RNAPII, pRNAPII S5 and pRNAPII S2 on chromatin versus DNA content from samples treated as in (A). Non-UV irradiated cells (−) are shown in grey, and samples harvested at 15min (UV 15min), 30min (UV 30min), and 2h after UV (UV 2h) in colors as indicated. Barcoded control cells (shown in black) were added to all individual samples prior to staining, separated from the samples during analysis (as in Figure 1G), and shown in scatterplots together with the sample cells. Note that in the non-UV irradiated (−) sample the barcoding cells (black), largely overlap with sample (grey), but in the UV treated samples the sample cells are frequently shifted either higher or lower than the barcoding cells, showing that the chromatin levels of RNAPII, pRNAPII S5 and pRNAPII S2 change after UV. (**C**) Flow cytometry histograms showing RNAPII, pRNAPII S5 and pRNAPII S2 levels on chromatin vs cell count in individual G1 cells (determined as in Figure 1F). (**D**) Mean median RNAPII, pRNAPII S5 and pRNAPII S2 levels on chromatin in cells treated as in A) and normalized to barcoding cells. UV-treated samples were further normalized to non-treated sample ($n = 3$), significance tested by the two-tailed one sample *Student's* test. Error bars represent SEM. **(E)** Mean median RNAPII, pRNAPII S5 and pRNAPII S2 levels on chromatin in RPE cells treated as in A) and analyzed as in D) ($n = 3$), significance tested by the two-tailed one sample *Student's* test. Error bars represent SEM. (**F**) Mean fold changes 2h after UV of RNAPII, pRNAPII S5 and pRNAPII S2 levels on chromatin in individual phases of the cell cycle (determined as in Figure 1F), and normalized to barcoding cells. ($n = 3$), significance tested by the two-tailed one sample *Student's* test. Error bars represent SEM.

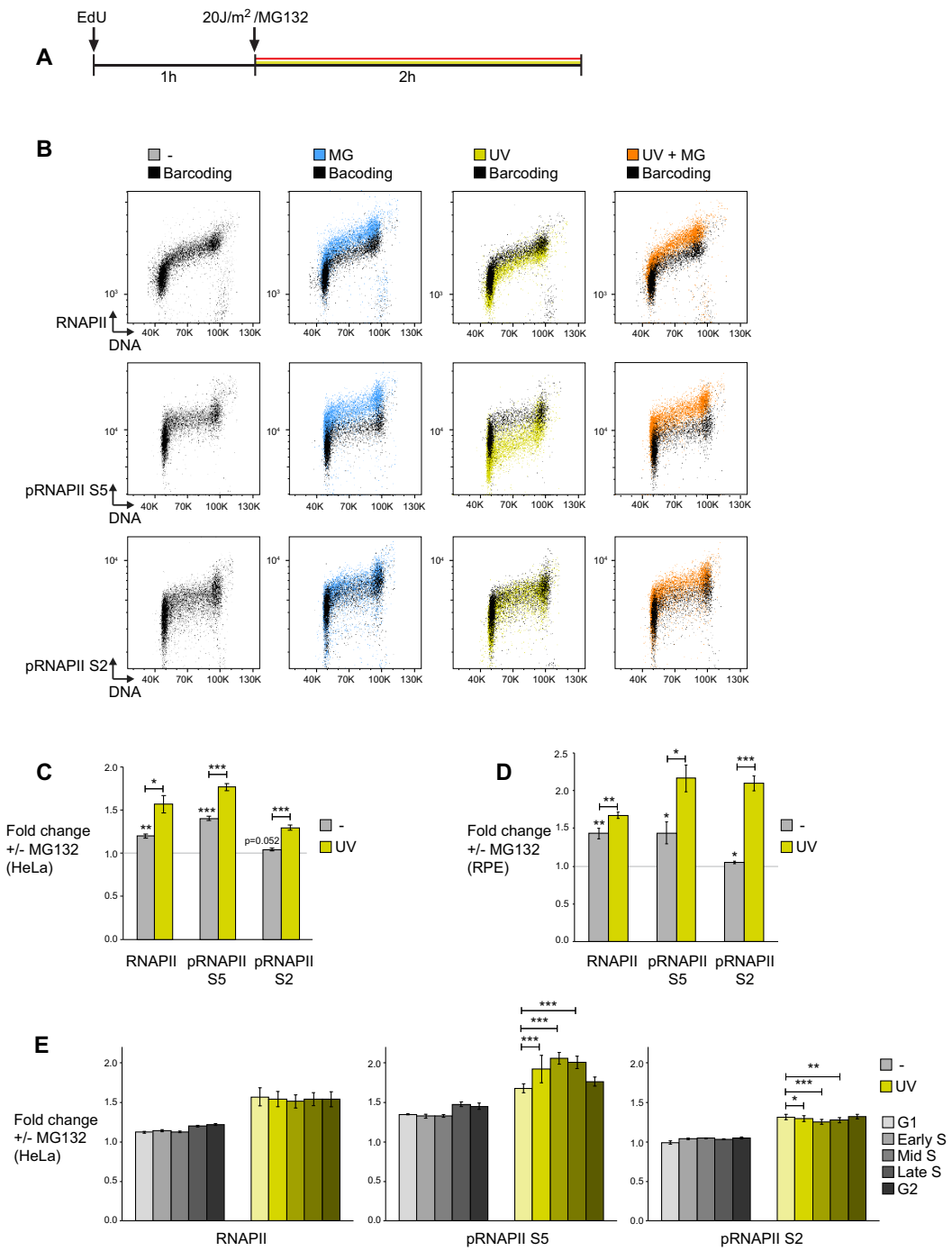

Figure 3. pRNAPII S5 is degraded on chromatin in the presence and absence of UV. (**A**) Overview of experimental set up. EdU was added to HeLa cells 1h prior to UV irradiation with 20 J/m^2 and addition of 50 μM MG132. Samples were harvested, extracted and fixed for flow cytometry analysis at 2h after UV/ addition of MG132. (**B**) Flow cytometry scatter plots showing levels of RNAPII, pRNAPII S5 and pRNAPII S2 on chromatin versus DNA content from samples treated as in A). Non-treated cells (−) are shown in grey, and samples treated with UV and/or MG132 are shown in colors as indicated. Barcoded control cells (shown in black) are shown in scatterplots together with the sample cells as in Figure 2B. (**C**) Mean fold changes after MG132 treatment (chromatin levels with MG132 / chromatin levels without MG132) in the presence (yellow) or absence (grey) of UV, from experiments as in B). Note that even in the absence of UV, the mean fold change after MG132 is above 1 (meaning MG132 increases the chromatin binding) for RNAPII and pRNAPII S5, but less so for pRNAPII S2. After UV, the average fold changes for all the RNAPII forms are increased. ($n = 3$), significance tested by the two-tailed one sample Student's *t*-test. Error bars represent SEM. (**D**) As in C) except showing fold changes after MG132 in RPE cells. ($n = 3$), significance tested by the two-tailed one sample *Student's t*-test. Error bars represent SEM. (**E**) Mean fold changes after MG132 treatment (as in C) in individual phases of the cell cycle (determined as in Figure 1F). ($n = 3$), significance tested by the two-tailed one sample Student's *t*-test. Error bars represent SEM.

MG132 treatment alone both in HeLa and RPE cells (Figure 3B–D), suggesting the productively elongating fraction is less degraded under unperturbed conditions. After UV, proteasome mediated degradation of all forms of RNAPII was enhanced both in HeLa and in RPE cells (Figure 3B–D). Notably, the enhanced degradation of pRNAPII S5 after UV was unexpected, as promoter proximal RNAPII has been thought to avoid degradation with and without UV (21,41). In addition, proteasome mediated degradation of pRNAPII S5 was higher in S phase versus G1 phase after UV in HeLa cells (Figure 3E), showing that the lower levels of pRNAPII S5 in S phase vs G1 at 2h after UV (Figure 2F) were caused by increased degradation (more removal). On the other hand, pRNAPII S2 was less degraded in S versus G1 phase both in HeLa cells and in RPE cells after UV (Figure 3E, Supplementary Figure S3A), in line with the higher stability of the elongating RNAPII fraction in S phase after UV (Figure 2F, Supplementary Figure S2D, F).

Promoter proximal RNAPII is subjected to proteasome-mediated degradation on chromatin in unperturbed conditions

Our results with pRNAPII S5 using MG132 suggested proteasome-mediated degradation of promoter proximal paused RNAPII occurs on chromatin under non-perturbed conditions. We hypothesized that enhancing promoter proximal pausing might increase RNAPII degradation. To address this, we added the widely used transcriptional inhibitor DRB, which prevents the release of RNAPII from the promoter proximal pause site into productive elongation (42). Several recent ChIP-seq experiments have confirmed that DRB causes a widespread arrest of RNAPII at the 5′ end of genes (43–45), though a few DRB-insensitive genes have also been reported (46). As expected, levels of pRNAPII S2 were decreased and levels of pRNAPII S5 were increased after treatment with DRB (Figure 4A–D). Moreover, in line with our hypothesis, total RNAPII chromatin levels were lower after DRB, and were completely reversed with MG132 (Figure 4A-D). Strongly supporting that proteasome-mediated degradation of the promoter proximal form of RNAPII was responsible for the lower levels of RNAPII on chromatin after DRB, the levels of pRNAPII S5, but not pRNAPII S2, were greatly enhanced by DRB + MG132 (Figure 4B–D). Moreover, pRNAPII S5 chromatin binding was lower in early S phase compared to G1 phase after DRB treatment (Figure 4E), suggesting enhanced promoter proximal RNAPII pausing by DRB causes more degradation of RNAPII in early S phase. As the majority of actively transcribing chromatin is early replicating (47), the distinct effects in early S vs G1 suggest that transcription replication conflicts involving promoter proximal RNAPII may be dealt with by degrading RNAPII.

Promoter proximal RNAPII is subjected to proteasome-mediated degradation on chromatin after UV

Enhanced levels of pRNAPII S5 on chromatin after UV and MG132 (Figure 3) suggested promoter proximal RNAPII may be subjected to proteasome-mediated degradation also after UV. However, productively elongating RNAPII is widely considered to be the form that is degraded after UV (21,41). We reasoned that if the productively elongating form was the only form that was degraded after UV, then inhibiting productive elongation should globally suppress UV-mediated degradation of RNAPII. To address this, we added DRB prior to UV treatment. Remarkably, RNAPII and pRNAPII S5 were more removed from chromatin after co-treatment with DRB and UV compared to either UV or DRB treatment alone (Figure 5A–C). Furthermore, MG132 reversed the lower levels of RNAPII and pRNAPII S5 after DRB and UV (Figure 5B, C), indicating proteasome-mediated degradation. UV-mediated degradation of RNAPII thus does not depend upon productive elongation. Rather, our results suggest that the promoter proximal form of RNAPII is degraded after UV. As expected, productive elongation was inhibited after DRB treatment, as levels of pRNAPII S2 were lower both with and without UV or MG132 (Figure 5B-C). Moreover, continuous release of RNAPII into productive elongation was required for maintenance of high pRNAPII S2 levels on chromatin 2h after UV in HeLa cells (Compare UV to UV + DRB, Figure 5B, C). Notably, co-treatment with DRB and UV caused a greater reduction in pRNAPII S2 than DRB alone (Figure 5B, C). This is likely due to UV- mediated degradation of productively elongating RNAPII that was either ongoing prior to addition of DRB or present at DRB-insensitive genes. Supporting that degradation of pRNAPII S2 occurred after DRB and UV co-treatment, MG132 counteracted this effect (Figure 5B,C compare pRNAPII S2 UV + DRB to UV + DRB + MG132). However, the increase in chromatin levels of pRNAPII S5 was greater than the increase in pRNAPII S2 after the triple treatment with UV + DRB + MG132 compared to UV + DRB, in line with more promoter proximal RNAPII being degraded than elongating RNAPII (Figure 5B, C). Degradation of promoter proximal paused RNAPII thus contributes to regulation of global RNAPII levels on chromatin after UV. Interestingly, DRB also caused a relatively greater reduction in pRNAPII S2 levels in G1 and G2 phase compared to S phase after UV (Figure 5D, E), supporting higher stability of the productively elongating fraction in S phase after UV.

Initiation is required for enhanced proteasome mediated degradation of promoter proximal RNAPII after UV

Enhanced degradation of promoter proximal RNAPII after UV was unanticipated, as this form of RNAPII does not travel very far along the DNA molecule and is thus not expected to encounter much DNA damage directly. In light of our result suggesting that initiation is likely enhanced and leads to more promoter proximal stalling after UV (Figure 2), together with the finding that DRB promoted RNAPII degradation (Figure 4), we hypothesized that the degradation might be triggered by abnormally high levels of promoter proximal stalled RNAPII after UV. To address this, we added THZ1, which inhibits RNAPII at a step prior to promoter proximal pausing (38,48). As expected, THZ1 caused the release of a large fraction of RNAPII from chromatin in all cell cycle phases (Figure 6A–D). However, the levels of pRNAPII S5 on chromatin were not further reduced by UV upon THZ1 treatment (Figure 6B, C). New transcription initiation leading to the production of new

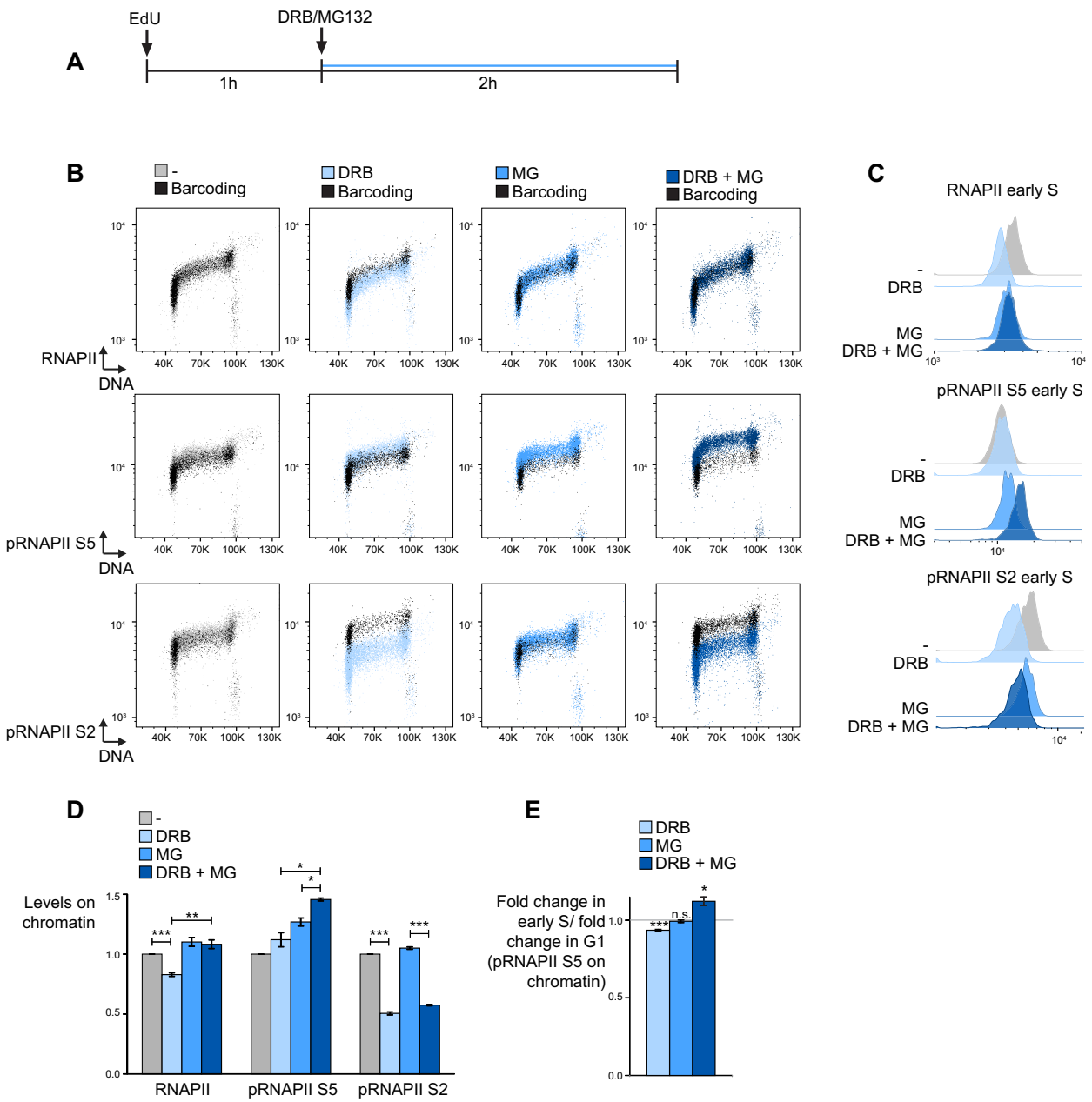

Figure 4. Promoter proximal RNAPII is subjected to proteasome-mediated degradation on chromatin in unperturbed conditions. (**A**) Overview of experimental set up. EdU was added to HeLa cells 1h prior to addition of 100 μM DRB and/or 50 μM MG132. Samples were harvested, extracted and fixed for flow cytometry analysis after 2h. (**B**) Flow cytometry scatter plots showing levels of RNAPII, pRNAPII S5 and pRNAPII S2 on chromatin versus DNA content from samples treated as in (A). Non-treated cells (−) are shown in grey, and samples treated with DRB and/or MG132 are shown in colors as indicated. Barcoded control cells (shown in black) are shown in scatterplots together with the sample cells as in Figure 2B. (**C**) Flow cytometry histograms showing RNAPII, pRNAPII S5 and pRNAPII S2 levels on chromatin vs cell count in individual cells in early S phase treated as in A). (**D**) Mean median RNAPII, pRNAPII S5 and pRNAPII S2 levels on chromatin in cells treated as in (A) and normalized to barcoding cells. Samples treated with DRB and/or MG132 were further normalized to non-treated cells ($n = 3$), significance tested by the two-tailed two sample Student's *t*-test. Error bars represent SEM. (**E**) Mean fold changes after DRB, MG132 and MG132 + DRB treatment in early S cells divided by the mean fold changes in G1 cells. ((chromatin levels in treated/non-treated early S cells)/(chromatin levels in treated/non-treated G1 cells)). With DRB this value goes below 1, meaning pRNAPII S5 is more removed in early S versus G1 phase. With DRB and MG132 the value goes above 1, meaning MG132 treatment increases pRNAPII S5 levels on chromatin more in early S versus G1 cells in the presence of DRB. With MG132 alone this value is equal to 1, showing there is no significant difference in the effect of MG132 in early S versus G1. ($n = 3$), significance tested by the two-tailed two sample Student's *t*-test. Error bars represent SEM.

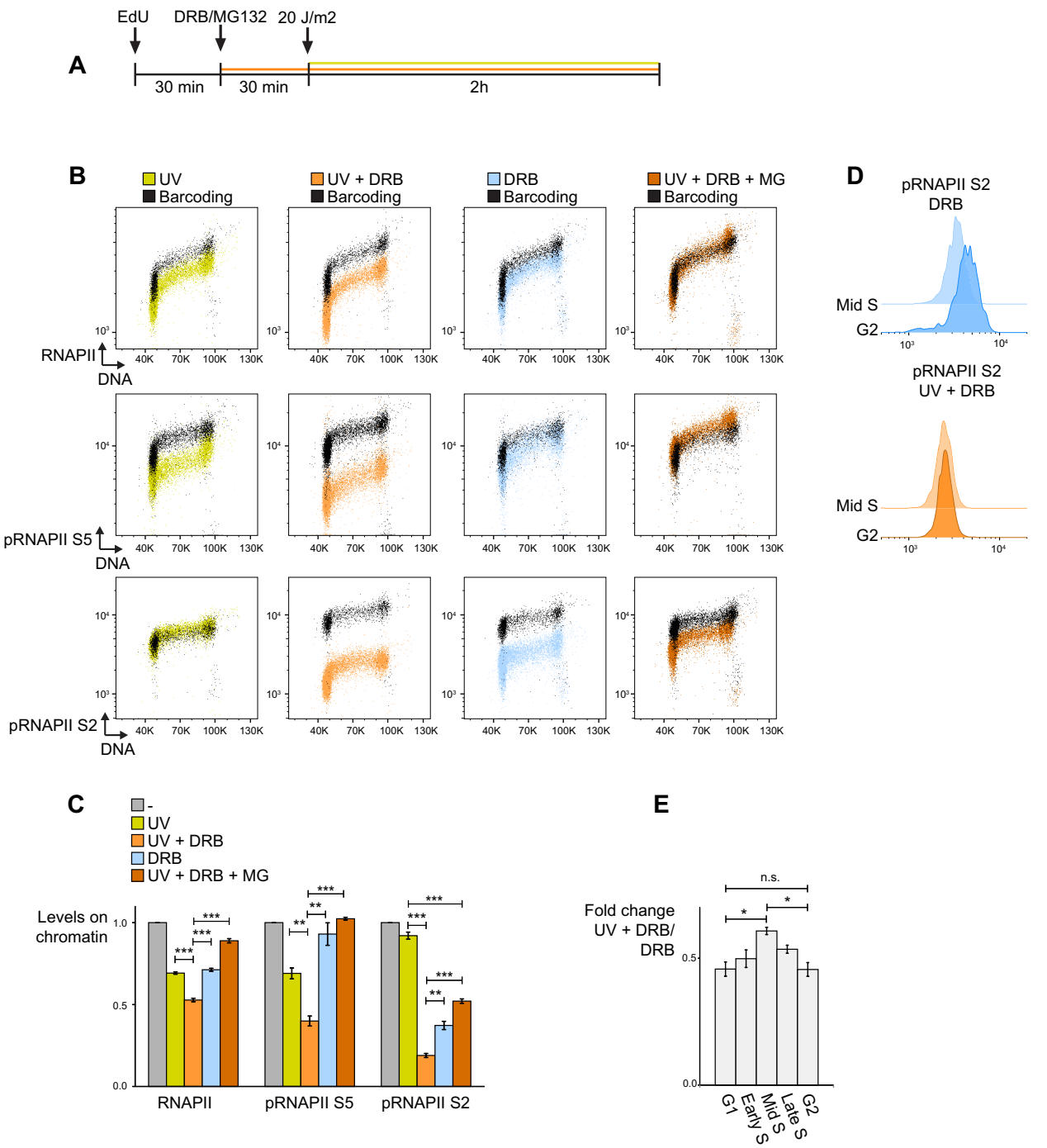

Figure 5. Promoter proximal RNAPII is subjected to proteasome-mediated degradation on chromatin after UV. (**A**) Overview of experimental set up. EdU was added to HeLa cells 30min prior to addition of 100 μM DRB and/or 50 μM MG132. 30min after this, samples were UV irradiated with 20 J/m^2. After 2h, samples were harvested, extracted and fixed for flow cytometry analysis. (**B**) Flow cytometry scatter plots showing levels of RNAPII, pRNAPII S5 and pRNAPII S2 on chromatin versus DNA content from samples treated as in (A). Samples treated with UV, UV + DRB, DRB and UV + DRB + MG132 are shown in colors as indicated. Barcoded control cells (shown in black) are shown in scatterplots together with the sample cells as in Figure 2B. (**C**) Mean median RNAPII, pRNAPII S5 and pRNAPII S2 levels on chromatin in cells treated as in (A) and normalized to barcoding cells. Samples treated with UV or inhibitors were normalized to non-treated sample (−) ($n = 3$), significance tested by the two-tailed two sample Student's t-test. Error bars represent SEM. (**D**) Histograms showing RNAPII pS2 levels on chromatin versus cell count in mid S and G2 phases of the cell cycle from the same experiment as in (B). Cell cycle phases were identified based on DNA content and EdU levels, as shown in Figure 1F). (**E**) Mean fold changes of RNAPII pS2 levels on chromatin in UV + DRB-treated cells relative to mean fold changes in DRB-treated cells, from experiments such as in (B). Results are shown for individual phases of the cell cycle. Note that UV reduces pRNAPII S2 levels in chromatin less in S phase in the presence of DRB. ($n = 3$), significance tested by the two-tailed two-sample Student's t-test. Error bars represent SEM.

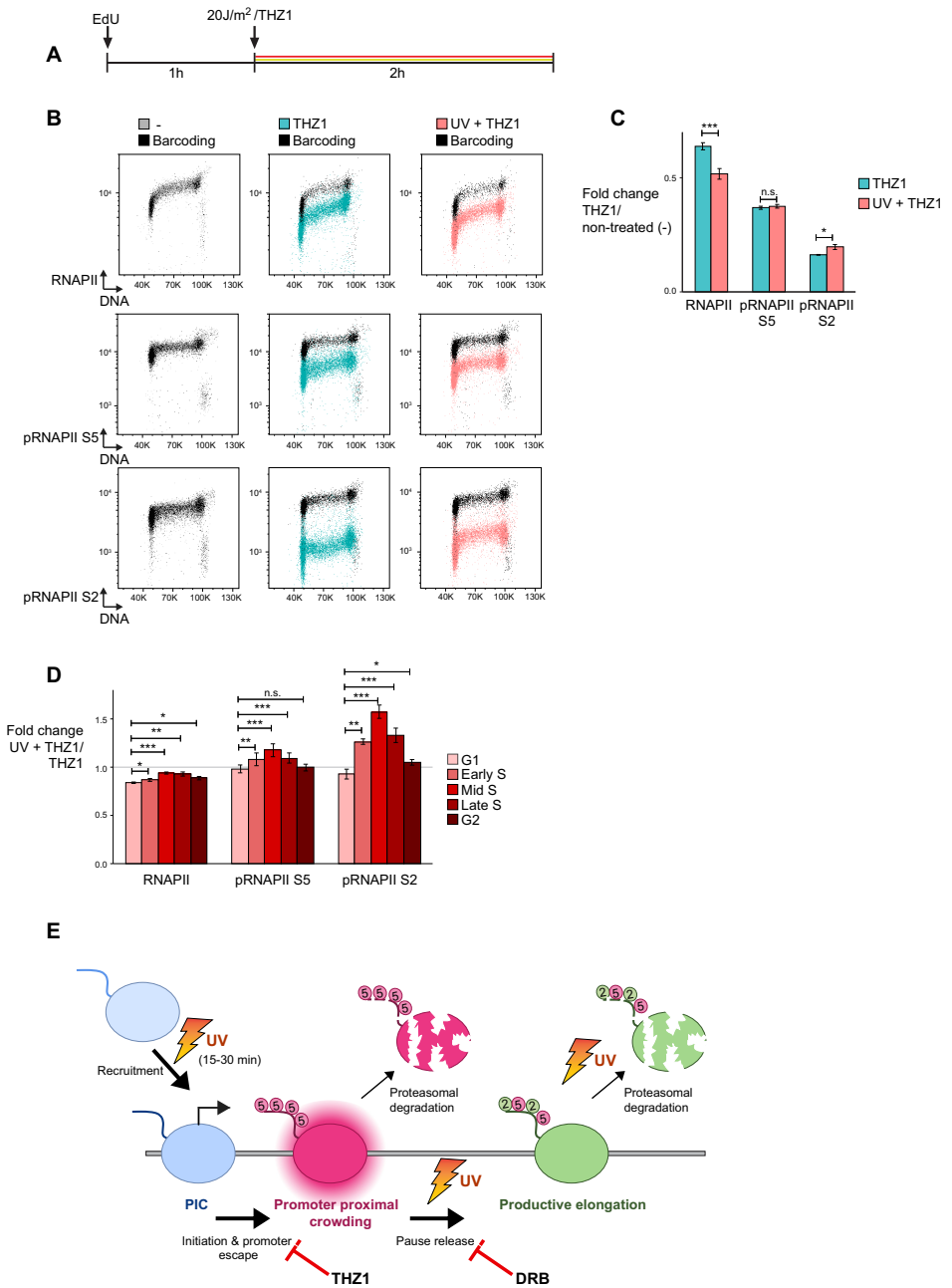

Figure 6. Initiation is required for enhanced proteasome mediated degradation of promoter proximal RNAPII after UV. (**A**) Overview of experimental set up. EdU was added to HeLa cells 1h prior to UV irradiation with 20 J/m^2 and/or addition of 1 μM THZ1 (added directly after UV irradiation). Samples were harvested after 2h, extracted and fixed for flow cytometry analysis. (**B**) Flow cytometry scatter plots showing levels of RNAPII, pRNAPII S5 and pRNAPII S2 on chromatin versus DNA content from samples treated as in A). Non-treated cells (−) are shown in grey, and samples treated with THZ1 +/− UV are shown in colors as indicated. Barcoded control cells (shown in black) are shown in scatterplots together with the sample cells as in Figure 2B. (**C**) Mean fold change after THZ1 +/− UV for RNAPII, pRNAPII S5 and pRNAPII S2 levels on chromatin in cells treated as in A) and normalized to barcoding cells. *(n = 3)*, significance tested by the two-tailed one sample Student's *t*-test. Error bars represent SEM. (**D**) Mean fold changes of RNAPII, pRNAPII S5 and pRNAPII S2 levels on chromatin in UV + THZ1 relative to mean fold changes in THZ1-treated cells. Results are shown for individual phases of the cell cycle (determined as in Figure 1F) ($n = 3$), significance tested by the two-tailed one sample Student's *t*-test. Error bars represent SEM. (**E**) Revised model for the effect of UV on the transcription cycle. Our results suggest that at early timepoints after UV, initiation is enhanced, leading to more promoter proximal stalling. The enhanced promoter proximal stalling causes 'crowding' (see main text for details) around the promoter proximal pause site, pushing RNAPII into productive elongation or degradation (premature termination). Treatment with DRB will exacerbate promoter proximal crowding by preventing pause release, and further enhance degradation of promoter proximal paused RNAPII after UV. THZ1 counteracts crowding at the promoter proximal pause site, as it prevents promoter escape, and thus also UV-induced enhanced degradation. Work by others has shown that UV also enhances pause release (11,33,34,50) and degradation of productively elongating RNAPII (68), which likely directly encounters DNA damage.

promoter proximal RNAPII, is thus likely a requirement for its UV-induced degradation. Indeed, pRNAPII S5 appeared to be slightly more stable after UV in the presence of THZ1, especially in S phase (Figure 6D). Of note, this was similar to pRNAPII S2, which was also slightly more stable in S phase than G1 or G2 phases after UV and THZ1 (Figure 6D). Nevertheless, overall levels of pRNAPII S2 were strongly suppressed by THZ1 in the presence and absence of UV (Figure 6B–D), supporting that continuous initiation followed by release into productive elongation is required for the high pRNAPII S2 levels on chromatin 2h after UV in HeLa cells (Figure 2B–D). Altogether, the results with THZ1 strongly support that the promoter proximal form of RNAPII is being degraded after UV and suggest that the enhanced initiation after UV is required for such degradation.

DISCUSSION

Global regulation of RNAPII levels is involved in transcriptional shutdown, resumption and cell survival after UV (35). So far, the UV-mediated degradation of RNAPII has been thought to involve productively elongating RNAPII (21,41), which is the form that likely encounters DNA damage and participates in TC-NER. Here we show that promoter proximal RNAPII is degraded both in the presence and absence of UV, using a new flow cytometry assay that accurately measures levels of RNAPII, pRNAPII S5 and pRNAPII S2 on chromatin in individual cells through the cell cycle. Inhibiting productive elongation with DRB prior to UV further enhanced degradation of total RNAPII on chromatin, strongly suggesting degradation of promoter proximal RNAPII contributes to regulation of total RNAPII levels after UV. Furthermore, as chromatin loading of RNAPII and pRNAPII S5 were enhanced at early timepoints after UV and suppression of promoter proximal paused RNAPII inhibited UV-mediated degradation of pRNAPII S5 on chromatin, our results suggest enhanced initiation promotes degradation of promoter proximal paused RNAPII at early timepoints after UV. In addition, precise measurements of individual cell cycle transitions revealed that pRNAPII S5 is more degraded after DRB in early S compared to G1 phase in HeLa cells, indicating that transcription replication conflicts are resolved by degradation of promoter proximal RNAPII. On the other hand, pRNAPII S2, associated with productive elongation, was more stable in S phase after UV. As processing of DNA damage-stalled RNAPII is tightly linked to repair (49), the latter may indicate cell cycle specific differences in TC-NER.

Based on the work shown here, we propose a modified model for the effect of UV on transcription (Figure 6E). At early timepoints (15–30min) UV enhances initiation, which leads to more promoter proximal pausing and subsequent elongation. However, as the rate of release into productive elongation is lower than the rate of initiation, UV may cause 'crowding' of RNAPII molecules around the promoter proximal pause site, leading to degradation of promoter proximal paused RNAPII. Inhibiting release into productive elongation by DRB further enhances 'promoter proximal crowding', and increases degradation of promoter proximal RNAPII after UV. Vice versa, suppressing 'promoter proximal crowding' with THZ1 suppresses UV-induced degradation of pRNAPII S5. Notably, increased release from promoter proximal pausing into productive elongation is known to occur after UV (11,33,34,50), but is not conflicting with our model as we simply propose that, at early timepoints after UV, the global rate of initiation vs release into productive elongation is higher causing an accumulation of promoter proximal RNAPII on chromatin. Importantly, the rate of release into productive elongation may still be higher compared to non-UV treated cells. 'Promoter proximal crowding', described here, shares similarity with the previously described 'transcription traffic jam' shown to occur behind RNAPII molecules stalled at DNA damage sites (49). However, in gene-internal regions the stretches of DNA are larger, and can encompass more molecules. From the pre-initiation complex to the promoter proximal pause site there is only ∼47 bp (51). As RNAPII occupies ∼33 bp (52), there is simply not room for a queue. Thus, though conceptually related, 'promoter proximal crowding' is not the same as a 'transcription traffic jam'.

Degradation of RNAPII at the promoter proximal pause site, as shown here, necessarily involves premature termination. A major implication of our work is thus that premature termination, which frequently occurs at the promoter proximal pause site (16,53,54), likely also involves RNAPII degradation on chromatin. Of note, previous reports have not observed enhanced degradation of RNAPII after DRB and UV (55,56). However, a major difference is that these studies measured RNAPII levels in whole cell lysates (55,56), while we measure the chromatin bound fraction in individual cells, used different antibodies and accurate quantification including the barcoding approach. The phospho-specific antibodies used here have been tested in vitro to detect pRNAPII S2 and S5 (57). Moreover, in this work we have used pRNAPII S5 as a marker for promoter proximal RNAPII. It is well established and easily observed in ChIP experiments that the majority of the pRNAPII S5 signal during normal transcription derives from promoter proximal pausing (58). Nevertheless, this does not exclude a role for pRNAPII S5 downstream of promoter proximal pause sites. Indeed, pRNAPII S5 plays a role at splice sites (59), and is found within 8 kb of transcriptional start sites of poised genes (60). After UV and THZ1 treatment, a small fraction of pRNAPII S5 was more stable in S phase (Figure 6). This is reminiscent of the more stable fraction of elongating pRNAPII S2 in S phase after UV, in line with this fraction being dually phosphorylated on S2 and S5. As pRNAPII S5 has been reported to be refractory to degradation (21), this may indicate that promoter proximal paused RNAPII and productively elongating RNAPII may be degraded by different pathways, and that pRNAPII S5 may play different roles in these.

Our results suggest initiation is enhanced after UV leading to more promoter proximal pausing at early timepoints. Notably, most previous work has dealt with later timepoints after UV. However, one study showed global hyperphosphorylation of RNAPII at 1h after UV by western blotting (61) which is consistent with enhanced initiation, as RNAPII becomes phosphorylated during the first steps of transcription (20). Furthermore, RNA synthesis from

all transcription start sites was higher at 1h after UV by nRNA-seq (33), also in line with enhanced initiation. In addition, enhanced promoter proximal stalling after UV is supported by the redistribution of RNA reads toward the 5′ ends of genes upon labeling 0-45min after UV by BruUV-seq (62) and TT-seq (35). Nevertheless, the common view is that UV downregulates transcription initiation (63). In line with the latter, RNAPII levels at transcription start sites were lower at 1.5h after UV by ChIP-seq (33), and RNA reads were reduced at promoter proximal sites at 2h after UV by GRO-seq (11) and at 3h after UV by TT-seq (35). Notably, downregulation of transcription initiation after UV is thought to occur via reduction of the global RNAPII pool by proteasome-mediated degradation of elongating RNAPII (35), and by enhanced expression of the early response gene ATF3 (64), both of which take some time to occur. We therefore propose that the findings can be reconciled by separating the effects after UV into early response (<1h), where initiation and promoter proximal pausing are enhanced, and late response (>1h), where they are suppressed. Such a hypothesis fits well with our results, as RNAPII and pRNAPII S5 loading were enhanced at 15–30min, but reduced at 2h after UV (Figure 2).

The effect of the cell cycle on RNAPII chromatin binding after UV has been little studied, likely because, until now, a good technique to study this has been lacking. Overall, UV induced changes on RNAPII chromatin binding occurred globally in all cell cycle phases. However, cell cycle specific effects could still be detected. As RNAPII processing is tightly linked to TC-NER in human cells (49), the most relevant cell cycle effect with regard to DNA repair is likely the higher stability of elongating RNAPII in S phase after UV. Though TC-NER can occur throughout most of the cell cycle, several of the factors required for the later steps of NER are shared with replication and are expressed in a cell cycle dependent manner (65). Moreover, another cell cycle difference we observed in this work is the enhanced degradation of pRNAPII S5 in S phase compared to G1 or G2 phases after UV in HeLa cells (Figure 2). Furthermore, more pRNAPII S5 was degraded on chromatin in early S phase compared to G1 phase after DRB (Figure 4). This suggests promoter proximal degradation of RNAPII is promoted by replication. Degradation of promoter proximal RNAPII may thus be a mechanism by which the cells deals with collisions between promoter proximal paused RNAPII and replication. Such a mechanism is likely important, as promoter proximal RNAPII can be stable for ∼1h (66).

An advantage of flow cytometry versus other available techniques is statistical strength, which is due to the measurement of thousands of individual cells per sample per experiment. In addition, flow cytometry is rapid, and multiparameter data processing is highly feasible. As it provides an internal control in each sample for normalization, including barcoding greatly facilitates quantifications and sensitivity. The barcoded cells are divided, mixed and stained with each of the samples, so that sample to sample variation during staining is eliminated. Furthermore, EdU incorporation and pH3S10 staining allows the study of RNAPII levels in different cycle phases without having to synchronize cells. It also adds another layer of accuracy, as the contribution of e.g. replication can be specified. This is illustrated in Supplementary Figure S2A, where enhanced levels of RNAPII were detected on chromatin in G1, but not in S phase cells at 30min after UV. Furthermore, in our assay, cells were extracted prior to fixation, causing the release of un- or weakly bound proteins from chromatin. Confirming the accuracy of our method, mitotic cells showed similarly low levels of chromatin binding of RNAPII and its phosphorylated forms by flow cytometry as by western blotting. Several other transcription-related proteins are also released from chromatin in mitosis (26,67), and lower mitotic staining can thus likely be used to verify the accuracy of flow cytometry chromatin binding assays for other proteins as well. This method may further be useful to study mitotic repression of transcription at the G2/M transition. Indeed we found that high mitotic pH3S10 levels occurs prior to the release of RNAPII from chromatin at the G2/M transition (Figure 1), in agreement with another study which found that nascent transcription can be observed in pH3S10 positive cells in early prophase (24). Moreover, using transcriptional inhibitors, we also show that this method can be used to study the transcription cycle itself. Notably, DRB, a well-known inhibitor of release from promoter proximal pausing (42), maintained levels of pRNAPII S5 while strongly suppressing pRNAPII S2. On the other hand, THZ1, which inhibits the transition from initiation into promoter proximal pausing (38), as expected lowered the levels of both pRNAPII S5 and pRNAPII S2.

All in all, here we have developed a rapid, highly sensitive and quantitative assay to study chromatin binding of RNAPII and its phosphorylated forms through the cell cycle. In combination with transcriptional and proteasome inhibitors it can be used to study the transcription cycle and follow the fate of RNAPII on chromatin. Using this method we show that elongating RNAPII becomes more stable in S phase after UV, suggesting cell cycle specific effects in TC-NER. Furthermore, we show that promoter proximal RNAPII is degraded on chromatin in the absence and presence of UV DNA damage, and propose a new modified model for the effect of UV on the transcription cycle. Our results suggest degradation of promoter proximal paused RNAPII substantially contributes to the regulation of the 'RNAPII pool', and may thus be important for transcription resumption and cell survival after UV.

DATA AVAILABILITY

The data has been deposited to the FLOW repository (https://flowrepository.org/) with IDs: FR-FCM-Z5CR, FR-FCM-Z5CE, FR-FCM-Z5CQ, FR-FCM-Z5CX and FR-FCM-Z5CP.

SUPPLEMENTARY DATA

Supplementary Data are available at NAR Online.

ACKNOWLEDGEMENTS

We are grateful for assistance and use of the flow cytometry core facility at the Radium Hospital, Oslo University Hospital.

FUNDING

Norwegian Research Council [275918]. Funding for open access charge: Norwegian Research Council [275918].
Conflict of interest statement. None declared.

REFERENCES

1. Tudek,A., Candelli,T. and Libri,D. (2015) Non-coding transcription by RNA polymerase II in yeast: Hasard or nécessité? *Biochimie*, **117**, 28–36.
2. Gaul,L. and Svejstrup,J.Q. (2021) Transcription-coupled repair and the transcriptional response to UV-Irradiation. *DNA Repair (Amst.)*, **107**, 103208.
3. Lesage,E., Clouaire,T. and Legube,G. (2021) Repair of DNA double-strand breaks in RNAPI- and RNAPII-transcribed loci. *DNA Repair (Amst.)*, **104**, 103139.
4. Montaldo,N.P., Bordin,D.L., Brambilla,A., Rösinger,M., Fordyce Martin,S.L., Bjørås,K., Bradamante,S., Aas,P.A., Furrer,A., Olsen,L.C. *et al.* (2019) Alkyladenine DNA glycosylase associates with transcription elongation to coordinate DNA repair with gene expression. *Nat. Commun.*, **10**, 5460.
5. Enoiu,M., Jiricny,J. and Schärer,O.D. (2012) Repair of cisplatin-induced DNA interstrand crosslinks by a replication-independent pathway involving transcription-coupled repair and translesion synthesis. *Nucleic Acids Res.*, **40**, 8953–8964.
6. Mulderrig,L., Garaycoechea,J.I., Tuong,Z.K., Millington,C.L., Dingler,F.A., Ferdinand,J.R., Gaul,L., Tadross,J.A., Arends,M.J., O'Rahilly,S. *et al.* (2021) Aldehyde-driven transcriptional stress triggers an anorexic DNA damage response. *Nature*, **600**, 158–163.
7. Landsverk,H.B., Sandquist,L.E., Sridhara,S.C., Rødland,G.E., Sabino,J.C., de Almeida,S.F., Grallert,B., Trinkle-Mulcahy,L. and Syljuåsen,R.G. (2019) Regulation of ATR activity via the RNA polymerase II associated factors CDC73 and PNUTS-PP1. *Nucleic Acids Res.*, **47**, 1797–1813.
8. Lindsey-Boltz,L.A. and Sancar,A. (2007) RNA polymerase: the most specific damage recognition protein in cellular responses to DNA damage? *Proc. Nat. Acad. Sci. U.S.A.*, **104**, 13213–13214.
9. Jackson,S.P. and Bartek,J. (2009) The DNA-damage response in human biology and disease. *Nature*, **461**, 1071–1078.
10. Lans,H., Hoeijmakers,J.H.J., Vermeulen,W. and Marteijn,J.A. (2019) The DNA damage response to transcription stress. *Nat. Rev.*, **20**, 766–784.
11. Williamson,L., Saponaro,M., Boeing,S., East,P., Mitter,R., Kantidakis,T., Kelly,G.P., Lobley,A., Walker,J., Spencer-Dene,B. *et al.* (2017) UV irradiation induces a Non-coding RNA that functionally opposes the protein encoded by the same gene. *Cell*, **168**, 843–855.
12. Mayne,L.V. and Lehmann,A.R. (1982) Failure of RNA synthesis to recover after UV irradiation: an early defect in cells from individuals with Cockayne's syndrome and xeroderma pigmentosum. *Cancer Res.*, **42**, 1473–1478.
13. Ratner,J.N., Balasubramanian,B., Corden,J., Warren,S.L. and Bregman,D.B. (1998) Ultraviolet radiation-induced ubiquitination and proteasomal degradation of the large subunit of RNA polymerase II. Implications for transcription-coupled DNA repair. *J. Biol. Chem.*, **273**, 5184–5189.
14. Woudstra,E.C., Gilbert,C., Fellows,J., Jansen,L., Brouwer,J., Erdjument-Bromage,H., Tempst,P. and Svejstrup,J.Q. (2002) A Rad26-Def1 complex coordinates repair and RNA pol II proteolysis in response to DNA damage. *Nature*, **415**, 929–933.
15. Core,L. and Adelman,K. (2019) Promoter-proximal pausing of RNA polymerase II: a nexus of gene regulation. *Genes Dev.*, **33**, 960–982.
16. Contreras,X., Benkirane,M. and Kiernan,R. (2013) Premature termination of transcription by RNAP II: the beginning of the end. *Transcription*, **4**, 72–76.
17. Jensen,T.H., Jacquier,A. and Libri,D. (2013) Dealing with pervasive transcription. *Mol. Cell*, **52**, 473–484.
18. Eaton,J.D. and West,S. (2020) Termination of transcription by RNA polymerase II: BOOM! *Trends Genet.: TIG*, **36**, 664–675.
19. Cossa,G., Parua,P.K., Eilers,M. and Fisher,R.P. (2021) Protein phosphatases in the RNAPII transcription cycle: erasers, sculptors, gatekeepers, and potential drug targets. *Genes Dev.*, **35**, 658–676.
20. Harlen,K.M. and Churchman,L.S. (2017) The code and beyond: transcription regulation by the RNA polymerase II carboxy-terminal domain. *Nat. Rev.*, **18**, 263–273.
21. Somesh,B.P., Reid,J., Liu,W.F., Sogaard,T.M., Erdjument-Bromage,H., Tempst,P. and Svejstrup,J.Q. (2005) Multiple mechanisms confining RNA polymerase II ubiquitylation to polymerases undergoing transcriptional arrest. *Cell*, **121**, 913–923.
22. Yasukawa,T., Kamura,T., Kitajima,S., Conaway,R.C., Conaway,J.W. and Aso,T. (2008) Mammalian Elongin a complex mediates DNA-damage-induced ubiquitylation and degradation of Rpb1. *EMBO J.*, **27**, 3256–3266.
23. Delgado-Román,I. and Muñoz-Centeno,M.C. (2021) Coupling between cell cycle progression and the nuclear RNA polymerases system. *Front. Mol. Biosci.*, **8**, 691636.
24. Liang,K., Woodfin,A.R., Slaughter,B.D., Unruh,J.R., Box,A.C., Rickels,R.A., Gao,X., Haug,J.S., Jaspersen,S.L. and Shilatifard,A. (2015) Mitotic transcriptional activation: clearance of actively engaged Pol II via transcriptional elongation control in mitosis. *Mol. Cell*, **60**, 435–445.
25. Gottesfeld,J.M. and Forbes,D.J. (1997) Mitotic repression of the transcriptional machinery. *Trends Biochem. Sci*, **22**, 197–202.
26. Martínez-Balbás,M.A., Dey,A., Rabindran,S.K., Ozato,K. and Wu,C. (1995) Displacement of sequence-specific transcription factors from mitotic chromatin. *Cell*, **83**, 29–38.
27. Gomez-Gonzalez,B. and Aguilera,A. (2019) Transcription-mediated replication hindrance: a major driver of genome instability. *Genes Dev.*, **33**, 1008–1026.
28. Poli,J., Gerhold,C.B., Tosi,A., Hustedt,N., Seeber,A., Sack,R., Herzog,F., Pasero,P., Shimada,K., Hopfner,K.P. *et al.* (2016) Mec1, INO80, and the PAF1 complex cooperate to limit transcription replication conflicts through RNAPII removal during replication stress. *Genes Dev.*, **30**, 337–354.
29. Landsverk,H.B., Sandquist,L.E., Bay,L.T.E., Steurer,B., Campsteijn,C., Landsverk,O.J.B., Marteijn,J.A., Petermann,E., Trinkle-Mulcahy,L. and Syljuåsen,R.G. (2020) WDR82/PNUTS-PP1 prevents transcription–replication conflicts by promoting RNA polymerase II degradation on chromatin. *Cell Rep.*, **33**, 108469.
30. Wang,J., Rojas,P., Mao,J., Mustè Sadurnì,M., Garnier,O., Xiao,S., Higgs,M.R., Garcia,P. and Saponaro,M. (2021) Persistence of RNA transcription during DNA replication delays duplication of transcription start sites until G2/M. *Cell Rep.*, **34**, 108759.
31. Rudé,J.M. and Friedberg,E.C. (1977) Semi-conservative deoxyribonucleic acid synthesis in unirradiated and ultraviolet-irradiated xeroderma pigmentosum and normal human skin fibroblasts. *Mutat. Res.*, **42**, 433–442.
32. Mailand,N., Falck,J., Lukas,C., Syljuåsen,R.G., Welcker,M., Bartek,J. and Lukas,J. (2000) Rapid destruction of human Cdc25A in response to DNA damage. *Science (New York, N.Y.)*, **288**, 1425–1429.
33. Liakos,A., Konstantopoulos,D., Lavigne,M.D. and Fousteri,M. (2020) Continuous transcription initiation guarantees robust repair of all transcribed genes and regulatory regions. *Nat. Commun.*, **11**, 916.
34. Lavigne,M.D., Konstantopoulos,D., Ntakou-Zamplara,K.Z., Liakos,A. and Fousteri,M. (2017) Global unleashing of transcription elongation waves in response to genotoxic stress restricts somatic mutation rate. *Nat. Commun.*, **8**, 2076.
35. Tufegdžić Vidaković,A., Mitter,R., Kelly,G.P., Neumann,M., Harreman,M., Rodríguez-Martínez,M., Herlihy,A., Weems,J.C., Boeing,S., Encheva,V. *et al.* (2020) Regulation of the RNAPII pool is integral to the DNA damage response. *Cell*, **180**, 1245–1261.
36. Boeing,S., Williamson,L., Encheva,V., Gori,I., Saunders,R.E., Instrell,R., Aygun,O., Rodriguez-Martinez,M., Weems,J.C., Kelly,G.P. *et al.* (2016) Multiomic analysis of the UV-Induced DNA damage response. *Cell Rep.*, **15**, 1597–1610.
37. Geijer,M.E., Zhou,D., Selvam,K., Steurer,B., Mukherjee,C., Evers,B., Cugusi,S., van Toorn,M., van der Woude,M., Janssens,R.C. *et al.* (2021) Elongation factor ELOF1 drives transcription-coupled repair and prevents genome instability. *Nat. Cell Biol.*, **23**, 608–619.
38. Steurer,B., Janssens,R.C., Geverts,B., Geijer,M.E., Wienholz,F., Theil,A.F., Chang,J., Dealy,S., Pothof,J., van Cappellen,W.A. *et al.* (2018) Live-cell analysis of endogenous GFP-RPB1 uncovers rapid turnover of initiating and promoter-paused RNA polymerase II. *Proc. Nat. Acad. Sci. U.S.A.*, **115**, E4368–E4376.

39. Håland,T.W., Boye,E., Stokke,T., Grallert,B. and Syljuåsen,R.G. (2015) Simultaneous measurement of passage through the restriction point and MCM loading in single cells. *Nucleic Acids Res.*, **43**, e150.
40. Parsons,G.G. and Spencer,C.A. (1997) Mitotic repression of RNA polymerase II transcription is accompanied by release of transcription elongation complexes. *Mol. Cell. Biol.*, **17**, 5791–5802.
41. Noe Gonzalez,M., Blears,D. and Svejstrup,J.Q. (2021) Causes and consequences of RNA polymerase II stalling during transcript elongation. *Nat. Rev.*, **22**, 3–21.
42. Yamaguchi,Y., Shibata,H. and Handa,H. (2013) Transcription elongation factors DSIF and NELF: promoter-proximal pausing and beyond. *Biochim. Biophys. Acta*, **1829**, 98–104.
43. Salifou,K., Burnard,C., Basavarajaiah,P., Grasso,G., Helsmoortel,M., Mac,V., Depierre,D., Franckhauser,C., Beyne,E., Contreras,X. *et al.* (2021) Chromatin-associated MRN complex protects highly transcribing genes from genomic instability. *Sci. Adv.*, **7**, eabb2947.
44. Sheridan,R.M., Fong,N., D'Alessandro,A. and Bentley,D.L. (2019) Widespread backtracking by RNA Pol II is a major effector of gene activation, 5′ pause release, termination, and transcription elongation rate. *Mol. Cell*, **73**, 107–118.
45. Erickson,B., Sheridan,R.M., Cortazar,M. and Bentley,D.L. (2018) Dynamic turnover of paused Pol II complexes at human promoters. *Genes Dev.*, **32**, 1215–1225.
46. Gomes,N.P., Bjerke,G., Llorente,B., Szostek,S.A., Emerson,B.M. and Espinosa,J.M. (2006) Gene-specific requirement for P-TEFb activity and RNA polymerase II phosphorylation within the p53 transcriptional program. *Genes Dev.*, **20**, 601–612.
47. Pope,B.D., Hiratani,I. and Gilbert,D.M. (2010) Domain-wide regulation of DNA replication timing during mammalian development. *Chromosome Res.*, **18**, 127–136.
48. Nilson,K.A., Guo,J., Turek,M.E., Brogie,J.E., Delaney,E., Luse,D.S. and Price,D.H. (2015) THZ1 reveals roles for Cdk7 in Co-transcriptional capping and pausing. *Mol. Cell*, **59**, 576–587.
49. Nakazawa,Y., Hara,Y., Oka,Y., Komine,O., van den Heuvel,D., Guo,C., Daigaku,Y., Isono,M., He,Y., Shimada,M. *et al.* (2020) Ubiquitination of DNA damage-stalled RNAPII promotes transcription-coupled repair. *Cell*, **180**, 1228–1244.
50. Studniarek,C., Tellier,M., Martin,P.G.P., Murphy,S., Kiss,T. and Egloff,S. (2021) The 7SK/P-TEFb snRNP controls ultraviolet radiation-induced transcriptional reprogramming. *Cell Rep.*, **35**, 108965.
51. Shao,W. and Zeitlinger,J. (2017) Paused RNA polymerase II inhibits new transcriptional initiation. *Nat. Genet.*, **49**, 1045–1051.
52. Saeki,H. and Svejstrup,J.Q. (2009) Stability, flexibility, and dynamic interactions of colliding RNA polymerase II elongation complexes. *Mol. Cell*, **35**, 191–205.
53. Brannan,K., Kim,H., Erickson,B., Glover-Cutter,K., Kim,S., Fong,N., Kiemele,L., Hansen,K., Davis,R., Lykke-Andersen,J. *et al.* (2012) mRNA decapping factors and the exonuclease Xrn2 function in widespread premature termination of RNA polymerase II transcription. *Mol. Cell*, **46**, 311–324.
54. Wagschal,A., Rousset,E., Basavarajaiah,P., Contreras,X., Harwig,A., Laurent-Chabalier,S., Nakamura,M., Chen,X., Zhang,K., Meziane,O. *et al.* (2012) Microprocessor, Setx, Xrn2, and Rrp6 co-operate to induce premature termination of transcription by RNAPII. *Cell*, **150**, 1147–1157.
55. Luo,Z., Zheng,J., Lu,Y. and Bregman,D.B. (2001) Ultraviolet radiation alters the phosphorylation of RNA polymerase II large subunit and accelerates its proteasome-dependent degradation. *Mutat. Res.*, **486**, 259–274.
56. McKay,B.C., Chen,F., Clarke,S.T., Wiggin,H.E., Harley,L.M. and Ljungman,M. (2001) UV light-induced degradation of RNA polymerase II is dependent on the Cockayne's syndrome A and B proteins but not p53 or MLH1. *Mutat. Res.*, **485**, 93–105.
57. Chapman,R.D., Heidemann,M., Albert,T.K., Mailhammer,R., Flatley,A., Meisterernst,M., Kremmer,E. and Eick,D. (2007) Transcribing RNA polymerase II is phosphorylated at CTD residue serine-7. *Science (New York, N.Y.)*, **318**, 1780–1782.
58. Heidemann,M., Hintermair,C., Voss,K. and Eick,D. (2013) Dynamic phosphorylation patterns of RNA polymerase II CTD during transcription. *Biochim. Biophys. Acta*, **1829**, 55–62.
59. Nojima,T., Rebelo,K., Gomes,T., Grosso,A.R., Proudfoot,N.J. and Carmo-Fonseca,M. (2018) RNA polymerase II phosphorylated on CTD serine 5 interacts with the spliceosome during Co-transcriptional splicing. *Mol. Cell*, **72**, 369–379.
60. Brookes,E. and Pombo,A. (2009) Modifications of RNA polymerase II are pivotal in regulating gene expression states. *EMBO Rep.*, **10**, 1213–1219.
61. Rockx,D.A., Mason,R., van Hoffen,A., Barton,M.C., Citterio,E., Bregman,D.B., van Zeeland,A.A., Vrieling,H. and Mullenders,L.H. (2000) UV-induced inhibition of transcription involves repression of transcription initiation and phosphorylation of RNA polymerase II. *Proc. Nat. Acad. Sci. U.S.A.*, **97**, 10503–10508.
62. Andrade-Lima,L.C., Veloso,A., Paulsen,M.T., Menck,C.F. and Ljungman,M. (2015) DNA repair and recovery of RNA synthesis following exposure to ultraviolet light are delayed in long genes. *Nucleic Acids Res.*, **43**, 2744–2756.
63. van den Heuvel,D., van der Weegen,Y., Boer,D.E.C., Ogi,T. and Luijsterburg,M.S. (2021) Transcription-Coupled DNA repair: from mechanism to human disorder. *Trends Cell Biol.*, **31**, 359–371.
64. Kristensen,U., Epanchintsev,A., Rauschendorf,M.A., Laugel,V., Stevnsner,T., Bohr,V.A., Coin,F. and Egly,J.M. (2013) Regulatory interplay of Cockayne syndrome B ATPase and stress-response gene ATF3 following genotoxic stress. *Proc. Nat. Acad. Sci. U.S.A.*, **110**, E2261–E2270.
65. Mjelle,R., Hegre,S.A., Aas,P.A., Slupphaug,G., Drabløs,F., Saetrom,P. and Krokan,H.E. (2015) Cell cycle regulation of human DNA repair and chromatin remodeling genes. *DNA Repair (Amst.)*, **30**, 53–67.
66. Chen,F., Gao,X. and Shilatifard,A. (2015) Stably paused genes revealed through inhibition of transcription initiation by the TFIIH inhibitor triptolide. *Genes Dev.*, **29**, 39–47.
67. Muchardt,C., Reyes,J.C., Bourachot,B., Leguoy,E. and Yaniv,M. (1996) The hbrm and BRG-1 proteins, components of the human SNF/SWI complex, are phosphorylated and excluded from the condensed chromosomes during mitosis. *EMBO J.*, **15**, 3394–3402.
68. Wilson,M.D., Harreman,M. and Svejstrup,J.Q. (2013) Ubiquitylation and degradation of elongating RNA polymerase II: the last resort. *Biochim. Biophys. Acta*, **1829**, 151–157.

Supplementary information for

‘A novel, rapid and sensitive flow cytometry method reveals degradation of promoter proximal paused RNAPII in the presence and absence of UV’

Lilli T. E. Bay, Randi G. Syljuåsen and Helga B. Landsverk

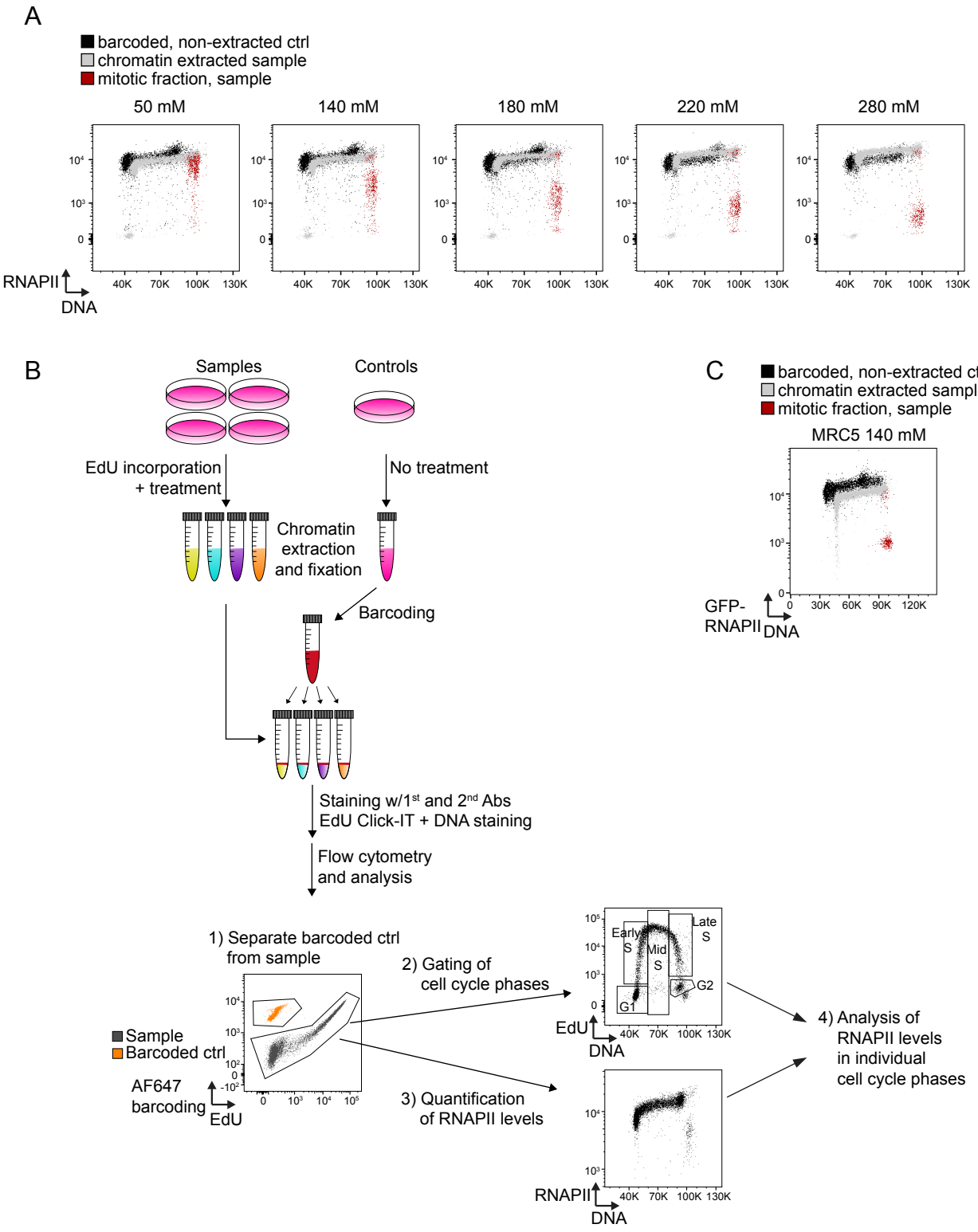
A
barcoded, non-extracted ctrl
chromatin extracted sample
mitotic fraction, sample
50 mM
140 mM
180 mM
220 mM
280 mM
RNAPII
DNA
B
Samples
Controls
EdU incorporation + treatment
No treatment
Chromatin extraction and fixation
Barcoding
Staining w/1st and 2nd Abs EdU Click-IT + DNA staining
Flow cytometry and analysis
1) Separate barcoded ctrl from sample
Sample
Barcoded ctrl
AF647 barcoding
EdU
2) Gating of cell cycle phases
Early S
Mid S
Late S
G1
G2
EdU
DNA
3) Quantification of RNAPII levels
RNAPII
DNA
4) Analysis of RNAPII levels in individual cell cycle phases
C
barcoded, non-extracted ctrl
chromatin extracted sample
mitotic fraction, sample
MRC5 140 mM
GFP-RNAPII
DNA

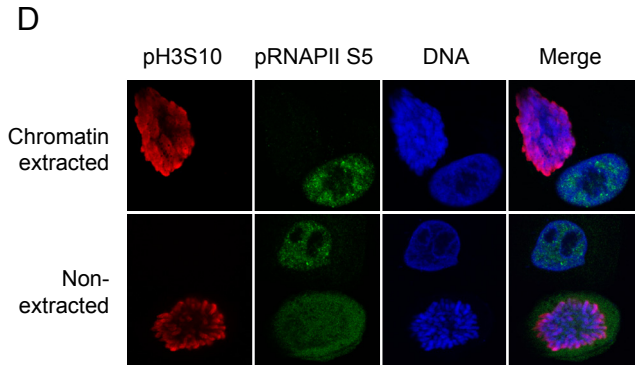
D
pH3S10
pRNAPII S5
DNA
Merge
Chromatin extracted
Non-extracted

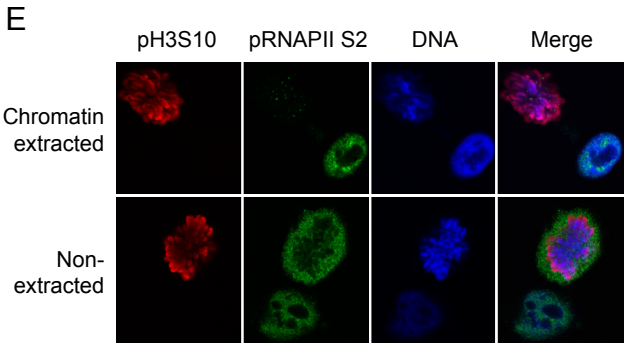
E
pH3S10
pRNAPII S2
DNA
Merge
Chromatin extracted
Non-extracted

Figure S1.

A) Flow cytometry scatter plots of RNAPII levels versus DNA content. A barcoded, non-extracted control (black color) of HeLa cells was added to all individual samples prior to antibody staining. Each sample was subjected to chromatin fractionation of varying concentrations of NaCl in the extraction buffer, ranging from 50 mM to 280 mM (samples are in grey and red color). Mitotic fraction of the sample was identified by pH3S10 staining, as shown in Figure 1A-C, and is visualized in red.

B) Overview of experimental procedure for chromatin extraction, staining and flow cytometry analysis. Samples of cells in culture dishes were treated with EdU, UV and/or inhibitors. Both sample and non-treated control cells were harvested, transferred into tubes, chromatin extracted and fixed. After fixation, non-treated controls cells were barcoded and distributed to all the individual samples. Samples (now also containing the barcoded non-treated control cells) were stained with primary and secondary antibodies, followed by EdU Click-IT reaction and DNA staining. During flow cytometry analysis, barcoded non-treated control cells (Barcoded ctrl) were separated from sample cells (Sample) based EdU content and AF647 signal (from barcoding). Samples were further gated into cell cycle phases (as shown), and levels of RNAPII were visualized and quantified. Levels of RNAPII on chromatin in barcoded cells were used for normalization.

C) Flow cytometry scatter plot showing levels of GFP RNAPII on chromatin versus DNA content in MRC5 cells expressing knock-in GFP tagged RNAPII (MRC5-GFP-RNAPII cells), after extraction with 140 mM NaCl. Non-extracted control (ctrl) of MRC5-GFP-RNAPII cells were barcoded (black) and added to the extracted cells prior to staining with pH3S10 to identify the mitotic cells. Extracted cells are shown in grey (pH3S10 negative) and red (pH3S10 positive).

D) Immunofluorescence analysis of chromatin extracted (140 mM NaCl) or non-extracted cells using antibodies to pRNAPII S5 and pH3S10. DNA was stained with Hoechst 33342.

E) As in D), but for pRNAPII S2

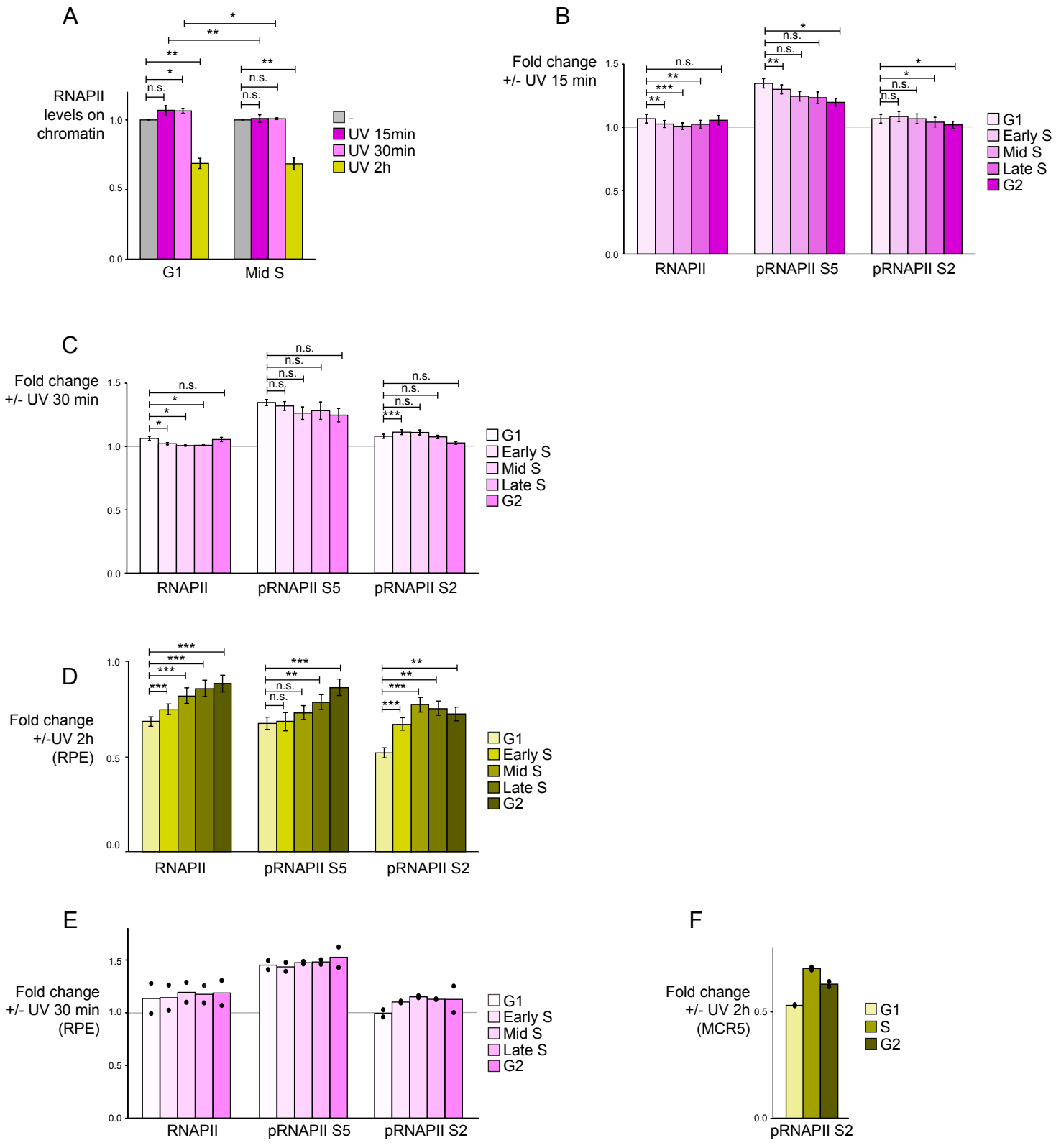
A
RNAPII levels on chromatin
1.0
0.5
0.0
G1
Mid S
-
UV 15min
UV 30min
UV 2h
B
Fold change +/- UV 15 min
1.5
1.0
0.5
0.0
RNAPII
pRNAPII S5
pRNAPII S2
G1
Early S
Mid S
Late S
G2
C
Fold change +/- UV 30 min
1.5
1.0
0.5
0.0
RNAPII
pRNAPII S5
pRNAPII S2
G1
Early S
Mid S
Late S
G2
D
Fold change +/-UV 2h (RPE)
1.0
0.5
0.0
RNAPII
pRNAPII S5
pRNAPII S2
G1
Early S
Mid S
Late S
G2
E
Fold change +/- UV 30 min (RPE)
1.5
1.0
0.5
0.0
RNAPII
pRNAPII S5
pRNAPII S2
G1
Early S
Mid S
Late S
G2
F
Fold change +/- UV 2h (MCR5)
0.5
0.0
pRNAPII S2
G1
S
G2

Figure S2.

A) Mean median RNAPII, pRNAPII S5 and pRNAPII S2 levels on chromatin in G1 and Mid S phase, from experiment performed as in Figure 2A-E. *(n=3)*, significance tested by the two-tailed one sample *Student's* test. Error bars represent SEM.

B) Mean fold change for RNAPII, pRNAPII S5 and pRNAPII S2 levels on chromatin at 15 min after UV vs non-treated cells, from experiment performed as in Figure 2 and analyzed similar as in 2F). *(n=3)*, significance tested by the two-tailed one sample *Student's* test. Error bars represent SEM.

C) As in B), but at 30 min after UV. *(n=3)*

D) As in B), but in RPE cells at 2h after UV. *(n=3)*, significance tested by the two-tailed one sample *Student's* test. Error bars represent SEM.

E) As in B), but in RPE cells at 30 min after UV. *(n=2)*

F) As in B) but in MRC5-GFP-RNAPII cells, for pRNAPII S2 levels on chromatin at 2h after UV. Here EdU was omitted, and cell cycle phases were therefore determined by DNA content. *(n=2)*

A

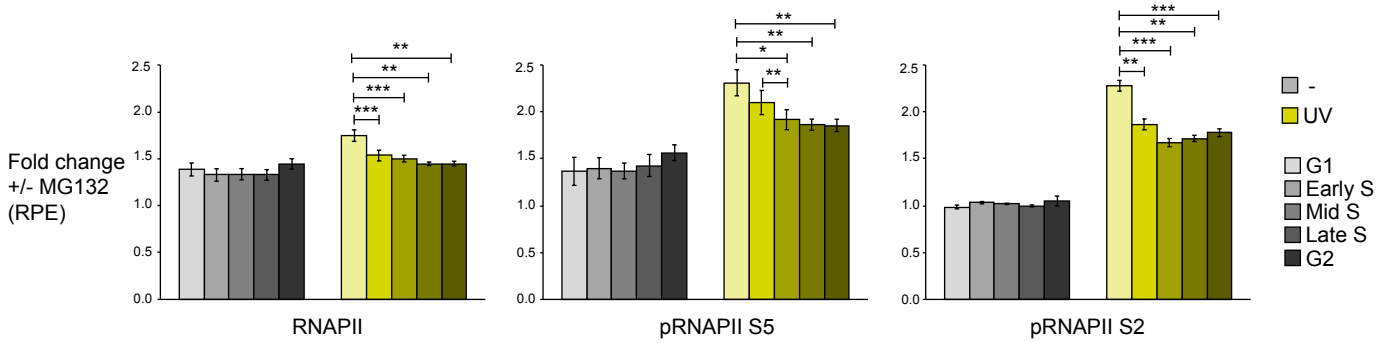
Fold change
+/- MG132
(RPE)
2.5
2.0
1.5
1.0
0.5
0.0
**
**
***
***
RNAPII
**
**
*
**
pRNAPII S5
***
**
***
**
pRNAPII S2
-
UV
G1
Early S
Mid S
Late S
G2

Figure S3.

A) As in Figure 3E), but in RPE cells. *(n=3)*, significance tested by the two-tailed one sample *Student's* test. Error bars represent SEM.

III